Structural Modelling of Plasterboard-Clad, Light Timber-Framed Walls in Fire

A Thesis Submitted in Fulfilment of the Requirements of the higher degree of

Doctor of Philosophy

by

Scott Young

Centre for Environmental Safety & Risk Engineering

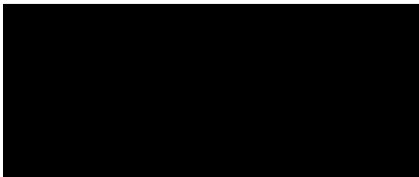Faculty of Engineering and Science

Victoria University of Technology

Victoria

Australia

2000

Declaration

I declare that the following work has been performed by myself and has not be submitted previously in whole or any part in respect to any other award. To my knowledge, the work reported in this thesis is original and contains no material published by other investigations, except where appropriate reference has been given to the source of the material.

Scott Young

8/12/2000

Date

i

Abstract

The building regulations in Australia and other countries are being reformed from a prescriptive basis of designing fire safety system requirements to a performance basis, which requires the application of engineering principles. Under the prescriptive regulations, fire resistant construction elements were tested using a standard fire resistance test heating regime, which is invariably quite different from the characteristics of real fires. The engineered approach requires the ability to predict the performance of elements of construction that may have different details those tested under the standard heating regime and under different heating regimes.

This thesis comprises part of a comprehensive research program undertaken at the Centre for Environmental Safety and Risk Engineering, Victoria University of Technology to develop a comprehensive framework to determine the time dependent probability of failure of timber-framed assemblies subjected to real fires.

The objective of the thesis is to determine the structural response of plasterboard-clad, timber-framed walls subject to fire and is a key component that is incorporated into the framework to determine the probability of failure of timber-framed assemblies subjected to fire. The structural model simulates dominant phenomena, which have conventionally been ignored in the determination of the structural response of timber-framed walls in fire. The phenomena considered include the degradation in mechanical properties of materials due to thermal effects, non-linear mechanical and geometric effects caused through buckling, partial composite interaction with the plasterboard sheeting, thermal expansion and shrinkage and varied end restraint conditions.

These phenomena have been modelled using common frame analysis methods to provide a computationally efficient and robust model. A transient, second-order direct stiffness approach has been utilised, with specific elements devised to consider the partial composite interaction.

In conjunction with the development of the model, a comprehensive experimental program has been undertaken, to provide a means of comparison of the model predictions, and to obtain data found to be lacking in the literature. A series of full-scale experiments were conducted on timber-framed assemblies under ambient and elevated temperature conditions. The variability, end restraint conditions and contribution of the sheeting were carefully controlled and examined in the experiments. The literature review identified that there was a lack of data detailing the reduction in the modulus of elasticity in compression with temperature. This was considered the most critical mechanical property in determining the time-to-failure of a load bearing timber-framed wall and so a series of experiments was undertaken on short lengths of timber to determine the reduction in the mechanical properties in compression with temperature.

The full-scale experiments demonstrated the significance of end restraint and the influence of plasterboard sheeting on the time-to-failure. The full-scale experiments also showed an apparent rapid drop in the apparent stiffness of the timber framing as it approached a mean temperature of approximately 100°C through the cross-section.

The reduction in the mechanical properties of radiata pine in compression due to elevated temperature exposure was determined directly from tests. It was determined that there was a significant reduction in the mechanical properties in compression of moist timber specimens heated to 70°C, compared with dry specimens. This finding was consistent with results from the full-scale experiments.

The structural response model was successfully validated against closed form and finite element solutions and the predictions of the model compared closely with results from a series of full-scale experiments undertaken as part of the research. The deformation induced in the full-scale experiments was irrecoverable and may have been associated with a mechano-sorptive type creep phenomenon, although further research is required to study this phenomenon. This is one several areas requiring future research that has been identified by the author.

Publications Arising from Research Undertaken towards this Thesis

Young, S.A., Clancy, P., Beck, V.R. & Leicester, R.H., "Model for the Performance of Timber Framed Assemblies in Real Fires", 1994, *Proceedings of Australasian Conference Structural Engineering Conference*, Sydney, Australia, 21-23 September 1994, Vol. 2, pp. 705-712

Young, S.A., Clancy, P. & Beck, V.R., "Structural Modelling of Timber Walls in Fire", 1996, *Proceedings of the First Australasian Conference on Applied Mechanics*, Melbourne Australia, 21-23 February 1996, pp. 707-712

Young, S.A. & Clancy, P., "Compression-Load Deformation of Timber Walls in Fire", 1996, *Proceedings of the Third International Conference, Wood and Fire Safety*, 6-9 May 1996, The High Tatras, Hotel Patria, Slovak Republic, pp. 127-136

Young, S.A. & Clancy, P., "Degradation of the Mechanical Properties in Compression of Radiata Pine in Fire", 1998, *5th World Conference on Timber Engineering*, August 17-20 1998, Montreux, Switzerland, Vol. 1, pp. 246-253

Young, S.A. & Clancy, P., "Full-scale Ambient Tests on Timber Framed Walls", Internal Report, Centre for Environmental Safety & Risk Engineering, Victoria University of Technology, Australia, 164 pp.

Young, S.A. "Elevated Temperature Mechanical Properties of Radiata Pine in Compression", 1996, Internal Report, Centre for Environmental Safety & Risk Engineering, Victoria University of Technology, Australia, 147 pp.

Young, S.A., "Structural Modelling of Plasterboard Clad, Light Timber-Framed Walls in Fire", 2000, Internal Report IR 00-001, Centre for Environmental Safety & Risk Engineering, Victoria University of Technology, Australia

Young, S.A. & Clancy, P., "Structural Modelling of Light-timber Framed Walls in Fire", 2000, *Fire Safety Journal*, manuscript submitted, accepted for publication

Young, S.A. & Clancy, P., "Compression Mechanical Properties of Wood at Temperatures Simulating Fire Conditions", 2000, *Fire & Materials*, manuscript submitted

Clancy, P., Young, S.A., Beck, V.R. & Leicester, R.H., "Modelling of Timber Framed Assemblies in Real Fires", 1994, *Proceedings of the Pacific Timber Engineering Conference*, Gold Coast, Australia, July 1994, Vol. 2, pp. 282-293

Clancy, P. & Young, S.A., "Models for Light Timber Framed Assemblies in Real Fires", 1995, *Proceedings of the Fifth East Asia-Pacific Conference on Structural Engineering and Construction*, Gold Coast, Australia, 25-27 July 1995, pp. 2271-2276

Clancy, P. & Young, S.A., "Full Scale Furnace Tests on Timber Framed Walls", 1996, Report, Department of Civil & Building Engineering, Victoria University of Technology, Australia, 268 pp.

TABLE OF CONTENTS

3. Structural Model   3-1

7. Comparisons of Model Predictions with Experimental Results 7-1

Appendix 1: Derivation of the Strain Induced through the Composite Elements by Consideration of Partial Composite Action

1. Introduction

1.1 Background

In Australia and other countries, building regulations are in the process of being reformed with respect to fire safety design of buildings. The reform has involved a move from a prescriptive-based approach to allowing a performance-based approach.

In allowing for a fire safety system to be designed for a building on a performance basis, the fire protection systems must achieve the required objectives agreed upon by the engineer, the building regulatory authority and other stakeholders; for example the objectives may be life safety but not property protection. Undertaking a performance-based approach to the design of fire safety systems within buildings as has been identified in reports, such as those prepared by the Warren Centre Project (1989), and can result in design flexibility while achieving potential significant cost savings. These outcomes can be achieved without necessarily increasing the risk of fatality for occupants exposed to fire compared with the risk inherent in building designs based on prescriptive regulations. The use of performance-based design approaches can provide new opportunities for the use of timber-framed construction for passive fire protection where it was not permitted in certain circumstances under a prescriptive regulatory regime; namely exclusion of combustible construction. In addition, there are opportunities to reduce the costs of passive fire protection in buildings that incorporate the use of timber-framed construction.

Gypsum plasterboard-clad, timber-framed wall partitions have been previously used for passive fire protection in buildings of certain types of construction; namely those which permitted combustible construction. The prescriptive building regulations would require a barrier separating element to have a demonstrated ability to sustain a period of exposure to a specified testing regime. In Australia, this requirement is referred to as a Fire Resistance Level (FRL). The relevant testing regime in Australia is AS1530.4 (1997) "Methods for Fire Tests on Building Materials, Components and Structures Part 4 - Fire-Resistance Tests of Elements of Building Construction"; other similar regimes are BS476 Part 20, ISO 834 and ASTM E119. For practical designs of

barrier separating elements, there may be many different forms of construction required that differ from the tested prototype tested in accordance with these standard testing regimes. For example increased heights that are not practical to be tested on a furnace, different loads or framing member dimensions and timber stress grades. Such variations require an analysis to be undertaken to determine the performance of these varied configurations, extrapolated from the results of a tested prototype of the barrier separating element subjected to the standard testing regime.

A performance-based fire safety engineering design approach requires consideration of the interaction of fire safety sub-systems within a building, and depending on the depth of analysis, may require the modelling of fire growth and spread within the building. In the case of the Building Code of Australia (BCA-1996), the relevant performance requirements are CP1 and CP2. These performance requirements must be considered in a performance based design involving load-bearing timber-framed, plasterboard-clad barriers. Performance requirements CP1 and CP2 are shown in Figure 1.1.

These clauses require the determination of the performance of building passive fire protection systems, such as plasterboard-clad, timber-framed barriers, when subjected an appropriate design fire intensity. The design fire intensity to which a barrier is subjected is represented by a compartment gas temperature versus time relationship. In the case of real fires, this can be predicted through the use of fire growth and spread models, or reference to appropriate test data. Reference to selected compartment gas temperatures from full-scale compartment fire tests and comparison with the heating regime of a standard fire resistance test demonstrates that the heating conditions are likely to be very different for a real design fire compared with those of a standard fire resistance test.

CP1

A building must have elements which will, to the degree necessary, maintain structural stability during a fire appropriate to-

(a) the function or use of the building; and

(b) the *fire load*; and

(c) the potential *fire intensity*; and

(d) the *fire hazard*; and

(e) the height of the building; and

(f) its proximity to *other property*; and

(g) any active *fire safety systems* installed in the building; and

(h) the size of any *fire compartment*; and

(i) *fire brigade* intervention; and

(j) other elements they support.

CP2

A building must have elements which will, to the degree necessary, avoid the spread of fire-

(a) to *exits*; and

(b) to *sole-occupancy units* and *public corridors*; and

Application:
CP2(b) only applies to a Class 2 or 3 building or Class 4 part.

(c) between buildings; and

(d) in a building,

appropriate to-

(i) the function or use of the building; and

(ii) the *fire load*; and

(iii) the potential *fire intensity*; and

(iv) the *fire hazard*; and

(v) the number of *storeys* in the building; and

(vi) its proximity to *other property*; and

(vii) any active *fire safety systems* installed in the building; and

(viii) the size of any *fire compartment*; and

(ix) *fire brigade* intervention; and

(x) other elements they support; and

(xi) the *evacuation time*

***Figure 1.1:** Relevant Performance Clauses CP1 and CP2 from the BCA-1996*

It is feasible for a single building that there will be a multitude of realistic compartment design fires due to the different uses in the building, fuel loads, compartment sizes, ventilation provisions and wall lining materials. It is possible therefore for a building with passive fire protection, designed on a performance basis, that the performance of the barrier systems will need to be considered for exposure to a multitude of realistic fires. Accordingly, a model is required to determine the performance of barrier systems subjected to various fire conditions.

A number of models to predict the performance of plasterboard-clad, timber-framed barrier systems if subjected to heating conditions of a standard fire resistance test have been developed, for example, White (1988) and Collier (1991). However, these have generally been empirically derived from standard fire resistance tests for specific construction configurations and are not suited to predicting the performance of varied construction configurations, subjected to a multitude of realistic fire conditions.

Approaches have been developed to relate the heating characteristics of realistic fires to a standard testing heating regime. These approaches have been derived in terms of an "equivalent" time of exposure to the standard heating regime and such methods have been summarised by Harmathy (1987). These methods have been demonstrated to be suitable in predicting the performance of unprotected structural steel (Latham, 1987). However, the use of an "equivalent" time of exposure to a standard heating regime may not be readily applicable to plasterboard-clad, timber-framed barriers. The approach may be suitable for steel at relatively low stress levels, due to the steel being an excellent conductor and having close to idealised linear elastic mechanical behaviour through much of the stress-strain range. There is no evidence that such an approach can be used to predict the performance of materials, which have highly insulative, non-linear, transient properties such as plasterboard and timber. It is therefore apparent that for plasterboard-clad, timber-framed barriers existing fire resistance test data and models derived empirically from it, cannot be readily adapted through the use of an "equivalent" fire resistance approach. Therefore it is necessary to develop a model to predict the performance of these barriers when exposed to realistic fires by considering all relevant phenomena in the analysis.

Based on this need to develop a model to predict the performance of plasterboard-clad, timber-framed barriers for a multitude of realistic fires through the consideration of relevant phenomena, Clancy (1999) in 1992 defined a framework to perform the modelling (Figure 1.2).
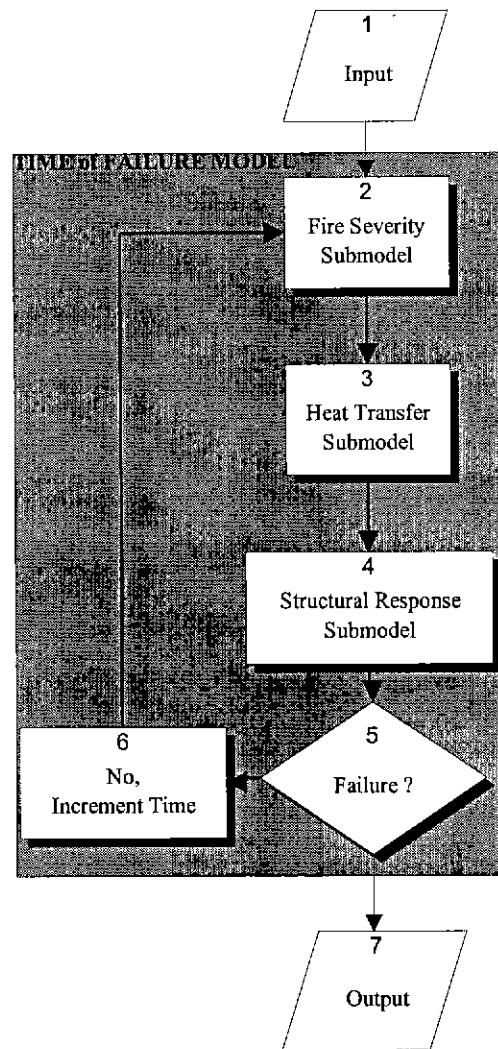
Figure 1.2: Flow-chart depicting the Framework Developed by Clancy (1999)

1.2   The Overall Project Framework of Clancy

The aim for the framework developed by Clancy (1999) was to develop models to predict the time-dependent probability of failure of gypsum plasterboard-clad, timber-framed barriers in real fires. The framework required detailed models to be developed to define the performance of timber-framed barriers in fire; a probabilistic model was incorporated to allow the work to be utilised in a risk analysis for the purposes of being used in comparative studies of alternative fire safety sub-systems. The framework required models to be developed to determine both the thermal and structural response of the barrier when exposed to fire.

The general requirements of these models were as follows:

- The models were to be interlinked, to allow for the consideration of input parameters and probabilistic distributions of properties. Therefore, the models should ideally consist of a stand alone source code.

- In order to determine the cumulative probabilistic distribution of the time of failure, many simulations or runs would be required. Therefore, the models must be both efficient with regard to solution speed, but be robust and capable of many repeated runs without requiring manual intervention; (for example, manually altering material properties during phases of the analysis).

Clancy (1999) has developed a sophisticated model for heat transfer that allows for a range of timber wall sections with complex cavities to be incorporated into the framework, in addition to allowing for the use of a number of fire severity models. The responsibility for the development of the structural model rested with the author of this thesis.

The research described in this thesis was associated with the development of a model compatible with this framework, which would predict the structural response of timber-framed, plasterboard-clad barriers in real fires through discretely considering relevant phenomena.

1.3   Research Required to Develop the Structural Model

An examination of the literature revealed that many of the developments in the modelling of timber-framed assemblies in fire applied empirically derived methods for design purposes that were based on the reduction in cross-section (the char rate) when exposed to a standard heating regime; for example, White (1988). The use of such approaches for different heating regimes has not been extensively verified, although Hadvig (1981) has made some correlations. In addition, such approaches cannot be used to predict the performance of construction systems that are substantially different from the tested system for which the empirical relationship was derived.

Fundamental theoretical methods have been developed by Knudson *et al* (1975), Gammon (1987) and Thomas (1996) to predict the performance of timber-framed assemblies. The methods of Knudson *et al* (1975) and Gammon (1987) generally concentrated on development of the heat transfer analysis model. These authors utilised equations based on the ultimate stress for a beam in bending or an Euler expression for buckling for a column to model structural behaviour and predict the time-to-failure. These authors did not consider some of the key phenomena identified in the literature as being important in defining the structural performance of a timber-framed member under ambient conditions, as had been demonstrated by Polensek (1976), Thompson *et al* (1976) and Foschi (1982). For example, the authors did not consider the significance of the additional flexural stiffness provided through the composite action provided by the plasterboard sheeting.

Thomas (1997) utilised finite element analysis software packages to determine the time to failure of timber-framed walls in fires. The use of such an approach was not considered appropriate to incorporate within the framework of Clancy (1999) as it necessitated manual intervention during the analysis to change the mechanical properties of elements as the stresses changed from being in compression to tension. Other reasons for not utilising a finite element analysis software package were possible difficulties in linking the finite element software with the output from the heat transfer analysis from Clancy (1999) and difficulties in trapping potential numerical instabilities.

The literature review did not reveal studies of the contribution of the various phenomena associated with the structural response of load-bearing light timber-framed walls in fire. It was therefore necessary to examine the phenomena, which are associated with the structural response of timber-framed assemblies in ambient and elevated temperature conditions, and incorporate these within the model. The examination of relevant phenomena is considered in the literature review in Chapter 2.

The development of a model to determine the structural response of a timber-framed wall in fire requires that the effect of thermal degradation on the mechanical properties be correctly defined. A load-bearing timber-framed wall in fire is a slender column and the failure mode is likely to be associated with the buckling phenomenon (equation 1.1). For a constant applied load, the critical

parameter defining the time to failure of a timber-framed wall exposed to fire is the change in flexural stiffness with time. The flexural stiffness is dependent on the modulus of elasticity, and thus it is essential that the effect of temperature on the modulus of elasticity of timber in compression be considered.

The literature revealed a lack of test data on the degradation of the mechanical properties with temperature of timber in compression, in particular the modulus of elasticity. The reduction in these properties was inferred from tests conducted in bending or tension. Given that different constituents of timber provide the mechanical characteristics in compression and tension (Dinwoodie, 1989) and that these constituents degrade at different temperatures (Schaffer, 1973), it is reasonable to assume that the degradation in mechanical properties in compression and tension with temperature will be different. Thus the properties derived from tensile or bending tests could not be readily applied.

To have confidence in the predictions made by a model, the results predicted by the model should be compared with test results under carefully controlled conditions, including known boundary conditions. However, the literature revealed there was a lack of detailed full-scale load-bearing wall tests, which contained satisfactory detail or control, to be used to compare with predictions of a detailed structural model. Important test details such as having well defined support conditions, uniform heating conditions or measuring the flexural stiffness of the framing members from which the walls were built appear to have been ignored.

The structural model developed to predict the response of a timber-framed barrier should be capable of predicting the response of walls under ambient conditions, in addition to elevated temperature conditions. However, no details were revealed in the literature of models that were used to predict the structural response of timber-framed walls in fire, being used to predict the load-deflection response for a timber-framed walls under ambient conditions.

1.4   Aims of this Thesis

The general aim for this research was the development of a model, to predict the structural response of the timber-framed, gypsum plasterboard-clad barrier when subject to a wide range of given temperature-time conditions.

Within this general aim, the scope of the research was limited to the following specific aims:

(i)   To identify the dominant phenomena associated with the structural response of timber-framed, plasterboard-clad walls in fire.

(ii)   To model dominant phenomena identified in (i) to enable their significance to be determined, with regard to their effect on the time-to-failure of timber-framed, plasterboard-clad walls in fire.

(iii)   To develop a computationally efficient structural model; that is, it should determine the structural response of a timber-framed wall assembly in fire in a short period of time to allow many simulations, possibly thousands, to be conducted for a risk analysis.

(iv)   To develop an algorithm that is able to be readily integrated into the framework developed by Clancy (1999) that incorporates the heat transfer, fire severity and probabilistic models. That is, the algorithm developed should be robust for a wide range of variables to be generated over a wide range of values and be capable of many repeated runs without requiring manual intervention.

1.5   Methodology

The methodology that was adopted for this research to achieve the aims outlined in §1.4 is summarised as follows:

(i)   Literature was reviewed to evaluate the relevant dominance of phenomena and consider modelling procedures employed for timber-framed barriers in ambient and elevated temperature conditions.

(ii)   A fundamentally rigorous model, utilising commonly used frame analysis methods, was developed to determine the structural response of gypsum plasterboard-clad, timber-framed walls exposed to a wide range of temperature conditions.

(iii)   Any mechanical properties, which were determined to be fundamental to the model predictions, but lacking in detail in the literature, were determined through experimentation.

(iv)   The model was mathematically validated against closed-form and finite element solutions.

(v)   Predictions made by the model were compared with results from a series of carefully controlled, full-scale ambient and fire resistance experiments.

(vi)   Studies on sensitivity and the significance of phenomena were determined based on the results of comparisons with the full-scale tests.

(vii)   Areas of future research were identified.

1.6   Significance of the Research

The outcome of this research is a structural model that can be used for the design of light-timber-framed barriers subjected to real. The model incorporates advances over models developed previously such as the use of a common frame analysis method that provided a fast and robust model, the consideration of partial composite action between the plasterboard sheeting and timber framing, changed end restraint and loading conditions and the inclusion of phenomena that was identified as important for the performance of the wall.

The model that was developed has advantages over the use of conventional finite element analysis software in that it had automatic handling of stress-reversal without manual intervention required during execution, a faster solution time for the level of detail incorporated and greater robustness with regard to numerical convergence.

As part of the research, measurements were obtained from experiments under well-controlled conditions that do not appear to have been undertaken previously. These controlled conditions included:

• Full-scale ambient experiments on frames and walls, selected from the same batches of timber and constructed at the same time as the full-scale furnace experiments.

• Clearly defined end support conditions at the top and bottom supports.

- Clearly known degrees of composite action between the plasterboard sheeting and timber framing to the structural behaviour in a fire resistance test.

- Clearly known uniform heating conditions of the load bearing timber studs.

The structural behaviour of a load-bearing, timber-framed wall in fire is primarily dependent on the buckling capacity, which is directly related to the modulus of elasticity in compression with temperature (equation 1.1). The reduction of this property and the ultimate strength in compression with temperature was determined for the first time through direct measurement of heated samples in compression.

For the first time, model predictions were compared with both full-scale ambient and wall furnace experiments in which the walls were constructed from the same selected batch of timber. The structural model satisfactorily predicted both the ambient response and the elevated temperature response of timber-framed, plasterboard-clad prototype wall panels.

The model has successfully been incorporated into the Clancy (1999) framework to predict the time-dependent probability of failure of timber-framed, plasterboard-clad wall panels in real fires.

In addition, the model can be used to undertake designs based on prescriptive regulations since it can predict the likely performance of barriers, which may be substantially different from a tested prototype when subjected to a standard fire resistance test. Such differences may be tall partitions (>3m), different stud sizes, load levels etc. Thus the model can be a useful tool, within the context of a design, with untested forms of fire resistant construction, and therefore providing a greater field of application than empirically derived models.

2. Literature Review

2.1 Introduction

The objective of this research project was to develop a phenomenologically based model to determine the structural response of timber-framed walls in fire. A constraint for the model development was that it had to be capable of being readily incorporated into a framework developed by Clancy (1999) to determine the time-dependent probability of failure of timber walls in real fires.

The following literature review considers the current state of knowledge with regard to modelling timber-framed assemblies for fire resistance. It considers the fundamental issues, which determine the response of the components of a wall in fire and then examines the global issues of overall structural behaviour. In particular, the review examines the phenomena that are associated with the structural response of a timber-framed wall in a fire. The response due to exposure to elevated temperatures of the microstructure and chemical constituents of timber and plasterboard is considered, with the corresponding change in mechanical properties. Structural models developed to determine the structural response of timber-framed assemblies in ambient conditions and elevated temperatures are examined to determine their suitability for use in achieving the aims of this project. Structural models for the elevated temperature structural modelling of reinforced concrete and steel have been considered, with regard to the applicability of techniques developed for these materials being used for the structural analysis of a timber-framed wall in fire.

2.2 Phenomena Affecting the Structural Response of Timber Framing in a Fire

2.2.1 Typical Temperature Distributions in Timber Elements

The temperature distribution through the timber studs is determined by the rate of the transfer of heat through the timber element. A generic diagram detailing the conditions through the cross-

section of a timber element exposed to fire is shown in Figure 2.1. As heat is transferred into timber, moisture is removed, pyrolysis occurs and char forms. The term pyrolysis is used to describe the process of timber being degraded thermally into char and volatiles (Johnsson *et al*, 1985).

Surface protected from exposure to fire

Cool wood – no chemical degradation

"Pyrolisis Zone" – wood degrading to char and gas

Char

Ablation – char converted to gas
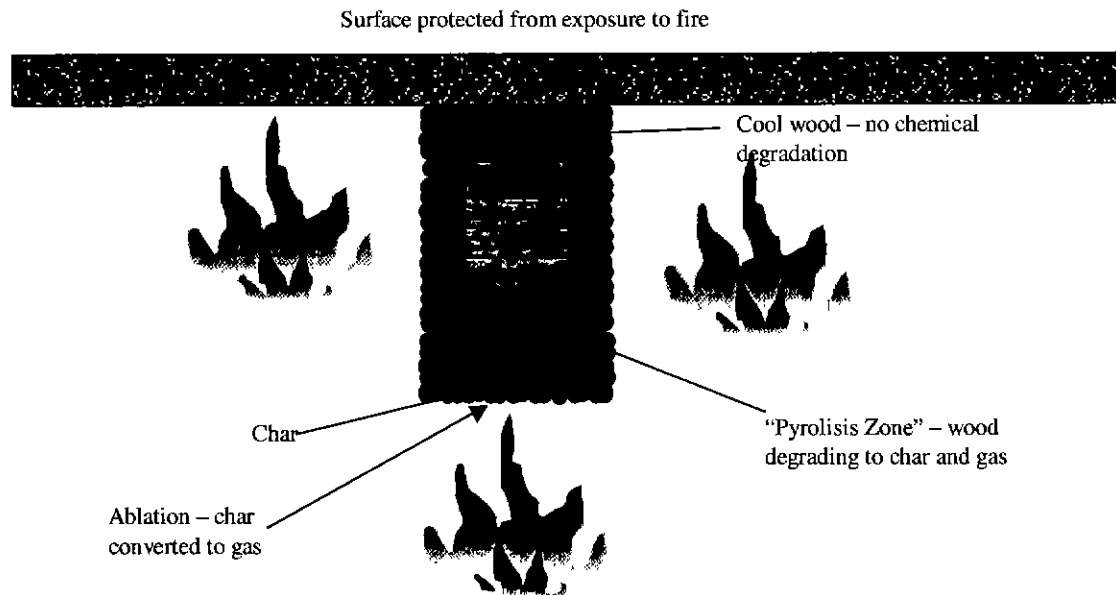
Figure 2.1: *Degradation of the Cross-Section of Timber Elements due to Fire on Three Sides*

Hadvig (1981) determined that for a timber element of minimum cross-section dimension greater than 80mm, the rate of charring beneath all surfaces could be considered as uniform. However, for timber elements with a minimum cross-section dimension less than 80mm, the reduction in cross-section due to charring was faster and could not be assumed to be uniform. This was apparent in measurements made by White *et al* (1981), Collier (1991) and König (1991), where temperatures were measured within timber elements and it was shown that temperature varied in two-dimensions through the cross-section. The approximate temperature of char formation was 288°C (Shaffer, 1973). White *et al* (1981) demonstrated that there was a significant variation in the moisture content through the cross-section of timber elements in fire resistance tests. However, consideration of the movement of moisture lies outside the scope of this project, which requires the structural response to be determined based on a temperature distribution calculated through the cross-section.

2.2.2 Response of the Timber Microstructure when Exposed to Elevated Temperatures

2.2.2.1 Constituents of the Microstructure

Softwoods, which are most commonly used in fire-resistant drywall construction in Australia, consist primarily of five constituents, which are listed in Table 2.1.

Table 2.1: Constituents of Softwood Timber (After Dinwoodie, 1989)

Constituent	Percentage by Mass
Cellulose I	40-45
Hemicellulose – galactoglucomannans	15-20
Hemicellulose – arabinoglucuronoxylan	10
Lignin	26-34
Extractives	0-5

The structure of wood on a macroscopic level has been described by Dinwoodie (1989) as being a fibre reinforced composite, consisting of microfibrils with crystalline cellulose forming the fibres and a combination of non-crystalline cellulose, hemicellulose and lignin forming the matrix. The structure of a microfibril is shown in Figure 2.2. The microfibrils are not continuous throughout a piece of wood, having amorphous regions, which exhibit little characteristic strength.
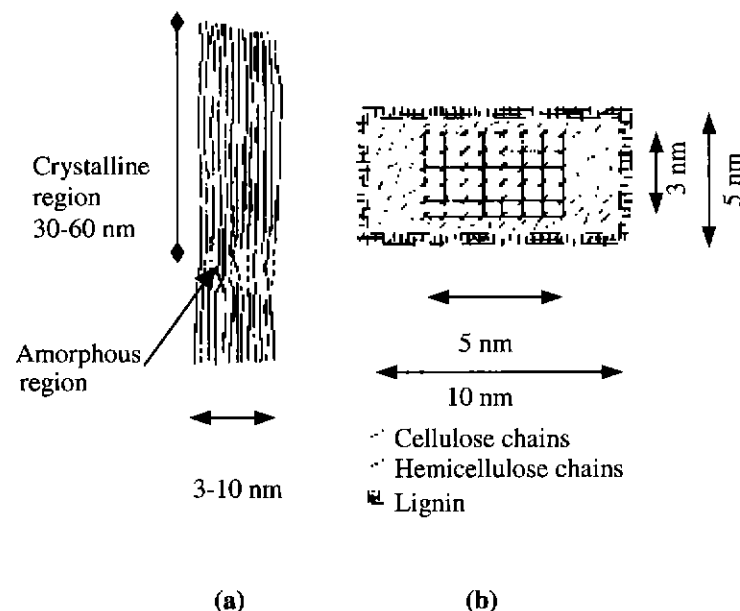
Figure 2.2: Composition of a microfibril: (a) crystalline core in longitudinal section. (b) Transverse section of core and surrounding matrix. (from Dinwoodie, 1989)

In summary from Dinwoodie (1989), the tensile mechanical properties are governed by the

crystalline cellulose core of the microfibril, which is impermeable to moisture. Thus the tensile

mechanical properties are considered to be dependent on the cellulose. The mechanical behaviour

in compression is related to the lignin. It is indicated in Dinwoodie (1989) that the 'compression

wood', present in areas of softwood trees in which are subjected to compression, has a higher

concentration of lignin, and a correspondingly lower proportion of cellulose.

2.2.2.2   Response of Microstructure to Elevated Temperatures

Increasing temperature causes chemical changes within timber. The changes in the chemical

properties of the constituents of timber result in a change in the mechanical performance. The

chemical changes occurring within timber due to increased temperature are summarised in Table

2.2.

Table 2.2: Effect of Temperature on Timber Constituents (after Schaffer, 1973)

Temperature		Effect
50		
	55	Natural lignin structure is altered. Hemicellulose begins to soften.
	70	Transverse shrinkage of wood begins.
100		
	110	Lignin slowly begins weight loss
	120	Hemicellulose content begins to degrease. α-cellulose begins to increase. Lignins begin to soften.
	140	Bound water is freed.
150		
	160	Lignin is melted and begins to re-harden.
	180	Hemicelluloses begin rapid weight loss after losing 4%. Lignin in torus flows.
200		
		Wood begins to lose weight rapidly. Phenolic resin begins to form. Cellulose dehydrates above this temperature.
	210	Lignin hardens, resembles coke. Cellulose softens and depolymerizes. Endothermic reactions change to exothermic.
	225	Cellulose crystallinity decreases and recovers.
250		
	280	Lignin reaches 10% weight loss. Cellulose begins to lose weight.
288		Assumed wood charring temperature.

Given different constituents of the wood govern the tension and compression mechanical

characteristics, depending on the temperature at which these constituents degrade, the percentage

change in mechanical properties in tension and compression due to exposure to elevated temperatures are likely to differ at the same temperature.

2.2.3 Change in Mechanical Properties of Timber Due to Exposure to Elevated Temperatures

2.2.3.1 Introduction

This section reviews the effect of temperature on the mechanical properties in tension and compression. The reductions will be considered and evaluated in light of the known behaviour of the constituents. Reviews of the reduction in mechanical properties of timber due to exposure to elevated temperatures have been presented in papers published by Gerhards (1982), Schaffer (1984), Östman (1985) and Gammon (1987). Additional consideration will be made of phenomena that are associated with the mechanical behaviour of timber in ambient conditions subjected to the combined actions of compression and bending as identified in Buchanan (1986).

The following changes in mechanical properties due to the effects of elevated temperatures have been considered in this review:

- Tensile strength

- Compression Strength

- Modulus of Elasticity in Compression and Tension

- Flexural Properties

- Size Effects

- Thermal Expansion/Shrinkage

- Stress-Strain Characteristics

- Creep

2.2.3.2   Degradation of Tensile Strength Versus Temperature for Timber, Parallel to
the Grain
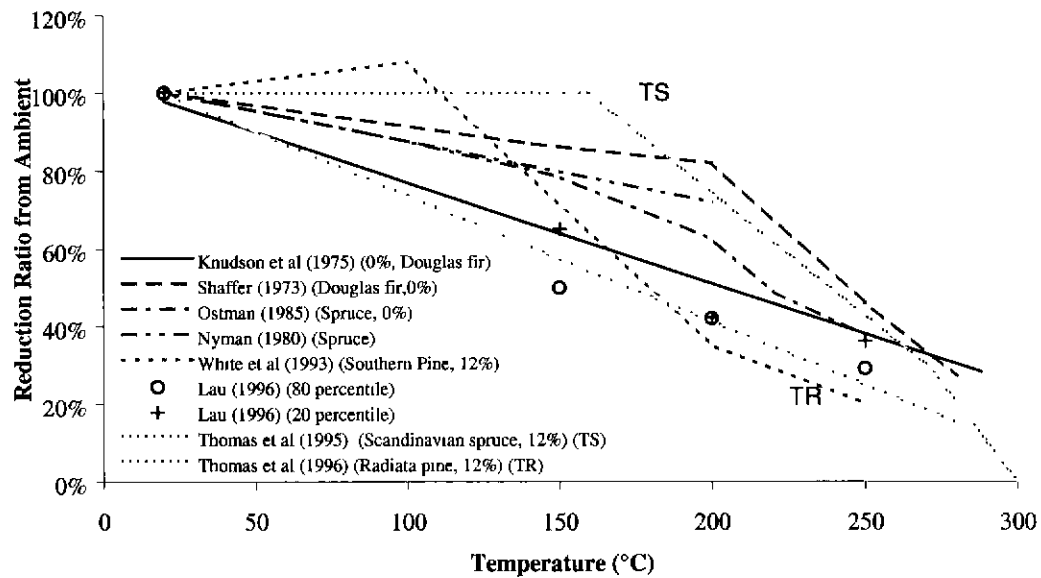
Figure 2.3: Effect of Temperature on Tensile Strength

The effect of temperature on the tensile strength for timber is shown in Figure 2.3. The results of

Nyman (1980) have been obtained from the review presented by Östman (1985). The results of

Schaffer (1973) and Östman (1985) give a similar trend in behaviour, indicating the feasibility of

using a bi-linear function to represent the reduction in property. There is a slight reduction in the

tensile strength as the temperature approaches approximately 200°C. Above this temperature, there

is a much more rapid reduction to a complete loss of tensile strength as char is formed as

temperatures approach 300°C (Schaffer, 1973). The increased rate of tensile strength degradation

above 200°C can be explained because the cellulose begins to degrade above this temperature

(refer to Table 2.2), which has been demonstrated to be associated with the mechanisms of

providing tensile strength for timber (Dinwoodie, 1989).

The results presented from White *et al* (1993) indicate an increase in the tensile strength as the

specimen temperature approaches 100°C, possibly being related to the drying out of the specimen.

2-6

Lau (1996) tested structural sized specimens and did not heat them to a uniform temperature, but used a regression technique to derive the mechanical properties. The temperatures indicated were described as a "temperature of exposure", the actual temperature within the timber element varied, being invariably less than the exposure temperature.

Thomas *et al* (1996) did not conduct tests, but based the derivations on fitting a model with experimental results of König (1991) and Collier (1991). This involved modelling the structural response of a beam in bending and assuming a reduction in the modulus of elasticity and compression properties at the same time.

It is interesting to note that the reduction in tensile strength with temperature obtained from structural size specimens such as experiments by Lau (1996) and derived by Thomas *et al* (1996), gave a linear relationship. This possibly indicates that macroscopic characteristics are more dominant in determining the strength of structural size specimens.

The tensile strength is not considered to play a significant role in determining the structural response of a timber-framed wall in fire, due to the failure mode being most likely associated with buckling in compression and thus the modulus of elasticity in compression. Hence any approximation in the magnitude of the reduction in the mechanical property with temperature is not considered to significantly affect the results predicted by the model. The reduction in tensile strength versus temperature considered most appropriate for use within the model will be based on the linear reduction as presented by Thomas *et al* (1996). This is because the results obtained from the extensive study conducted by Lau (1996) and the calibrations performed by Thomas *et al* (1996) were for structural grade specimens and that the data points tend to coincide in Figure 2.3.

2.2.3.3 Degradation of Compression Strength Versus Temperature for Timber, Parallel to the Grain
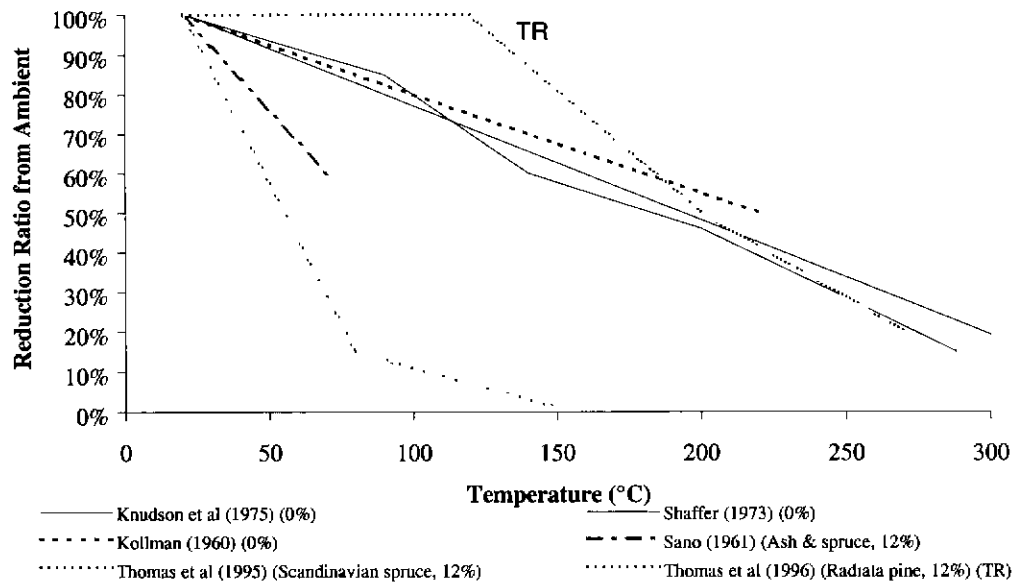
Figure 2.4: Effect of Temperature on Compression Strength

Reductions in compression strength with temperature effects from the literature are shown in Figure 2.4. Results presented for Kollman (1960) and Sano (1961) were obtained from expressions for the reduction presented in a review by Gammon (1987). The results of Knudson *et al* (1975), Schaffer (1973) and Kollman (1960) for 0% moisture content samples are in quite close agreement, giving an approximately linear reduction in compression strength versus temperature.

There is evidence that the reduction in compression strength is significantly greater for specimens with approximately 12% moisture content than those with 0% moisture content. The results for Sano (1961) for timber with approximately 12% moisture content indicated a sharp reduction in compression strength at 70°C. The results presented by Thomas *et al* (1995) and (1996) were derived by comparison with bending and wall tests conducted by other authors and are very different. However, those derived for tests involving Scandanavian Spruce also indicated a sharp decrease in strength with increasing temperature, similar to the results of Sano (1961). Konig (1991) demonstrated from a series of tests of loaded beams heated by a furnace, that the loss in flexural stiffness when the side in compression was exposed to fire was considerably larger than if the tensile side was exposed to fire. This indicates that the effect of exposure to elevated

temperatures affects the mechanical properties in compression at a lower temperature than in tension. This is consistent with the degradation of Lignin commencing at approximately 110°C (Table 2.2)

Given that Konig (1991) has demonstrated that compression dominates over tension in the reduction in mechanical performance in flexure and that the model is to consider the structural response of a wall, which is axially loaded in compression, the conflict between results presented by Thomas *et al* (1995 & 1996) and the limited data available in the literature, further experiments are required to determine the reduction in compression strength for timber at elevated temperatures.

2.2.3.4   Degradation of Modulus of Elasticity versus Temperature for Timber, Parallel to the Grain

Knudson et al (1975) (Douglas fir, 0%)
Gerhards (1982) (~12%, various)
Suzuki et al (1982) (White fir, 0%)
White et al (1993) (Southern Pine, 12%)
Thomas et al (1996) (Radiata Pine, 12%, Compression)

Shaffer (1973) (Douglas fir, 0%)
Ostman (1985) (Spruce, 0%)
Sano (1961) (Ash & spruce, 12%)
Thomas et al (1996) (Radiata Pine, 12%, Tension)
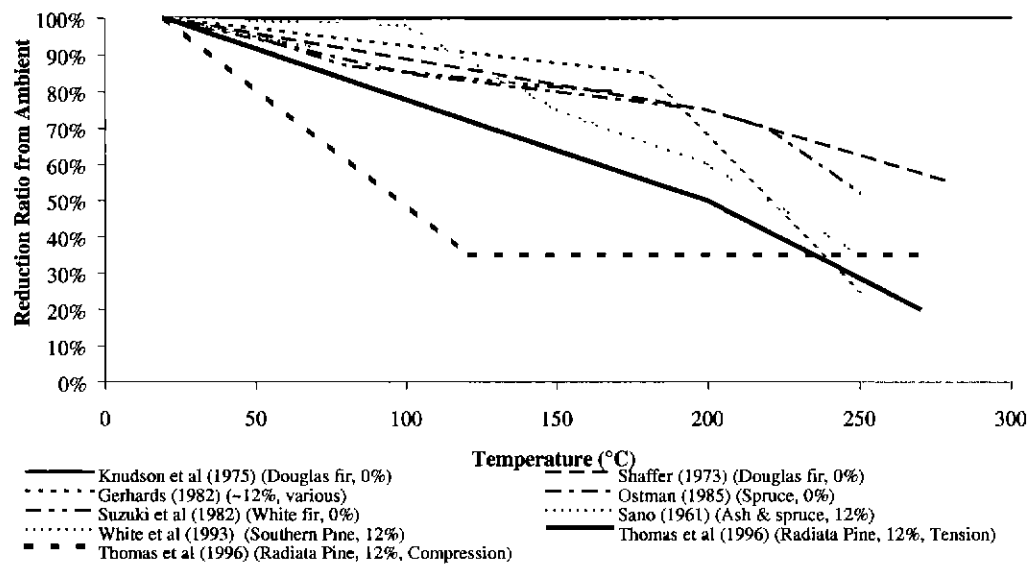
Figure 2.5: Effect of Temperature on Modulus of Elasticity

The modulus of elasticity is considered the most important mechanical property associated with this research, as the dominant mode of failure of an axially loaded column (ie. timber stud) with a high slenderness ratio would be expected to be due to buckling as opposed to crushing.

Results from the literature, which detail the effect of elevated temperature on the modulus of elasticity, are presented in Figure 2.5. These results have generally been derived from tests performed in bending or tension. There was little data for the reduction in the modulus of elasticity in compression at elevated temperatures that has been obtained directly from compression tests.

Malhotra *et al* (1980) stated that for ambient conditions, the modulus of elasticity in tension and compression can be generally considered to be the same. However, given that different constituents (refer to §2.2.2.1) of the timber contribute to the tension and compression properties, and these constituents degrade at different temperatures (refer to §2.2.2.2), it seems more likely that the reduction in modulus of elasticity due to elevated temperatures is different in tension and compression. This has been indicated by Thomas *et al* (1996), whose values were derived from calibration with results from tests performed by Collier (1991).

The results presented by Knudson *et al* (1975) conflict with those reported by other authors in that they found that there was a negligible change in the modulus of elasticity versus temperature. The method employed by Knudson *et al* (1975) involved the use of dynamic means to determine the modulus of elasticity. However, due to a lack of data in calibrating this method, may have been responsible for the discrepancy with results of other authors. It should be noted that the results from White *et al* (1993) did show considerable scatter, especially through the temperature range 150°C - 250°C. It was also observed in the results of White *et al* (1993) that the specimens heated for a longer period of time (60 minutes) had higher strength and stiffness than those heated for a 30 minute interval. An explanation for this result may be that a greater surface temperature is required to heat the sample in a shorter period of time causing excessive degradation in the region of the surface compared with the sample heated over a longer interval. However, the scatter in results due to the variation in timber mechanical properties may account for this result.

It has been established that there is an apparent lack of experimental data in the literature for the reduction in the modulus of elasticity of timber obtained directly from tests in compression and that the flexural stiffness is dominant in determining the structural response of a loaded wall frame. It is therefore imperative that the degradation of the modulus of elasticity in compression

due to exposure to elevated temperatures is clearly established through a series of experiments. Due to the difference in the reduction of the modulus of elasticity with temperature in compression and tension, the experiments will require the mechanical properties of timber to be derived directly from specimens subjected to elevated temperature and tested in pure compression.

2.2.3.5 Effect of Duration of Exposure on Mechanical Properties of Timber

The effect of duration of exposure is relevant to the method of determining the mechanical properties of timber at elevated temperatures. The time for a timber specimen to be heated in a standard fire resistance test will generally be considerably faster than a controlled experiment in which the reduction in mechanical properties are to be determined – a standard fire resistance test will subject the timber to higher temperatures and steeper thermal gradients. In applying a temperature substantially greater than the desired test temperature to the surface of the test specimen to heat it more quickly may result in irreversible degradation in the surface layers.

MacLean (1953, 1954 and 1955) performed a study examining the duration of exposure of several species of timber to elevated temperature through oven drying, heating in steam and water, this being associated with the preservation of wood. Although the specimens were tested under ambient conditions, it was demonstrated that an increased time of exposure (from 30 minutes to 8 hours) at temperatures of 300°F ($\approx$ 150°C) and 350°F ($\approx$ 175°C) substantially reduced the bending strength and modulus of elasticity of the timber specimens. For example, there was an additional reduction of 20% in the modulus of elasticity of a specimen heated at 175°C for a period of 8 hours compared with 30 minutes.

Troughton *et al* (1974) performed tests to determine the effect of heating medium and duration on the tensile properties of thin sections of Douglas Fir and White Spruce. Using sections only 100 microns thick, the specimens were exposed to temperatures of 200°C for oven, hot press and oil bath environments, and a temperature of 183°C in superheated steam. The authors found that the reduction in ultimate tensile strength was least in the case of heating in the oil bath, which

indicated that oxidation reactions were already occurring in the timber specimens heated in the oven and hot press at these temperatures.

Knudson *et al* (1975) examined the relationship between compression and tensile strength and time of exposure at 260°C for a period of between 5 minutes - 60 minutes. It was reported that the compression strength was not substantially affected and the tensile strength showed a slight reduction (approximately 5%) with increased exposure time. It should be noted that these conclusions were derived from only four test specimens tested in compression and tension.

Schaffer (1982) examined the creep of dry Douglas Fir and in the process found that there was a reduction in the modulus of elasticity for an increased time of exposure for temperatures in the range (140°C - 275°C) for the period of exposure of 800 seconds to 7200 seconds. However, due to the scatter of the results the reduction could not be readily quantified.

Except for the findings of Knudson *et al* (1975), it is apparent that the degradation of timber is dependent on the duration of exposure at elevated temperature. Hence mechanical property tests for timber specimens would be expected to determine greater reductions in the mechanical properties compared with a specimen in a fire resistance test, which will be heated more quickly. Thus predictions made by a structural model using mechanical properties derived directly from tests will tend to predict an earlier time-to-failure, and thus be conservative if used for design purposes.

2.2.3.6   Thermal Expansion and Shrinkage of Timber

Little data are available in the literature that defines the coefficient of thermal expansion or shrinkage of timber at temperatures of the range experienced during fire conditions. More frequently the results reported in the literature associated with the shrinkage of green timber due to the reduction in moisture content over time are more concerned in considering the long-term effects in construction for example, bowing in beams and gaps in walls.

Thermal expansion in directions perpendicular and radial to the grain were stated in the Forest

Products Handbook (1987) to be 5 to 10 times greater than that parallel to the grain. The thermal

expansion of wood during heating tends to be counteracted by shrinkage induced by a change in

moisture content and thermal degradation.

Values presented in the Forest Products Handbook (1987) for thermal expansion of oven dry

timber in the direction parallel to the grain were stated to be between $3.1*10^{-6}$ /°C and $4.5*10^{-6}$

/°C. This range of values is consistent with the results of Schaffer (1982), who measured the

coefficient of thermal expansion across the temperature range of 20°C to 275°C for dry specimens

of Douglas Fir expansion as being normally distributed about $3.52*10^{-6}$ /°C across the temperature

range.

König (1994) investigated the effect of thermal expansion and shrinkage with regard to overall

element behaviour and reported that in furnace tests on one side of timber beams that the curvature

was not substantially influenced by thermal gradient. He demonstrated that load-bearing

deflections were considerably greater than the effect of thermal expansion/shrinkage.

From the literature it is apparent that thermally induced shrinkage and expansion of timber induce

no significant net strain. Thus these phenomena are not considered to significantly affect the

structural response and require no further investigation.

2.2.3.7 Creep of Timber

It is well established in structural timber design codes such as AS1720.1 (1988) that creep effects

can result in a significant increase in the deflection of timber structures over an extended period

after the initial application of the load. For example, deflections can treble during long term

loading (≥1 year) for members in bending in compression for a maximum initial moisture content

of greater than 25%. The design codes also identify that the magnitude of creep is dependent on

the moisture content. However, there are little data in the literature considering the short-term

creep behaviour of timber under fire conditions.

Schaffer (1977) proposed a model to represent the creep behaviour of timber and presented a study on the influence of heat on the longitudinal creep of dry Douglas fir. Schaffer (1982) fitted an equation based on a non-linear viscoelastic-plastic model to experimental results. The model is the simplified equation (2.1) which gives creep strain, ε_{creep}, in terms of the time of exposure, t, stress, σ, and temperature, T.

$$\varepsilon_{creep} = \sigma t^{0.25} 0.27 * 10^{-4} e^{0.042T} \qquad - (2.1)$$

The simplified model derived did not consider the effect of the moisture content. The model shows that creep strain increases with temperature. Schaffer (1984) summarised that creep rate was magnified from that at ambient by ten fold at 125°C and by fifty fold at 250°C.

The results from Schaffer (1984), in conjunction with the requirements of design codes in considering the effects of creep over a period of one year must be put into the context of the period of exposure that a timber-framed element way be subjected for in a fire. That is, the fire resistance for a load-bearing, timber-framed, plasterboard-clad wall may be generally of a maximum duration of 120 minutes (eg. Boral Plasterboard, 1994). The changing conditions and stress levels, which are appropriate for creep to occur, may only exist for a fraction of this time. Hence when this period is compared with multiplication factors from design codes such as AS1720.1 and the multiplier of creep rate from Schaffer (1984), the time period of significance does not indicate a substantial magnitude of creep. That is a fifty fold increase in the creep rate from one year is equivalent to a period of seven days. Hence from Schaffer's (1984) assertion, creep at 250°C is not significant.

Due to the lack of data available in the literature associated with the creep of moist timber at elevated temperatures, the significance is uncertain. For dry timber, it has been demonstrated that creep strains induced in timber will not be significant for a relatively short period of exposure during a real fire or fire resistance test. Consequently, further consideration of the creep phenomenon for moist specimens should be considered to determine its significance.

2.2.3.8   Degradation in Mechanical Properties of Timber related to Moisture Content

White *et al* (1981) established that during the exposure of timber to a fire resistance test, there was

a significant increase (approximately double) of the moisture content within parts of the specimen.

It is well known that changing the moisture content can alter the mechanical properties of timber.

Gerhards (1982) demonstrated that there was a reduction in the ultimate strength in compression

and tension and the modulus of elasticity with increasing moisture content.

The results from Gerhards (1982) that are summarised in Table 2.3 and Madsen (1992) showed

that the strength in compression was more highly sensitive than the strength in tension to a change

in moisture content in the range (10%-25%). The results are consistent with the knowledge that the

tensile strength of timber is governed by the crystalline cellulose core of the microfibril

(Dinwoodie, 1989), which is impermeable to moisture.

The modulus of elasticity was described as being somewhat sensitive to moisture content by

Madsen (1992) and Gerhards (1982). The method of determining the modulus of elasticity in the

results summarised by Gerhards were based on timber specimens tested in tension and flexure.

Results were not presented that were derived directly from compression tests.

Table 2.3: Effect of Moisture Content on the Mechanical Properties of Timber (from Gerhards

(1982))

Mechanical Property	Reduction in Mechanical Property as Moisture Content Changes from 12% to 25%
Ultimate Strength in Compression (Parallel to the grain)	50%
Ultimate Strength in Tension (Parallel to the grain)	75%
Modulus of Elasticity (Parallel to the grain)	85%
Ultimate Strength in Bending	65%

There was insufficient information that could be gleaned from the literature to define the reduction in mechanical properties associated with both elevated temperature and moisture content. The model of Clancy (1999) does not consider moisture transfer, hence the effects cannot be implemented within the structural model at this stage. However, it is apparent that the moisture content of timber can affect the mechanical properties and the significance of moisture content on the mechanical properties of timber in full-scale fire resistance tests should be examined in the experimental programs outlined in this thesis.

2.2.4   Stress-Strain Behaviour of Timber

Timber does not exhibit the same behaviour in compression and tension up to failure. Zakic (1973) presented an approximation for the stress-strain relationship of timber assuming elastic behaviour in tension and a parabola in compression, with the peak stress occurring at the peak strain (Refer to Figure 2.6).

Malhotra *et al* (1980) presented a literature review of stress-strain models, which were used to predict the bending strength of timber beams. These authors criticised the approach of Zakic as incorrect by assuming that the peak compressive stress occurred at the most extreme fibre in compression in a beam at failure. Malhotra *et al* (1980) proposed a bilinear function to describe the stress-strain behaviour of timber in compression (Refer to Figure 2.6). In addition, they claimed that the elastic modulus in compression and tension could be reasonably assumed the same, based on experimental results that showed the difference was in the order of only a few percent.

Buchanan (1986) developed a model to predict the strength of timber subjected to combined actions of bending and compression. He also reviewed several stress-strain relationships for the behaviour of timber in compression and selected the curve represented by the expression

$$f = E\varepsilon - A\varepsilon^n \qquad \qquad -(2.2)$$

where   f = stress

ε = strain in compression

E = elastic modulus of elasticity

A, n are constants which are derived on the basis of peak stress occurring at 1.35 times the equivalent elastic strain

In tension, the stress-strain relationship by the authors previously mentioned in this section was stated to be linear elastic until the ultimate failure strain was achieved through brittle failure. In compression, timber exhibits non-linear behaviour as the ultimate stress is approached. The expression presented by Buchanan (1986) is considered the most appropriate as he compared model predictions using the expression against many test results. Buchanan (1986) incorporated a linear descending branch from the peak compression strain, the gradient of which was determined empirically. Examination of the interaction diagrams prepared by Buchanan (1986) indicated that the gradient of this descending branch was most important in predicting the capacity of members with combined actions with a high proportion of stresses induced through bending.
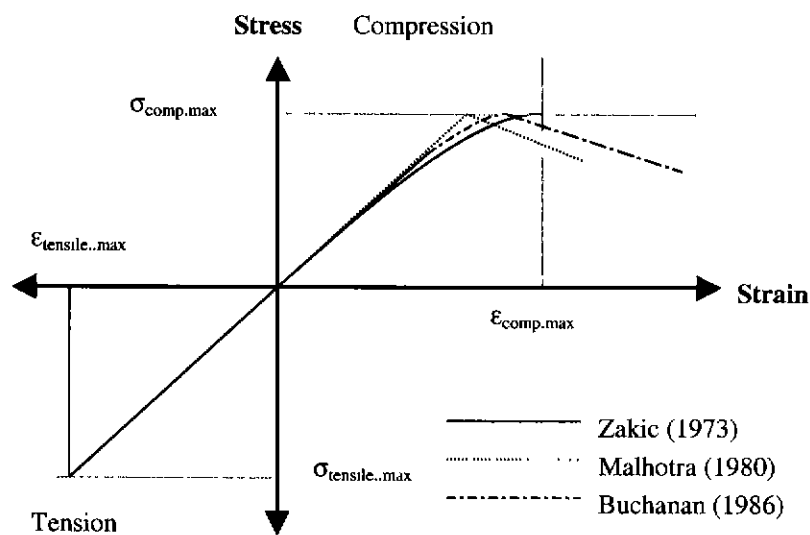
Figure 2.6: Stress-Strain Relationships for Timber

It must also be noted that both Malhotra *et al* (1980) and Buchanan (1986) included terms considering the statistical nature of predicting the strength of timber, referred to as size and length effects. However, there are insufficient data in the literature detailing the reduction in mechanical properties at elevated temperatures to appropriately define these statistical parameters.

Consequently, the phenomenon of size effects is therefore considered outside the scope of this thesis.

2.3 Phenomena Affecting the Structural Response of Plasterboard Sheeting in a Fire

2.3.1 Typical Temperature Distributions

The typical temperature distribution within a plasterboard sheet, when exposed to a fire resistance test as have been provided in the Gypsum Association Fire Resistance Design Manual (1997) are listed in Table 2.4 and qualitatively shown in Figure 2.7. The results presented are for a 6 inch (150mm) thick plasterboard barrier after two hours exposure to the heating conditions specified in ASTM E119.

Table 2.4: Temperatures through the Cross-Section of a 6 inch (150mm) Thick Plasterboard Barrier after Two Hours Exposure to the Standard Heating Regime Specified in ASTM E119.

Distance from Exposed Face	Approximate Temperature
Exposed surface	1040°C
25mm	510°C
50 mm	104°C
100 mm	82°C
Unexposed face (150mm)	54°C

Fire side of plane of calcination – insulation barrier, but exhibits shrinkage and cracking.

Plane of Calcination, temperatures generally less than 100°C

Indicative temperature profile through cross-section
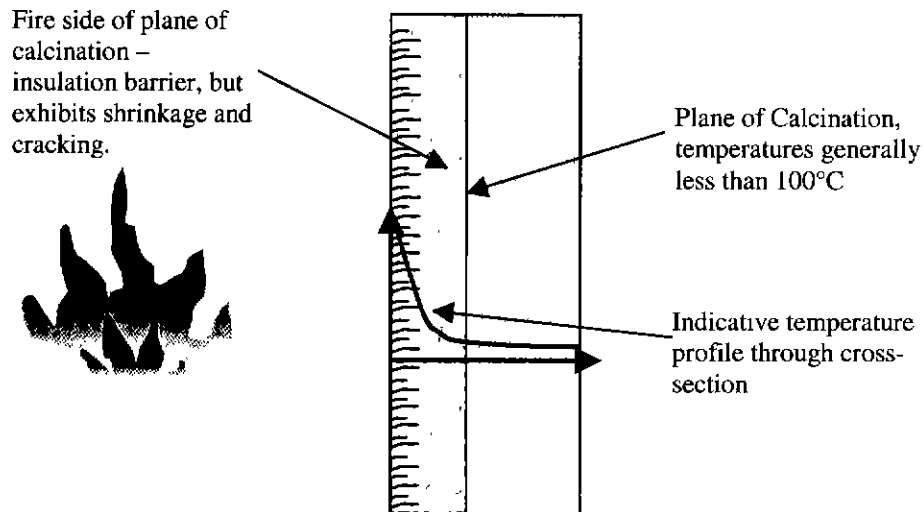
Figure 2.7: *Qualitative Description of the Response of Plasterboard to a Fire Resistance Test*

Plasterboard sheeting provides an insulative barrier to prevent the spread of fire between compartments. The gypsum material has characteristics that are favourable to preventing the spread of fire. Fire resistant plasterboard sheets have additional additives to enhance the ability to provide a barrier resistant to the spread of fire.

2.3.2 Constituents of the Microstructure

Plasterboard consists primarily of gypsum. In addition, fire resistant boards have several additives, including glass fibres, vermiculite and fly ash (Boral Plasterboard, 1977). The primary chemical constituents of the Boral fire resistant plasterboard are shown in Table 2.5. Non-fire-rated plasterboard generally does not have the additives to improve performance in fire (glass fibres and vermiculite) and is substantially less dense.

Table 2.5: Constituents of Fire Resistant Plasterboard by Mass

Constituents	% by Mass (n.b. round-off means does not add to 100%)
Gypsum	80
Impurities	8
Fly Ash	6
Vermiculite	4
Glass fibres	0.34
Paper	

The constituents listed in Table 2.5 contribute the following characteristics to the plasterboard:

- The paper on the outside of the board improves the tensile strength and provides a protective cover for the gypsum.

- Glass fibres increase the tensile strength and hold the board together as the matrix of gypsum degrades with heating.

- Vermiculite is incorporated to enhance the properties of the material by counteracting the shrinkage of the gypsum at high temperatures .

- Fly ash is added to improve the workability of the plaster during manufacture.

2.3.3   Physical Changes in the Constituents of Plasterboard with Temperature

Gypsum has approximately 21% water content by weight. The degradation of the plasterboard is associated with the removal of bound water from the gypsum. The gypsum (calcium sulfate dihydrate) is converted to calcium sulfate hemi-hydrate, which commences at 42°C (Mould *et al*, 1974). However, the reaction rate was described by Mould *et al* (1974) as being dependent on the temperature, the rate being appreciable at 100°C. The mass loss versus temperature for fire resistant plasterboard (Mehaffey, 1991) is shown in Figure 2.8. The bulk of the mass loss occurred in the range 100°C-160°C. It should be noted that Mehaffey *et al* (1994) considered the rate of heating between ranges which he stated were comparable for the heating of the bulk of a gypsum plasterboard sheets for a fire resistance test ie. 2°C/ min and 20°C/min. A second reaction where the calcium sulfate hemi-hydrate converts to calcium sulfate, identified by Mould *et al* (1974) to occur at 400°C was not clearly obvious.
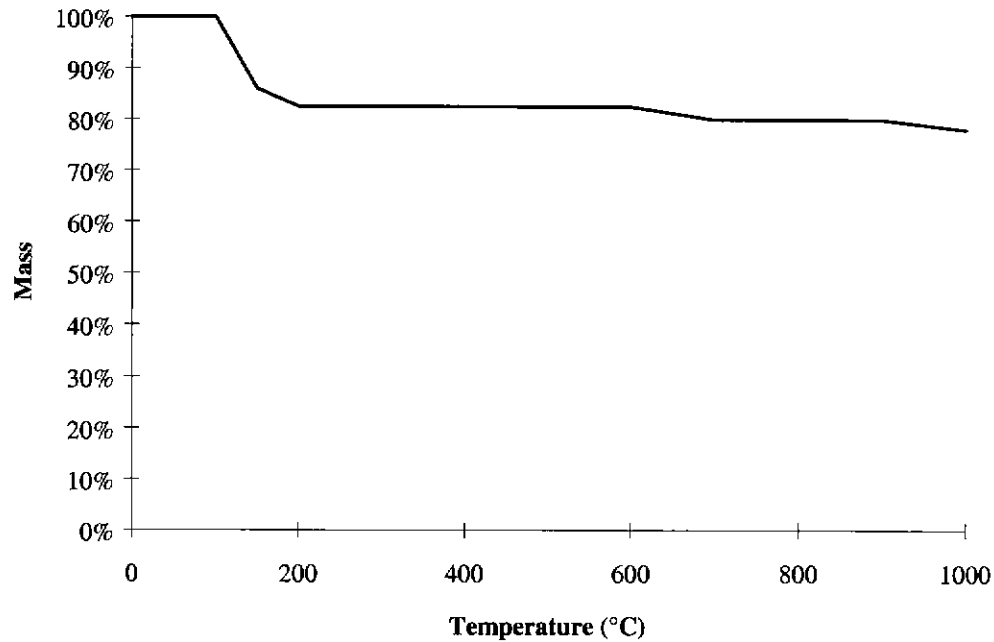
Figure 2.8: Change in Mass of Fire Rated Gypsum Plasterboard versus Temperature (after

Mehaffey, 1991)

The paper on the outside face of the sheeting is assumed to degrade at the same temperatures as

timber, hence, at temperatures of approximately 300°C, it is assumed to have charred.

Plasterboard from different manufacturers have a noticeably different response to elevated

temperatures. This is evidenced by the cracking pattern observed on the furnace exposed face of

test specimens in a comparative test conducted by Warrington Fire Research (1997) (refer to

Figure 2.9).

The plasterboard exhibits extensive shrinkage as the moisture is removed from the gypsum

(Mehaffey, 1991, Walker *et al*, 1995), the glass fibres provide tensile strength and help to hold the

sheet in place. Figure 2.10 demonstrates the contribution of glass fibres in reinforcing a fire

resistant plasterboard sheet exposed to fire. The viscosity of the glass fibres reduces rapidly at a

temperature of approximately 700°C-745°C (Carne, 1995).

2-21
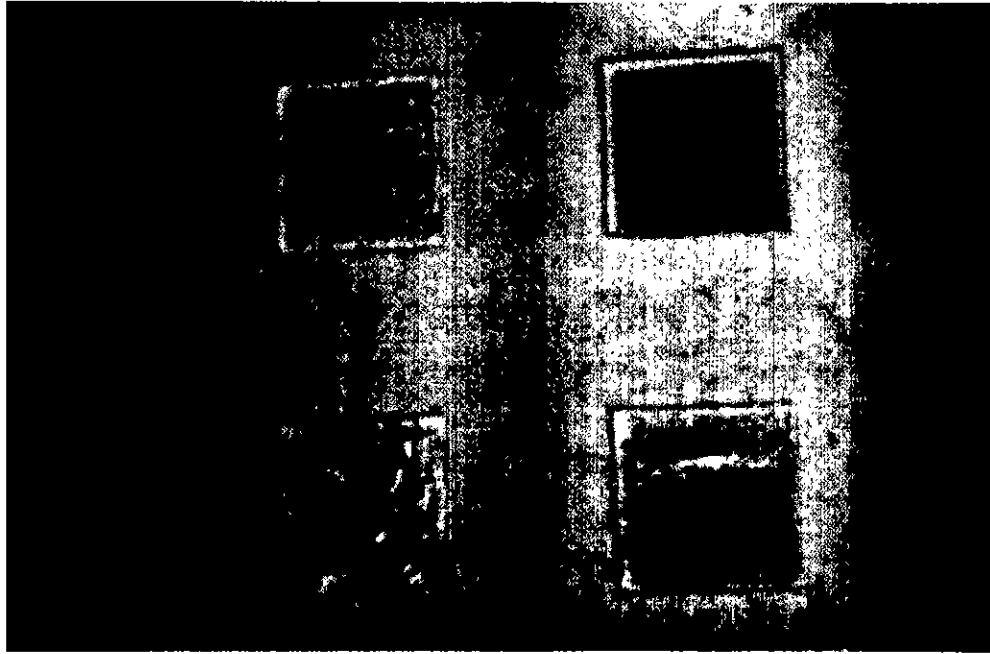
Figure 2.9: *Exposed Face of a Pilot Test Comparing Different Australian Plasterboard Manufacturer Fire Rated Sheets and a Calcium Silicate Board.(After Three Hours exposure to the Heating Regime Specified in AS1530.4-1997)*
Note the different cracking pattern of the plasterboard samples.
(Courtesy Warrington Fire Research Aust, 1997)

Large tears in exposed face
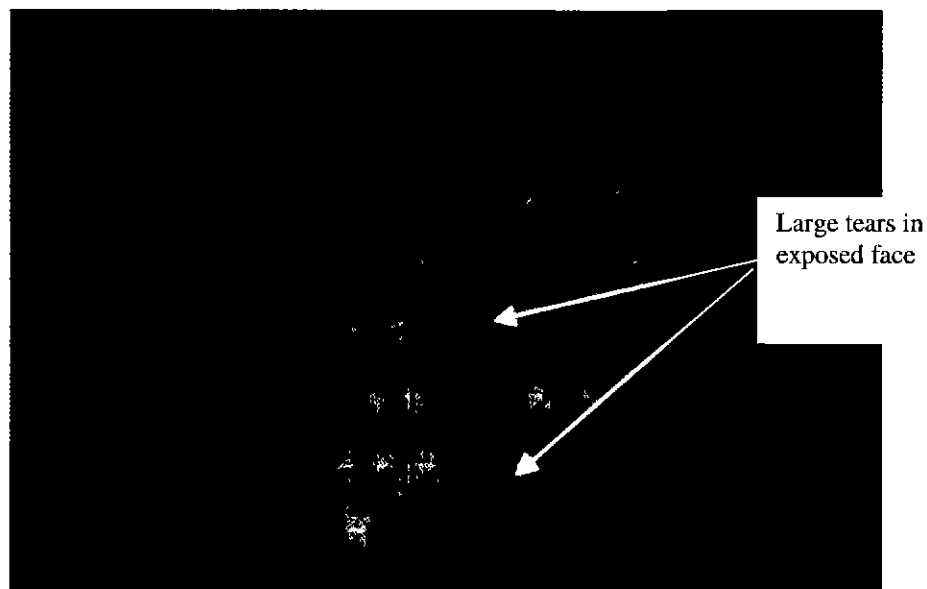
Figure 2.10: *Plasterboard on the Exposed Face during a Fire Resistance Test of a Steel Framed, Plasterboard-clad Wall. Note the cracks opening up to allow the passage of hot gases into the cavity.*
(Courtesy Warrington Fire Research Aust, 1998)

2.3.4 Degradation of Tensile Strength Versus Temperature for Gypsum Plasterboard

The use of plasterboard for fire protection has tended to consider the material as a barrier against hot gas movement rather than contributing to a load-bearing element. However, in ambient conditions, it could contribute significantly to the structural response of a wall (Polensek, 1976). Examination of the literature did not glean readily available data on the reduction in the mechanical properties of gypsum plasterboard with temperature. All data presented in the literature considered the contribution of plasterboard in tension, which is consistent with the observed behaviour of timber-framed, plasterboard-clad walls in fire resistance tests, which bow outward at the centre from the furnace (Collier, 1991).

The data that details the reduction in mechanical properties of plasterboard versus temperature (refer to Figure 2.11) have been based on work performed at Victoria University of Technology performed during the period of study for this doctoral thesis. Walker *et al* (1995) performed tests to determine the reduction in mechanical properties of fire rated gypsum plasterboard from several Australian manufacturers (Boral 'Firestop', CSR Gyprock 'Fyrchek' and Pioneer "Fireshield'). Goncalves *et al* (1996) repeated the work of Walker *et al* (1995), increasing the size of the data set. Data in the region of less than 300°C were not obtained by the authors of either report because of difficulties in maintaining stable temperatures in a gas-fired furnace within that range.

Both Walker *et al* (1995) and Goncalves *et al* (1996) have linearly interpolated results between a sparse number of data points over large temperature ranges. Defining the reduction in strength as the proportion of total mass loss, based on the results presented by Mehaffey (1991) (refer to Figure 2.8), may indicate that a substantial proportion of the strength is lost during the conversion from gypsum to calcium hemi-hydrate. The plateau of remaining strength (approximately 10-15%) at temperatures above this value is most likely due to the contribution of the glass fibres within the board.

It is therefore considered doubtful that significant structural resistance is provided after calcination has been completed. Hence the interpreted reduction presented in Figure 2.11 was adopted. This

reduction was assumed to be related to the calcination process of gypsum, decreasing linearly from

100% of the ambient value at 100°C to 0% of the ambient value at 150°C.
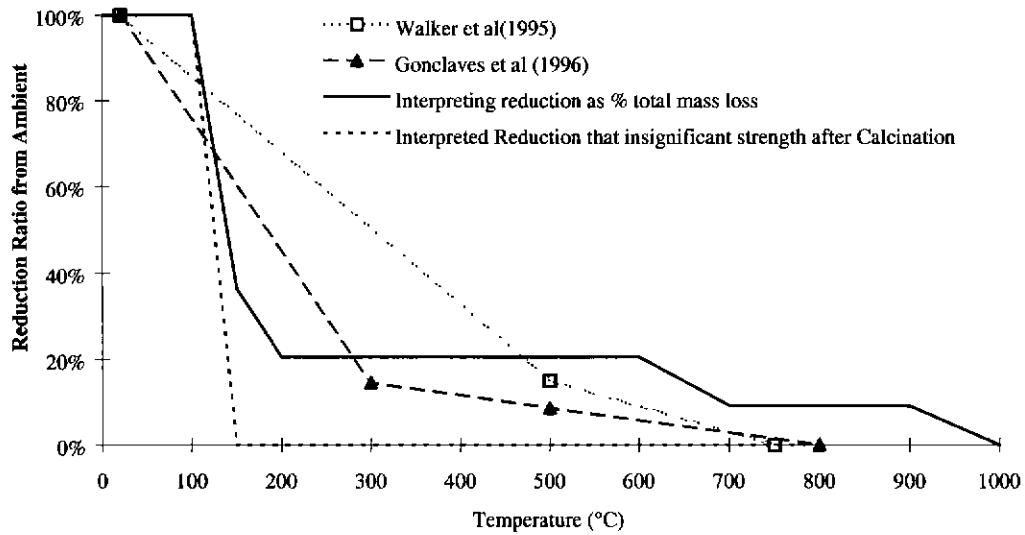
Figure 2.11: Change in Tensile Strength of Fire Rated Gypsum Plasterboard versus Temperature

(Without Paper)

2.3.5 Degradation of Modulus of Elasticity versus Temperature for Gypsum Plasterboard

As with the reduction in tensile strength of plasterboard at elevated temperatures, little data were

available in the literature detailing the change in modulus of elasticity associated with exposure to

elevated temperatures. The data that exists were those obtained by Walker *et al* (1995) and

Goncalves *et al* (1996) who also examined the reduction in tensile strength as a component of the

same studies performed at Victoria University of Technology during the period of this doctoral

thesis.
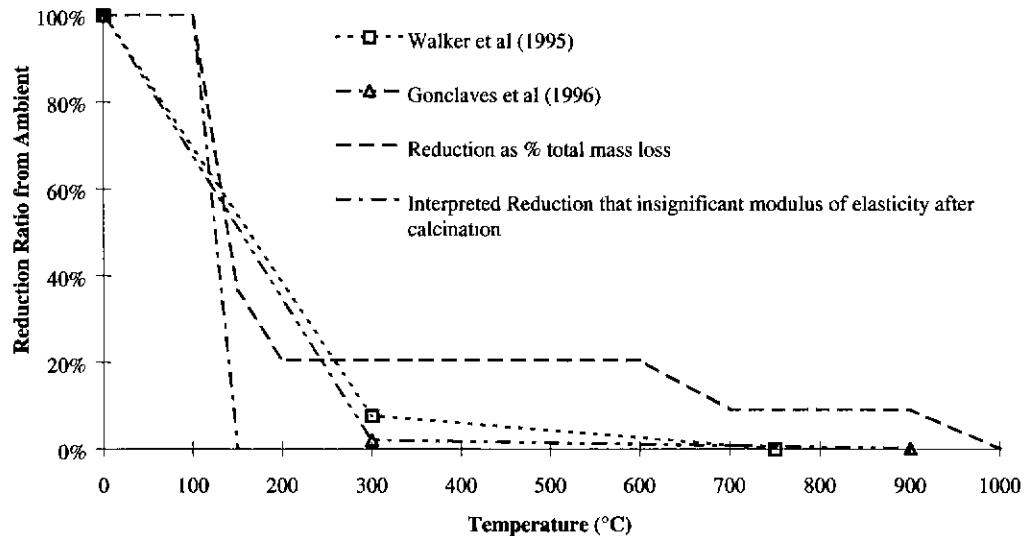
Figure 2.12: *Change in Modulus of Elasticity of Fire Rated Plasterboard versus Temperature*

(Without Paper)

The data presented by Walker *et al* (1995) and Goncalves *et al* (1996) (Refer to Figure 2.12) indicates that the modulus of elasticity reduces to a very small proportion (approximately 3%) of the ambient value at 300°C. The authors, due to the difficulty of maintaining stable furnace temperatures, could not reliably obtain the data in the region below 300°C. As with the strength properties, the reduction in the modulus of elasticity is calculated based on the reduction in total mass and is plotted in Figure 2.12. However, the comparison with test results indicated a far greater reduction than predicted directly by the proportion of total mass loss. Based on the results presented, it is apparent that the modulus of elasticity may be related to the proportion of gypsum, with a very minor contribution to the modulus of elasticity provided by the glass fibres. Hence the reduction in modulus of elasticity of the sheeting was assumed as related to the calcination process of gypsum, decreasing linearly from 100% of the ambient value at 100°C to 0% of the ambient value at 150°C. This interpreted relationship shown in Figure 2.12 will be adopted for use in the model.

2.3.6 Thermal Expansion / Shrinkage of Gypsum Plasterboard

The thermal expansion of plasterboard is a property dependent on the manufacturer of the board (refer to Figure 2.9) and the type of board used. For example, boards designed specifically for fire

rated barrier construction have additives such as vermiculite to reduce the shrinkage and glass

fibres to retain strength of the material after calcination. The results of studies to determine the

shrinkage of plasterboard versus temperature have been performed by Mehaffey (1991) and

Walker *et al* (1995) and are presented in Figure 2.13.
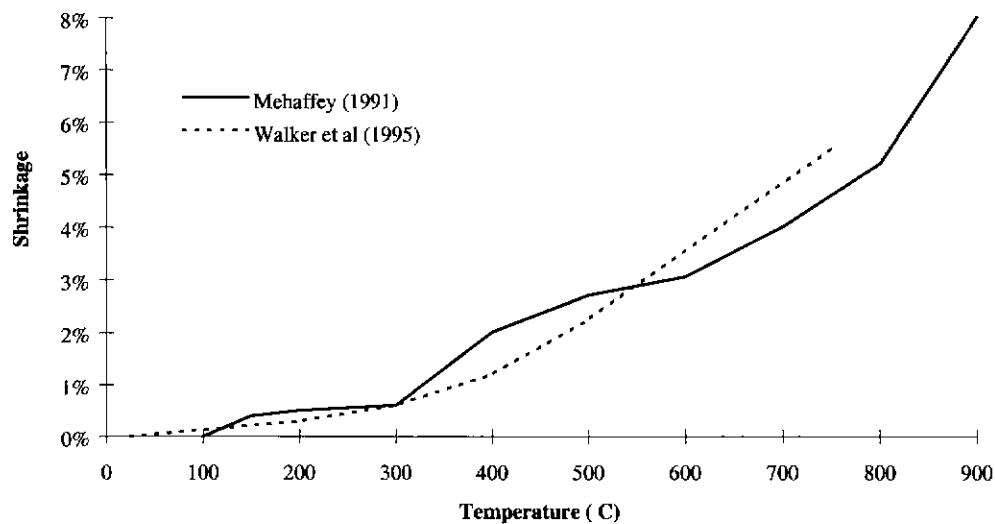
Figure 2.13*: Shrinkage of Fire Rated Plasterboard versus Temperature*

The results of Mehaffey (1991) indicate that a small amount of thermal expansion occurred at

temperatures under 100°C, before significant calcination had commenced. In terms of structural

modelling, this is important as the mechanical properties at lower temperatures are less degraded

and therefore the thermal expansion will have a greater overall impact on structural response. This

is explained in that the stress induced by restraining an element from free thermal expansion or

shrinkage is directly proportional to the modulus of elasticity, if the modulus of elasticity is very

low, the stresses will be very low. Hence at temperatures where the modulus of elasticity is very

low (ie. at temperatures of 150°C and above), the effect of shrinkage will not significantly impact

on the structural behaviour of a wall.

2.3.7   Creep of Gypsum Plasterboard

No quantitative data were found in the literature for the creep of gypsum plasterboard due to

elevated temperatures. A brief examination was performed by Goncalves *et al* (1996), however the

experiment was relatively crudely performed and a comparative assessment between the ability of

Australian manufacturer's boards to sustain load at elevated temperature was the only outcome

from the experiment. The contribution of creep to the overall structural response of a timber-

framed wall in fire is not considered to be important due to the small temperature range in which

the material contributes structurally to the wall.

2.4   Known Structural Behaviour of Timber-framed Walls Exposed to Fire

Collier (1991) has probably presented the most detailed reports for fire resistance tests of load-

bearing plasterboard-clad timber-framed walls. It should be noted that plasterboard manufacturers,

e.g. Boral (1994) have undertaken fire resistance tests for fire resistant construction systems to

provide evidence to building regulators, however, the results of such tests are confidential and

generally do not give detailed observations of phenomena.

From the observations and by interpretation of the raw data given in Collier (1991), the diagram in

Figure 2.14 details the derived response of a timber wall in a standard fire resistance test. Light

timber-framed walls exposed to fire resistance tests tend to deflect outward from the furnace and

the sheet of plasterboard on the exposed face loses strength rapidly. The timber element degrades

in strength and the neutral axis of the timber framing member moves toward the unexposed face.

Load Applied
via Top Plate

Stud

Soft

Fastener Creating
Partial Composite
Action

Stiff — Fastener

Movement
of Centre of
Axial Stiffness
Towards Stiff
Wood

Gypsum
Board

Plasterboard on
fire exposed side
cracks and
degrades and is
not structurally
effective

Fire Side

Stiff   Ambient Side

A

A

Ambient
Side

Tension
in Plasterboard
on Ambient Side

Original
Position
of Stud

when deflections become
large

Reaction at
Bottom Plate

Vertical Section Through

Typical Timber Framed Wall

Section AA

Figure 2.14: Schematic Diagram Detailing the Response of a Timber-framed Wall Exposed to

Fire

The behaviours presented in Figure 2.14 are generally well established in the literature. Despite the

quantity of data measured from fire resistance tests e.g. Collier, 1991, boundary conditions for

structural response have not been adequately controlled for validation of models: namely the end

restraint of the walls and the uniform heating of load-bearing members. For example, examination

of the deflection data of Collier (1991) reveals that the studs located nearest each side of the wall

had less deflection than the three studs located in the central area of the wall. This indicates that

these outer studs were possibly exposed to less severe heating conditions than the inner studs.

Similarly, the restraint at the ends of the wall was not clearly defined, the results predicted by a

structural model assuming rotation at the ends is allowed compared with one which has rotation

prevented can be very different. The significance of end restraint is demonstrated by considering

the Euler buckling equation (1.1) for a column. The effective length of a member with rotation prevented at the ends is half that of a member where the ends can freely rotate. Hence, the theoretical capacity of a member where the ends cannot rotate is four times that of a member, where no rotational restraint is provided.

To validate the structural model with confidence, a series of carefully controlled full-scale experiments for load-bearing timber-framed, plasterboard-clad walls are required. Such a series of carefully controlled tests are not available in the literature. The methods employed by Collier (1991) with regard to temperature measurement are considered sound and a similar approach should be adopted. The end conditions must be specifically defined, allowing free rotation or preventing rotation. All load-bearing timber framing elements should be subjected to the same heating conditions. The timber elements should be carefully selected to reduce the likelihood of variability between specimens.

2.5 Models

2.5.1 Introduction

The literature review in this section will consider the developments in models to determine the structural response of timber and timber-framed barriers exposed to fire. In addition, there will be a brief consideration of techniques employed to model the structural behaviour of other construction materials in fire to determine if the methods can be readily applied to achieving the aims defined in this thesis.

2.5.2 Timber

2.5.2.1 Introduction

The methods employed to determine the response of timber element exposed to fire generally follows two distinct streams. The first major stream is based on a char rate or reduced section

technique. The second is based on performing a discrete analysis of the material through the cross-section of the element.

2.5.2.2   Reduced Section Techniques – Char Rate

The bulk of the literature associated with the use of reduced section techniques was concerned with heavy structural timber elements including laminated timber beams and columns. The reduced section techniques do not require analysis of the heat transfer through the cross section of the timber, but assume a uniform rate of reduction in the cross section, called the "char rate". White (1988) in his review of reduced section type models referred to these as "empirical α models". The reduced section is then used in an analysis involving the application of elementary structural analysis formulae for bending or compression in ambient timber design codes. Because of the simplicity in application, the char-rate method is thus well established in design codes (e.g. AS1720.4, Eurocode 5). Authors have introduced further "factors" to account for the rounding of edges (for example König, 1991, 1995), reduced restraint near failure (for example König, 1988) and the reduction in mechanical properties (for example Woeste *et al*, 1981). The char-rates are empirically derived, generally from tests for specimens exposed to the heating regime specified in standard fire resistance tests (e.g. AS1530.4, ISO 834). Reduced section techniques cannot therefore be used to determine the response of load-bearing timber elements in any other heating regime, nor can they be used to predict the time-to-failure of configurations significantly different from tested prototypes, from which calibrations of char rates were performed.

Collier (1991) presented a different approach for a reduced section model for designing load-bearing light timber-framed walls for fire resistance called the "charfactor" approach. The model utilises a modified secant approach based on an Euler formula with an extra term was included to incorporate the effect of furnace pressure. Collier (1991) assumed that three sides of the stud were exposed to fire. The "charfactor" was defined by relating the results from fire resistance tests to a change in cross section dimensions, which gave the same structural response. The method was empirically derived, and required fire resistance tests to be undertaken to calibrate the model for a particular wall configuration (refer to Collins *et al*, 1993 for such results).

In summary, the empirically derived models developed have generally allowed solutions for the fire resistance of unprotected timber elements to be readily calculated for design purposes. However, the primary concern in the application of such methods for general use in determining the fire resistance of timber-framed assemblies, is that the models do not consider the contribution of individual phenomena to the overall behaviour of the wall. The "char rates", "char factors" and other coefficients are defined for a specific field of application which means any configuration that differs from tested prototypes used to derive the coefficients for the empirical models may preclude the use of such models or require further calibration through testing. The most important consideration is that these empirical approaches are based on a 'standard' heating regime defined by a time-temperature curve such as that in ASTM E119, AS1530.4, ISO 834 and BS 476 Part 20, and for any other heating regime the results are not applicable.

The aims of the thesis are to develop a structural model, which is phenomenologically based to determine the structural response of a timber-framed, plasterboard-clad wall for a variety of fire severities, load levels and structural configurations. Thus, for the purposes of achieving the aims of this study, the use of a reduced section technique is not considered appropriate as the discrete effects of phenomena are ignored.

2.5.2.3   Discrete Modelling Techniques

The second stream of models uses discrete modelling techniques to allow for the contribution of individual phenomena to be considered.

The advantage in using discrete modelling approaches instead of empirically derived relations is that the discrete modelling overcomes the limited scope of reduced section techniques with regard to different fire severities and configurations from tested prototypes. Researchers have generally solved the heat transfer diffusion equation through either finite element or finite difference schemes. Composite section, or occasionally finite element, techniques have then been utilised to perform the structural analysis of timber members. The composite section technique is a

conventional analytical technique generally used for structural elements, which are composed of materials with dissimilar mechanical properties, in particular with different modulii of elasticity. The technique of composite section analysis is contained within general reference texts for structural analysis eg. Popov (1978). A key assumption in utilising composite section theory is that the strain distribution through the cross-section is assumed to be linear, that is, plane sections remain plane.

Knudson *et al* (1975) developed a combined thermal and structural model to determine the performance of timber members exposed to fire. The temperature distribution through the cross section was determined by solving the generalised heat diffusion equation by a finite element technique. The temperatures calculated were used as input data for the structural analysis. Composite section theory was applied to determine the flexural stiffness properties. Deflections were calculated using standard formulae for beams. Failure of beams was determined by the calculated capacity of the beam being exceeded by the applied moment. Failure of a column exposed to fire was calculated by determining of the radius of gyration and considering the slenderness ratio for the remaining section, elementary formulae for either crushing or Euler buckling were applied. Result comparisons with large cross section beams and columns were described by the authors as giving "surprisingly good predictions". However, the mechanical properties derived by the authors were not consistent with other property values that have been published (refer to Section 2.2.3). In addition, their model was not developed for composite action involving sheeting.

Do *et al* (1983a, 1983b) developed a model to predict the time of failure of wooden beams during fire. The method was based on determining if the maximum fibre stress in bending was exceeded using elementary beam strength formulae. The expressions assumed to represent the reduction in strength and modulus of elasticity were based on the proportion of total mass loss. The model was calibrated with experimental results for light timber sections (19.05 mm x 19.05 mm) exposed to a burner and then compared to structural grade specimens in a burn room test for floor joists. Given the model was calibrated assuming a constant surface fire temperature, results from standard fire resistance tests could not be used for validation. The approach to determine the reduction in

strength and flexural stiffness was dependent on a model which was based on the mass loss from the thermal analysis, not temperature, which meant the reductions in mechanical properties derived by of other authors (refer to Section 2.2) could not be readily utilised. This methodology was also incompatible with the model of Clancy (1999) which did not analyse mass loss. The model did not consider the contribution of sheeting to the structural response of a light timber-framed member or changed support conditions.

Gammon (1987) began a model to perform the reliability analysis of wood-frame wall assemblies exposed to fire, but only went as far as developing a time-to-failure model. A finite element approach was used to solve the heat transfer equation. The model to determine the structural response was based on a composite section analysis with mechanical properties within a mesh being determined from the calculated temperature distribution through the cross-section. The section properties determined from the composite section theory were utilised in the Euler equation for linear elastic buckling. The compression strength was also calculated. If the load carried by the stud exceeded the crushing or buckling load, then a failure was deemed to have occurred. The structural model developed was similar to that of Knudson *et al* (1975) and did not consider the interaction of sheeting or end support conditions.

Thomas (1997) used a combination of software packages to determine the fire resistance of timber-framed walls. TASEF-2 by Wickstom (1979) was used to perform the heat transfer analysis and the results were applied to define the mechanical properties through the cross section. The finite element analysis software ABAQUS was used to perform the structural analysis. The use of such an approach was not considered feasible for the technical requirements of this study; particularly as Thomas (1997) had to manually redefine tensile and compression elements within the model. Such an approach would prove cumbersome in both linking to the heat transfer model of Clancy (1999) and utilising the model to perform probabilistic simulations, where manual intervention was not suited, as many repeated runs of the model would be required (potentially thousands).

It has been demonstrated from considering the discrete modelling techniques that of the models which are 'stand alone', almost all used elementary structural analysis equations for bending of buckling combined with a composite section analysis are based on the reduction in mechanical properties through the cross-section with temperature. The concentration of most effort appears to have been in solving the problem of heat transfer. None of models considered the phenomena of composite action contributed by the sheeting, changed restraint conditions including partial restraint, non-linear mechanical properties (except for Thomas, 1997) or non-linear geometric effects.

2.5.3   Other Materials

Development of fire resistance models for other materials are more advanced in the areas of concrete and steel construction. The direct application of these techniques was considered.

The phenomena that occur amongst all typically used engineering materials due the effects of a fire are in many cases similar e.g. thermal expansion/shrinkage, creep and changing mechanical properties with temperature. The analysis techniques for non-linear geometric and mechanical properties should also be similar - the only difference is the values of the mechanical properties. There are, however, differences in the phenomena that dominates in the response of each type of construction to fire, which are related to the mechanical nature of the material. A lightweight timber-framed assembly has the additional consideration of the partial composite action through the cladding.

Models considering the analysis of steel construction in fire are either very simplistic when used for design purposes, being based on a limiting temperature approach such as used in design codes such as AS 4100 (1998), or are highly numerically advanced and generally incorporate plastic and creep behaviour. The mechanical properties of steel in elevated temperatures appear to be much more precisely defined than for timber. The homogeneity of steel means models to predict the behaviour in fire can readily utilise advanced analytical techniques involving non-linear finite element analysis. Finite element packages such as ABAQUS and ANSYS are most suited to

performing analysis of steel elements in fire. The use of such advanced techniques for timber members which contain growth characteristics, highly variable temperature distributions and reductions in mechanical properties that are not well defined, are not considered appropriate at this stage in the research. Similarly, the use of a limiting temperature approach is unsuitable as timber is a very good insulator, unlike steel, and cannot be assumed as being a uniform temperature throughout.

Analysis of reinforced concrete in ambient conditions can be said to have similarities to the mechanical behaviour of timber. The behaviour in compression is non-linear. The modulus of elasticity in compression and tension are different. The key phenomena, which are critical for elevated temperature behaviour are the coefficient of expansion of the material, and the reduction in mechanical properties. Extensive theoretical and experimental studies have been performed at Lund Institute of Technology in Sweden (Anderberg, 1976). The structural modelling for concrete structures was performed by modification of a program called "FIRES-RC". This program uses a non-linear direct stiffness approach and incorporates the stress-strain behaviour of concrete and steel elements. The approach used is based on a time-step iterative approach. The analysis assumed that secondary forces and moments are negligible and could not predict stability failure. The source code was not readily available to modify for timber, and did not incorporate any composite interaction with sheeting, however, the approach is considered suitable for use for timber elements.

An iterative model to determine the behaviour of precast reinforced concrete panels in fire was developed by O'Meagher *et al* (1991). The technique used by O'Meagher *et al* (1991) was based on an algorithm presented by Purkiss *et al* (1987) in development of the computer program to analyse reinforced concrete columns in fire (SAFE-RCC). The algorithm involved the following steps:

(i)   Determination of the initial shape at ambient conditions.

(ii)   Guessing a value for a moment and curvature for each segment that the column is subdivided, and each is adjusted until the column satisfies the conditions of equilibrium, compatibility and end restraint.

The analysis incorporated creep and transient strains. The models for concrete composite construction developed by O'Meagher *et al* (1991) were further refined to incorporate changed restraint by Buchanan *et al* (1991) and substantially redeveloped by Poh *et al* (1994) to consider biaxial behaviour. The source code for the code of O'Meagher (1991) was not readily available. The use of this approach for plasterboard-clad, timber-framed elements did not provide the ability to readily vary the boundary conditions or consider the effect of partial composite action between the timber framing and sheeting.

Models for other materials were not readily available to be implemented nor do they model all the actions and phenomena required. Hence it is necessary to develop a new modelling technique, which will utilise some similarities in approach to that of Anderberg (1976).

2.5.4   Ambient Structural Models for Timber-Framed Walls and Floors

2.5.4.1   Introduction

Generally in the structural design of timber-framed walls and floors, the contribution of sheeting to a timber-framed member to the load-bearing capacity of the member is ignored. Similarly for the models predicting the structural response in fire, the contribution of the sheeting has been ignored. Whilst ignoring the contribution of the sheeting in design may be considered acceptable as it provides an increase in the factor of safety, it will under-predict the actual capacity of an assembly. Several authors have performed studies examining the structural response of timber-framed elements in ambient conditions which incorporate the contribution of the sheeting to more accurately determine the capacity.

2.5.4.2   State of Knowledge

Armana *et al* (1967a,1967b) derived solutions for configurations of three types of plywood stressed-skin components with ribs. The solutions are derived by using orthotropic plate theory to represent the behaviour of the skin and a beam element to represent the rib. Interlayer slip was incorporated in deriving the expression for strain distribution through the cross-section. Fourier

series solutions were used to solve the differential equations derived for the stress functions defined for the assembly. The use of such solutions was not considered appropriate for this model as the derivation of differential equations for specific boundary conditions would not allow a model which could be readily varied with regard to end conditions and applied loading.

A model was developed to predict the response of a floor in the 1970s at the Forest Products Laboratory/Colorado State University, which incorporated the contribution of the sheeting. The program FEAFLO (Finite Element Analysis of FLOors) Thompson *et al* (1975,1976) was the result. Energy formulations were used to represent the components of the floor, which were solved by finite element techniques. The components comprising the floor were idealised as beams - plate elements were not used to represent the sheeting. Gaps in the connection between sections of sheeting were represented by short, low-stiffness elements. Research on several aspects of floor behaviour including the phenomenon of load-sharing between framing members were performed using the FEAFLO model, Criswell (1983) contains a summary of several aspects of these. The FEAFLO software is in the public domain, a listing of the source code was provided in Thompson *et al* (1976). However, although the model does consider the composite action between the sheeting and joist, it does not consider the effects of large deformations due to axial forces as required for a column or composite section theory for the components due to thermal effects. The issue of load-sharing (an important aspect of FEAFLO) at this stage is considered outside the scope of this thesis. However in the future, when the redistribution of load within a wall in fire conditions is required to be considered, or if the effect of non-uniform heating on a wall is considered, load-sharing would be required to be incorporated.

Foschi (1982) developed a finite element model to model floors. The enhancement over the FEAFLO model was the incorporation of the torsional contribution of the sheeting and the use of plate elements to represent the sheeting to consider the effective width of the sheeting acting between the joists. Due to the limited state of knowledge of the mechanical properties of timber, it was considered that such a refinement at this stage is not warranted.

Polensek (1976) developed a model to perform the finite element analysis of wood-stud walls. The wall was represented as a series of I-beam elements connected together with plate elements located at the middle plane to accommodate the phenomenon of load sharing between studs. The model incorporated non-linear geometry and some limited non-linear mechanical property phenomena. Polensek formulated the stiffness matrix of the I-beam elements using the solutions presented by Armana et al (1967a). The model compared axial deformations independently of transverse deformations in considering the non-linear analysis. Non-linearities were accounted for by using a step-by-step linear analysis technique. The model was combined further with probabilistic simulation techniques to determine a simplified analysis technique (Gromala *et al*, 1981). Polensek (1976) demonstrated the requirement to consider the non-linear geometric behaviour of a wall in predicting the load-deflection response.

McCutcheon (1977) presented a simpler formulation to represent the partial composite behaviour of a floor. The effective stiffness calculated was based on the consideration of the full composite section behaviour of a T-beam using a transformed area technique, and reducing the flexural stiffness with a factor to account for incomplete composite action due to the connection. The deflected shape, Δ, of a loaded floor was calculated using the following equation:

$$\Delta = \Delta_R \left[1 + f_\Delta \left(\frac{EI_R}{EI_U} - 1 \right) \right]$$

- (2.3)

where Δ_R = deflection calculated for rigid (full) composite action

EI_R = flexural stiffness if components are rigidly connected

EI_U = flexural stiffness is components are not connected

f_Δ = reduction factor to account for partial composite action

For three load cases applicable to floors (uniformly distributed load, quarterpoint and concentrated load) the value of f_Δ was approximated by

$$f_\Delta = \frac{10}{(L\alpha)^2 + 10}$$

- (2.4)

where   L = length of beam span

$$\alpha = \frac{h^2 S}{EI_R - EI_U} \left(\frac{EI_R}{EI_U} \right)$$

- (2.5)

2-38

where   h = distance between centroid of joist and sheathing

S = effective stiffness of slip connection (load per unit length to give one unit slip)

McCutcheon (1984) extended the model to incorporate load-sharing for joists by considering the sheathing to be a beam acting on elastic springs representing the stiffness of the mid-span of the joists. The model did not consider variation through the length of the beam and neglected the torsional stiffness of the components. McCutcheon (1986) further extended the technique to consider the behaviour of sections with sheeting on both sides. The method used by McCutcheon was compared to results from FEAFLO by Woeste (1990) and showed that the model generally gave conservative results, unless rigid gaps were assumed between the sheeting in FEAFLO. The disadvantage of the techniques employed in these models was that for different boundary conditions to the solutions provided, a complex differential equation must be solved, removing the versatility in utilising this approach.

2.5.4.3   Summary

The detailed models developed to perform structural analysis for walls and floors demonstrated clearly that the sheeting provides a significant contribution to the structural behaviour of the system. For ambient conditions, the sheeting must be considered in a structural model to accurately predict the failure load of a wall or floor and therefore the significance of the sheeting in determining the fire resistance of the wall needs to be investigated. Techniques have been developed to model the effect of partial composite action. Polensek (1976) demonstrated the necessity to consider non-linear geometric effects in modelling the structural response of a wall. The validity of a technique of defining a single flexural stiffness for a partially composite system consisting of sheeting and the timber element were demonstrated. Issues such as load sharing and the contribution of torsional rigidity were raised. The phenomenon of load sharing is outside the scope of this thesis. However, the use of orthogonal beams interlinking elements as detailed in the development of FEAFLO would be an approach that should be considered in modelling this phenomenon. The source code of FEAFLO has been published (Thompson *et al*, 1976). The source code of the models developed by Foschi (1982) and Polensek (1976) did not appear to be

freely available in the literature. However FEAFLO does not consider the effects of large

deformations due to axial forces as required for a column, discrete details through the cross-section

of the components due to thermal effects and the modifications required to the source code may

prove to be extensive and may take longer than to develop a new model and software.

2.5.5 Fastener Stiffness Between the Sheeting and Timber Framing

Several of the models describing the behaviour of a timber-framed assembly in ambient conditions

eg. FEAFLO developers, Polensek (1976), Foschi (1982) have assumed a linear relationship for

the load-deflection behaviour through the connection. In these models, the force transmitted

through the fasteners, P (N), is related to the slip between the sheeting and timber framing,

Δ_{slip}(m), by the 'slip modulus', k. (N/m)

$$P = k\Delta_{slip} \qquad - (2.6)$$

Several authors included the definition of k to include the stiffness per nail and spacing between

each nail.

The results from various authors (Collins, 1989, Polensek, 1976) show that the interconnection

stiffness is non-linear with respect to load (refer to Table 2.6), reducing dramatically with slip.

Extensions to model the actual behaviour of the connection to account for the true non-linear

behaviour have been based on assuming a logarithmic relationship, which is based an empirical

expression derived by McLain (1975) and has be used by Wheat *et al* (1983) and Pellicane *et al*

(1991).

$$P = A \log(1 + B\Delta) \qquad - (2.7)$$

The constants A & B are derived empirically. Pellicane *et al* (1991) further present values for the

constants based on tests, which are calculated in terms of the specific gravity of each of the

components, with reduction factors introduced to account for effects such as the interlayer gap,

sheeting thickness and nail diameter. Further extensions with regard to empirically defining the

constants for several species are contained in Sa Ribeiro *et al* (1992).

Table 2.6. Shear stiffnesses established by Collins (1989), Aloysius (1996) and Polensek (1976) for nails fastening gypsum board to timber framing.

Researcher	th_{board} (mm)	Board (Density)	Nail length x dia.	Stiffness (kN.mm^{-1}) for various amounts of : (i) Fastener slip of gypsum board wrt timber,			
				0.25 mm slip	1 mm slip	2 mm slip	3 mm slip
Collins (1989)	12.5	Winstones (810 kg.m^{-3})		1.17	.43	.24	.16
	16	Winstones (810 kg.m^{-3})		1.20	.48	.28	.19
Alloysius (1996)	16	Boral Firestop (810 kg.m^{-3})	50 x 2.8mm	na	na	na	.22
				(ii) Out-of-plane load (kPa)			
				0-0.14	0.14-0.38	0.38-0.958	0.958-
Polensek (1976)	13	N/a	39 x 2.23mm	17.50 kN.mm^{-1}	12.25 kN.mm^{-1}	1.365 kN.mm^{-1}	0.21 kN.mm^{-1}

Notes: na   = not available.

th_{board} = thickness of gypsum board

wrt   = with respect to

dia   = diameter

An alternative technique used to derive the interconnection stiffness was based on the components connected and the connector. Wilkinson (1971,1972) derived an expression relating the load and slip based on the solution of beams on elastic foundations. The relationship derived was a linear function, based on the mechanical properties of the components of the joint. Foschi (1974) presented a detailed analysis of nail behaviour within a connection, utilising an elasto-plastic finite element analysis using beam elements.

It is apparent that a non-linear relationship is more correct as demonstrated by the test results presented in Table 2.6 and Wheat *et al* (1983). However non-linear modelling is considered too refined for this project as there are insufficient data in the literature detailing the change in material properties due to heating effects on the nail, plasterboard and timber and hence the connector behaviour. The nail through the plasterboard is an excellent conductor, potentially allowing localised heating in the region of the joint in advance of the general heating conditions experienced by the assembly, this has been detailed in work by Fuller *et al* (1992). The thermal

model of Clancy (1999) does not consider the heat transfer in the region of the joint, which would require a complex three-dimensional heat transfer analysis. Thus insufficient detail exists to apply a model such as that presented by Foschi (1974) or Wilkinson (1972). To apply such a model using temperatures not calculated in the specific region implies a false degree of certainty. Application of a logarithmic expression with empirically derived constants would require an experimental program to derive the values.

The load level considered in the structural model, simulating the performance of a wall in a fire resistance test would be assumed to relate to a design load which could be crudely assumed as 30% of the short-term capacity of the wall. Thus the behaviour of the connection would be assumed to be comfortably in the linear portion of the range. Therefore a linear elastic load-slip relationship appears an acceptable method of incorporating partial composite action between the timber and plasterboard. The significance of composite action at elevated temperatures requires further consideration.

2.6   Methods of Analysis

Based on the literature review undertaken, it is apparent that phenomena which should be considered in the development of a structural model to analyse timber-framed, plasterboard-clad walls in fire are listed as follows:

- The degradation of the mechanical properties through the cross-section with temperature

- Partial composite interaction between the timber framing and sheeting

- Non-linear geometric (P-Δ) effects

- Varied end restraint

- Varied loading conditions

- Thermal expansion / shrinkage of the plasterboard sheeting

In addition to the phenomena listed, the model must be a 'stand alone' algorithm, which can be readily integrated within the framework developed by Clancy (1999). The model is required to be

flexible with regard to changing temperatures and random variations of and readily allow data interchange with models from this framework.

The options available to perform the structural analysis to consider the phenomena mentioned were:

(i)   Use of conventional finite element analysis software, using three-dimensional elements e.g. (STRAND 6.1, ABAQUS, ANSYS)

(ii)   Derivation of a closed form solution to describe the model

(iii)   Constitutive iterative approach (e.g. O'Meagher *et al*, 1991)

(iv)   Use of a numerical technique such as a direct stiffness approach, with a composite section technique to take into account the change in mechanical properties (e.g. Andeberg, 1976) and partial interaction between the sheeting and timber framing

Commercially available finite element packages such as ANSYS, ABAQUS and STRAND 6.1 are capable of solving the numerical problem, as has been demonstrated by Thomas *et al* (1995). The following concerns were had with respect to the use of finite-element packages:

- The solution time can be very slow when three-dimensional elements are used in conjunction with non-linear analysis.

- The software cannot be readily integrated with the work of Clancy (1999), especially if the code is to be portable and 'stand alone'.

- Thomas *et al* (1995) identified limitations in the non-linear analysis routines in some finite element analysis software, with regard to the definition of mechanical properties for compression and tension. The properties had to be separately defined if the stress-strain relationships were different in tension and compression. This would result in a cumbersome model, which could not practically be used for probabilistic simulation as it would require continual revision of the input data in order to perform the analysis whenever there is stress reversal in elements during iteration.

- The model may become numerically unstable at the location of a specific node due to the interaction of a restraint or force, which may slow the solution procedure considerably. This

is unsuitable for risk modelling, which requires stability over many simulations with a wide range of values generated from random variables.

The use of a closed form solution would allow the fastest solution procedure. However the derivation of a closed form solution to incorporate all of the phenomena considered in the review would be impractical. No author in the literature for fire analysis of timber or other materials has developed such as solution - the problem is intractable.

The iterative approach of O'Meagher *et al* (1991) may require many trials to converge, and indeed may not always converge. This approach is therefore not considered to be best suited for risk modelling, as the solution process may be slow, or stall.

The direct stiffness approach as detailed in most structural engineering texts (eg. Coates *et al* , 1989) is a well-established technique for the analysis of beam-column elements, which allows great flexibility in defining boundary conditions to consider restraint and also load configurations, and a fast solution time. A version of the method was employed in the determination of the fire resistance of reinforced concrete columns by Anderberg (1976). The technique has been used in many commercially available structural analysis software packages used for frame analysis eg. Space Gass, Microstran. Techniques to perform non-linear analysis for the direct stiffness approach have been well established and are presented in generalised texts such as Chen *et al* (1987).

2.7   Summary

Based on the review of literature, the phenomena that should be considered in the development of a structural model to analyse timber-framed, plasterboard-clad walls in fire have been outlined, and are listed as follows:

- The degradation of the mechanical properties through the cross-section with temperature.

- Partial composite interaction between the timber framing and sheeting.

- The significance of the plasterboard sheeting on the time-to-failure of timber-framed, plasterboard-clad walls.

- Non-linear geometric (P-Δ) effects.

- Varied end restraint.

- Varied loading conditions.

- Thermal expansion / shrinkage of the plasterboard sheeting.

With consideration of the requirements of the model to be a stand-alone algorithm for incorporation into the framework of Clancy (1999) and be used in probabilistic simulation, and the phenomena required to be considered, the models in the literature did not have the capabilities to satisfy these requirements, hence a new model is required.

To model the phenomena, a composite section technique as identified by several authors in analysing timber elements appears credible. In order to consider the partial composite interaction of the sheeting - stud, an expression defining the flexural stiffness should be derived, in a similar manner to that performed by McCutcheon (1984).

The use of a second order direct-stiffness approach was considered to be the most appropriate as the basis for the development of the structural model, due to it offering both flexibility in loading and end restraint and having a fast solution time compared to a finite element approach.

The literature review also identified a significant lack of knowledge with regard to the reduction in mechanical properties of timber tested in pure compression. There was also a lack of information for full-scale fire-resistance tests of load-bearing timber-framed wall panels, which had well defined, controlled conditions required to validate a model. Thus it has been demonstrated that a significant program of experimentation is required to:

(i) Define the reduction in mechanical properties in compression of the timber, radiata pine, commonly used in the construction of Australian timber-framed, plasterboard-clad partitions.

(ii)   A series of full-scale tests with well defined, known boundary conditions and detailed

instrumentation should be conducted to provide an more accurate means of comparison

with the model developed.

3. Structural Model

3.1 Introduction

From the aims in Section 1.4 and the relevant phenomena that should be considered in the determining the structural response of a timber framed barrier identified in the Literature Review (§2.7), the following specific aims were required to be achieved in developing the structural model:

(i)   It must have a fast solution speed.

(ii)   It must be able to model individual phenomena, namely:

- The degradation of the mechanical properties through the cross-section with temperature

- Partial composite interaction between the timber framing and sheeting

- Non-linear geometric (P-Δ) effects

- Varied end restraint

- Varied loading conditions

- Thermal expansion / shrinkage of the plasterboard sheeting

(iii)   It must be readily integrated with other models developed to allow probabilistic simulation associated with the models developed by Clancy (1999) within the overall framework developed for the research (refer to Figure 1.3).

The literature review considered several analytical approaches in determining a suitable approach for the model development (§2.6). Based on the available approaches, and with consideration of the aims the model must satisfy, it was concluded that the model should be developed on the following basis:

- Second-order direct stiffness approach for numerical efficiency and flexibility in considering changed load and restraint conditions.

- Composite section theory to account for the temperature distribution through the cross-section of the timber elements.

- Derivation of a stiffness element to take into account the partial composite action between the timber framing and sheeting, in a similar manner to McCutcheon (1984).

For the reasons outlined in Section 2.6, the use of a conventional finite element software package was considered unsuitable in achieving the aims of this thesis and was not used for the modelling. However finite element analysis was considered to be a useful tool in both validating components of the structural model and further investigating assumptions made, such as the effective width of the plasterboard sheeting.

3.2   Overview of Model

3.2.1   General

The structural model calculates the out-of-plane deformations versus time up to the time of collapse. The assemblies are modelled as beam elements, with section properties accounting for the partial composite actions of the sheeting with the timber framing and the thermal degradation of the mechanical properties. The model incorporates a transient second-order direct stiffness approach. The model has the capability to consider non-linear geometric and mechanical property phenomena. A generalised flow chart of the model for calculating the structural response at a given time step is presented in *Figure 3.1*. The model uses an iterative procedure. The initial data for the model to commence the solution process are read from an input file and the structural response is calculated based on the initial geometry assuming ambient mechanical properties (box 1). The iterative procedure employed (boxes 2-9) uses the direct stiffness method and incorporates the change in the mechanical properties due to temperature and the stress-strain characteristics of the materials. If the wall does not fail, the structural response is calculated for subsequent time steps, utilising the corresponding temperature data to determine the mechanical properties. Each successive time step involves iterations continuing until one of the following conditions occurs:

(i)   If there is a failure of the wall (box 4 "no" branch or box 8 "yes" branch).

(ii)   The required convergence occurs (box 9 "yes" branch).

(iii)   The maximum allowable number of iterations is performed (box 9 "yes" branch).

The wall may fail through either geometric instability or crushing mechanisms.
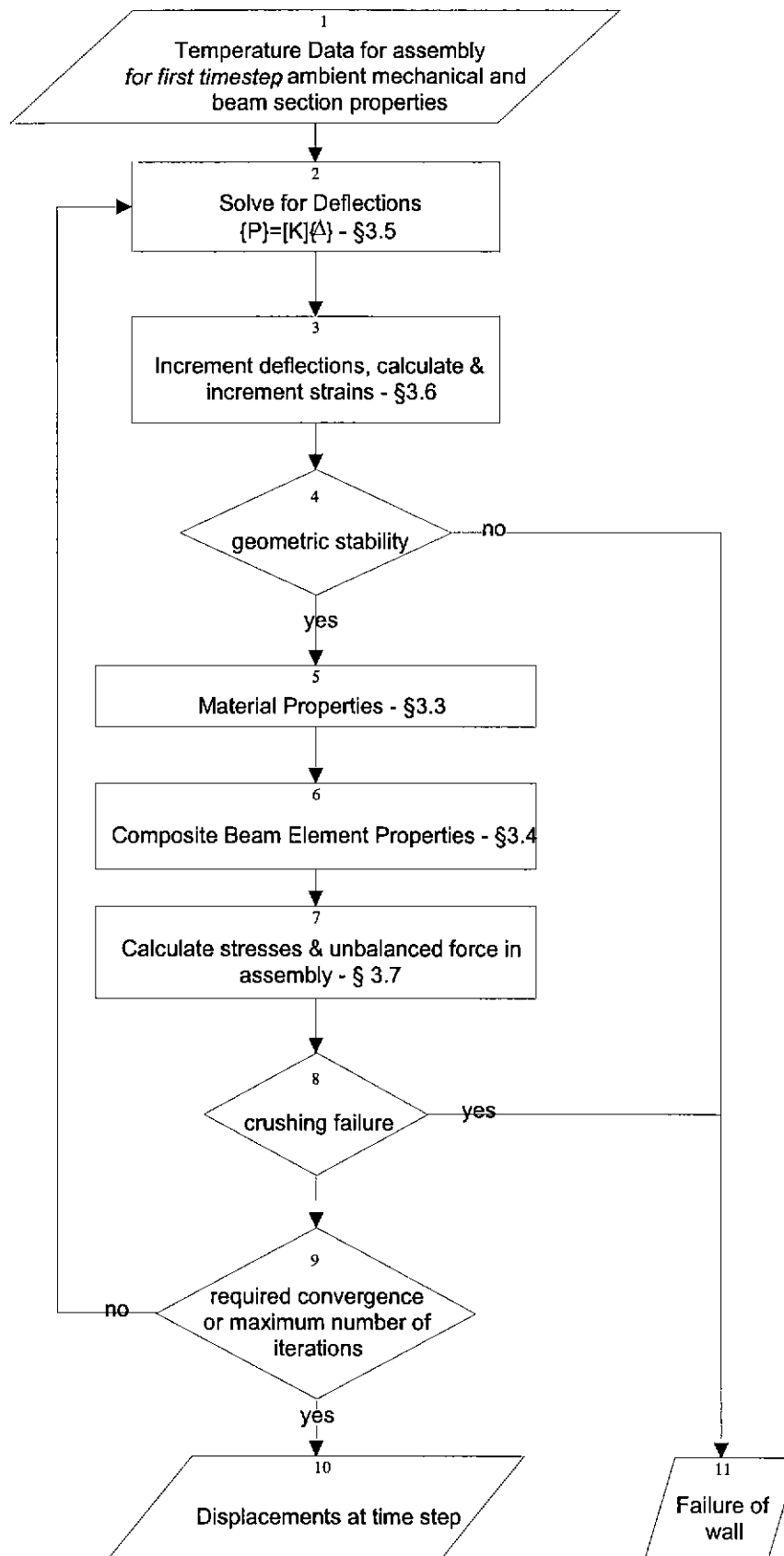
Figure 3.1: *General Flowchart of Model*

3.2.2   Discretisation of Wall-Framing Assembly

The model converts the cross-section consisting of a timber stud with two flanges of plasterboard

sheeting into an equivalent line member that is suitable for use by the direct stiffness approach.

Refer to *Figure 3.2* for the diagram depicting the discretisation of the assembly in the model. The

cross section of each segment is discretised into elements; each having a uniquely assigned

property based on the temperature and mechanical response. The wall-framing assembly is

discretised into segments along the length. The axial and flexural stiffness of the segment is

calculated based on the mechanical properties through the cross-section as detailed in Section

3.4.3.
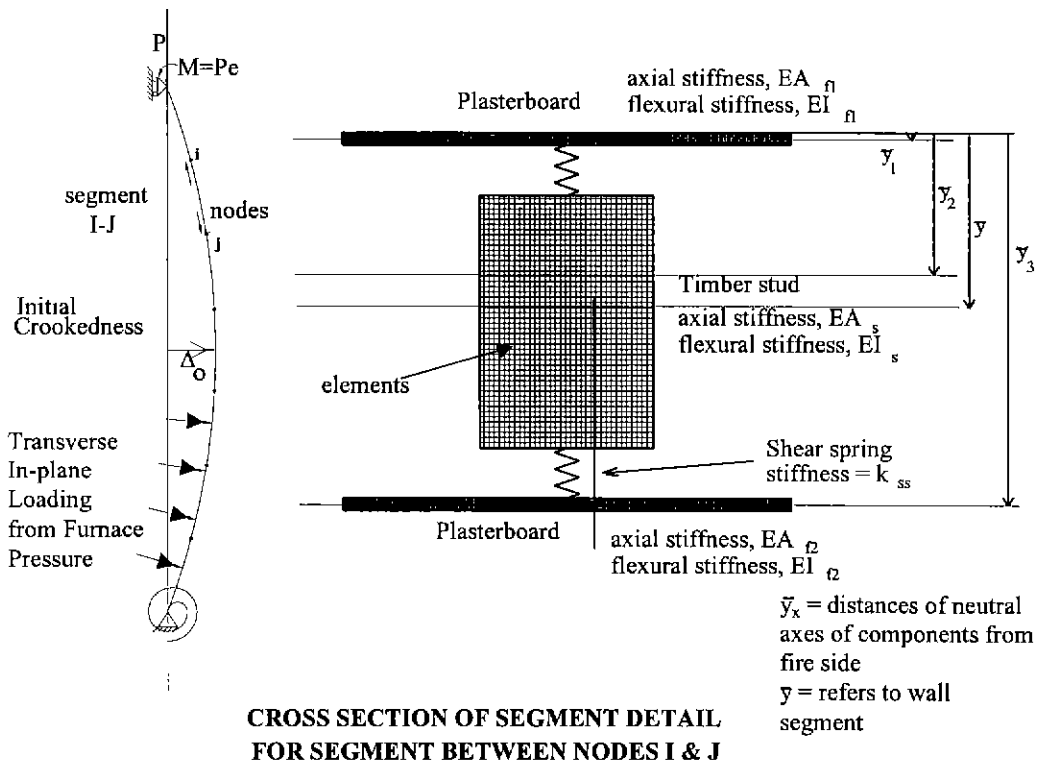
Figure 3.2: Discretisation of a Timber-Framed, Plasterboard-Clad Wall Assembly

3.2.3   Assumptions

The following assumptions were made in developing the structural model:

- Plane sections remain plane in components, that is, the strain distribution is linear.

- The position of restraint at the supports was at the neutral axis of the specimen. This method

  differs with restraint positions adopted in applying finite element analysis software, where the

  location of the restraint is fixed at a nodal location.

- The curvature of the stud and plasterboard sheeting were assumed the same at each section.

- Lateral in-plane deformation of the studs were assumed negligible, due to restraint provided by the plasterboard, hence only out-of-plane deformation is considered.

3.2.4 Non-Linear Solution Algorithm of the Frame Analysis

The non-linear analysis technique is based on an iterative algorithm for second-order elastic analysis for framing members presented in Chen *et al* (1987). The algorithm was selected as a well-established technique of performing the non-linear analysis in conjunction with a direct-stiffness matrix approach. The algorithm for non-linear analysis is summarised in the diagram *Figure 3.3* and the associated flowchart in Figure 3.4. The non-linear analysis considers both phenomena associated with non-linear geometry (large deflection known as P-Delta effects) and non-linear mechanical properties, which are detailed in the following Section 3.3.2, and utilises a secant approach.
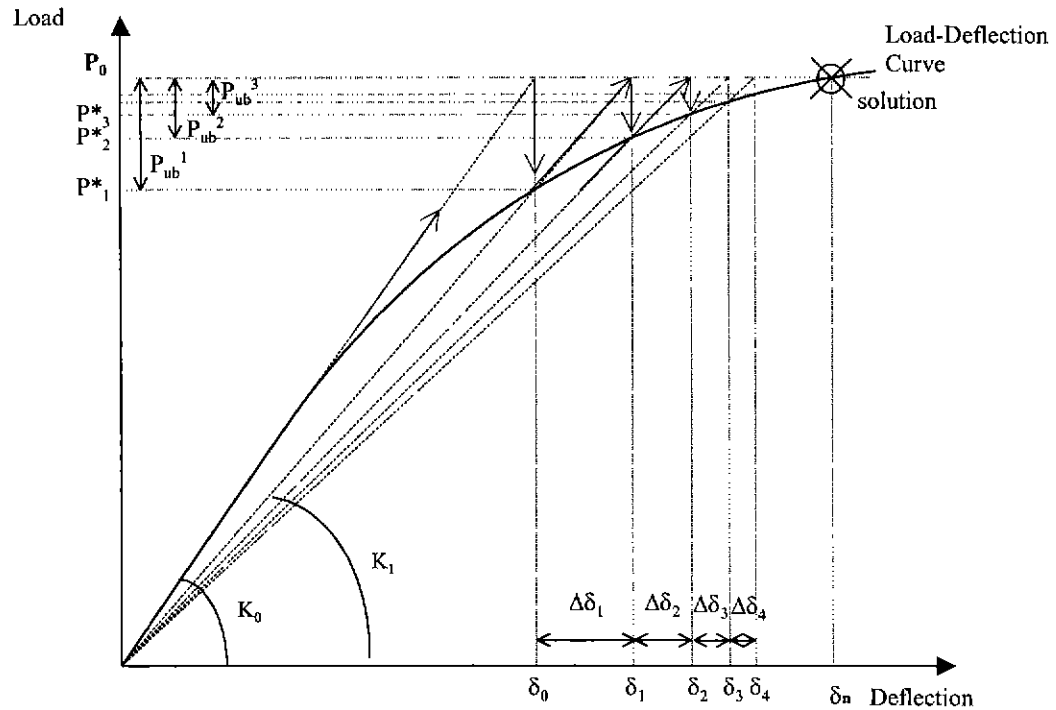
Figure 3.3: Non-Linear Analysis Iteration Algorithm

The calculation procedure involves an initial determination of the deflection, δ_0, based on the first order linear elastic properties (a structure stiffness represented by K_0) for the externally applied

load, P_0. The force calculated within the structure, P^*_1, based on this deflected shape is then calculated. The unbalanced force, P_{ub}^1 is then calculated, which is the difference between the externally applied force and the force required to induce the deflection δ_0. The unbalanced force is reapplied to the structure with the stiffness K_1 and the deflection $\Delta\delta_1$ is calculated. The total deflection of the structure, δ_1, is calculated and the required force to induce the deflection, P^*_2 is calculated. The unbalanced force between P^*_2 and the externally applied force is calculated and this is reapplied to the structure. The iterative procedure (2)-(7) as shown in Figure 3.4 is repeated until an acceptable level of convergence is achieved.

3.2.5   Transient Solution Algorithm of the Frame Analysis

The transient solution algorithm (refer to *Figure 3.5*) is an extension of the non-linear analysis algorithm described in Section 3.2.4. To represent the change in properties during a time step, δt, the deflection is held constant (path A in *Figure 3.5*) and the analysis 'moves' via path B to another load-deflection curve representing the load-deflection behaviour with the mechanical properties relating to conditions at the new time step. The change in stiffness of the assembly due to the change in temperature over the time interval results in a change in the load, P^*, required to achieve the deformation Δ_t.
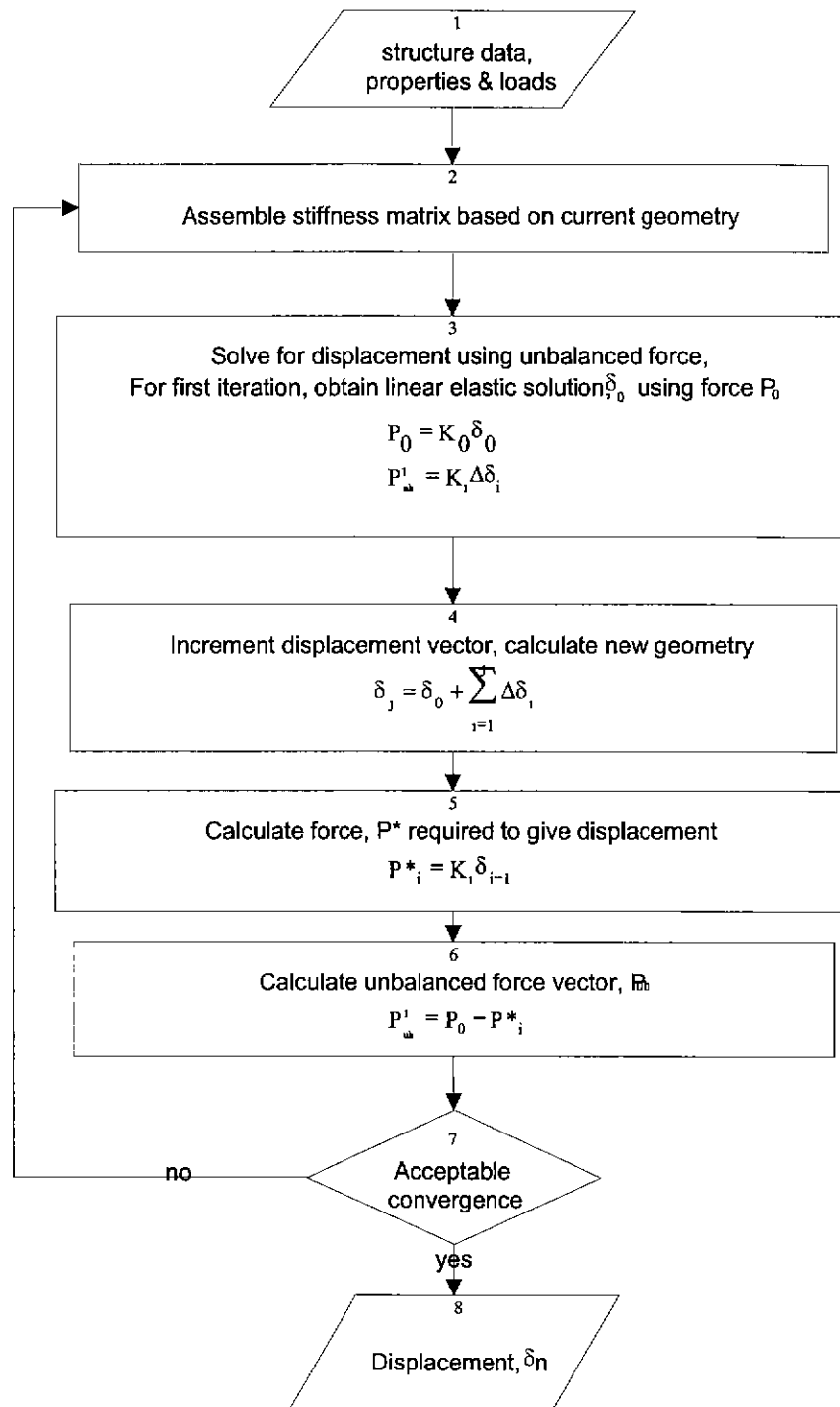
Figure 3.4: Non-Linear Analysis Iteration Routine – Flowchart

(Note: symbols are defined in Section 3.2.4)
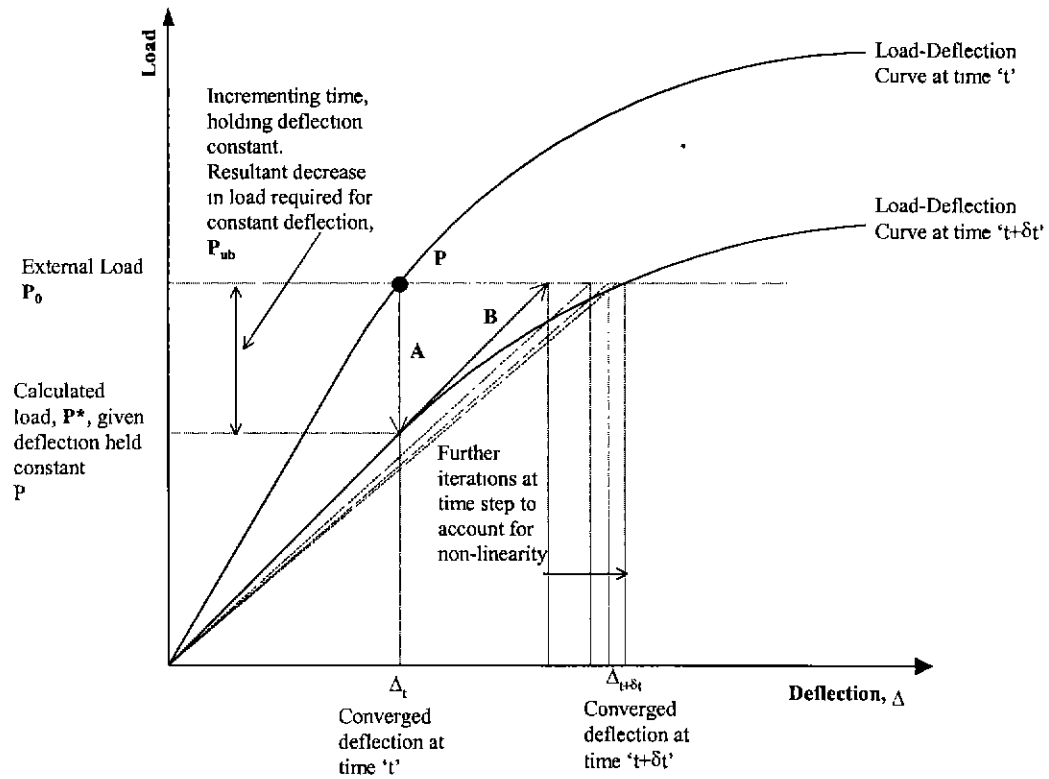
***Figure 3.5:** Transient Solution Algorithm*

The unbalanced force vector, P_{ub} is calculated in the same manner as the non-linear algorithm

detailed in Section 3.2.4, except the effect of changing mechanical properties is incorporated in

this particular iterative step. Further iterations for the temperature conditions at the time step are

performed to account for non-linear geometric and mechanical behaviour. A flow chart depicting

the analysis algorithm in more detail than presented in *Figure 3.1* is shown in *Figure 3.6*.
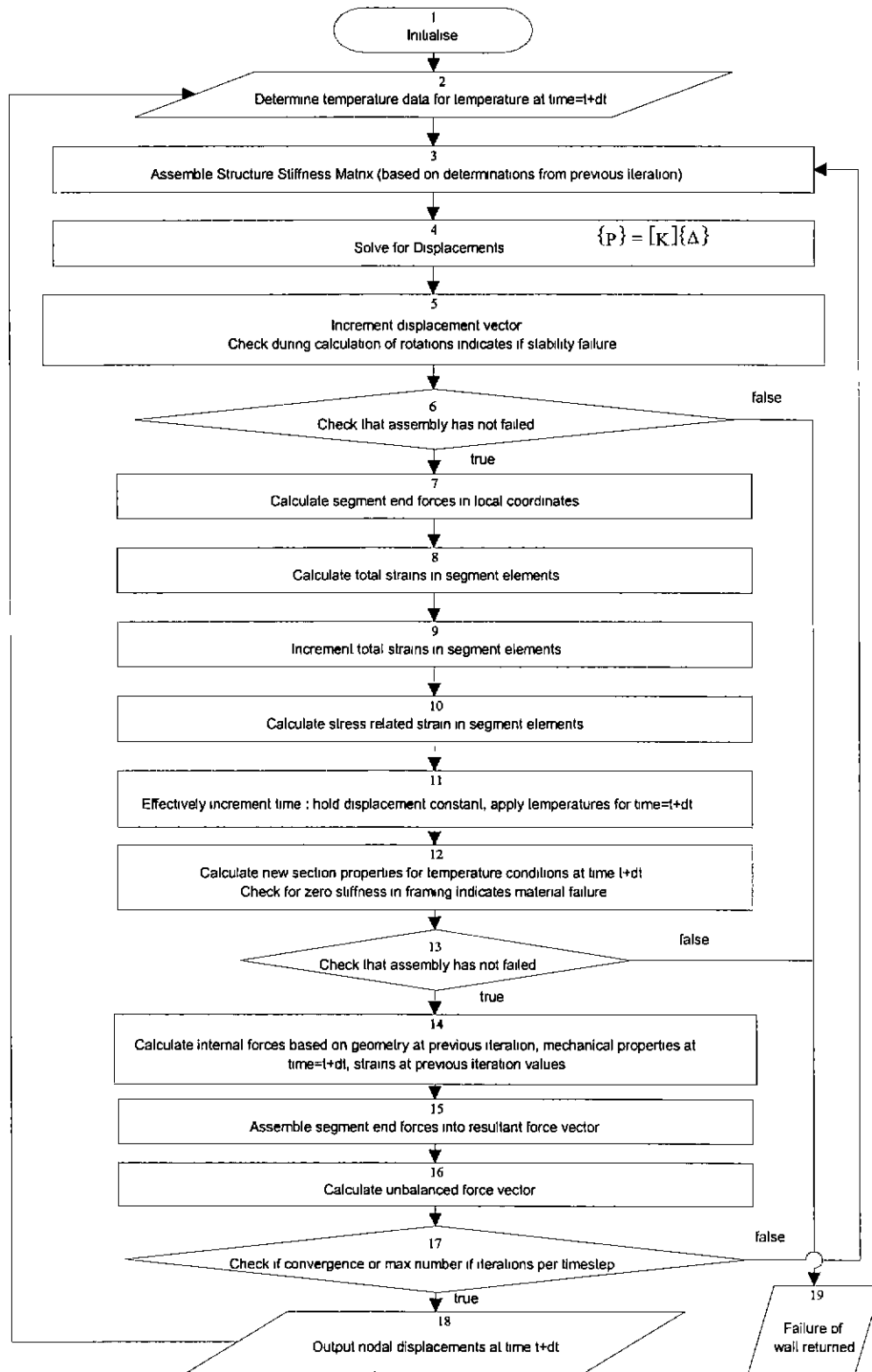
Figure 3.6: Flowchart of Transient Structural Model Solution Procedure

Note: For the initial pass of the algorithm, the structure stiffness matrix [K] is assembled from element stiffness matrixes based on the ambient section properties. The applied load to solve for displacements is the external load vector.

3.3 Material Mechanical Properties

3.3.1 Introduction

The mechanical properties adopted in the model were represented as functions of the properties at ambient conditions as detailed in §3.3.2. The functions were a simple scaling factor which were dependent on the temperature and are described in §3.3.3.

3.3.2 Mechanical Behaviour of Materials in Ambient Conditions

The model requires the stress-strain relationship adopted for timber to be specified as either purely linearly elastic or a non-linear expression presented by Buchanan (1986) for ambient conditions (*Figure 3.7*).

The relation in tension was assumed to be linearly elastic until the ultimate tensile stress was achieved.

$$\sigma_t = E\varepsilon \qquad\qquad - (3.1)$$

where σ_t is the stress in tension

       E is the modulus of elasticity

       ε is the strain

The stress-strain relationship in compression was assumed to be represented by the expression

$$\sigma_c = E\varepsilon - A\varepsilon^n \qquad\qquad - (3.2)$$

where σ_c is the stress in compression

       ε is the strain

       A, n are constants defined such that the peak stress in compression at 1.35 times the equivalent elastic strain, $\varepsilon_{equiv\ max}$.

       Buchanan (1986) also incorporated a linear drop-off after the peak stress in compression was reached. The gradient of this line was calibrated against test data. For the purposes of this study, the linear gradient drop-off was not incorporated, as the timber studs comprising the wall are very slender elements and are likely to be subjected to a higher proportion of axial load compared to bending moment and the effect of the shape beyond

this peak was shown to not be significant in Buchanan's paper. Use of the model in predicting the behaviour of floor elements will require a more detailed consideration of the nature of the reduction in compression stress versus strain beyond the peak compression strength.
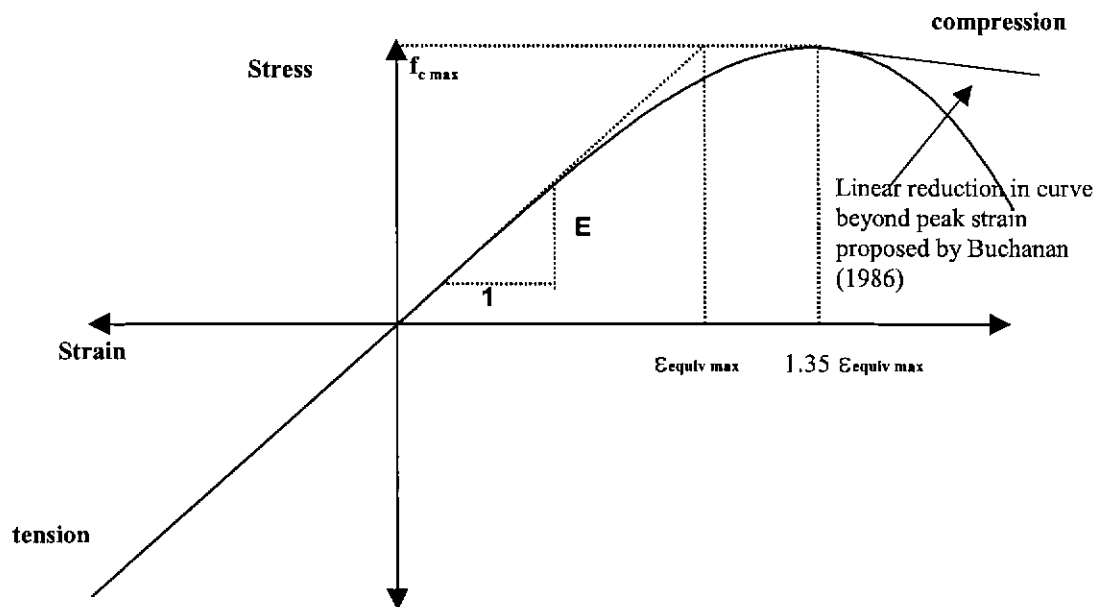
Figure 3.7: *Stress-Strain Relationship adopted for the Mechanical Behaviour of Timber (after Buchanan, 1986)*

Considerations of length and size effects to account for the distribution of defects within timber specimens were not performed due to the lack of applicable data for elevated temperature (§2.2.4).

Two alternative relationships for the stress-strain behaviour of plasterboard can be selected in the model:

(i)   Purely linear-elastic

(ii)   Non-linear - Idealised elasto-plastic behaviour in compression in combination with brittle elastic behaviour in tension (Walker *et al*, 1995).

3.3.3 Change in Mechanical Properties With Temperature

The change in mechanical properties with temperature was accounted for by use of a reduction

factor, $\phi_{Temp}(T)$, related to the initial ambient value of the property, $P_{ambient}$. The property, $P(T)$ at

temperature T was calculated by

$$P(T) = \phi_{Temp}(T)P_{ambient} \qquad\qquad - (3.3)$$

The relation between reduction factor for a particular mechanical property and temperature was

based on relationships from the literature such as those in Figures 2.2 – 2.5, experimental results,

engineering judgment and calibration with experimental results. The examination of the

mechanical property reductions, in particular in compression is considered in Section 7.

3.4 Composite Beam Segment Properties

3.4.1 Introduction

The timber framed assembly was considered as a 'sandwich' construction element, consisting of

one or two flanges of sheeting connected by a shear spring to the framing (refer to *Figure 3.2*).

The model considers both the effect of the temperature distribution through each component of the

assembly (§3.4.2) and the partial composite interaction between the components by use of shear

spring sub-models for fasteners (§3.4.3) to obtain the overall axial and flexural stiffness of the

segments (§3.4.4) assuming the effective width of the sheeting is equal to the timber framing

spacing (§3.4.5).

3.4.2 Composite Section Behaviour

Each component of the "sandwich" construction was discretised into a mesh of elements through

the cross-section as shown in *Figure 3.8*. Each element had a unique property assigned based on

the temperature at the centre of the element and the strain conditions of the element. The flexural

and axial stiffness values of the timber framing and sheeting for a given temperature distribution

were calculated by utilising composite section theory which employed a transformation of area technique (Popov, 1978 and §2.5.2.3).
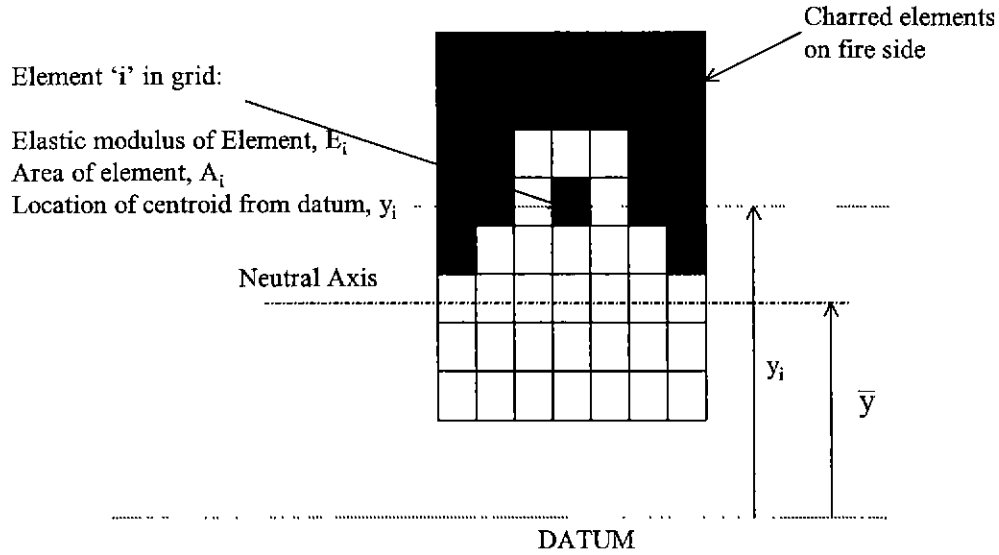
Figure 3.8*: Discretisation of Framing Element to Determine the Component Flexural & Axial*

Stiffness

The axial stiffness, EA, for the framing and sheeting components was calculated by summing the stiffness contribution of each element within each component.

$$EA = \sum_A E_i A_i \qquad \text{- (3.5)}$$

The neutral axis of the component was calculated with respect to a datum using

$$\bar{y}_i = \frac{\int_A yEdA}{\int_A EdA} \cong \frac{\sum_A E_i A_i y_i}{\sum_A E_i A_i} \qquad \text{- (3.6)}$$

where y_i = location of the centroid of the element with respect to a datum

E_i = modulus of elasticity of the element

A_i = cross section area of the element

The flexural stiffness of each component was then calculated using the transformation of axis theorem and summing the contribution over the area of the cross section, A.

3-13

$$EI = \sum_A E_i A_i (\bar{y} - y_i)^2 + \sum_A E_i I_i \qquad - (3.7)$$

where $\quad I_i = \dfrac{b_i d_i^3}{12}$ = moment of inertia of an element, with b_i = breadth of element, d_i = depth of

element

3.4.3   Fastener Behaviour

The fastener connecting the framing to the sheeting was modelled by a shear spring connected

between the sheeting and the stud. The magnitude of slip between the framing and sheeting, Δ_{slip},

was represented by the expression:

$$\Delta_{slip} = \frac{P_{flange}}{k_{ss}} \qquad - (3.8)$$

where $\quad P_{flange}$ = magnitude of force transmitted through the shear spring into the sheeting flange

of the sandwich construction (N).

k_{ss} = shear spring stiffness of the connection (N/m) for the length of the segment

3.4.4   Composite Action Between the Timber Framing and Sheeting

Sheeting was demonstrated in the literature review for ambient conditions to provide a

considerable increase in the load-bearing capacity of timber walls and floors (for example,

Thompson *et al*, 1975, Polensek, 1976).

Considering the partial composite action demonstrated to be provided by the sheeting, the

following expressions were derived to calculate the centroid, axial stiffness and flexural stiffness

of the sandwich panel construction:

$$\text{The centroid of segment, } \bar{y} = \frac{\sum_{i=1}^{3} \bar{y}_i k_i}{\sum_{i=1}^{3} k_i} \qquad - (3.9)$$

where $\quad \bar{y}_i$ = location of neutral axis of the sandwich panel component from a datum

The terms, k_i, represent the effective axial stiffness contribution of each component of the sandwich panel (i=1 represents one sheet of plasterboard, i=2 represent the timber framing and i=3 represents the other sheet of plasterboard). L is the length of the segment

where $\quad k_1 = \dfrac{EA_1 k_{ss}}{EA_1 + Lk_{ss}}$ — (3.10a)

$k_2 = EA_s$ — (3.10b)

$k_3 = \dfrac{EA_2 k_{ss}}{EA_2 + Lk_{ss}}$ — (3.10c)

the terms EA_x are the axial stiffness of the segment components, calculated by summing the elements comprising each of the respective segment components.

i.e. $\quad EA_x = \displaystyle\sum_{A_x} E_{xi} A_{xi}$ — (3.11)

the segment axial stiffness, EA, was determined from the expression

$EA = L \displaystyle\sum_{i=1}^{3} k_i$ — (3.12)

the segment flexural stiffness, EI, was determined from

$EI = \displaystyle\sum_{i=1}^{3} \left[Lk_i \left(\bar{y} - \bar{y}_i \right)^2 + EI_i \right]$ — (3.13)

3.4.5   Effective Width of the Sheeting

This is the first study considering the effect of sheeting on the structural resistance of timber framed, plasterboard-clad walls in fire. Based on Criswell (1983), who considered floors in ambient conditions, the effect of shear lag is not considered to be significant. However, the accuracy of this assumption will be considered in the further detail in Section 4.

3.5   Solution for Displacements

The direct stiffness approach was used to calculate the displacement of the assembly for a given load, geometry and mechanical properties. The relationship between force acting on the assembly,

{P}, and the resultant displacement, {Δ}, of the structure is dependent on the stiffness of the structure, [K] and is represented by the fundamental equation.

$$\{P\} = [K]\{\Delta\}$$ - (3.14)

The stiffness matrix of the assembly was determined by combining the stiffness matrices of the segments into which it has been discretised.

3.5.1 Segment Stiffness Matrices
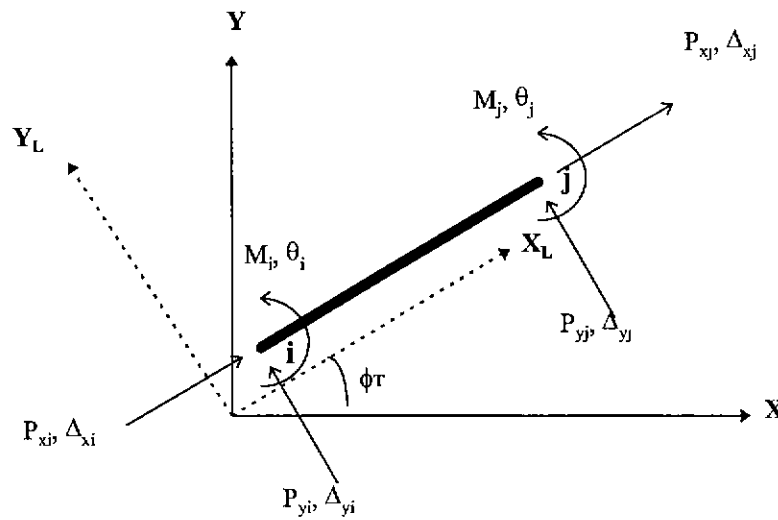
Figure 3.9*: Depiction of Direction of Forces and Corresponding Displacements on a Beam-Column Orientated in the local coordinate plane X_L, Y_L rotated an angle ϕ_T from the global plane X, Y*

The expression relating force and displacement for a beam-column in a local coordinate system was determined from the well established stiffness relations and can be found in several texts on matrix structural analysis including Coates *et al* (1988). The relationship between the end forces acting on the segment (as shown in Figure 3.10) and corresponding displacement is given by the expression:

$$
\begin{Bmatrix} P_{xi} \\ P_{yi} \\ M_i \\ P_{xj} \\ P_{yj} \\ M_j \end{Bmatrix} = \begin{bmatrix} \dfrac{EA}{L} & 0 & 0 & -\dfrac{EA}{L} & 0 & 0 \\ 0 & \dfrac{12EI}{L^3} & \dfrac{6EI}{L^2} & 0 & -\dfrac{12EI}{L^3} & \dfrac{6EI}{L^2} \\ 0 & \dfrac{6EI}{L^2} & \dfrac{4EI}{L} & 0 & -\dfrac{6EI}{L^2} & \dfrac{2EI}{L} \\ -\dfrac{EA}{L} & 0 & 0 & \dfrac{EA}{L} & 0 & 0 \\ 0 & -\dfrac{12EI}{L^3} & -\dfrac{6EI}{L^2} & 0 & \dfrac{12EI}{L^3} & -\dfrac{6EI}{L^2} \\ 0 & \dfrac{6EI}{L^2} & \dfrac{2EI}{L} & 0 & -\dfrac{6EI}{L^2} & \dfrac{4EI}{L} \end{bmatrix} \begin{Bmatrix} \Delta_{xi} \\ \Delta_{yi} \\ \theta_1 \\ \Delta_{xj} \\ \Delta_{yj} \\ \theta_j \end{Bmatrix}
$$

- (3.15)

Where   L = length of the segment

EA = axial stiffness of the segment

EI = flexural stiffness of the segment

A generalised expression for the stiffness matrix of a segment, derived to allow for transformation into other coordinate systems was calculated from the stiffness relation for a segment in local coordinates is as follows:

$$
\left[K_{seg} \right] = [T]^T \left[K_{seg}^L \right] [T] \qquad\qquad - (3.16)
$$

where $\left[K_{seg}^L \right]$ is the stiffness matrix of the segment in local coordinates

$[T]$ is the transformation matrix

The transformation matrix is defined as

$$
[T] = \left[\begin{array}{ccc|ccc} C & S & 0 & 0 & 0 & 0 \\ -S & C & 0 & 0 & 0 & 0 \\ 0 & 0 & 1 & 0 & 0 & 0 \\ \hline 0 & 0 & 0 & C & S & 0 \\ 0 & 0 & 0 & -S & C & 0 \\ 0 & 0 & 0 & 0 & 0 & 1 \end{array} \right] \qquad - (3.17)
$$

where $C = \cos\phi_T$

$S = \sin\phi_T$

Performing the matrix multiplication using the transpose of the transformation matrix, $[T]^T$ and the transformation matrix [T] yields a generalized stiffness matrix for a beam-column.

$$[K_{seg}] = \begin{bmatrix} C^2\frac{EA}{L}+S^2\frac{12EI}{L^3} & CS\left(\frac{EA}{L}-\frac{12EI}{L^3}\right) & -S\frac{6EI}{L^2} & -\left(C^2\frac{EA}{L}+S^2\frac{12EI}{L^3}\right) & -CS\left(\frac{EA}{L}-\frac{12EI}{L^3}\right) & -S\frac{6EI}{L^2} \\ CS\left(\frac{EA}{L}-\frac{12EI}{L^3}\right) & S^2\frac{EA}{L}+C^2\frac{12EI}{L^3} & C\frac{6EI}{L^2} & CS\left(-\frac{EA}{L}+\frac{12EI}{L^3}\right) & -\left(S^2\frac{EA}{L}+C^2\frac{12EI}{L^3}\right) & C\frac{6EI}{L^2} \\ -S\frac{6EI}{L^2} & C\frac{6EI}{L^2} & \frac{4EI}{L} & S\frac{6EI}{L^2} & -C\frac{6EI}{L^2} & \frac{2EI}{L} \\ -\left(C^2\frac{EA}{L}+S^2\frac{12EI}{L^3}\right) & CS\left(-\frac{EA}{L}+\frac{12EI}{L^3}\right) & S\frac{6EI}{L^2} & C^2\frac{EA}{L}+S^2\frac{12EI}{L^3} & CS\left(\frac{EA}{L}-\frac{12EI}{L^3}\right) & S\frac{6EI}{L^2} \\ -CS\left(\frac{EA}{L}-\frac{12EI}{L^3}\right) & -\left(S^2\frac{EA}{L}+C^2\frac{12EI}{L^3}\right) & -C\frac{6EI}{L^2} & CS\left(\frac{EA}{L}-\frac{12EI}{L^3}\right) & S^2\frac{EA}{L}+C^2\frac{12EI}{L^3} & -C\frac{6EI}{L^2} \\ -S\frac{6EI}{L^2} & C\frac{6EI}{L^2} & \frac{2EI}{L} & S\frac{6EI}{L^2} & -C\frac{6EI}{L^2} & \frac{4EI}{L^2} \end{bmatrix}$$

- (3.18)

3.5.2 Assembly of Structure Stiffness Matrix

The stiffness matrix for the wall was assembled by using the well established techniques defined for the direct stiffness approach as detailed in Coates *et al* (1988). Terms from segment stiffness matrices in the global coordinate scheme corresponding to the same force and the corresponding degree of freedom were added.

3.5.3 End Restraint of the Assembly

To account for end restraint conditions of the assembly, the model had the option of full restraint or partial rotational restraint. Full restraint for a given degree of freedom was applied using the standard technique of placing 1's on the diagonals of the relevant degree of freedom and zeroes on the corresponding row and columns for the force and displacement restrained. Rotational restraint was applied by adding a torsional spring, of a stiffness corresponding to the degree of rotational restraint at the ends of the member, to the term relating the rotational degree of freedom and corresponding moment.

3.5.4 Solution for the Displacement of the Assembly

The displacement of the assembly was calculated by solving the system of simultaneous equations (equation 3.14) by use of algorithms from Press *et al* (1992). An LU decomposition was performed of the stiffness matrix. A back substitution of the LU decomposed stiffness matrix

using the load vector was performed to obtain the unknown vector of displacements. The node displacements were calculated with respect to the global coordinates of the assembly.

3.6   Incrementation of Deflections, Calculation & Incrementation of Strains

3.6.1   Incrementation of Deflections

The node deflections were incremented during each iteration step by adding the additional displacement calculated for the given iteration step to the total displacement of all previous iteration steps. Refer to the flow chart and diagrams in *Figure 3.3* and Figure 3.4.

3.6.2   Calculation of Segment End Forces

To calculate the strain distribution of the elements within a segment, the end forces in the segment as shown in *Figure 3.9* were first calculated. Segment end forces in local coordinates were calculated using the equation (3.15). Node displacements were extracted from the assembly displacement vector and were converted into local coordinates for the segment using the expression:

$$\left\{\Delta_{seg}^{L}\right\} = [T]\left\{\Delta_{seg}\right\}$$
- (3.19)

3.6.3   Calculation of Strains from End Forces

The framing was assumed to be the only load carrier in the segment and so the distribution of strain induced in the framing was assumed identical to that carried through the segment.

The framing strain was calculated based on the average end forces of each segment and the flexural stiffness of the segment. The total strain of an element, $\varepsilon_{total,i}$, located at a position, y_i was calculated using

$$\varepsilon_{total\,i} = \frac{N}{EA} + \frac{M(\bar{y} - y_i)}{EI}$$
- (3.20)

where   N = average end axial force acting on segment

M = average end bending moment acting on segment

EA = segment axial stiffness

EI = segment flexural stiffness

$\overline{y}$ = location of neutral axis of segment

y_i = location of element 'i'

The magnitude of strain transferred to the sheeting flanges was related to the interconnection shear spring stiffness. Curvature was assumed to remain constant for the framing and sheeting. A diagram showing the strain distribution through a segment is shown in *Figure 3.10*. The expression derived (refer to Appendix 1 for the derivation) for the strain within the sheeting at a location y_i, was

$$\varepsilon_{total\ pb} = \frac{N}{EA}\left(1 - \frac{EA_p}{Lk_{ss} + EA_p}\right) + \frac{M}{EI}\left((\overline{y} - y_i) - (\overline{y} - \overline{y}_p)\frac{EA_p^{\ 2}}{EA(EA_p + Lk_{ss})}\right) \qquad - (3.21)$$

where EA_p = axial stiffness of the plasterboard sheeting

y_p = location of neutral axis of plasterboard sheeting

k_{ss} = interconnection spring stiffness between framing and sheeting
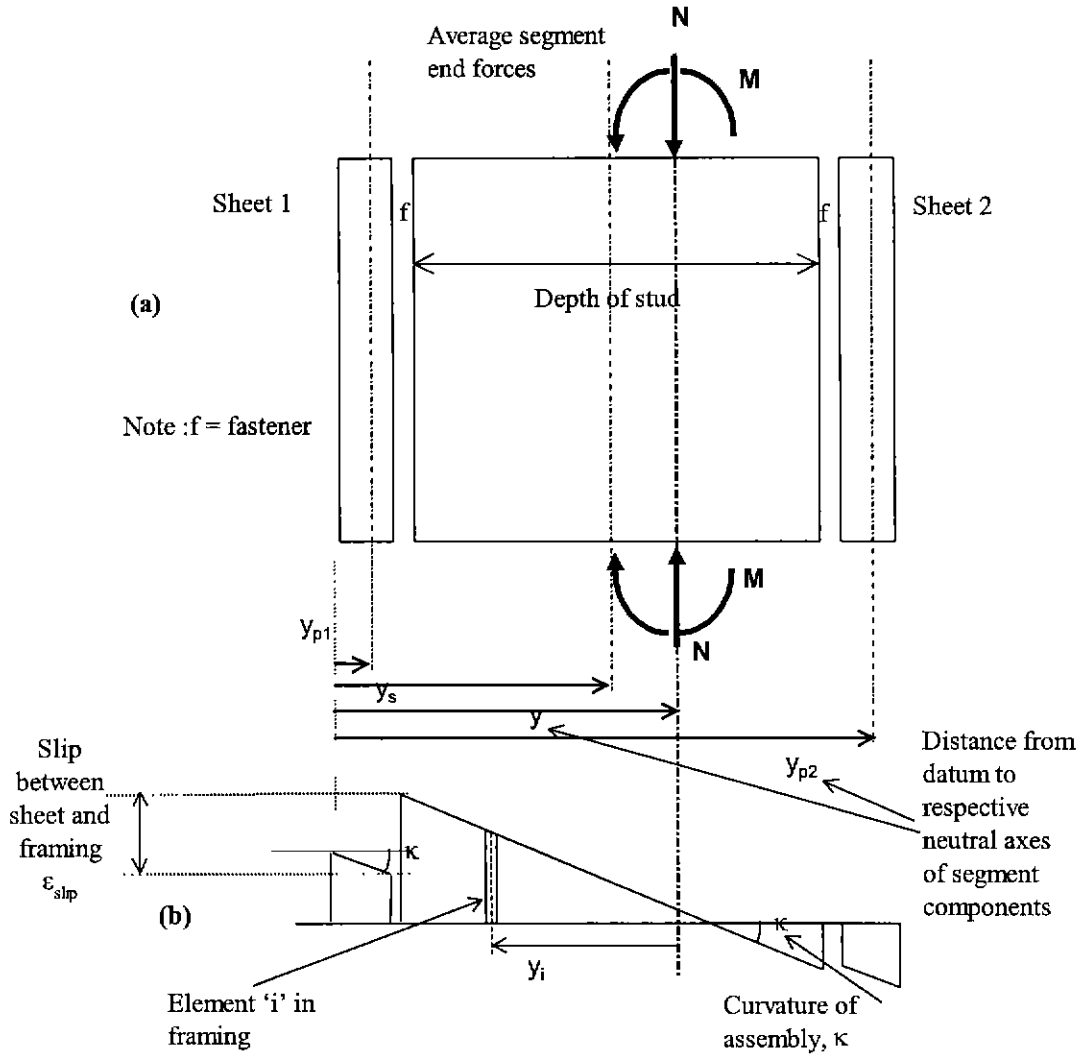
Figure 3.10: *(a) Part Vertical Section through Stud in Wall*
(b) Strain Distribution through Segment

3.6.4 Constitutive Strain Model

The constitutive strain model adopted defined the total strain, ε_{total} as

$$\varepsilon_{total} = \varepsilon_{\sigma} + \varepsilon_{creep} + \varepsilon_{thermal} \qquad\qquad - (3.22a)$$

where ε_{σ} = stress related strain

  ε_{creep} = strain due to creep

  $\varepsilon_{thermal}$ = strain due to thermal expansion

The stress related strain was calculated from rearranging the constitutive equation.

$$\varepsilon_\sigma = \varepsilon_{\text{total}} - \varepsilon_{\text{creep}} - \varepsilon_{\text{thermal}} \qquad \text{- (3.22b)}$$

The strain due to thermal expansion was calculated from

$$\varepsilon_{\text{thermal}} = \alpha_T(T)\Delta T \qquad \text{- (3.23)}$$

where $\alpha_T(T)$ = coefficient of thermal expansion, a function of temperature and the material

comprising the element

ΔT = change in temperature of the element from the reference temperature which defined

the thermal expansion versus temperature relationship

The strain due to creep was not implemented in the model due to a lack of experimental data

available in the literature. Incorporation of creep implicitly in determining appropriate elastic

modulus versus temperature was performed (refer to Chapter 7 for model comparisons with

experimental results). The shortcoming of this technique in considering creep is directly related to

the dependence of creep strain on time and temperature at a given stress level. If stress levels are

different then the mechanical properties implicitly incorporating creep may not be applied to

another situation where the wall configuration is different. This is listed as one of the

recommendations for future research in Chapter 9.

3.7   Calculation of the Unbalanced Force

3.7.1   Introduction

The unbalanced force, $\{P_{ub}\}$ acting on the assembly is defined as the difference between the actual

force applied to the assembly, $\{P\}$ and the calculated force required to attain the deflected shape of

the assembly, $\{P^*\}$. That is:

$$\{P_{ub}\} = \{P\} - \{P^*\} \qquad \text{- (3.24)}$$

The magnitude of the relative difference between the applied force and calculated force gives an

indication of the degree of convergence of the non-linear solution procedure.

The force contribution of each element must be combined to calculate segment end forces, which are in turn used to assemble the vector, {P*}.

3.7.2   Calculation of Stresses in the Partial Composite Section

The stresses were calculated in the elements comprising the partial composite section by inserting the stress related strain calculated in equation (3.22b) into the stress-strain model assumed for the material (§3.3).

3.7.3   Calculation of Forces from Stress-Related Strains

The axial force components, P_{xi}, P_{xj} were calculated by summing the contribution of the axial force in each element within the respective ends of a segment.

$$P_{xi} = \sum_A f_i A_i \qquad\qquad - (3.25)$$

The bending moment components M_i, M_j were calculated by summing the moment contribution of each element within the end of a segment.

$$M_i = \sum_A (\bar{y} - \bar{y}_i) f_i A_i \qquad\qquad - (3.26)$$

where $\bar{y}_i$ is the centroid of stress related strain of an element from a datum

The shear components P_{yi} and P_{yj} are calculated by summing the moment at each end of a segment and dividing by the length of the segment.

$$P_{yi} = \frac{M_i + M_j}{L} \qquad\qquad - (3.27)$$

$$P_{yj} = -P_{yi} \qquad\qquad - (3.28)$$

3.7.4   Assemblage of Calculated Load Vector

The calculated load vector, {P*} for the structure is assembled by converting the segment end forces into global coordinates and adding the contribution of each segment.

3.7.5   Calculation of Unbalanced Force Vector

The unbalanced force vector, $\{P_{ub}\}$ was calculated using equation (3.24). The unbalanced force

vector was reapplied to the structure for the next iteration of the analysis as detailed in Sections

3.2.4 and 3.2.5.

3.8   Failure Criteria

3.8.1   Failure of an Element

The failure of an element within the cross-section of a segment was based on it either exceeding

the maximum allowable stress related strain for the material at a given temperature, or exceeding

the maximum allowable stress for an element. The criterion could be selected was dependent on

the analysis technique used in the model (linear elastic compared with non-linear stress-strain

characteristics). The model can perform analysis using either and some investigation will be

performed to determine the sensitivity in using non-linear stress strain characteristics. However,

the use of non-linear stress strain curves made use of the ultimate stress technique difficult to

implement because the stress may decrease with increased strain beyond that at which the ultimate

stress occurs.

3.8.2   Failure of a Joint Between the Plasterboard Sheets

The model allowed for the horizontal placement of sheets, as is conventional in construction of fire

resistant timber-framed plasterboard-clad walls in Australia (Boral Plasterboard, 1994). Such

placement requires horizontal joints, which are backed by timber noggings, to be covered with

paper tape and gypsum cement. Failure in such a joint was deemed to occur if the tensile stress

related strain on the edges with a segment containing the joint exceeded the maximum allowable

joint strain. The contribution to the segment stiffness of the plasterboard flange in which the joint

had failed was taken as zero.

3.8.3 Failure of the Wall

The failure of a wall was deemed to occur if numerical instability occurred in the solution process. Instability would occur when deflections became large, resulting in a solution of the deflected shape that would not converge through successive iterations or the stiffness matrix being singular. The singularity in the stiffness matrix was indicative of the calculated deflected shape of the wall being impossible.

3.9 Convergence Criterion

The degree of convergence of the analysis was calculated based on the percentage change in mid-height deflection in the out-of-plane direction between iterations. If the percentage change was less than the convergence criterion then another iteration would be performed at the current time-step. At convergence of the solution, the deflections were output and the thermal analysis would recommence until the next time step at which the structural analysis was required to be performed.

3.10 Conclusion

A structural model has been developed to predict the structural response of a timber-framed, plasterboard-clad wall in fire, that considers the relevant phenomena identified in the literature review (§2.7).

The source code for the model, written in Lahey Fortran 77 Level 3 (Lahey, 1992), is listed in Young (2000) - Appendix 2.

4 Mathematical Validation of the Numerical Analyses

4.1 Introduction

This chapter details the mathematical validations of the structural model that were undertaken.

These were to:

(i)   Check the accuracy of the numerical routines employed and

(ii)   Check the validity of the assumption that the sheeting could be represented as a beam

element. That is, the effects of shear lag within the sheeting are not significant.

The following sections briefly detail comparisons for specific cases between the model and both

closed form solutions and where required, finite element analysis (FEA) solutions using

commercially available software to verify the numerical validity of the program.

The final section of this chapter demonstrates the validity in modelling the sheeting as a beam

element. FEA software has been utilised in order to study the effective width of the plasterboard

sheeting, with the sensitivity of parameters associated with the plasterboard sheeting examined to

determine a range of application in assuming a beam element to represent the structural

contribution of the sheeting.

4.2 Mathematical Validation to Check the Accuracy of the Numerical Routines Employed

4.2.1 Introduction

The mathematical validations involved comparisons with elementary cases of out-of-plane elastic

analysis and cases involving combinations of structural phenomena, where the circumstances

precluded the use of a closed form solution due to the complexity, validation was performed using

FEA software, STRAND 6.13 (G+D Software, 1993).

The specific cases considered in the validations were as follows:

- Closed form solutions

  (i)   Linear elastic analysis – deflection of a simply supported beam

  (ii)   Non-linear geometry elastic analysis – deflection of a column with an eccentrically

         applied load

  (iii) Non-linear stress-strain behaviour – uniaxial compression of a column

- Finite Element Analysis with a software package

  (i)   Composite Section Analysis – Thermal expansion of a simply supported beam with

         an applied load.

  (ii)   Shrinkage of the Plasterboard Sheeting – Interaction between sheeting and stud.

The validation cases performed considered most aspects of the structural model analysis

capability. However, in some instances, the FEA software had limitations, which prevented the

direct validation of some aspects including more complicated examples with non-linear

mechanical properties and partial composite action. Such limitations included the inability to

consider different stress-strain characteristics in compression and tension, and numerical

instabilities induced with non-linear mechanical properties at supports or connectors between the

sheeting and framing. The structural model predictions were further validated by comparison with

full-scale ambient and fire endurance tests being performed as detailed in Chapter 7.

4.2.2   Linear Elastic Analysis - Deflection of a Simply Supported Beam

Load, P

P = 1000 N
E = 8*10⁹ Pa
L = 3m
D = 90 mm
B = 45 mm

Length, L

X
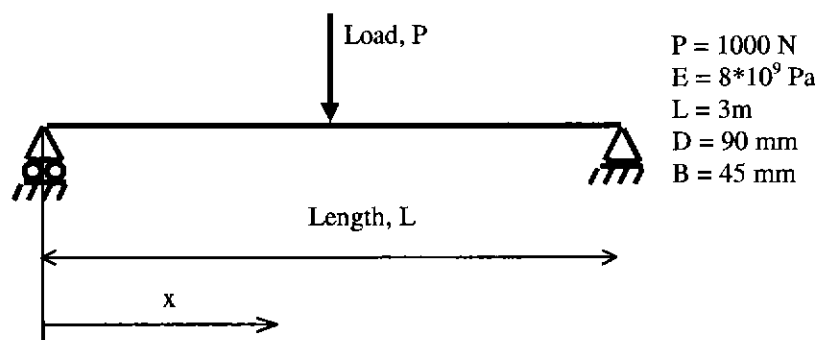
Figure 4.1: Structural System Considered for a Simply Supported Beam

The closed form solution to described the deflected shape, δ (x), for a beam of length, L, along the

length (x) with the flexural stiffness, EI and applied load, P is given in Timoshenko (1955) as:

$$\delta(x) = \frac{Px}{12EI}\left(\frac{3L^2}{4} - x^2\right) \qquad \text{for } x \le L/2 \qquad \text{- (4.1a)}$$

$$\delta(x) = \frac{PL}{24EI}\left(2Lx - x^2 - \frac{L^2}{4}\right) \qquad \text{for } x \ge L/2 \qquad \text{- (4.1b)}$$

The comparison between the closed form solution and predictions for the structural model for this

case are shown in Figure 4.2. Very close agreement has been demonstrated for this case.
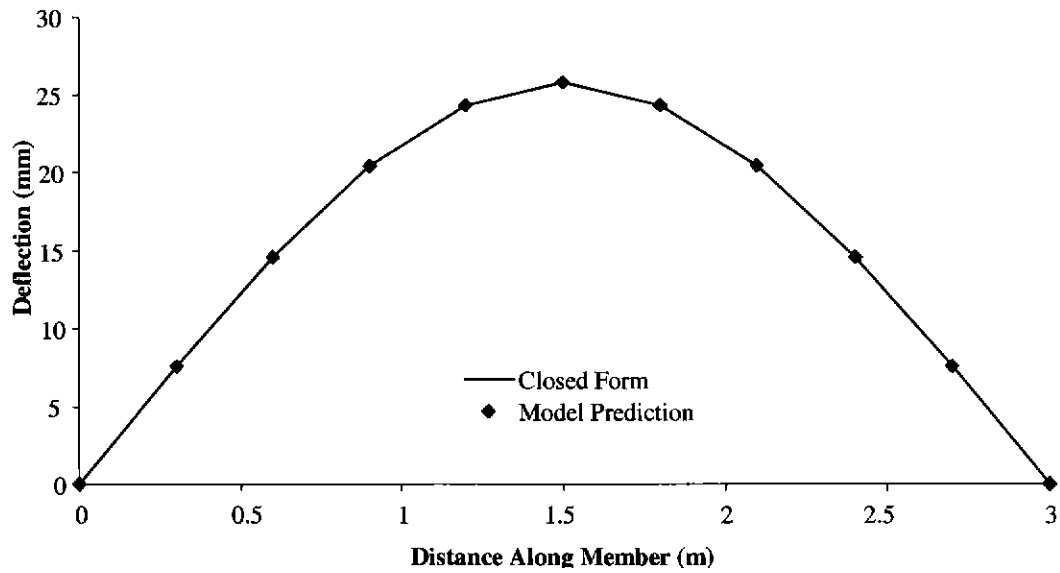
Figure 4.2: *Comparison between the Deflections Determined for the Closed Form Solution and*

Structural Model for a Simply Supported Beam with Applied Load and Linear Elastic Material

Properties

4.2.3 Non-Linear Elastic Analysis - Deflection of a Column with an Eccentrically Applied Load with Combined Bending and Compression

The closed form solution for the deflected shape, δ (x) of a column of flexural stiffness, EI, length, L, with a load, P, applied at an eccentricity, e, (refer to *Figure 4.3*) from Timoshenko (1956) is:

$$\delta(x) = e\left(\frac{\sin\rho x}{\sin\rho L} - \frac{x}{L}\right)$$

- (4.2)

where $\rho = \sqrt{P/EI}$

e $\leftrightarrow$ Load, P, applied at eccentricity, e

P = 14400 N
E = 8*10^9 Pa
L = 3m
D = 90 mm
B = 45 mm
e = 10mm

Length, L

x
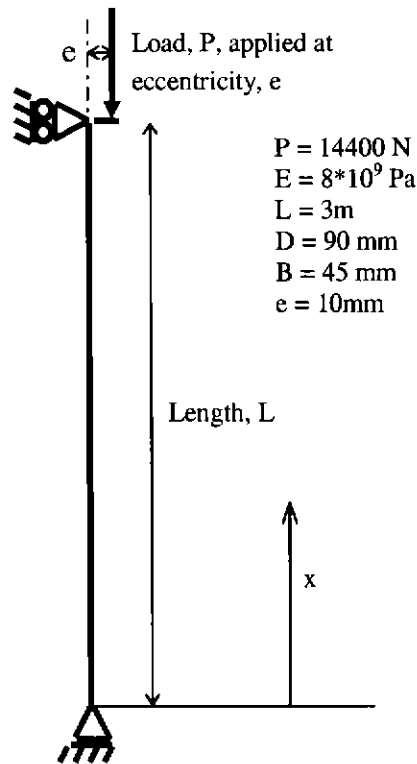
Figure 4.3: Representation of the Structure Considered for the Validation of the non-linear

Geometry Routine

The comparisons between the deflected shape and closed form solutions are shown in Figure 4.4. The load level applied was 60% of the Euler buckling load. A sensitivity study of the number of elements that the column has been divided along the length was performed. The results indicate an accurate prediction of the mid-height deflection even with ten elements along the length.
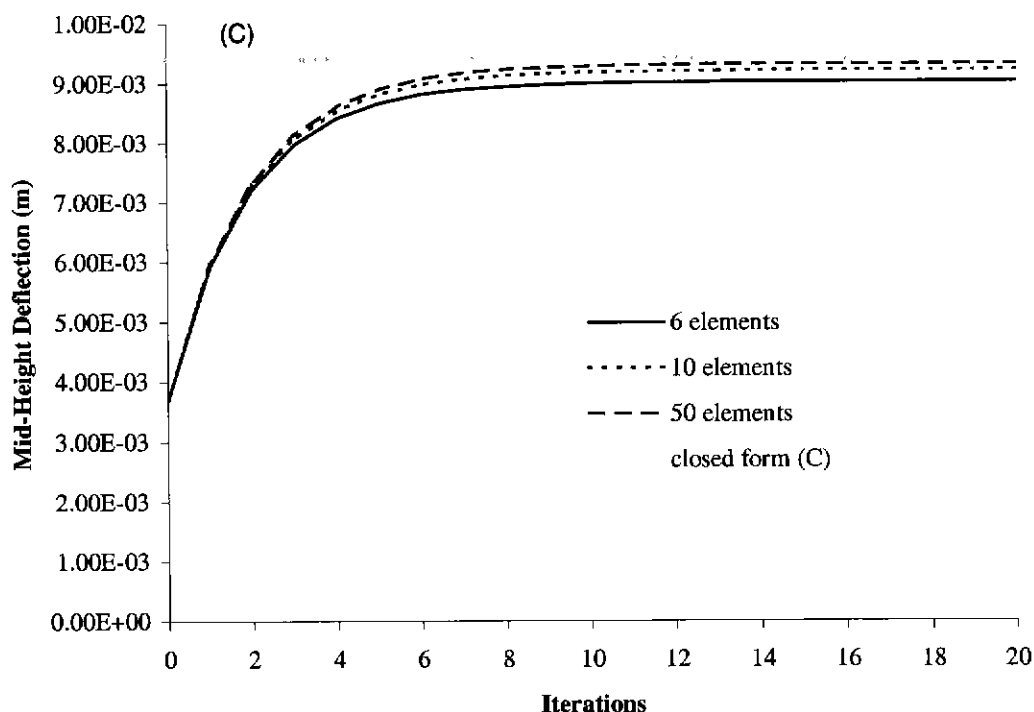
Figure 4.4: Comparison between Closed Form Solution and Structural Model Predictions, for Different Numbers of Subdivided Elements along the Length versus the Number of Iterations Required to Converge to a Solution

4.2.4 Non-Linear Stress-Strain Behaviour

A column assumed to be loaded purely with axial compression force was considered with the aim to verify the accuracy of the iterative routines employed in the structural model to consider non-linear stress-strain behaviour. The results from the structural model were compared with the theoretical axial compression calculated from the stress-strain curve selected for timber in compression (equation 3.2).

A column 1 m long, with cross-section 90mm x 45mm was selected. The modulus of elasticity was 8 GPa, the ultimate strength in compression was 24 MPa. An axial load of approximately 90 kN was applied to the column, equivalent to a theoretical strain of 0.0032. The theoretical axial deformation was 3.2mm, the model predicted 3.24mm assuming convergence between iterations of 0.1%. It was difficult to increase the axial load to follow further on the non-linear portion of the curve due to numerical round off effects that would induce small out-of-plane deflections and

result in the member buckling. The comparison indicated that the non-linear stress-strain algorithm within the structural program would correctly follow a non-linear stress-strain curve.

The Strand 6.13 FEA software (1993) had some limitations in considering non-linear mechanical property behaviour, in particular, it could not differentiate between compression and tension for a defined stress-strain relationship. The FEA software was therefore not used to consider more complicated methods of analysis involving non-linear mechanical properties. Thus for the particular application associated with the thesis, the model developed was more capable than the generic FEA software.

4.2.5 Composite Section Analysis - Thermal Expansion of Simply Supported Beam, with an Applied Load

The following analysis is to determine the validity in using the composite section theory in conjunction with phenomena of thermal expansion and a loaded member. A linear thermal gradient was assumed through the depth of the beam as shown in Figure 4.6 and the relationship shown in Figure 4.7 for the degradation in mechanical properties with temperature.
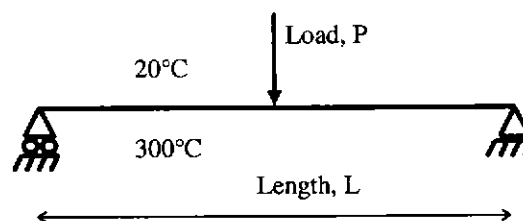
Figure 4.5: Structural System Considered for a Simply Supported Beam, With other Phenomena
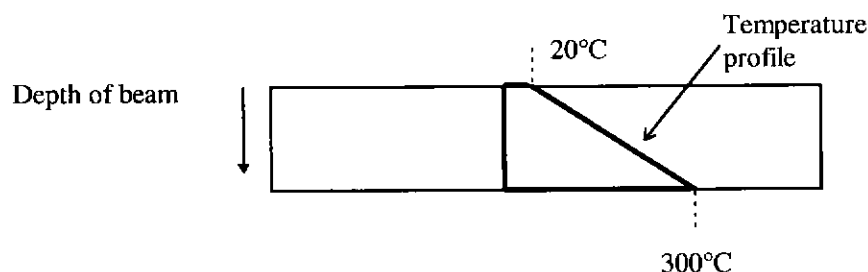
Figure 4.6: Assumed Temperature Profile Within Beam (constant distribution through width).
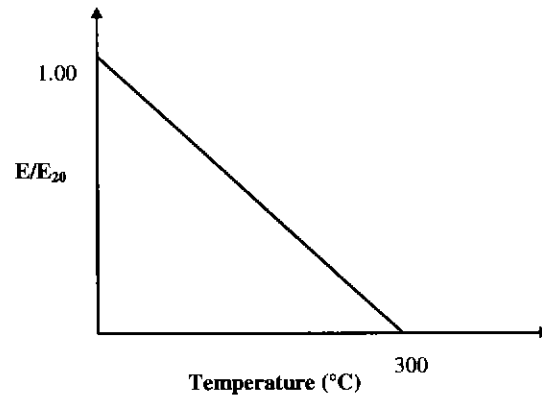
Figure 4.7: Assumed Reduction in Mechanical Properties for Numerical Validations

The deflection results in Figure 4.9 obtained from the FEA (Figure 4.8) and structural model can

be seen to give a very close comparison for this case.
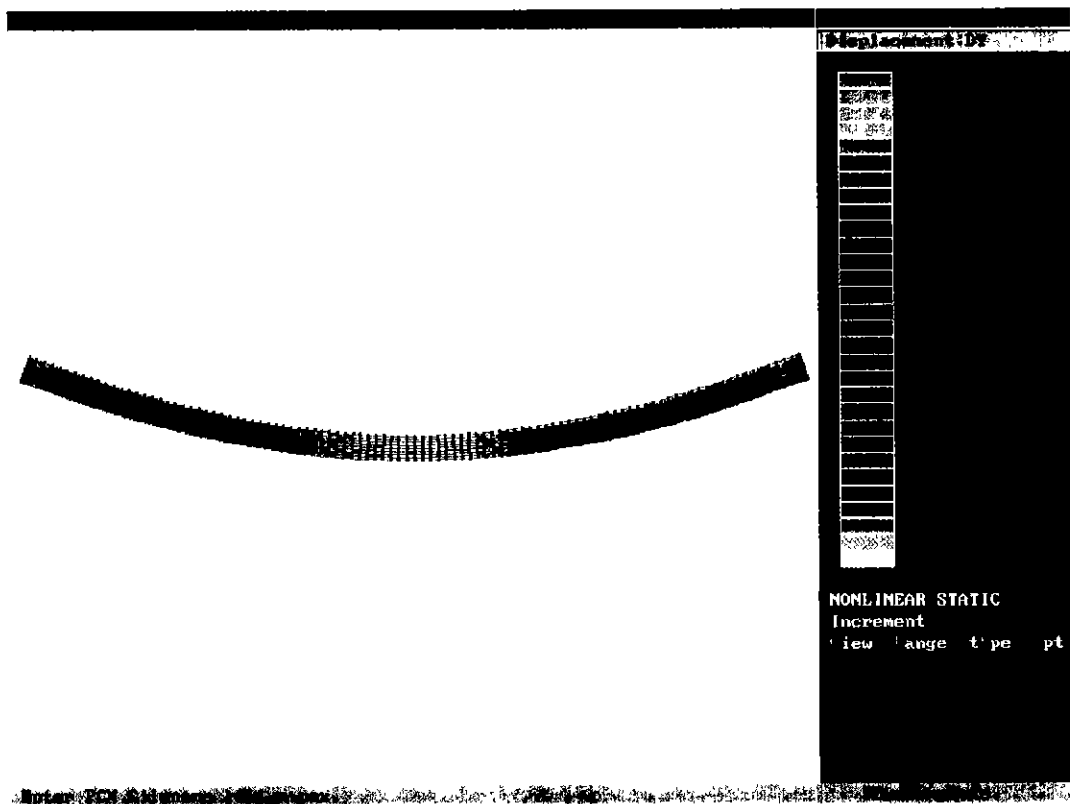
Figure 4.8: FEA Model from STRAND 6.13 (1993) – Output from Considering the Effects of a

Distribution of Temperature with Thermal Expansion and Change in Modulus of Elasticity with

Temperature and an Applied Load
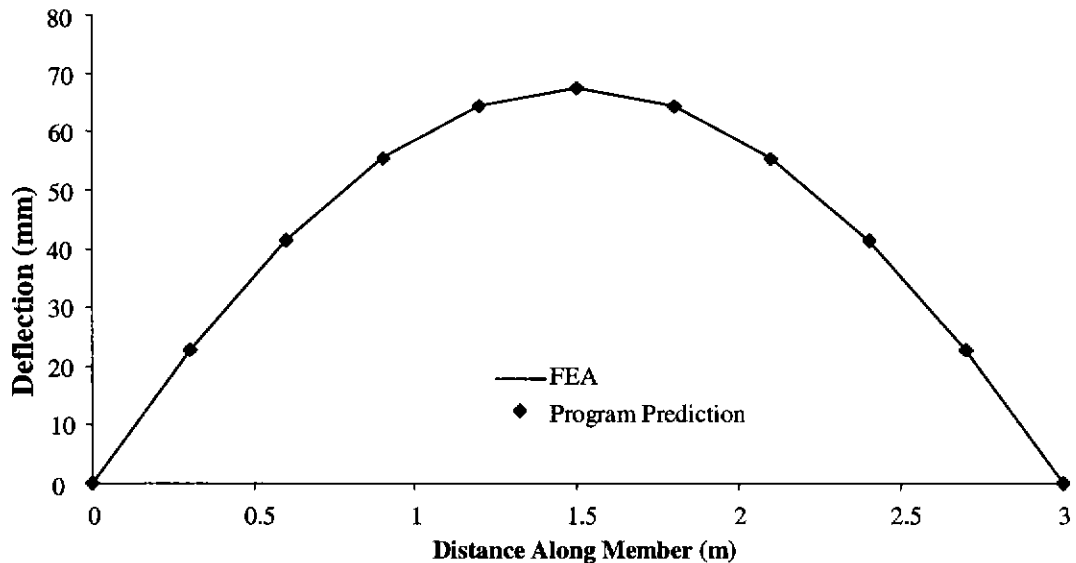
Figure 4.9: *Comparison Between FEA by STRAND 6.13 (1993) and Structural Model Predictions*

Considering the Effects of a Distribution of Temperature with Thermal Expansion and Change in

Modulus of Elasticity with Temperature and an Applied Load

4.2.6   Shrinkage of the Plasterboard Flange

The efficacy of modelling the composite action provided by the sheeting, and also the transfer of

thermal strain induced into the sheeting to the remaining components of the assembly was

examined. The configuration used for validation was as follows:

- A column 3 m long, timber stud was 90 mm x 45 mm, modulus of elasticity timber 8 GPa,

- Plasterboard sheeting 600 mm wide, 10 mm thick, modulus of elasticity 1 GPa.

In the analysis it was assumed that one of the sheets of plasterboard had a different and uniform

temperature applied that resulted in a shrinkage strain of 0.0029. Full composite action was

assumed. The output from the FEA is shown in Figure 4.10.
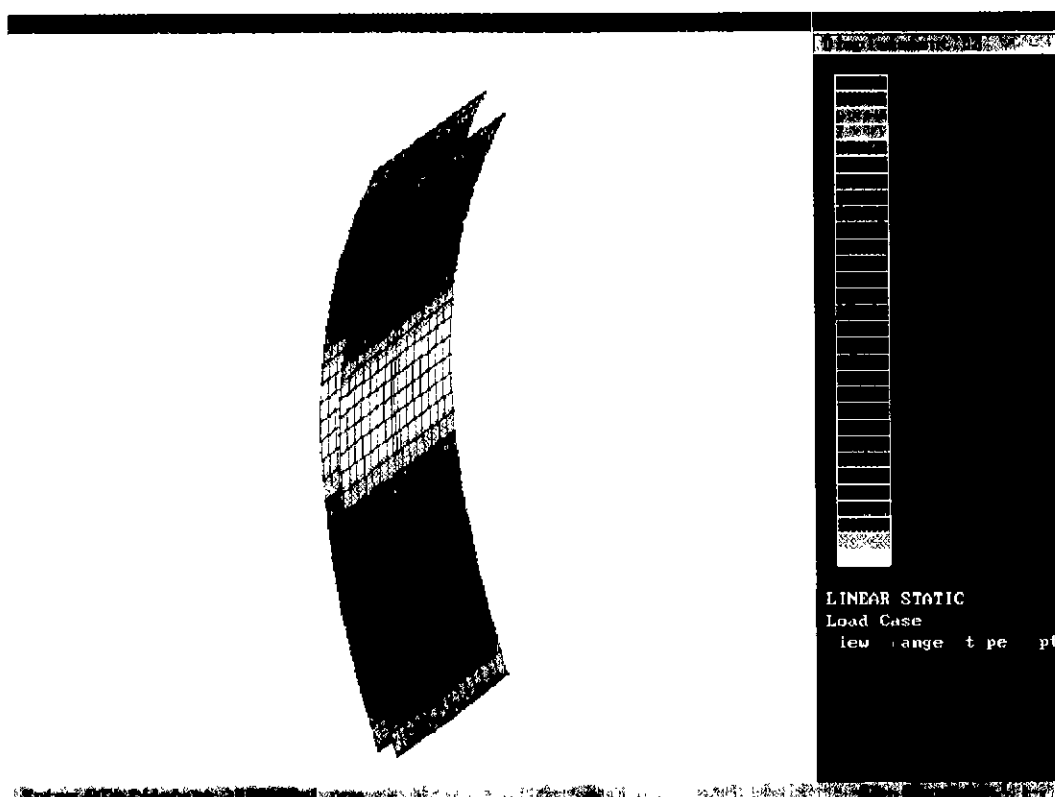
Figure 4.10: *Output from the FEA Model using STRAND 6.13 (1993) –Considering the Shrinkage*

of the Plasterboard Sheeting Flange

Figure 4.11 demonstrates that the results from the FEA and predictions made by the structural model were very close – being within 2.5%. The main discrepancy was identified to be associated with the assumption of the effective width of the sheeting being equal to the stud spacing.

Reducing the width of the plasterboard sheeting to 560mm from 600mm in the structural model resulted in a closer comparison between the two results. This is indicative of the phenomenon of shear lag. A study has been conducted later in this Chapter (§4.3) which examines the assumption that the effects of shear lag in the plasterboard sheeting for conventional construction spacings are insignificant and can be ignored.
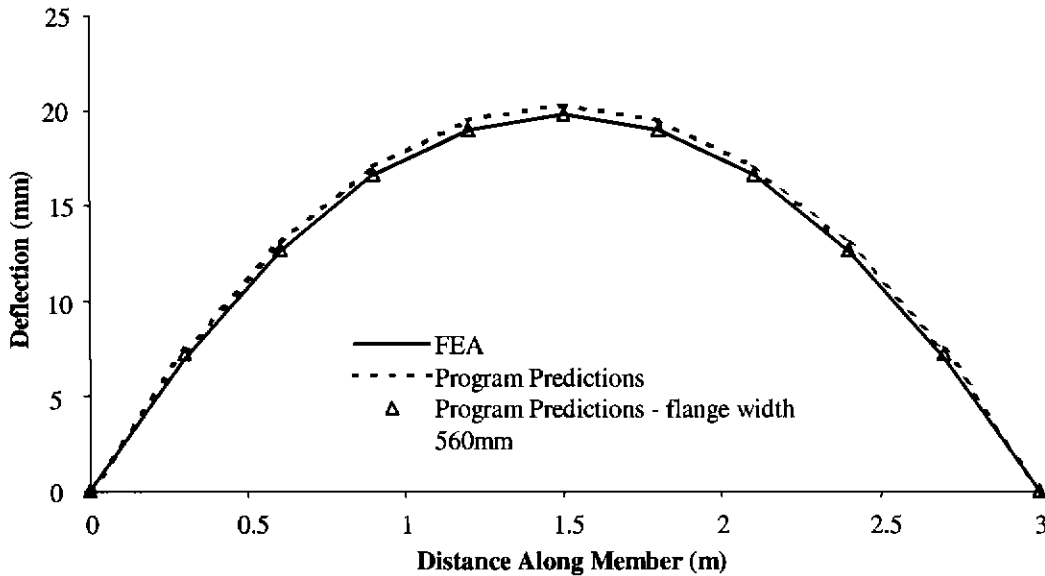
Figure 4.11: *Comparison between FEA and Structural Model Predictions considering the*

Scenario of the Shrinkage of the Plasterboard Sheeting Flange

4.2.7   Additional Considerations in Validating the Structural Model with FEA software

Validations could not be reliably performed for members with all of the phenomena considered by both methods - the structural model with the FEA software. In some instances, meaningful correlation between the two methods could not be performed due to the differing assumptions associated with the location of the position of restraint relative to the neutral axis. The assumption in the structural model was that the position of restraint was at the neutral axis of the member. The modelled load position was fixed, but the real position of restraint during fire exposure would tend to move with thermal degradation as shown in Figure 2.14. FEA software used in the validation fixes both the position of the load and the position of the restraint as these conditions are assigned to nodes. The construction of a wall loaded in compression will tend to result in a movement of the location of the restraint as the cross-section degrades due to the effects of fire. Thus the structural model assumptions with regard to the movement of the position of restraint are considered to be more representative of the real situation than could be represented in the FEA software, without reconstruction of the FE model at every time-step.

The phenomenon of partial fixity between the plasterboard sheeting and timber stud was not validated by comparing the structural model with FEA. The FEA software required small elements, which at low stiffness levels would become numerically unstable if a non-linear analysis was performed. For elements of a higher stiffness, numerical instabilities would be induced during non-linear analysis, in the region of the connector at high load levels. The model developed thus provided a more robust solution approach than generic FEA software for the range of partial fixity from no composite action to full composite action. The validation of the method of implementing partial fixity in the structural model was determined by manually checking the bounds of the calculated flexural stiffness for a range of interconnection stiffness values substituted into equations (3.10) – (3.13). An example of such a check is shown in Figure 4.12.
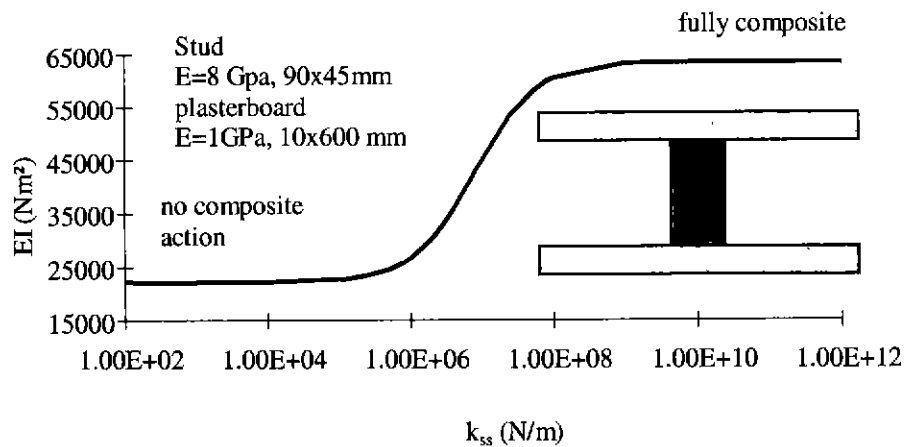
Figure 4.12: Example of Bounds Check of Partial Composite Action Insertion of Values into Equations (3.10)-(3.13) using Excel Spreadsheet Note the variation in the flexural stiffness has been exaggerated as the Y-axis does not commence at zero

The calculation of the flexural stiffness in the manner used in the structural model is shown to be bounded between that of the sum flexural stiffness of each of the components, to the flexural stiffness that is representative of full composite action. The actual calibration for the magnitude of the interconnection spring stiffness must be determined from comparisons with experimental data. This has been carried out in Chapter 7 using the results from the ambient experimental series in Chapter 5.

4.2.8 Conclusions from Mathematical Validation

The mathematical validations indicated a close comparison of the structural model developed with the closed form and FEA software solutions. The magnitude of difference was generally less than 1%.

4.3 Examination of the Validity in Ignoring Shear Lag in the Plasterboard Sheeting

4.3.1 Introduction

One assumption made in the structural model was that the effect of shear lag within the plasterboard sheeting was minimal and thus the entire width of the sheeting would be effective (That is, contributing equally to structural resistance). However, this does not occur in practice, as the resistance would be reduced (refer to Timoshenko *et al*, 1970) at locations in the plasterboard furthermost from the web (That is, the stud) due to the shear lag. The phenomenon of shear lag can be seen in a qualitative sense by considering the results of an FEA considering three different stud spacing widths (Figure 4.13). The greater distortion in the ends of the wider plasterboard flanges can be seen, as can the non-uniformity of displacement at a cross section taken through a given height.

(a)	**(b)**	**(c)**
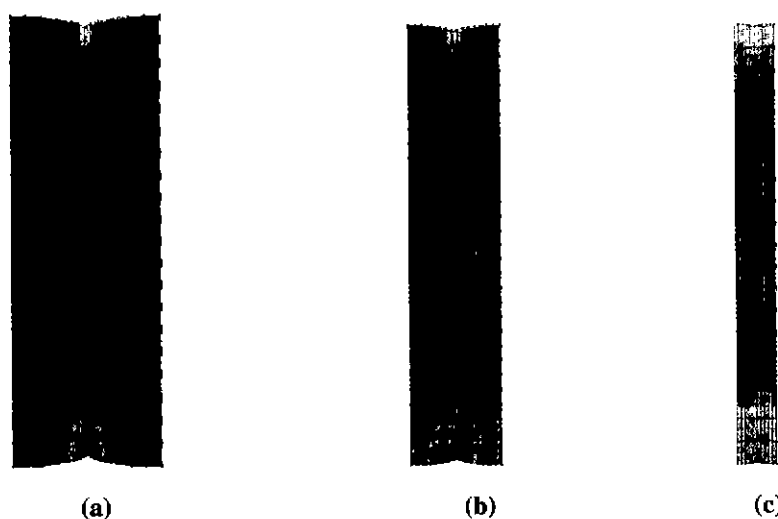
Figure 4.13: Reduced Shear Lag With Reduced Width of Plasterboard, for (a) 1000 mm, (b) 600 mm and (c) 250mm wide. Note that each shade of grey represents equal displacement.

The assumption in the model that the full width is effective has therefore examined in this section. The effective width of the plasterboard sheeting acting compositely with each stud in a light timber-framed wall will be determined by the use of FEA. FEA has been used due to the complexity in deriving closed form solutions to determine the effective width. The difference between the effective width with the actual width of the plasterboard (inter stud spacing) and the difference in the overall effect on structural behaviour is evaluated. The sensitivity of several parameters has been investigated in determining the value of the effective width and the resultant overall effect on the structural behaviour.

4.3.2 Methodology

4.3.2.1 General

The methodology applied in this study on shear lag was based on developing a representation of a timber wall using an FEA software package, STRAND 6.13 (1993). Closed form solutions for the structural response for the out of plane deflection of a simply supported beam and Euler buckling of a column were compared with the results obtained from the FEA. The effective width of the plasterboard sheeting was calculated by relating the closed form solution formulae to the results from the FEA.

The segment of a wall considered in the study was a composite 'I' section (refer to Figure 4.14 overleaf) the web being the timber stud and the flanges being the plasterboard sheeting, the width of which was equal to the stud to stud centreline spacing of the wall. It may be argued that a 'T' section may be more applicable in the case of a fire as the plasterboard sheet on the exposed face does not contribute to the structural response for the majority of a fire endurance test. However, the use of an 'I' section provides a greater proportion of the section that carries forces in the flanges and thus would give a more substantial demonstration of shear lag compared with the use of a 'T' section.

Full composite action was assumed to occur in the nailed connection because it is representative of an extreme case of force transfer into the plasterboard, that is, the case when the plasterboard is most active in providing structural resistance.

The FEA solution procedure employed was based on linear elastic mechanical and geometrical behaviour. The use of non-linear analysis with the FEA representation of the wall had resulted in numerical instabilities being introduced either within the elements representing the fasteners or in the interface between the fasteners and sheeting/framing.

4.3.2.2   Composite Beam Theory

The direct application of composite section theory was used to determine the flexural stiffness of the cross section of the wall.
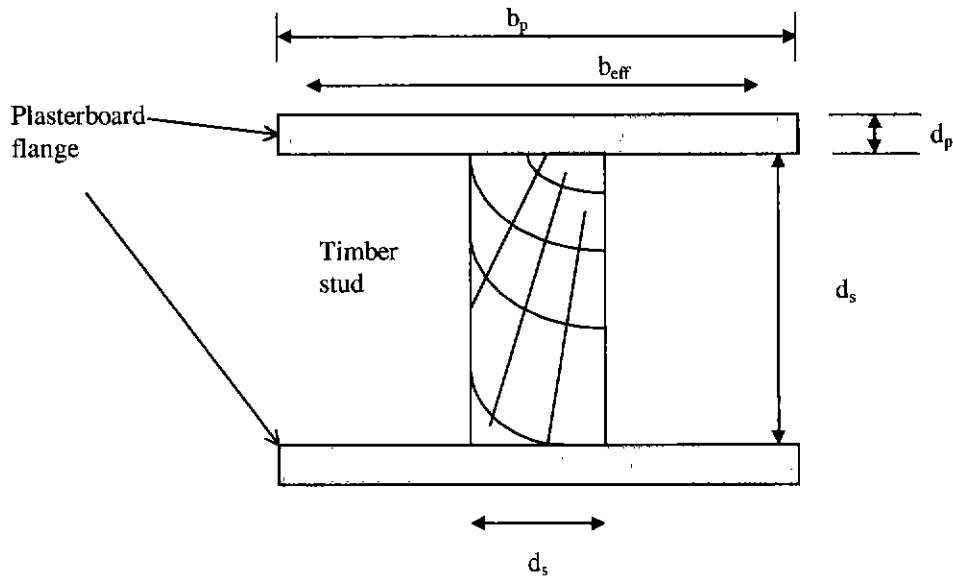
Figure 4.14*: Horizontal Cross Section of Representative Part of Wall*

Application of composite section theory assuming full shear transfer at the plasterboard/timber interface for the cross section shown in Figure 4.14 gives the flexural stiffness, EI as:

$$EI = 2\left(EA_p \left(\frac{d_p}{2} + \frac{d_s}{2} \right)^2 + EI_p \right) + EI_s \qquad \text{- (4.3)}$$

where EA_p, EI_p are the axial and flexural stiffness of the plasterboard flanges

EI_s is the flexural stiffness of the timber stud

4.3.2.3   Consideration of the Euler Buckling Solution of a Pin-Ended Column

This flexural stiffness was then applied directly in the Euler expression for the elastic buckling of a

pin-pin ended column from Timoshenko (1955). The Euler expression being:

$$P_{cr} = \frac{\pi^2 EI}{L^2}$$

$\qquad$ - (4.4)

where P_{cr} is the critical load at which elastic buckling occurs

L is the length of the column

Combining the results of (4.3) & (4.4), and assuming P_{cr} has been obtained from the finite element

analysis, the effective width of the plasterboard, b_{eff}, is calculated from:

$$b_{eff} = \frac{\dfrac{L^2 P_{cr}}{\pi^2} - EI_s}{2E_p \left[d_p \left(\dfrac{d_p + d_s}{2} \right)^2 + \dfrac{d_p^3}{12} \right]}$$

$\qquad$ - (4.5)

4.3.2.4   Consideration of out-of-plane deflection of a Simply Supported Beam

For a concentrated load, P applied at mid-span of a simply supported beam, the deflection from

Timoshenko (1955) is calculated with:

$$\delta = \frac{PL^3}{48EI}$$

$\qquad$ - (4.6)

again, as with equation (4.5), combining the results of equations (4.3) & (4.6) and assuming δ has

been calculated from a finite element analysis, the effective width of the plasterboard is

determined using

$$b_{eff} = \frac{\dfrac{PL^3}{48\delta} - EI_s}{2E_p \left[d_p \left(\dfrac{d_p + d_s}{2} \right)^2 + \dfrac{d_p^3}{12} \right]}$$ - (4.7)

4.3.2.5   Limitations of the technique

It must be noted that calculating the effective width in this manner assumes that the FEA

representation is ideal, that is, it was capable if the full width is effective of producing exactly the

same result as the closed form solution. The key assumption was therefore that the effective width

of the plasterboard is the *only* reason for discrepancy between the Euler / closed form solution and

finite element representation. Minor errors in calculation of the critical buckling load or

deflections due to the numerical idealisation of the wall will cause apparent changes in the

effective width. However these discrepancies are considered to be minor, particularly as two

different techniques have been used to consider the effective width. As the plasterboard

contribution to stiffness reduces relative to the wall, equations (4.5) & (4.7) will become more

affected by discrepancies between the closed form solution and FEA approximation. This

necessitates that a change in effective width should be put into context with the overall change in

structural response. Results presented in this study have therefore shown the overall effect on the

buckling load / out-of-plane deflection in comparing Euler / closed form deflections and FEA

solutions on the primary y-axis and the effective width calculated with equations (4.5) and (4.7) on

the secondary y-axis.

4.3.2.6   Finite Element Analysis Model

4.3.2.6.1   General

The FEA was performed using the Strand 6.13 software (1993). The model consisted of beam

elements representing the timber stud, plate elements representing the plasterboard flanges and

stiff beam elements connecting the stud to the plasterboard, representing the nails. Refer to Figure

4.15 to Figure 4.17 for a depiction of the finite element model. The plate elements representing the

plasterboard were plate-shell elements because of the need to consider primarily out-of-plane

deflections.
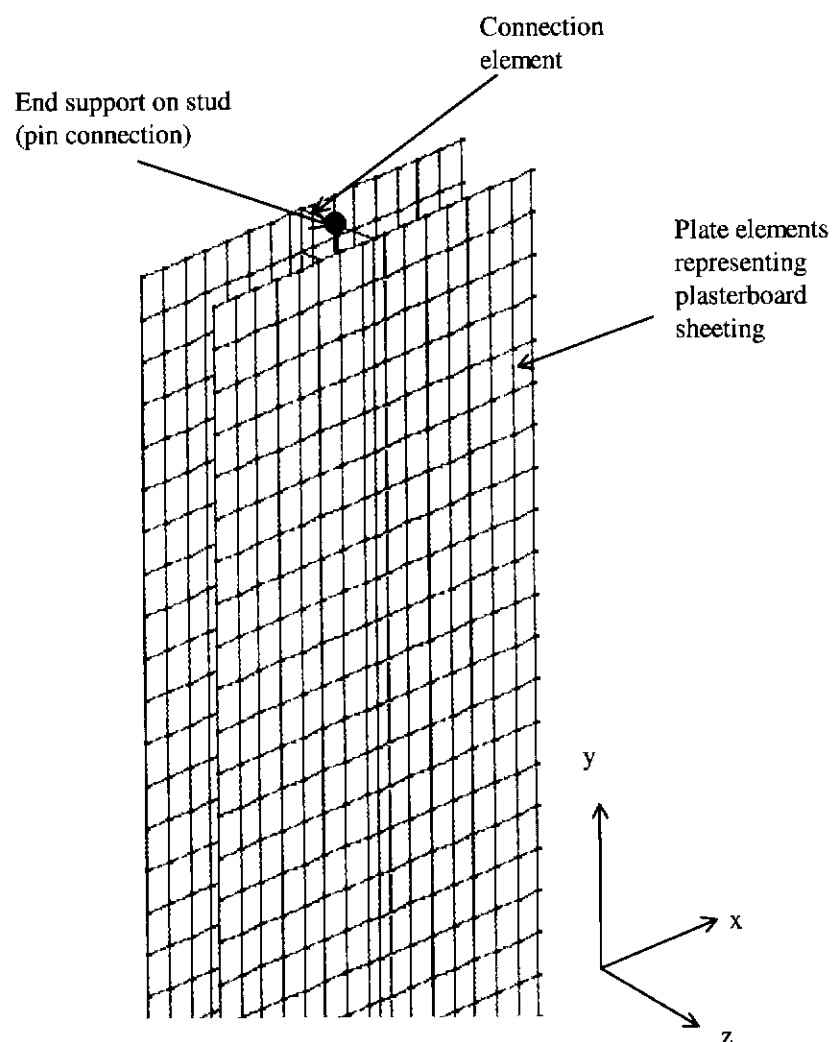
Figure 4.15: *Finite Element Model: Three Dimensional Representation*
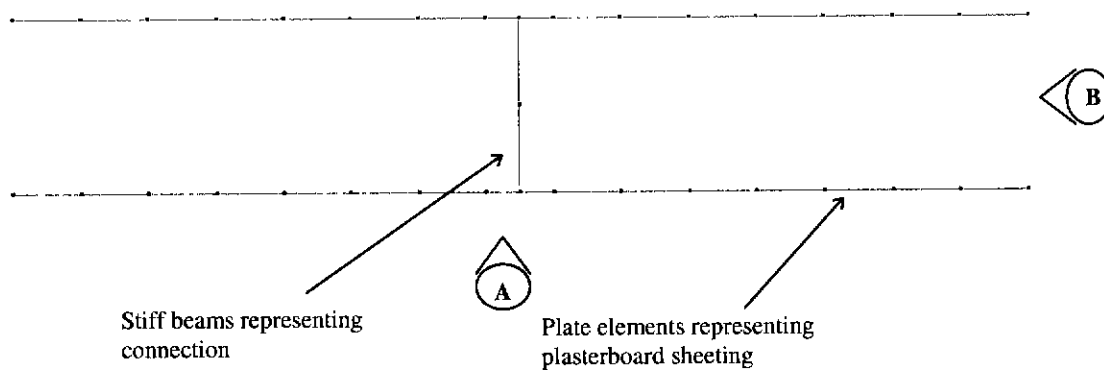
Figure 4.16: *Finite Element Model: Plan View*

P - load applied for buckling analysis

Fixity at end of stud :
DX=1,DY=0,DZ=1,
RX=0,RY=1,RZ=1

Note with regard to
restraint : DX refers to
displacement in the X
direction, RX refers to
rotation about the X-
axis. A restraint
condition of DX=1
means displacement
for this degree of
freedom is prevented.

Connection
elements (beams,
pin ended) between
stud and
plasterboard

Pδ - load applied for bending
(located at mid-height)

Fixity on nodes on
edge of wall segment:
DX=1,DY=0,DZ=0,
RX=0,RY=1,RZ=1

y

y

z

x

Fixity at end of stud :
DX=1,DY=1,DZ=1,
RX=0,RY=1,RZ=1

Figure 4.17: Finite Element Model - Front (A) & Side (B) Elevations Respectively

As shown in Figure 4.17, the stud is assumed to carry all load into the wall panel, and all load

carried by the plasterboard is passed via the connection elements from the stud. While this may not

be true in practice, it is an extreme situation assumed to provide a conservative solution with the

regard to the force transfer into the stud. Note that the loads applied P, Pδ were applied as two

distinctly separate load cases.

4.3.2.6.2   Restraint Conditions

The global restraint condition applied to all nodes was to prevent the panel twisting about the stud axis, thus the rotational degrees of freedom about the y and z axes (RY, RZ) were defined as fixed. The column end conditions were consistent with those of a pin-pin ended column / simply supported beam. Consistent with the restraint existing in a real wall, restriction to displacement in the plane of the wall (DX) was applied at the ends of the column, and on the nodes on the edges of the plasterboard flanges. While this can make the wall slightly stiffer due to Poisson's ratio effects, it is more closely representative of a wall in practice.

4.3.2.6.3   Fastener Behaviour

A sensitivity study on the role of the stiffness of the beam fastener was made to ensure the fastener element was stiff enough to assume full composite action occurring between the plasterboard and stud. The results of the study are shown in Figure 4.18. These show clearly that the transition between no composite action and full composite action occurs in the region with the elastic modulus of the fastener being between 10^3 Pa and 10^8 Pa. The value used in this component of the thesis was limited to that at which the phenomenon of full composite behaviour was certain to occur, where the proportion of force transferred into the sheeting would be maximised, and the phenomenon of shear lag associated with the effectiveness of the sheeting would be most apparent. It should also be noted that this study involved linear elastic analysis (linear buckling and bending) to avoid numerical instabilities induced by incorporating the spring stiffness in the FEA software in a non-linear analysis.
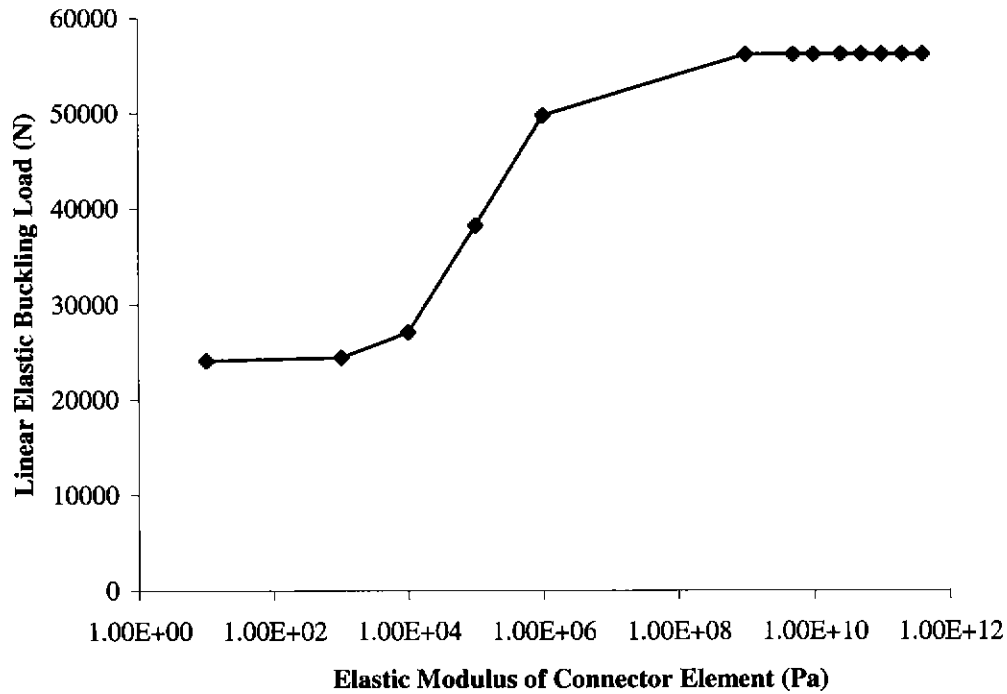
Figure 4.18: Sensitivity of Elastic Modulus of Connector Beam on Linear Elastic Buckling Load

4.3.2.6.4   Sensitivity of Parameters

The sensitivity of several key parameters on the effective width was considered in the analysis.

The parameters considered were those that were likely to be affected during the exposure of a

timber-framed wall to fire. The parameters were:

- Width of the plasterboard between studs.

- Height of the wall.

- Thickness of the plasterboard.

- Modulus of Elasticity of the plasterboard.

- Modulus of Elasticity of the timber stud.

The width of the plasterboard (stud spacing), height of the wall and thickness of the plasterboard

sheeting were considered with the aim of evaluating the range of application for which the

assumption of the full width of the plasterboard sheeting being applicable was valid.

Consideration of the effect of changing the modulus of elasticity of the plasterboard and timber

stud was performed because the mechanical properties of these materials when exposed to fire

change with temperature. The discretisation of the finite element model, global restraints applied

and interconnection performance were also considered during the developmental stages of the

model.

4.3.2.7   Results

4.3.2.7.1   Introduction

The results that follow demonstrate how the effective width determined from equations (4.5) and

(4.7) relate to the parameters that were to be considered in Section 4.3.2.6.4. The results presented

use both an elastic buckling analysis and a linear elastic analysis considering out-of-plane

deflections, to reduce the likelihood of inherent errors in finite element models in affecting the

calculated effective width with each parameter considered.

The graphs in the following section show on the y-axis on the left, the overall effect on the

structural response (buckling load or deflection) resulting from the assumption that the full width

is effective compared with the FEA solution. The y-axis on the right of the following graphs

shows the effective width calculated from equations (4.5) and (4.7) respectively.

Unless otherwise specified for the following results, the properties of the walls considered in this

study assume a 90 mm deep x 45 mm wide cross-section timber stud of elastic modulus 8 GPa, 10

mm thick by 600 mm wide plasterboard sheeting of elastic modulus 1 GPa. These values are

typical of wall construction in Australia (refer to AS1720.1 and Boral Plasterboard, 1994).

4.3.2.7.2   Changing Stud Spacing Between Plasterboard (Increasing Flange Width)

Referring to Figure 4.19(a) and Figure 4.19(b), these show that increasing the flange width

resulted in a corresponding increase between the closed form formulae and the FEA solution. This

result was expected in that the magnitude of the difference between the flange width and effective

width increase proportionally to the width of the flange. The magnitude of the error between the

closed form solutions, which assumed the full width was effective, and those from the FEA was of

prime importance. In this case, for conventional wall construction options of either 450 mm or 600

mm stud spacing, the assumption of the entire width of the plasterboard being effective was close.

For 600mm spacing, a discrepancy in buckling capacity of under 2% was calculated. The 2.4m

high wall shows a decrease in the effective width compared with the same corresponding 3.0m

high wall. Hence it was determined that the assumption to assume the entire width of the

plasterboard sheeting is effective for conventional constructions with stud spacing of 600mm and

less is reasonable.
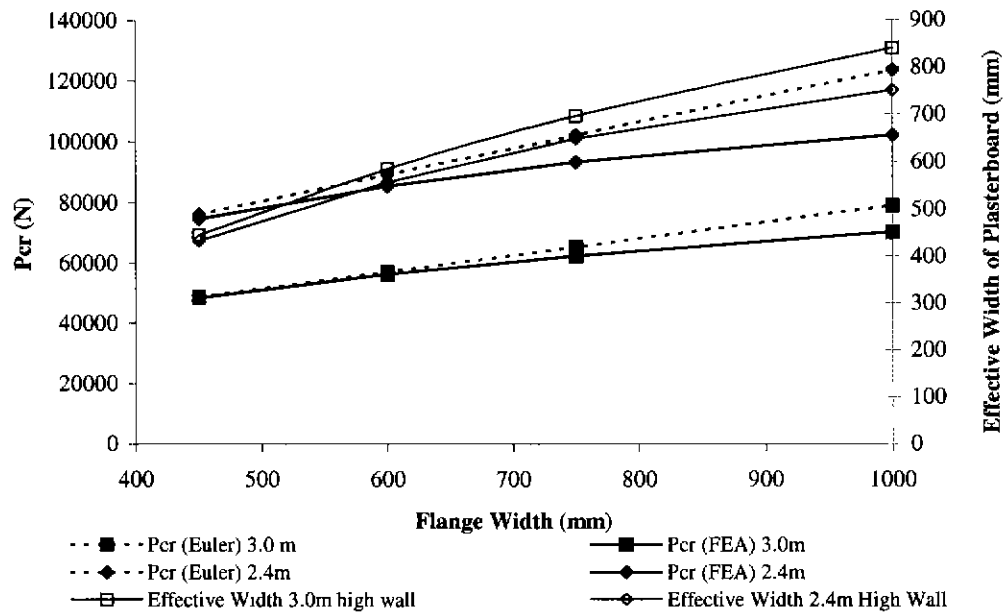
Figure 4.19 (a): Buckling Load Using Euler Solution and Finite Element Analysis & Effective

Width Calculated versus Flange Width
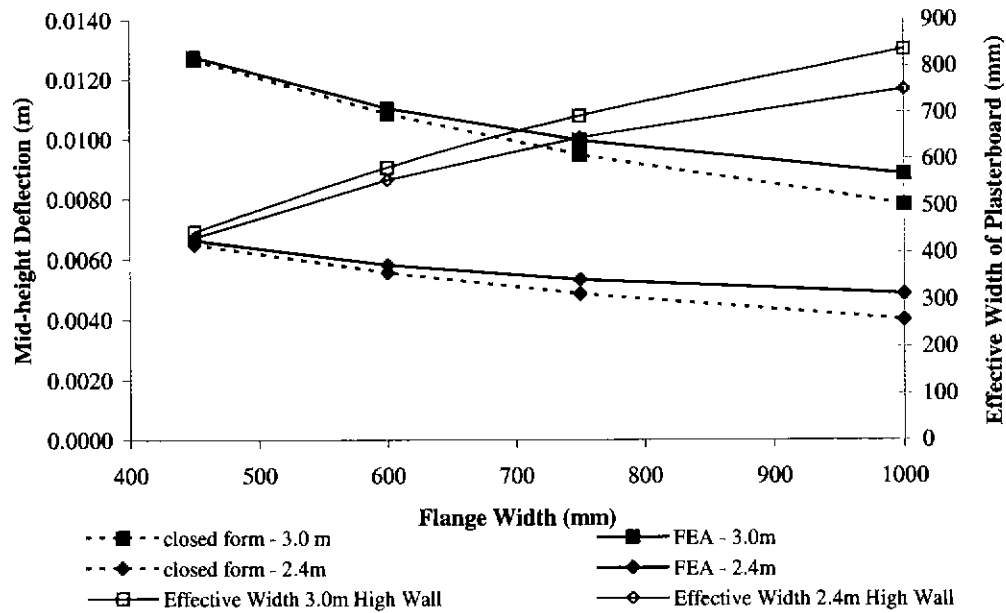
Figure 4.19(b): *Mid-height Deflection for 1kN load using Closed Form Solution and FEA &*
Effective Width Calculated Versus Flange Width

4.3.2.7.3   Changing Plasterboard Thickness

Figure 4.20 (a) and Figure 4.20 (b) highlight the insensitivity of the effective width of the

plasterboard to changing thickness for a stud spacing of 600 mm. The maximum reduction in the

effective width compared to the stud spacing is for 2.4m high walls.
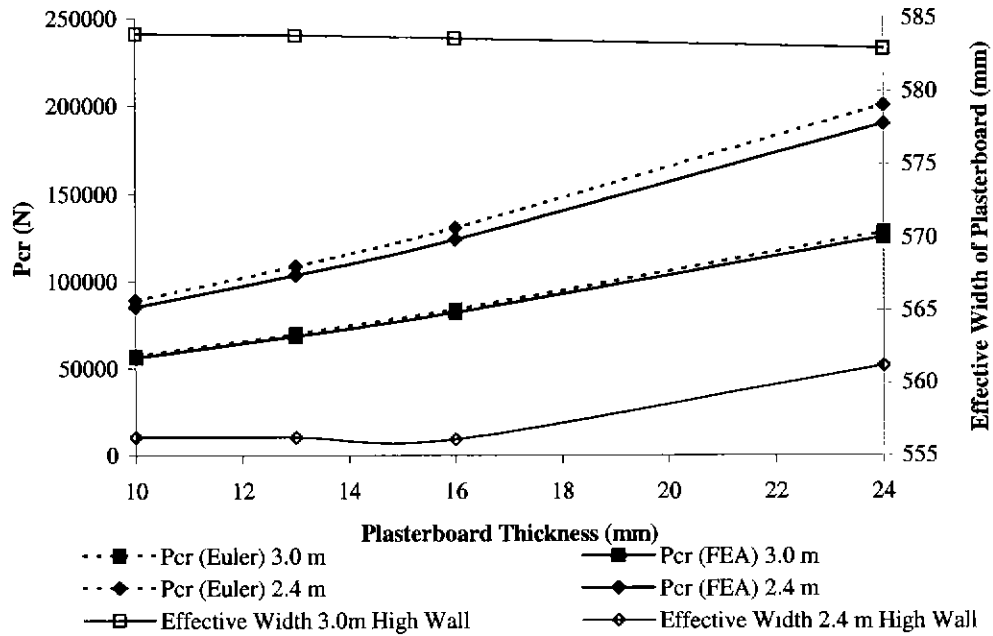
Figure 4.20(a): *Buckling Load Using Euler Solution and FEA & Effective Width Calculated versus Plasterboard Thickness*
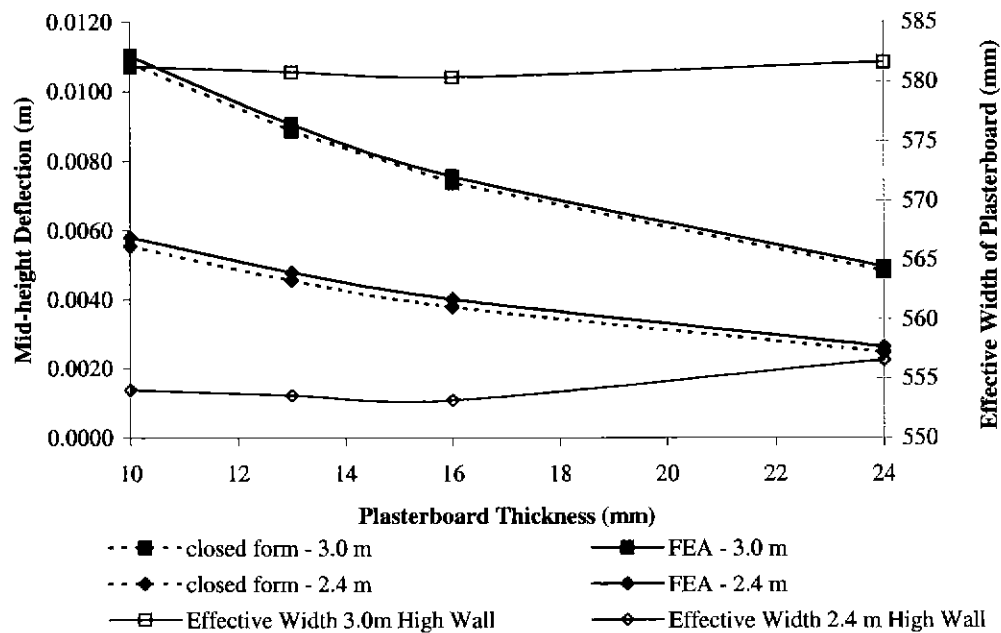
Figure 4.20 (b): *Mid-height Deflection for 1kN load using Closed Form Solution and FEA & Effective Width Calculated Versus Plasterboard Thickness*

4.3.2.7.4 Changing the Modulus of Elasticity of the Plasterboard

The effective width of the plasterboard was found to be largely insensitive to the modulus of elasticity of the material. The trends shown in Figure 4.21(a) and Figure 4.21(b) are highly

exaggerated by the vertical scale used on the right y-axis. A slight tendency to reduced effective

width may be apparent with increasing plasterboard modulus of elasticity.
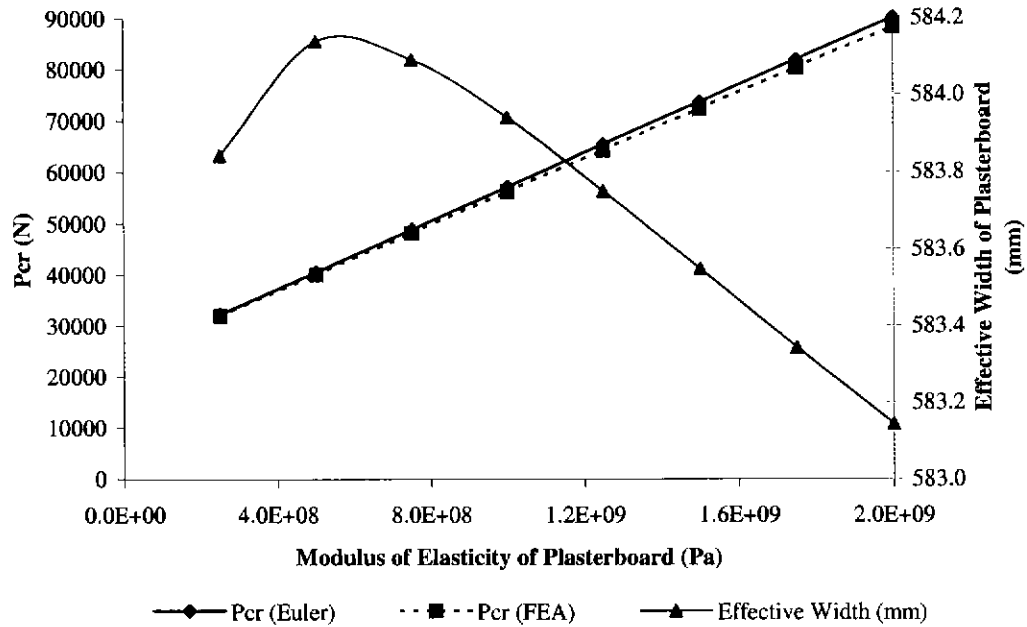
Figure 4.21(a): Buckling Load Using Euler Solution and FEA & Effective Width Calculated
Versus Modulus of Elasticity of Plasterboard – Note the highly exaggerated scale
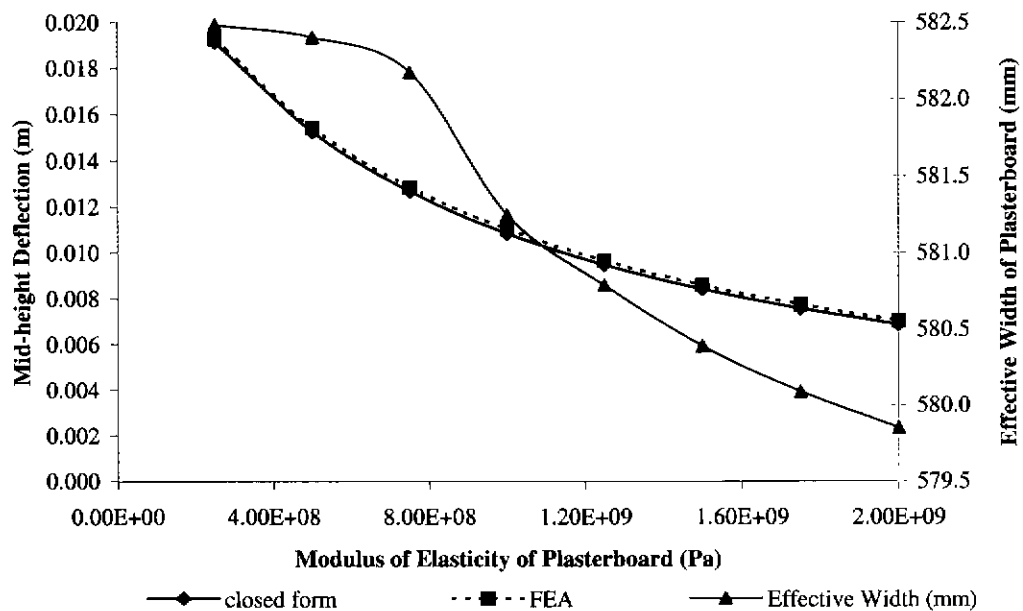
Figure 4.21(b): Mid-height Deflection for 1kN load using Closed Form Solution
and FEA & Effective Width Calculated Versus Modulus of Elasticity of Plasterboard – Note the
highly exaggerated scale

4.3.2.7.5   Changing the Modulus of Elasticity of the Timber Stud

Increasing the stiffness of the timber stud and keeping the plasterboard stiffness constant showed a clear relationship between the reduced effective width of the plasterboard versus increased stud stiffness (refer to Figure 4.22(a) and Figure 4.22(b)). However, the results demonstrated that the overall panel behaviour is insensitive to the changing the modulus of elasticity of the timber with regard to the effective width of plasterboard.
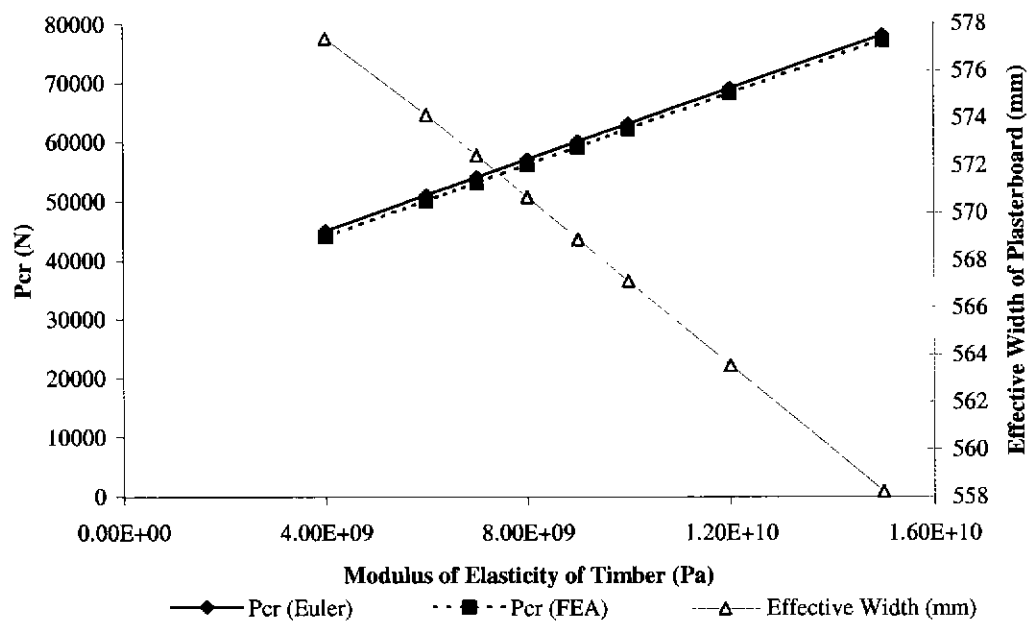
Figure 4.22 (a): Buckling Load Using Euler Solution and FEA & Effective Width Calculated versus Modulus of Elasticity of Timber
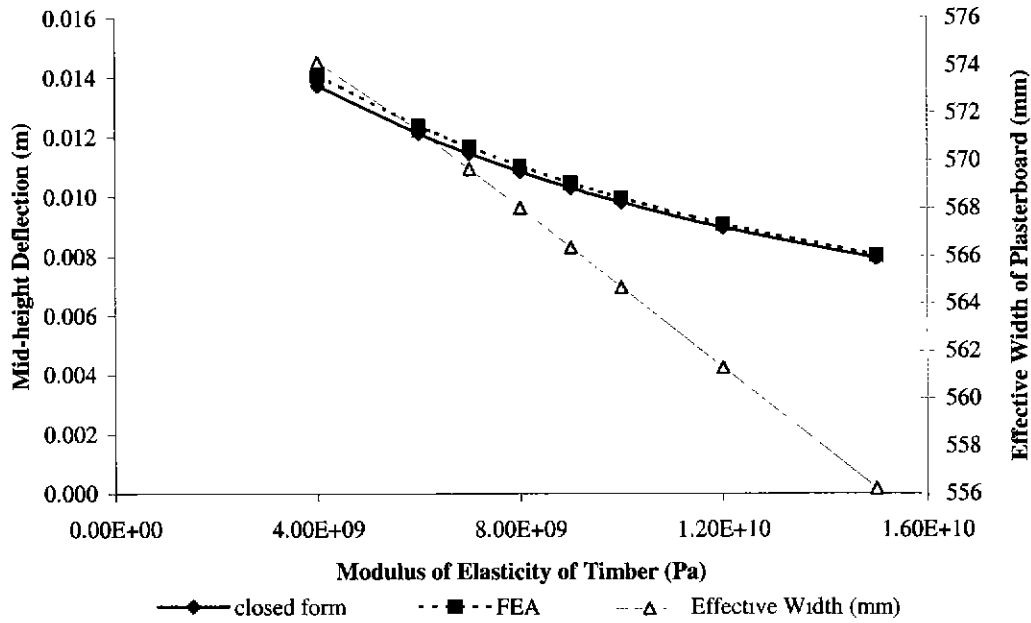
Figure 4.22 (b): *Mid-height Deflection for 1kN load using Closed Form Solution and FEA &*
Effective Width Calculated Versus Modulus of Elasticity of Timber

4.3.3   Conclusions

For conventional construction options of walls of plasterboard-clad, timber-framed walls which

are between 2.4m to 3 m high, plasterboard between 10mm and 24mm thick, and studs spaced of

either 450mm and 600mm, it has been demonstrated that assuming the stud spacing as the

effective width of the plasterboard sheeting is a good approximation.

The use of either a linear elastic buckling formulation or consideration of out of plane

deformations gave very similar results in determining the effective width of the plasterboard.

Given that an elastic analysis is required before commencement of a linear buckling solution

procedure, and the buckling solver takes considerably longer to solve, the technique of using the

out of plane deformations is a more efficient procedure.

Care must be taken in interpreting effective widths calculated by relating closed form solutions to

results from a finite element analysis. Inherent errors in the modeling procedure and given the

finite element technique only represents a numerical approximation means these errors may

dominate the actual values which are being determined. In this study, the effective width was calculated, but it was placed into a context of the overall effect on structural behaviour.

4.4   Conclusions from Mathematical Validations and Examination of the Validity in Ignoring Shear Lag in the Plasterboard Sheeting

The structural model has been successfully numerically validated using specific closed form and finite element models and was demonstrated to reliably predict the structural response related to these methods.

A study was undertaken to investigate the assumption of the effective width of the plasterboard sheeting to equal the stud spacing for a range of parameters. It was determined that for conventional construction of plasterboard-clad, timber-framed walls with stud spacing of either 450mm and 600mm, consideration of the structural behaviour of the stud combined with the full spacing width of plasterboard as a composite section was a reasonable approximation.

5. Full Scale Experimental Program

5.1 Introduction

For the purposes of ensuring reliable validation of the models developed and exploring the validity of assumptions made in the model development, a series of carefully controlled experiments were required.

The information obtained from temperatures measured following a standard fire resistance test procedure (AS1530.4) was inadequate for the detailed validation and calibration of the models developed. Standard fire resistance tests that are conducted in accordance with the requirements of an approach such as that defined in AS1530.4 generally prescribe a small number of locations where temperatures are to be measured during the test. In the case of AS1530.4, the requirement is for five thermocouples to be placed on the non-fire side of the unexposed face at quarter points and in the centre of the panel. Additional thermocouples may be located at positions on the unexposed face on the non-fire side that in the opinion of the testing laboratory will be hotter than those standard locations. No temperatures are required to be measured within the cavity or framing members, hence the use of previously conducted fire resistance tests was not considered suitable to perform a detailed validation of the models. From the literature, Collier (1991) appears to be the sole author reporting load-bearing timber-framed, plasterboard-clad wall fire resistance tests, who reported the results for the temperatures through the timber stud during a fire resistance test by installing a grid of thermocouples within a "dummy" timber stud. However, uncertainty regarding conditions of end and edge restraint, ambient wall capacity and the apparent non-uniform heating conditions of timber framing members made sole reliance on the data of Collier (1991) for the comparisons with the structural model unsuitable.

No references were found in the literature of full-scale fire resistance tests that had examined the conditions of end restraint or the effect of the contribution of the plasterboard sheeting on the non-fire side in increasing the structural capacity of the wall. The experiments to be performed thus allowed issues not adequately addressed in the literature to be examined for the first time,

including the effects of different conditions of end restraint and the contribution of the composite action of the plasterboard sheeting to the structural response.

An ambient series of experiments was conducted from the same batch of timber, which appeared in the literature to have not been done before. The timber used in the experiments was carefully selected to reduce variability, and allowed the structural response of the ambient framing and wall panels to be determined and related to the elevated temperature experiments. In addition, the ambient experiment series provided additional data for the validation and calibration of the structural model, and allowed the variability between the timber framing and wall panels to be determined.

It should be noted that full details of the full-scale experiments at ambient and elevated temperatures are contained in the reports Young *et al* (1996) and Clancy *et al* (1996). This chapter has focused on the issues and results, which are primarily associated with the structural response, with brief mention made of the thermal response.

5.2   Full-Scale Ambient Experimental Program

5.2.1   Introduction

The full-scale ambient experimental program involved the testing of full-scale timber frames and wall panels in compression at CSIRO Division of Building, Construction and Engineering at Highett, Melbourne.

The ambient series of experiments were used to determine the panel load ratio and variability with regard to load bearing capacity and structural response. This was to confirm the efficacy of the timber selection procedure, which was employed in an attempt to reduce variability between experiments, and to also determine the axial load bearing capacity to define the load level for the load bearing full-scale furnace experiments. If the ambient experiments demonstrated a low

variability then the scope of the elevated temperature experimental program would be increased, as less repetition of the same experiment would be required.

The results from these experiments were used for validation of the structural model developed and gave an indication of the structural contribution of the plasterboard sheeting with regard to the strength and stiffness of the wall panels.

The aims of the ambient full-scale experimental program were to:

(i)   Establish and verify the efficacy of the method of timber selection to reduce the variability in capacity of constructed frames.

(ii)   Determine reliably the ambient axial load capacities of the sheeted (panels) and timber frames.

(iii)   Determine an appropriate axial load for the full-scale furnace experiments.

(iv)   Determine the structural contribution due to the composite action provided by the plasterboard sheeting.

(v)   Obtain experimental results, which could be used for calibration and validation of the structural modeling for ambient conditions.

This series of experiments is hereafter referred to as Series I experiments and consisted of plasterboard sheeting attached to both sides of the timber framing ('I' sections) and frames without sheeting and steel bracing on the tension side.

The composite action between the timber studs and plasterboard sheeting during a substantial portion of the fire resistance experiments was observed to be similar to a 'T' section, that is, the plasterboard only being structurally effective on one side. The plasterboard on the exposed face during a fire resistance test is immediately exposed to the furnace atmosphere and is unlikely contribute significantly to the structural resistance of the wall for the majority of the test period. Thus it was assumed that there would be a closer relationship between the structural response of a 'T' wall panel with a standard wall panel tested in a fire resistance test. The final series of experiments was to determine to following:

(i) The capacity of a panel with plasterboard attached to only one side compared with the frames alone.

This series of tests hereafter are referred to as Series II experiments and consisted of plasterboard sheeting attached to a single side of the timber framing ('T' sections) and frames without sheeting and bracing attached to the compression side.

5.2.2 Schedule of Experiments

Table 5.1 summarises the schedule of ambient full-scale experiments that were performed:

Table 5.1: Schedule of Ambient Full Scale Experiments

Wall Panel/Frame Designation	Fastening of Plasterboard to Frame	Experiment Series	Comments
Panel A	16 mm Boral 'firestop' both sides	Ib	studs on outside were only cut at end, not at midspan, some bearing of plasterboard from end plate on end loading plate.
Panel B	16 mm Boral 'firestop' both sides	Ib	
Panel C	16 mm Boral 'firestop' both sides	Ib	
Panel D	16 mm Boral 'firestop' both sides	Ib	studs on outside were only cut at end, not at midspan, stiffens frame
Panel E	16 mm Boral 'firestop' both sides	Ib	
Frame F	none	Ia	bracing attached to tensile side
Frame G	none	Ia	bracing attached to tensile side
Frame H	none	Ia	bracing attached to tensile side
Frame I	none	Ia	bracing attached to tensile side
Frame J	none	Ia	bracing attached to tensile side
Frame K	none	IIa	bracing attached to compression side
Frame L	none	IIa	bracing attached to compression side
Frame M	none	IIa	bracing attached to compression side
Frame N	none	IIa	bracing attached to compression side
Frame O	none	IIa	bracing attached to compression side
Panel P	16 mm Boral 'firestop' to tensile side - 'T' Panel	IIb	
Panel Q	16 mm Boral 'firestop' to tensile side - 'T' Panel	IIb	
Panel R	16 mm Boral 'firestop' to tensile side - 'T' Panel	IIb	
Panel S	16 mm Boral 'firestop' to tensile side - 'T' Panel	IIb	
Panel T	16 mm Boral 'firestop' to tensile side - 'T' Panel	IIb	

5.2.3   Procedures

5.2.3.1   Timber Selection Criteria

The aim of the timber selection procedure was to minimise the variability in structural behaviour of the walls. The initial selection criteria in purchasing the timber were based on the density and stress grading from machine stress grading at the sawmill. The timber specimens were selected to be from within the lower band of the strength distribution. The density requirement was that the timber selected had an average density of close to 450 - 500 kg/m³, and must have contained at least some material within the F5 stress grade as defined in AS1720.1-1990. The characteristic bending strength of this grade is stated as being 16MPa in this standard.

The purchased timber was machine stress graded in a machine that CSIRO had extensively calibrated with mechanical property tests to determine a quantitative value of the modulus of elasticity (MOE) along the length of each stick. An average dynamic MOE was then calculated for each stud and they were then sorted on this basis. Excess studs remaining from those selected were used to construct the noggings, outer (cut) studs on the frames and end plates. These studs were either at the top or bottom of the range of average dynamic MOE of the group selected.

The three studs of timber to be used as the load bearing studs in each wall frame were carefully chosen so each frame had a close average MOE. Each frame had one stud selected from the lower third, one from the middle third and one from the upper third of the sorted list of studs based on the average dynamic MOE from machine stress grading. The density and average dynamic MOE for each stud used within each wall frame tested are shown in Table 5.2 and Table 5.3 for the series I and series II experiments respectively. The moisture content of the specimens during the machine stress grading was measured with a moisture meter and it was found they had a mean value of approximately 12%.

Table 5.2: Mechanical Properties of Timber Studs Used in Series I Experiments

Test	MOE$_{avge1}$ (GPa)	MOE$_{avge2}$ (Gpa)	MOE$_{avge3}$ (GPa)	MOE$_{avge\ studs}$ (GPa)	Density$_1$ (kg/m^3)	Density$_2$ (kg/m^3)	Density$_3$ (kg/m^3)	Density$_{avge}$ (kg/m^3)
Panel A	7.5	8 1	6.6	7.4	452	469	446	456
Panel B	6.7	7 6	8.0	7.5	519	460	481	487
Panel C	7.7	8.0	6.7	7.5	481	468	427	459
Panel D	7.3	6.8	7.9	7.3	478	427	516	474
Panel E	6.8	7.5	8.0	7.4	453	499	425	459
Frame F	6.7	7.3	7.7	7.2	445	412	487	448
Frame G	7.6	6.6	7.9	7.3	473	445	463	460
Frame H	7.8	6 8	7.2	7.3	468	425	442	445
Frame I	7.8	6.9	7.7	7.5	469	469	466	468
Frame J	7.8	7.5	6.9	7.4	448	463	430	447

Table 5.3: Mechanical Properties of Timber Studs Used in Series II Experiments

Test	MOE$_{avge1}$ (GPa)	MOE$_{avge2}$ (GPa)	MOE$_{avge3}$ (GPa)	MOE$_{avge\ studs}$ (GPa)	Density$_1$ (kg/m^3)	Density$_2$ (kg/m^3)	Density$_3$ (kg/m^3)	Density$_{avge}$ (kg/m^3)
Frame K	7.0	8 3	9.4	8.2	427	479	475	460
Frame L	9.0	8.0	7.5	8.2	479	446	415	446
Frame M	7.6	7.7	8.9	8.1	468	458	459	462
Frame N	8.0	7.6	8.5	8.0	441	441	504	462
Frame O	8.9	7.9	7.6	8.1	459	486	446	464
Panel P	7.1	9.1	8.2	8.1	458	480	479	472
Panel Q	7 2	8.0	9.4	8.2	428	422	480	444
Panel R	7.9	7.5	8.5	8.0	457	441	458	452
Panel S	8.0	7.3	8.5	8.0	491	455	465	470
Panel T	8.9	6.6	8.2	7.9	458	407	451	439

5.2.3.2   Construction and Erection of Timber Frames and Panels

5.2.3.2.1   General

The studs of radiata pine selected were at least three metres long and were 90 mm x 45 mm in

cross section. The reason that 90 mm x 45 mm sections were chosen rather than 90 mm x 35mm

was to increase the noticeable contribution of timber framing to time of failure and with

consideration to the full-scale furnace experimental series, to enable more thermocouples to be

inserted which would improve the accuracy of plots of temperature distributions in timber

sections.

A total of twenty timber frames, comprising ten unsheeted frames, five timber frames panels with plasterboard attached to both sides and five frames with plasterboard attached to only one side were constructed for the experiments. The plasterboard was 16mm "Firestop" manufactured by Boral Plasterboard, Melbourne. The selection of 16 mm fire rated board to attach to each side of the studs was in order to imitate a 'standard' (AS1530.4) 1-hour fire resistance level construction system. Three people lifted the panel/frame into position within the testing apparatus.

5.2.3.2.2   End Restraint

The end restraint selected for the experiments was to allow the structural model to be validated with known externally applied forces and rotational restraint. The end plates were attached to the ends of the panel/frame (refer to Figure 5.3 and the Photographs in Figure 5.4 and Figure 5.5). The end plates were designed to provide a known idealised 'pin' end restraint and negligible resistance to rotation. In addition, an eccentricity of 10mm was induced by the end plates, to allow for the direction of deformation to be predicted.

5.2.3.2.3   Series Ia Experiments –Timber Frames 'F'-'J' (Unsheeted)

The frames were constructed with details very similar to those of frames in the full scale wall furnace experiments. The centre to centre stud spacing was 380 mm (Refer to Figure 5.1 for details) instead of the conventional construction options of 450 mm or 600 mm. The reason for using a small spacing was to maximise the number of studs that shared load, in addition to having each load-bearing stud being exposed to similar heating conditions. Load sharing reduces the inherent variability of test results. Extra noggings and steel strapping were attached to the frames on the tensile side to prevent in-plane buckling.

Support details shown
in Figures 5.3, 5.4 and
5.5

600

1200

3000

1200

Steel
strapping to
prevent in-
plane
buckling.

3 studs @380
centers

805

Extra noggings at
midpoint of 1200mm
sections
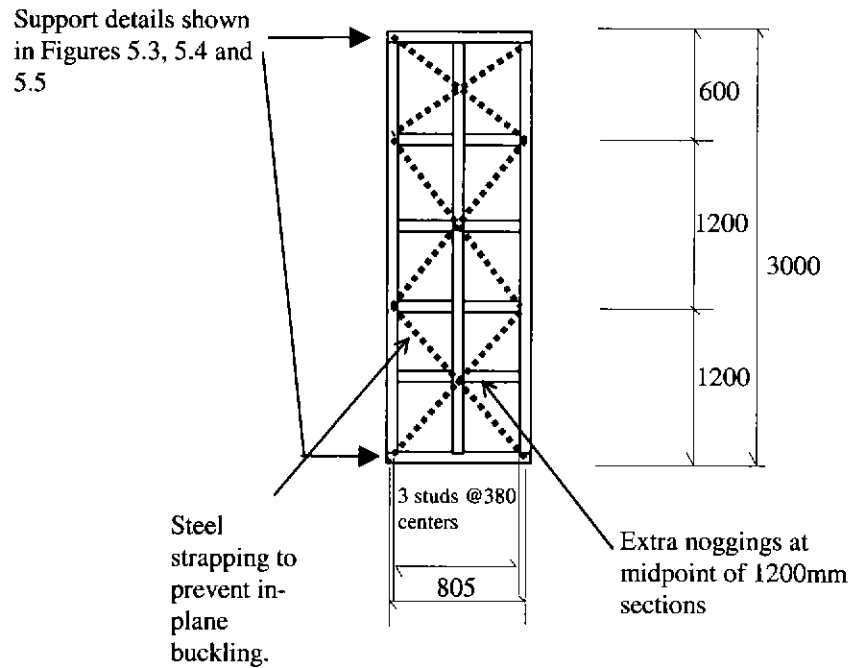
Figure 5.1: *Elevation of Typical Unsheeted Wall Frame Construction Detail*

5.2.3.2.4   Series Ib Experiments – Timber Panels 'A'-'E' (Sheeted)

The timber framing for the wall panels studs (refer to Figure 5.2) was constructed in the same

manner as the frames, except there was no requirement for steel strapping or the additional

noggings due to the plasterboard sheeting providing restraint against in-plane buckling. As the

studs at the edge of the wall were heated from one cavity only, they would not thermally degrade

to the same extent as the middle three studs, which were heated from two cavities. Accordingly for

the ambient tests, the edge studs were therefore structurally separated by firstly cutting a small

length off near the top plate in a similar manner to that of Collier (1991). However, the initial wall

panel experiments performed in these procedures revealed that three cuts were required to prevent

a substantial contribution to bending stiffness from double curvature of the plasterboard and hence

failure load. The plasterboard was fastened and joined with paper tape and Boral B300 stopping

material in accordance with the manufacturer's specifications for a standard one-hour fire rated

construction systems (for example Boral Plasterboard, 1994).

5.2.3.2.5   *Series IIa Experiments – Timber Frames 'K'-'O' (Unsheeted)*

The Series II experiments were carried out later than Series I and the elevated temperature

experiments. An additional batch of timber had to be obtained from which these frames would be

constructed. Also, timber frame experiments were required to provide a common basis for

comparing the results of Series II with Series I. The timber frames used in the Series IIa tests were

constructed in identical fashion to those in the Series I tests, except that the steel strapping was

placed on the compression side of the specimens. In tests for frames F-J, the bracing was placed on

the tensile side, which was found to effectively increase the stiffness the wall frame. Subsequently,

frames K-O had steel strapping placed on the compression side, which effectively reduced the

stiffness of the wall.

5.2.3.2.6   *Series IIb Experiments – Timber Panels 'P'-'T' (Sheeted)*

The 'T' panels were constructed as the Series Ib panels, except that the specimens had

plasterboard attached to only one side (refer to Figure 5.20). The load was applied at an

eccentricity of 10 mm from the centre of the timber stud away from the sheet, such that the

plasterboard sheeting was acting in tension to more closely represent the situation of a timber-

framed wall in a fire resistance test.
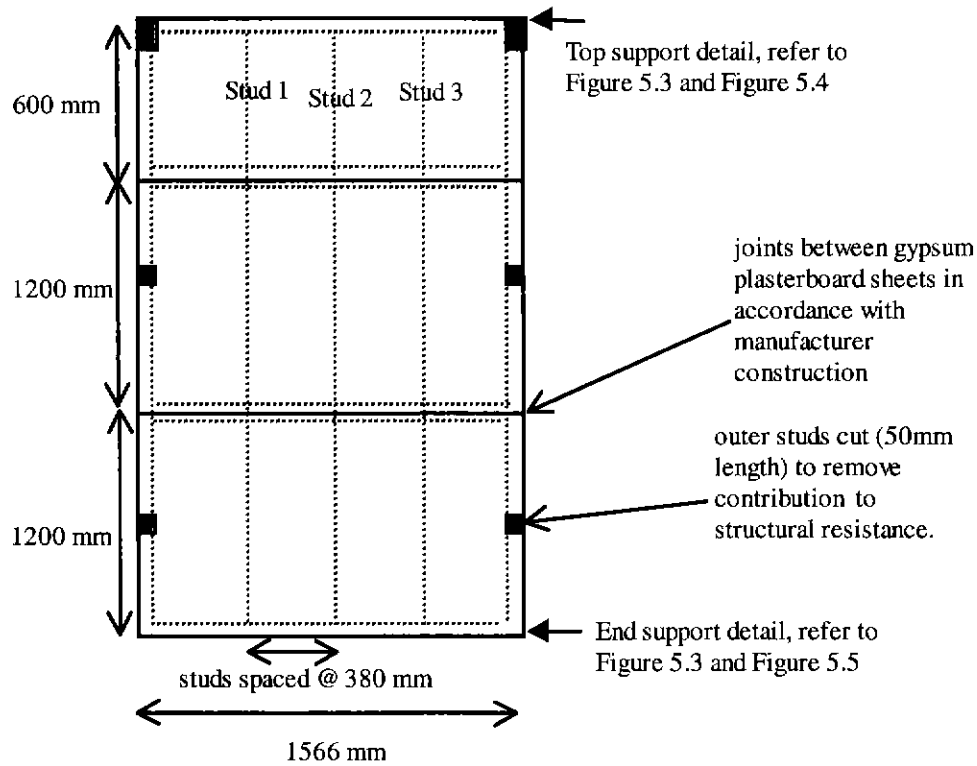
Figure 5.2: *Elevation of Typical Sheeted Wall Panel Construction Detail*
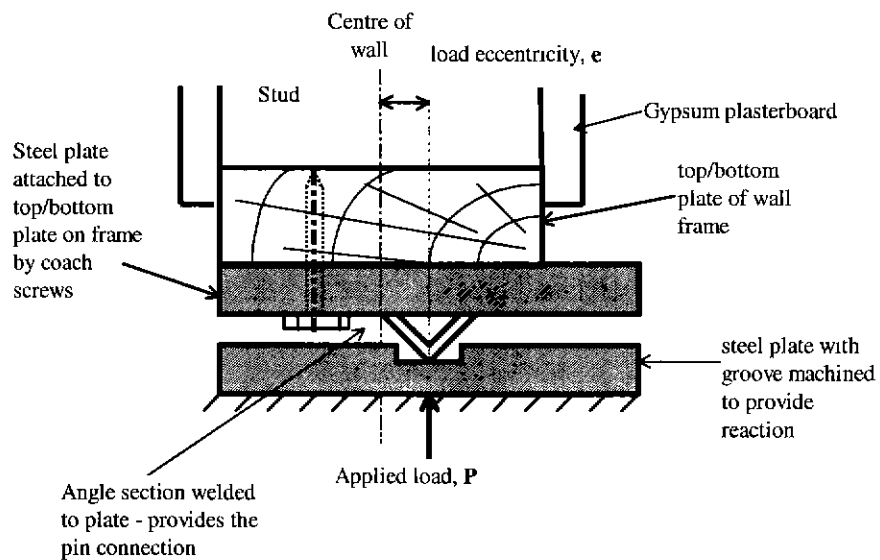
Figure 5.3: *End Support Detail Top and Bottom*
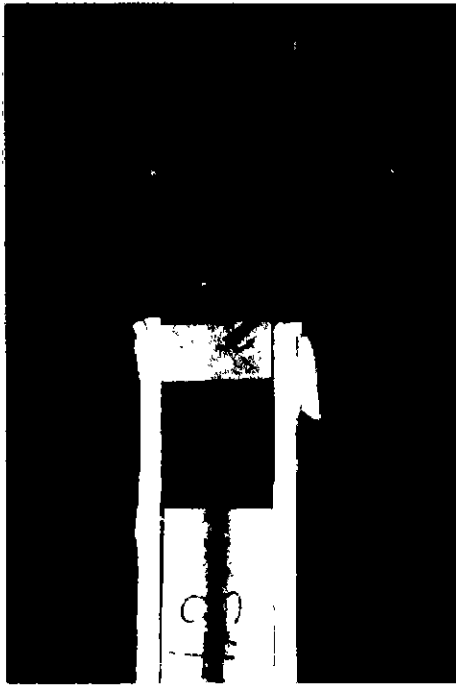
Figure 5.4 *: Photograph of the End Support at*
the Top of the Panel and Spreader Beam used
to Load the Specimen
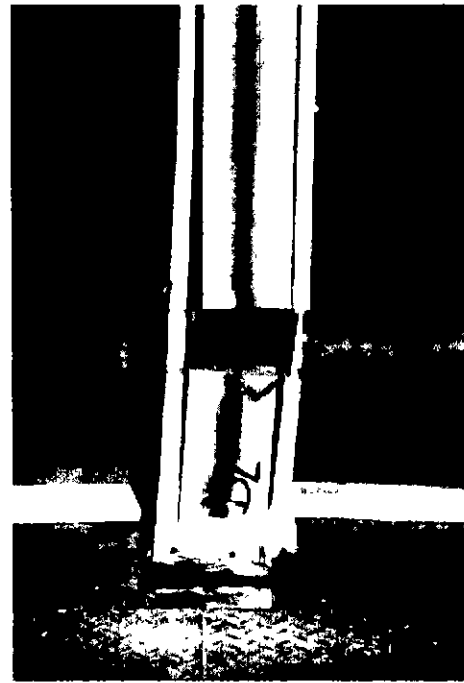
Figure 5.5 *: Photograph of the End Support at*
the Bottom of the Panel

5.2.3.3   Measurement of Deflection

Both out of plane and axial deflections were measured by use of dial gauges. These were placed at locations 1-7 identified in Figure 5.6 for the Series I experiments. The Series II experiments did not have dial gauges located at the quarter points vertically.
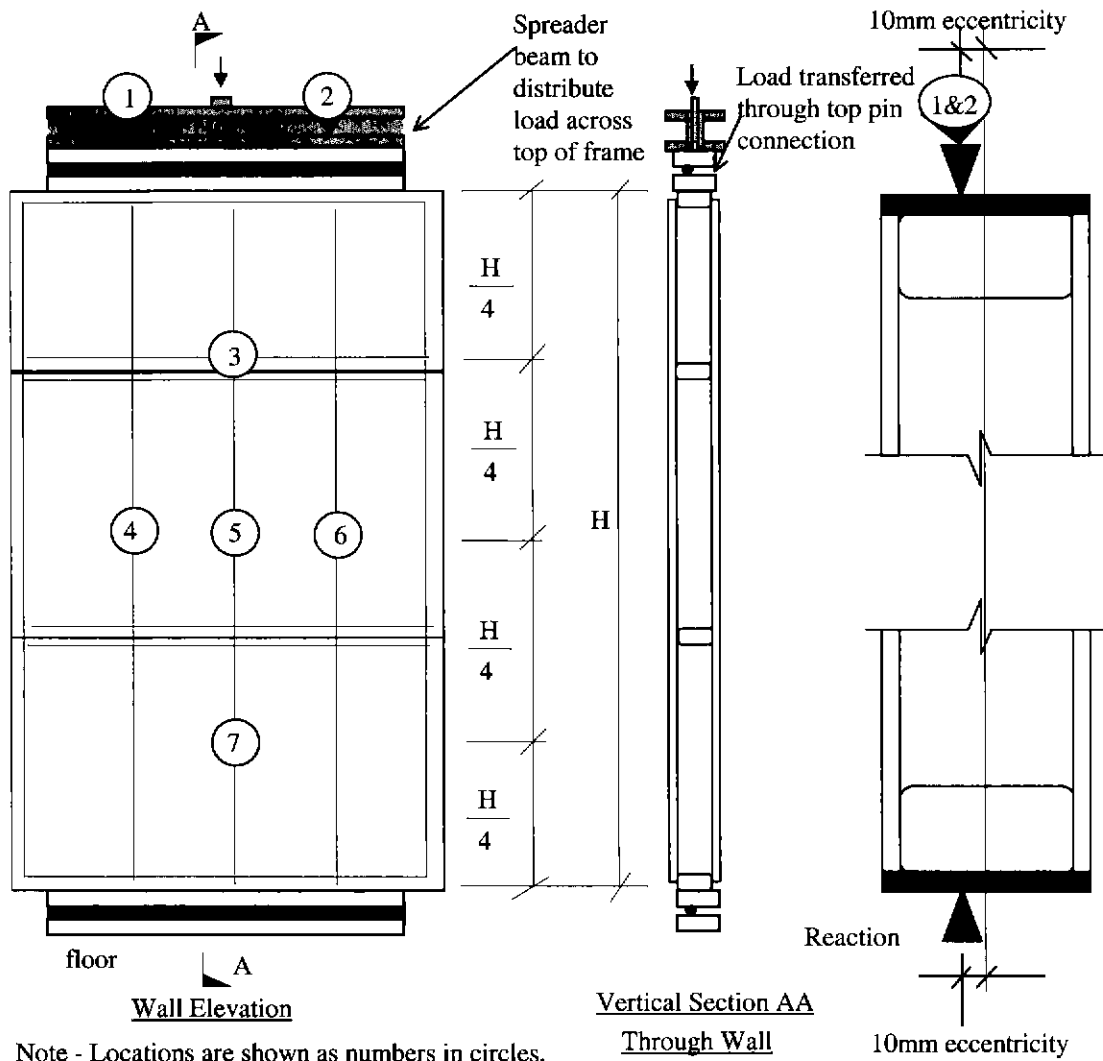
Figure 5.6: *Location of Deflection Measurement Points and Loading Technique*

Note: For Series II tests deflection measurements were not recorded at locations 3 and 7

5.2.3.4   Application of Loading

The wall frames/panels were loaded within a compression-testing machine, in specific increments

(generally in 5kN increments, near failure reduced to 2.5kN increments). The load was held

constant while three people read the dial gauges. Load versus deflection readings were recorded

until the dial gauges began to run out of travel at a deflection of approximately 25mm. At this

stage, the gauges were removed to reduce the likelihood of them being damaged when the frame or

panel failed. The general experiment configuration is shown in Figure 5.7.
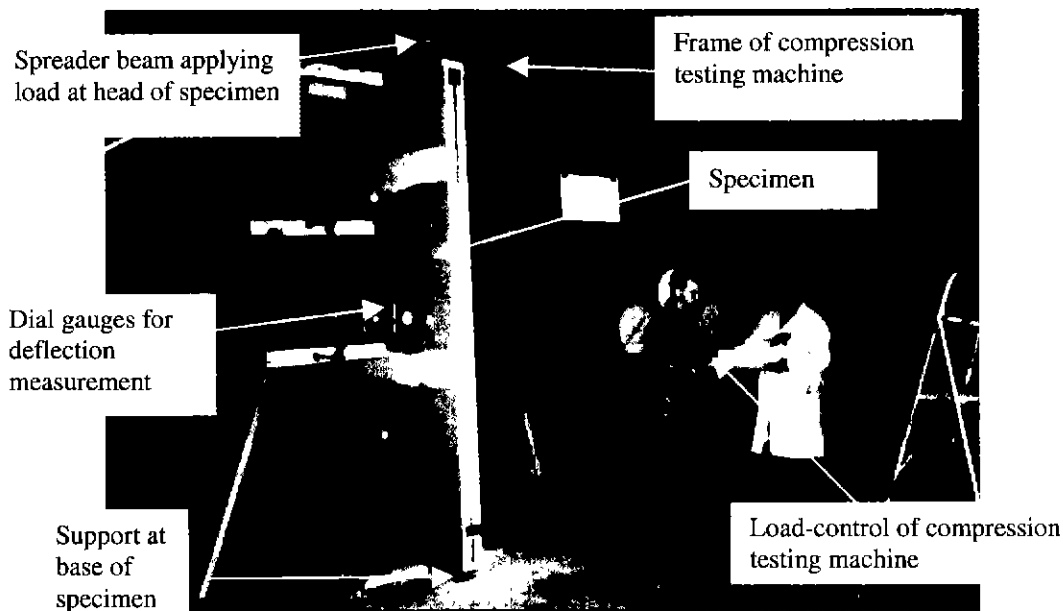
Figure 5.7: *Photograph Showing the General Configuration of the Apparatus used in performing*

the Ambient Experiments (S. Young left, R. McNamara, CSIRO right)

5.2.4   Discussion of Results

5.2.4.1   Series I Experiments – General Results

The results from the Series I experiments are summarised in Figure 5.8 and Figure 5.9.
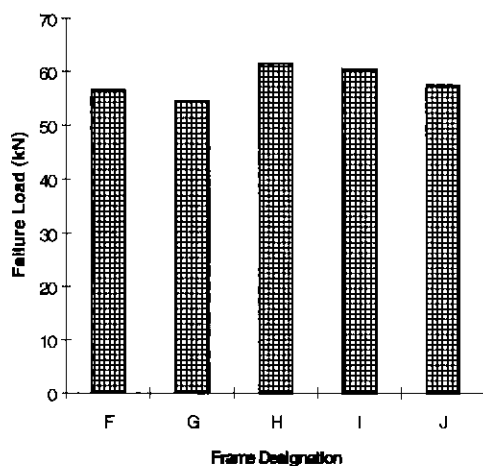
Figure 5.8: *Series Ia Experiments: Failure Loads for*
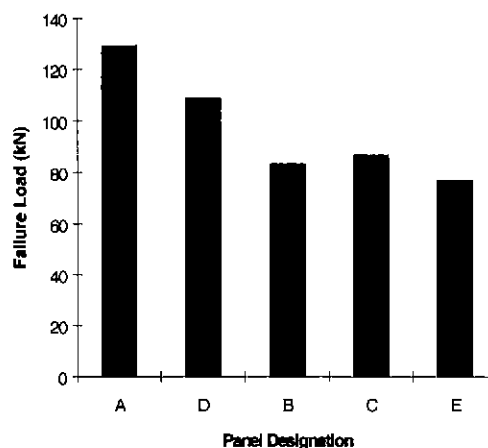
Unsheeted Frames

Figure 5.9: *Series Ib Experiments: Failure Loads for*

Sheeted Frames (Panels)

5.2.4.2   Series Ia Experiments - Unsheeted frames

Figure 5.10: *Load versus Out of Plane Deflection for Frames F, G, I & J*

n.b. Experimental data points are presented as points, the curve of best fit was obtained by using a

Polynomial Curve fit between the data points from Microsoft Excel 5.0.

The variation amongst the ultimate capacities of the unsheeted timber frames in the Series Ia

experiments was low (refer to Figure 5.8), an average capacity of 58.1 kN with a variation of ± 3.5

kN. The load versus deflection behaviour for the frames is shown in Figure 5.10. A photograph

demonstrating the specimen mounted in the testing machine is shown in Figure 5.11. The failure

mechanism was generally splitting around knots on the tension side of the studs (refer to Figure

5.12) within the middle third of the height of the wall. Attachment of the bracing to the tensile side

had the effect of slightly stiffening the frame in bending, but was necessary to prevent in-plane

buckling. The increase in the effective flexural stiffness was due to the steel strapping being in

tension and tending to straighten up the wall, further the stiffness in flexure through a degree of

composite action between the frame and bracing.

Figure 5.11: Photograph Showing the Deflected Shape Profile for the Loaded Frame

Figure 5.12 : Photograph Showing the Typical Failure Mode for the Loaded Frame

5.2.4.3 Series Ib Tests - Sheeted frames
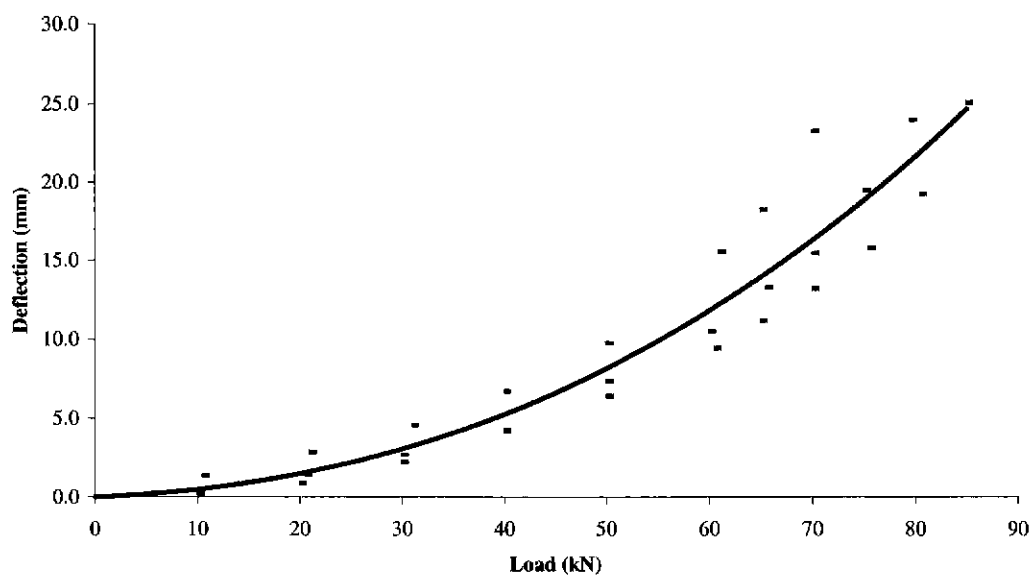
Figure 5.13: Load versus Out of Plane Deflection for Panels B, C & E

n.b. Experimental data points are presented as points, the curve of best fit was obtained by using a Polynomial Curve fit between the data points from Microsoft Excel 5.0.

5-15

The failure loads of the sheeted frames for the Series 1b experiments are shown in Figure 5.9. The first sheeted frame tested (A) gave a substantially greater capacity than predicted. The reasons for this include:

(i) The plasterboard sheeting was bearing on the loading plates, which provided an extra load path.

(ii) The timber studs on the outside of the frame, which were not supposed to contribute to the structural capacity of the wall, were stiffening the panel against bending as they were a continuous element for the majority of the height of the wall (Refer to Figure 5.7 compared with Figure 5.14); and provided a further path for the axial load

The second panel tested (D) had the ends of the outer studs cut to remove the load path to the support and the plasterboard shortened so it did not bear on the loading plates. However, the outer stud was still continuous along the length of the wall and was still providing considerable resistance against bending. The outside studs for subsequent tests (B,C,E) had 50 mm sections removed along the length to reduce the contribution of the outer studs to the bending stiffness of the wall. Panels B,C,E gave fairly uniform results, with the average ultimate capacity being 82 kN, the variation being ±4 kN. The load versus deflection for these panels is shown in Figure 5.13. A photograph demonstrating the specimen mounted in the testing machine is shown in Figure 5.14. This technique of removing sections of timber in the outer studs to minimise the structural contribution was subsequently implemented in the full-scale fire resistance tests.

Figure 5.14 : Photograph Showing the Deflected Shape Profile for the Loaded Panel
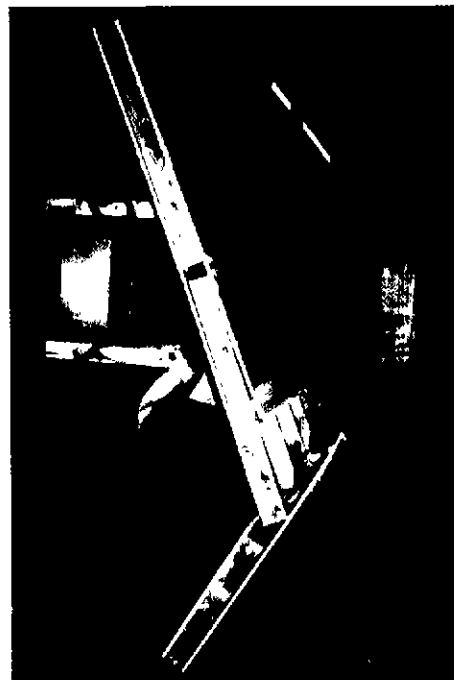
Figure 5.15: Photograph Showing the Typical Failure Mode for the Loaded Panel

The mode of failure was generally tearing at a joint on the tensile face of the plasterboard, before initiation of a brittle failure at a knot group located on the tensile side of the timber studs (Refer to Figure 5.15).

The increase in axial load capacity due to the composite action of the sheeting with the frame was of the order of 40% compared with the Series Ia frames alone. Given the Series Ia frames had bracing attached to the tensile side, which as discussed previously effectively increased the framing capacity, the increase in capacity due to composite action provided by the sheeting would be expected to be greater still. The in-plane deformation was negligible thus the plasterboard provided sufficient lateral restraint to prevent motion in this direction. The average ambient capacity of the walls in the full-scale furnace experiments was therefore predicted to be approximately 82 kN.

5.2.4.4   Series II Experiments – General Results

The results from the Series II experiments are summarised in Figure 5.16 and Figure 5.17.
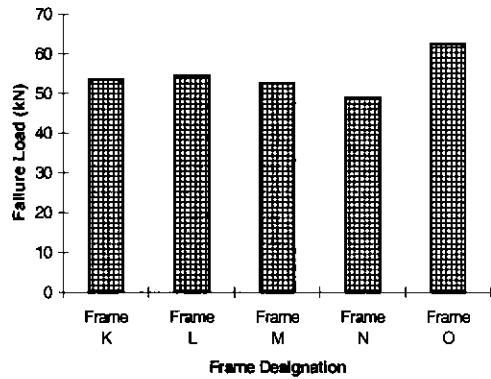
Figure 5.16 : *Series IIa Experiments: Failure*   **Figure 5.17**: *Series IIb Experiments: Failure*
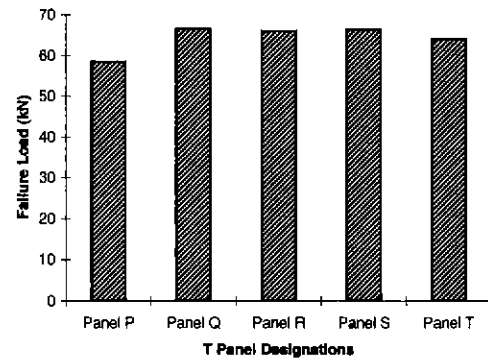
Loads for Unsheeted Frames   *Loads for Sheeted Frames ('T'Panels)*

5.2.4.5   Series IIa Experiments - Unsheeted frames
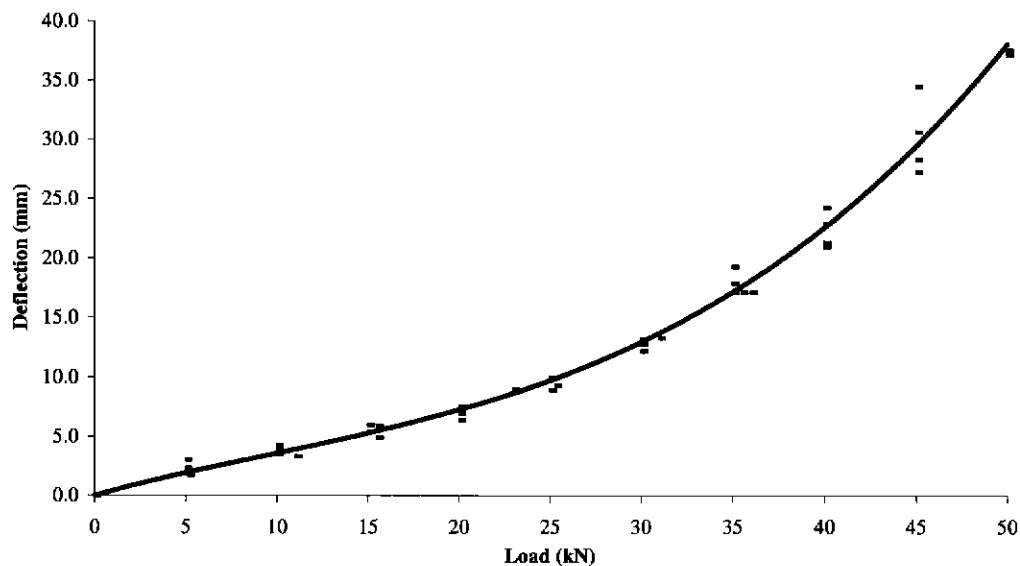
Figure 5.18: *Load versus Out of Plane Deflection for Frames K – N*

n.b. Experimental data points are presented as points, the curve of best fit was obtained by using a

Polynomial Curve fit between the data points from Microsoft Excel 5.0.

The variability of the ultimate capacity of the unsheeted timber frames was low (refer to Figure

5.16), except for a single test, Frame O. Frame 'O' contained a stud which had a hollow section

on an edge, which was the remnant of an encased knot and measured to have a low modulus of

elasticity when machine stress graded, but proved to be exceptionally strong. It was apparent that

5-18

the material in the region of the knot was of higher capacity. The results for test 'O' were not

therefore included in the graph of load versus deflection shown in Figure 5.18. The average

capacity neglecting frame 'O' was 52.4 kN ±3.4 kN. The flaw in using the machine stress grading

technique for strength and stiffness calculation was that the primary axis of bending was

orthogonal between the wall test orientation and the orientation used for the grading procedures.

The failure mechanism was generally one involving splitting around knots on the tension side

within the middle third of the height of the wall close to a knot group and principally where the

noggings were nailed into the timber.

The technique of attaching bracing on the compression side to prevent in-plane deformation tended

to not provide an increase in capacity as substantial as when it was attached to the tensile side.

The tensile force induced in the bracing, through in-plane movement of the framing, had a

tendency to pull the wall frame further in the direction of deflection, thus apparently reducing the

flexural stiffness of the frames.

5.2.4.6   Series IIb Experiments – 'T' Panels - Frames Sheeted on One Side

The results of the tests shown in Figure 5.17 and Figure 5.19 indicate the variability of the 'T'

panels was low, with an average strength of 64.4 kN ± 6 kN compared with the unsheeted frames

of 54.4 kN (52.4 kN if the anomaly of Frame O is neglected). The typical deflected shape before

failure is shown in Figure 5.20. An increase in capacity of 18% due to the sheeting was calculated.

It must be noted that this increase in capacity is potentially greater, except that the eccentricity of

the applied load is increased in the case of the 'T' section compared to a conventional wall panel

because it is non-symmetrical and the load is applied on the opposite side to the sheeting.

However, this must be countered in that the bracing on the frames was on the compressive side,

and tended to result in an underestimation of the frame capacity. The failure mode of the 'T'

section was initiated by a tensile tearing failure in the joint of the plasterboard sheeting, followed

by a very sudden failure in a knot group on the tensile side of one or more studs (refer to Figure
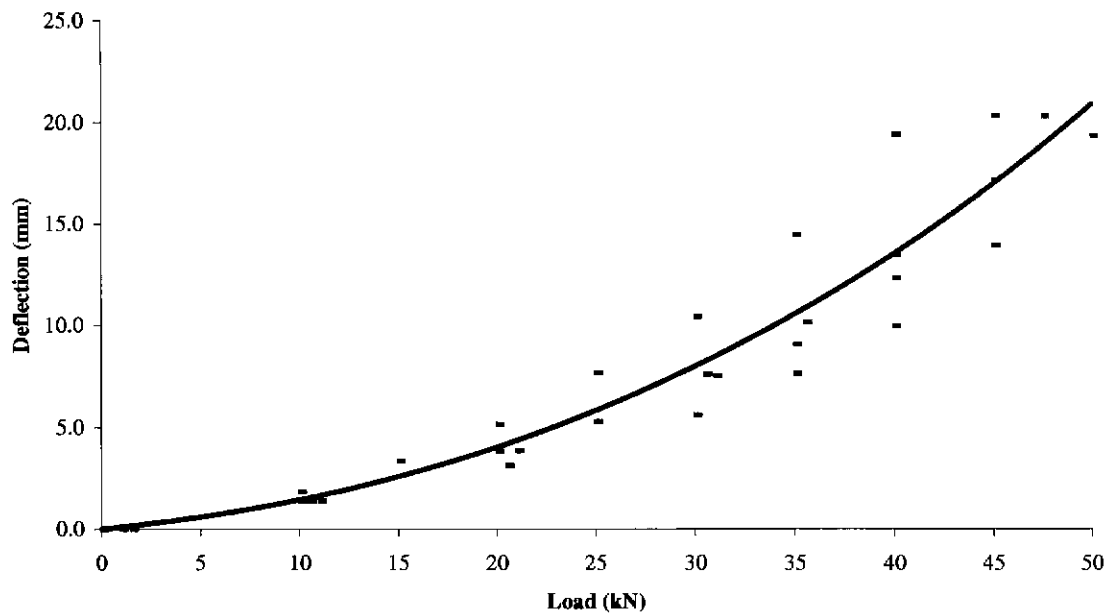
5.21).
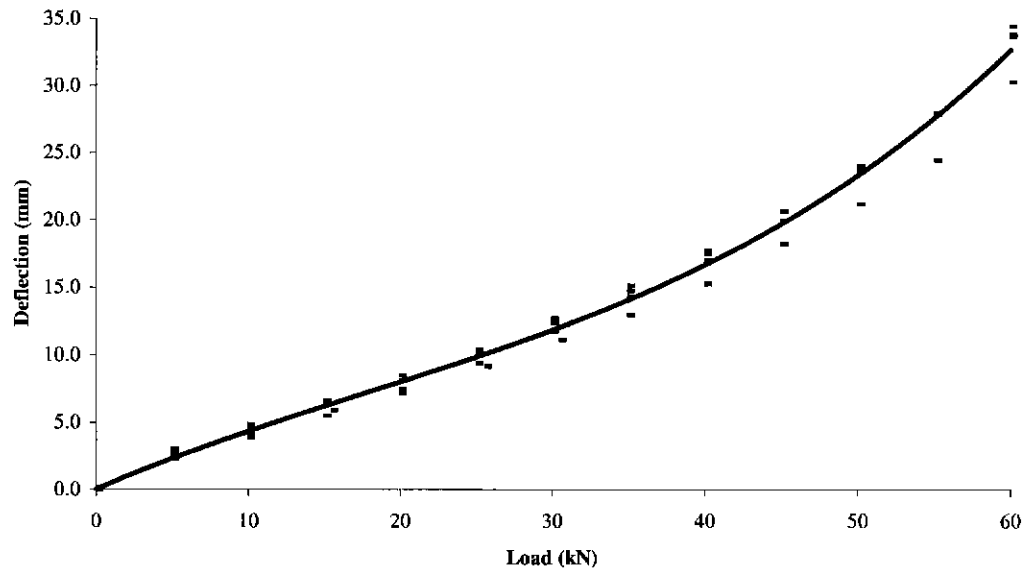
Figure 5.19: *Load versus Out of Plane Deflection for 'T' Panels Q-T*

n.b. Experimental data points are presented as points, the curve of best fit was obtained by using a

Polynomial Curve fit between the data points from Microsoft Excel 5.0.

Figure 5.20 : *Photograph Showing the Deflected Shape Profile for the Loaded 'T' Panel*

Figure 5.21: *Photograph Showing the Typical Failure Mode for the 'T' Panel*

5.2.5   Conclusions from the Full-Scale Ambient Experimental Program

The ambient capacities of the sheeted and unsheeted frames were determined and provided a reliable prediction of the strength of the walls used for the full-scale fire resistance experiments.

A valid selection technique for framing members was determined, which reduced the variability of the capacity of wall frames built from the members. The technique for timber selection was based on the use of a density criterion of about 450-500 kg/m^3 coupled with machine stress grading. Reduction of the variability of the wall capacity allowed the scope of the full-scale furnace experiments to be increased.

The panels with plasterboard sheeting on both sides had an increased load bearing capacity of 40% compared with the timber frames with bracing on the tensile side. This contribution would have been greater if no bracing was attached.

The timber frames with plasterboard sheeting attached only on the tensile side provided an increased load bearing capacity of 18% compared with the frames with bracing attached to the side in compression. This contribution would have been less if no bracing was attached.

The failure mechanism of the timber frames was one involving rupturing on the tensile side within a knot group in the middle third of the wall, occasionally in the region of a nogging.

The failure mechanism of the timber panels (framed with sheeting) was precipitated by a tensile rupture at a joint between the plasterboard sheets on the tensile face.

The ultimate bearing capacity of the frames was affected by the attachment of steel strapping to brace the frames to prevent an in-plane failure. The effects were to increase the frame capacity when the strapping was attached to the tensile face of the framing, and to reduce the frame capacity when attached to the compressive face of the framing. The sheeting was demonstrated to provide sufficient lateral restraint to prevent an in-plane failure.

The ambient tests provided load-deflection results, which provided results for validating the structural model.

5.3 Full-Scale Furnace Experimental Program

5.3.1 Introduction

The series of eight full-scale furnace experiments performed were required in order to validate the thermal models developed by Clancy (1994) and the structural model for this thesis. The experiments were performed on the 3 m high by 1.63 m wide vertical furnace at BHP Research, Melbourne Laboratories.

Additional issues such as the variability in time to failure, heat transfer, end restraint, load bearing, non-load bearing and the contribution of the plasterboard sheeting on the unexposed face through composite action were also examined in the procedures. The primary focus of the information that is reported in this section of the thesis are the issues associated with structural response. A more detailed presentation of the experimental results and procedures is presented in Clancy and Young (1996).

5.3.2 Aims

The aims of the full-scale fire resistance tests were as follows, to:

(i)   Provide data for the validation of the structural analysis model developed, including temperature distribution data, deflection data and times-to-failure

(ii)   Observe the variability of time-to-failure for experiments with similar configurations of restraint and loading to enable evaluation of inherent variability of the times-to-failure

(iii)   Establish the failure mechanism of the non-load bearing wall.

(iv)   Establish the effect of end restraint in examining the effect of rotational end restraint of a load bearing wall with regard to the time-to-failure and failure mechanism.

(v)   Establish the effect on the end restraint due to thermal degradation for the load bearing

       experiments.

(vi)   Determine the structural contribution of the partial composite action provided by the

       plasterboard sheeting on the unexposed face and the time-to-failure.

(vii) Deduce qualitatively a relation for the effective modulus of elasticity versus temperature, to

       compare with the results from the compression experiments reported in Chapter 6.

5.3.3   General Summary of Procedure

Eight frames which were constructed at the same time and from the same group of timber selected

for the ambient frames and panels tested in the Series I tests at CSIRO, were transported to BHP

Research, Melbourne Laboratories. The wall panels were successively assembled and tested.

Assembly was carried out by hoisting the timber frames into the steel frames that secured the wall

specimens against the furnace. After the timber frames were hoisted into position, thermocouples

were attached and plasterboard sheeting was affixed to the timber frame. Ceramic fibre was placed

around the perimeter of the walls to seal the furnace heat in and also to allow furnace pressure to

be maintained consistently in accordance with the requirements of AS1530.4-1990. Each wall was

then secured against the furnace. For load bearing experiments, three 800kg weights were placed

in loading devices at the top of the walls with a mobile crane, providing a loading of

approximately 8 kN per stud, to represent a load level of approximately 30% of the capacity of the

ambient panels. This load was consistent with the structural design loading of these timber framing

members, when designed in accordance with AS1720.1-1988 as calculated in an Appendix of

Clancy (1999). Thermocouple wires were then attached to calibrated data acquisition equipment

provided by BHP Research. The experiments were then undertaken in accordance with the heating

regime and pressure requirements of AS1530.4-1990 and lasted for a period of between 28 and 90

minutes. During the experiments visual observations were documented. A steel bar was secured

across the specimen in the furnace to help prevent the sudden outwards collapse of the wall panel

at failure, the bar allowed approximately 150mm outward deflection. At the conclusion of each

experiment, the wall panels were dismantled gradually and further observations regarding the

degradation documented.

5.3.4   Schedule of Experiments

Table 5.4 details the schedule of full-scale furnace experiments undertaken.

Table 5.4: Schedule of Full-Scale Wall Furnace Experiments

Wall Panel Designation	Experiment Designation	Fastening of Plasterboard to Timber Frame	Applied Load	Comments
1-2	BFT668 BFT669	Full fastening	None	Thermocouples placed in one nogging and one stud in each experiment for correlation. Pin supported top and bottom.
3	BFT676	Full fastening	None	No thermocouples in studs. Pin supported top and bottom.
4, 5	BFT679 BFT680	Full fastening	8.0 kN per stud	No thermocouples in studs. Pin supported top and bottom
6	BFT681	Full fastening	8.0 kN per stud	No thermocouples in studs. Fixed to prevent rotation at top and bottom supports.
7	BFT682	Minimal fastening refer to Clancy & Young (1996)	8.0 kN per stud	No thermocouples in studs Pin supported top and bottom. Substantial seals at plasterboard without providing composite action at joints.
8	BFT683	Minimal fastening as per Figure 5.23 on unexposed face	8.0 kN per stud	No thermocouples in studs Pin supported top and bottom. Normal joint detailing on fire side but substantial seals without providing composite action on the ambient side (refer to Figure 5.23).

5.3.5   Specific Procedural Details

5.3.5.1   Frame Construction & Erection

Eight timber frames were constructed at the same time as those in the first series of ambient experiments, from the same batch of timber selected. This allowed the likely ambient capacity and structural response of these specimens exposed to elevated temperatures to be estimated. The average modulus of elasticity and density of the load-bearing timber elements used in each wall are summarised in Table 5.5. The timber frames were hoisted into steel frames used to mount the wall in front of the furnace opening. The timber frames were secured into position, the required

thermocouples within the wall cavity were installed and plasterboard sheeting for the exposed face was attached to the timber frame. Thermocouples on the exposed face sheeting were then attached to the appropriate positions. Plasterboard sheeting was attached to the unexposed face of the wall. Plasterboard sheeting was attached (refer to Figure 5.22) to the wall in accordance with manufacturer specifications (Boral Plasterboard, 1994) for a one hour fire resistance level wall construction, except in the case of the walls with the structural contribution of the plasterboard removed (refer to Figure 5.23). The general configuration of the experimental configuration is shown in Figure 5.28.

For the experiment that was used to investigate the contribution of the sheeting was removed on the unexposed face only. The sheet on the exposed face and associated fasteners were considered to be heated rapidly and not contribute structurally to the performance of the wall, except in the initial stages of the experiment where failure of the panel was highly unlikely. The method of reducing the contribution of the connection between the sheeting and stud also had the potential for affecting the heat transfer conditions through the exposed face; for example, the sheet may fall into the furnace prematurely or hot gases may pass into the cavity through the slots created. Thus it was considered essential that the heating conditions for the timber framing were consistent for all tests to allow for a more reliable comparison between experiments to determine the structural contribution of the sheeting.

Table 5.5: Mechanical Properties of Timber Studs Used in Elevated Temperature Experiments

Experiment	MOE_{avge1} (GPa)	MOE_{avge2} (GPa)	MOE_{avge3} (GPa)	$MOE_{avge\ studs}$ (GPa)	$Density_1$ (kg/m³)	$Density_2$ (kg/m³)	$Density_3$ (kg/m³)	$Density_{avge}$ (kg/m³)
BFT 668	7.7	7.3	7.7	7.6	507	454	510	490
BFT 669	7.4	7.6	7.8	7.6	477	421	467	455
BFT 676	7.4	7.9	7.3	7.5	494	501	487	494
BFT 679	7.9	7.1	7.7	7.5	431	467	488	462
BFT 680	7.8	7.6	7.1	7.5	484	496	405	461
BFT 681	8.0	7.8	7.0	7.6	434	437	486	452
BFT 682	7.9	7.6	7.0	7.5	513	488	463	488
BFT 683	7.5	6.8	8.0	7.5	484	438	504	475

The moisture content of the timber specimens, measured with an electronic moisture meter was approximately 12%.

Exposed
Face

Unexposed
Face

Pairs of 50mm long x 2.8mm diameter
nails at 100 mm spacings covered with
Boral B300 bedding cement, paper tape
and a further layer of B300 over the tape.
Plasterboard sheets fastened with nails in
accordance with manufacturer
requirements on spacings

Plasterboard fastened
same as on fire side

Nogging

16 mm thick Boral
'Firestop' plasterboard
sheets

All timber framing 90mm x
45mm Radiata Pine

Figure 5.22: Plasterboard Joint Details per Boral Plasterboard Manual (Used for all experiments
except BFT 682, BFT683)

Exposed
Face

Unexposed
Face

Pairs of 50mm long x 2.8mm diameter
nails at 100 mm spacings covered with
Boral B300 bedding cement, paper tape
and a further layer of B300 over the tape.
Plasterboard sheets fastened with nails in
accordance with manufacturer
requirements on spacing

Plasterboard
strip screw fastened
at 200mm centers

Nogging

Ceramic fibre compressed to
form seal

Plasterboard sheets fastened with
nails as for walls 1-6

Plasterboard sheets fastened with
two nails at middle to each stud

All timber framing 90mm x
45mm Radiata Pine

16 mm thick Boral
'Firestop' plasterboard
sheets

Figure 5.23: Plasterboard Joint Details for Experiment BFT683

5.3.5.2   End Restraint

For the specimens without rotational restraint provided at the ends of the walls, the same detail as used in the ambient test series was employed, which is detailed in §5.2.3.2.2. In the case of the wall panel experiment where rotation was prevented, the gap between the plates at the ends of the specimen and frame, which provided clearance to allow free rotation were packed with steel pieces. These pieces were tightly fitted such that no rotation could occur at these supports. The remainder of the specimen was constructed identically to those with pinned supports, including the nailed connection of the top plate to the studs.

5.3.5.3   Thermocouple Construction

The thermocouples were constructed in accordance with the requirements of AS 1530.4-1990. All thermocouples used in the fire resistance experiments were of type K, Chromel Alumel, 2.4-3.0 mm diameter, and generally had fibreglass insulation on both the sheath and individual wires.

Ceramic fibre insulated cable was used in circumstances where either the exposed face surface temperatures of the plasterboard or temperatures within locations inside the furnace or a length of the cable was exposed to temperatures greater than 500°C for an extended period of time.

Thermocouple wires were made to a sufficient length to be connected directly to the data acquisition equipment with mini-thermocouple plugs.

At a time close to failure, all thermocouple wires were cut close to the wall being tested to reduce the risk of damage to the thermocouple wire. All thermocouple junctions were reconstructed for each experiment. Wiring was visually examined and any section of wiring which either appeared to have been thermally degraded, or with sharp bends induced in it where there was potential for junction formation, was removed and discarded.

5.3.5.4 Measurement of Temperatures within the Wall Cavity

Cavity temperatures were measured with thermocouples in open 50 mm diameter steel tubes wrapped in ceramic fibre. To observe whether there was any three dimensional variation of temperature, further thermocouples were placed throughout the walls to measure the temperature profile both through a central cavity and also arranged in a vertical line coincident with the central cavity being measured. Additional thermocouples were also arranged in several of the experiments in a horizontal line across walls, coincident with the cavity being measured. In several experiments, additional thermocouples were placed in a vertical line in the central cavity to measure any variation in temperature that could occur in that direction due to convection or other modes of heat transfer. Refer to Figure 5.25 for a generalised diagram detailing the thermocouple positions. Note: specific details of the locations of thermocouples for each individual experiment are detailed in Clancy & Young (1996).

5.3.5.5 Measurement of Temperatures within the Timber Framing

The temperature distribution through the cross section of the timber framing was measured with the use of noggings and studs containing a matrix of thermocouples (refer to Figure 5.24). The design was based on 'dummy' studs used for temperature measurement in fire resistance tests by Collier (1991).

The construction of the noggings involved the cutting of the timber element at a 60° angle and drilling holes 2.5mm in diameter to a depth of approximately 60mm. The thermocouples were orientated in this direction to increase the proportion of the length following the direction of minimum thermal gradient. Care was taken when drilling the holes to ensure that the holes followed a path parallel to the specimen. A drill press was used to drill the holes, a high drilling speed was used in conjunction with several short passes to ensure that the drill bit was always clear. Thermocouples created as hot junctions were inserted into the holes, the two sections of the temperature measurement section were covered with a calcium silicate based glue and clamped together to dry. Additional self-tapping screws were inserted through the joint on the non-fire side to increase to strength of the joint.

Two of the non-load-bearing experiments had both thermocoupled noggings and studs in order to calibrate temperatures measured between the two components. The use of noggings to measure the temperature distribution through the timber in the load-bearing experiments was deemed preferable to the technique of using 'dummy' studs within a cavity as employed by Collier (1991). It was considered that the effect on cavity temperatures due to the insertion of the dummy 'stud' could be more marked by the smaller size of the cavities the in experimental series than from those employed in conventional wall systems. The nogging temperatures would be affected by convection within the cavities above and below, the effect of this was examined in the course of the calibrations and was found to be generally most apparent during the initial phases of the tests when convective heat transfer dominated radiative heat transfer.
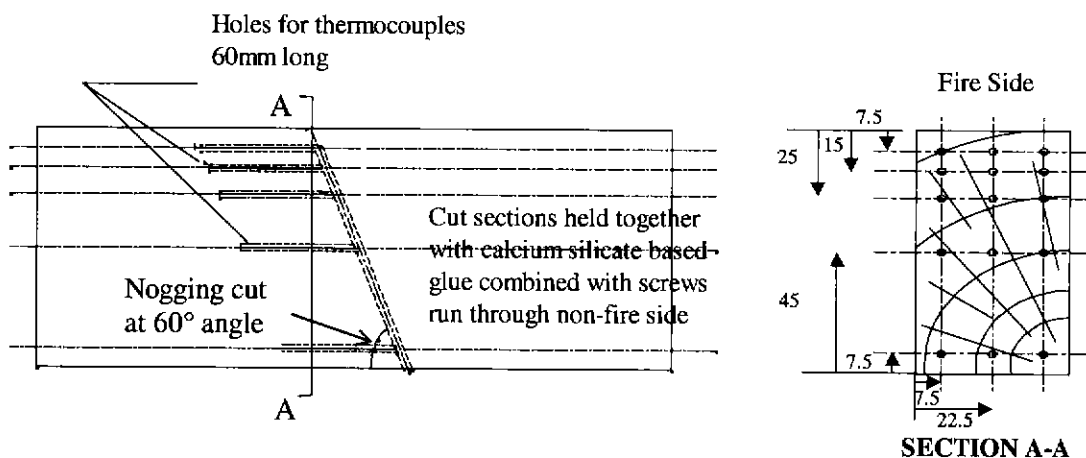
Figure 5.24: Timber Noggings (90mm x 45mm cross-section) Used for Temperature Measurement

Thermocouples were inserted at locations in the end plates on the top and bottom of the wall to monitor temperatures near the supports. Thermocouples were also inserted at two depths in the ends of the central stud to monitor the temperatures at the end of the stud and the condition of the supports during exposure.

A — Edge of Furnace

C5-8
P2(8)
x

x CX5,6
x CX3,4

L9,10

x
C9,10
L8

x CX1,2
P1(3)
x

L11,12

C11,12
x

Thermocouple marks
shown in grey were
used to validate
temperatures predicted
by heat transfer submodels.
(Other thermocouples for
checking assumptions.)

5 @ 600
= 3000

**ELEVATION OF WALL FRAME
VIEWED FROM AMBIENT SIDE**

22   A   22
4@380

1566

Fire Side

S1	S2	S3	7.5
S4	S5	S6	7.5
S7	S8	S9	10
S10	S11	S12	20
S13	S14	S15	7.5

7.5 15 15 7.5
45

THERMOCOUPLES IN STUD

Fire Side

Car engine gasket
sealant resistant
to 500°C

[1]	[1]	[2]		[3]	[1]	[1]	[1]
P1(3,8)	P1(4-6)	P2(6)		C2	C3	C4	C1
P2(3,8)				C6	C7	C8	C5
					CX2	C10	C9
Ceramic					CX4	C12	C11
Insulated					CX6		CX1
					L8		CX3
					L10		CX5
					L12		L9
							L11

Fibreglass Insulated

THERMOCOUPLES IN CAVITIES

[1] Surface thermocouple with pad and copper disc

[2] Surface thermocouple with copper disc, no calcium silicate pad.

[3] Cavity thermocouple shielded in a tube wrapped in ceramic fibre.

Figure 5.25: Thermocouple Locations in the Full-Scale Fire Resistance Test Series

5.3.5.6   Deflection Measurement

Deflection measurements were made at locations shown in Figure 5.26. Out-of-plane deflections were measured with the use of a graduated rule held in place and a dumpy level (refer to Figure 5.27). Axial deformations for the loaded tests were measured using a rule fixed in place and a dumpy level. The measurements were made until either smoke from the test obscured the view of the rule with the level or it was considered that failure was imminent and it was unsafe for measurements to be made in front of the wall panel. Deflections were recorded for the non-load-bearing tests at all locations every fifteen minutes. For the load-bearing tests with reduced times of failure, such as BFT680 and BFT683, deflections at important locations such as the mid-height position in the centre of the panel were recorded at approximately five minute intervals, whilst deflections at all points were recorded every ten minutes.
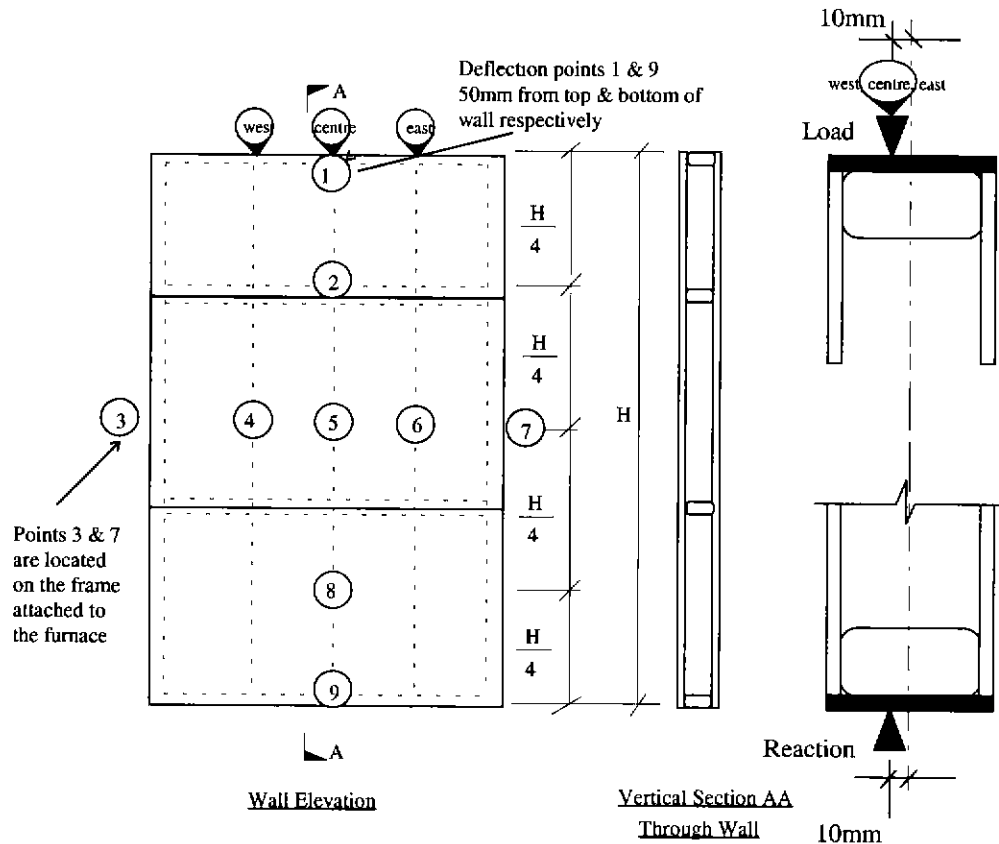
Figure 5.26: Deflection Point Locations
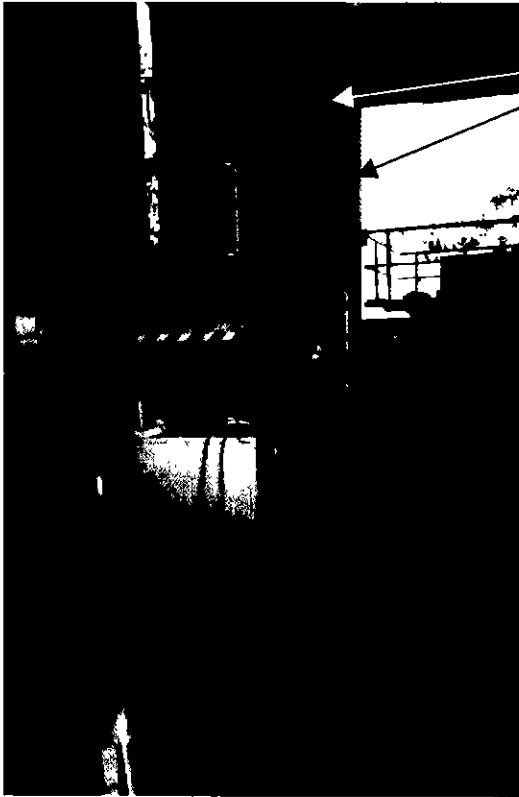
Figure 5.27 : Photograph Showing the Technique Employed to Measure Out-of-Plane Deflection
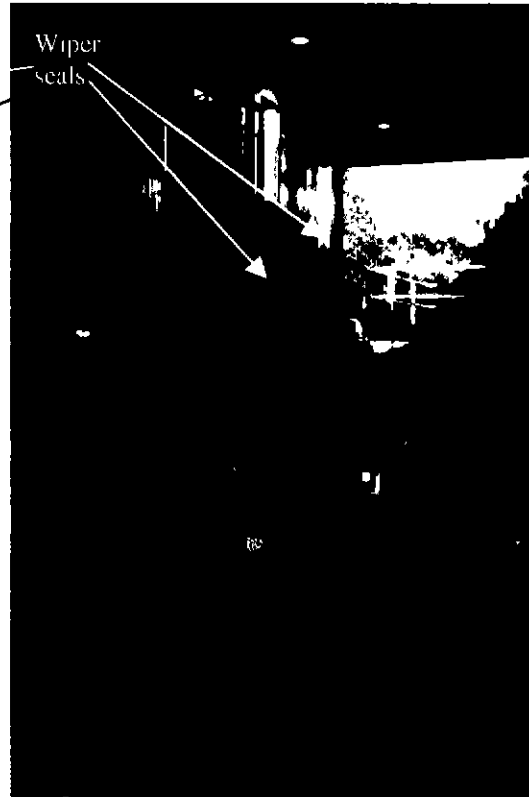
Figure 5.28 : Photograph Showing the General Configuration of the Experiment Apparatus, including the Furnace, Data Acquisition Equipment, Dumpy Level

5.3.5.7   Construction of Wiper Seals

Wiper seals were constructed to provide a seal between the timber panel tested and the steel frame used to mount the panel on the furnace (Refer to *Figure 5.29* for a horizontal section detailing the construction, Figure 5.27 and Figure 5.28 show photographs). The seals allowed the furnace pressure to be maintained in accordance with the requirements of AS1530.4-1990, whilst not allowing restraint against motion along the edges of the wall panel.
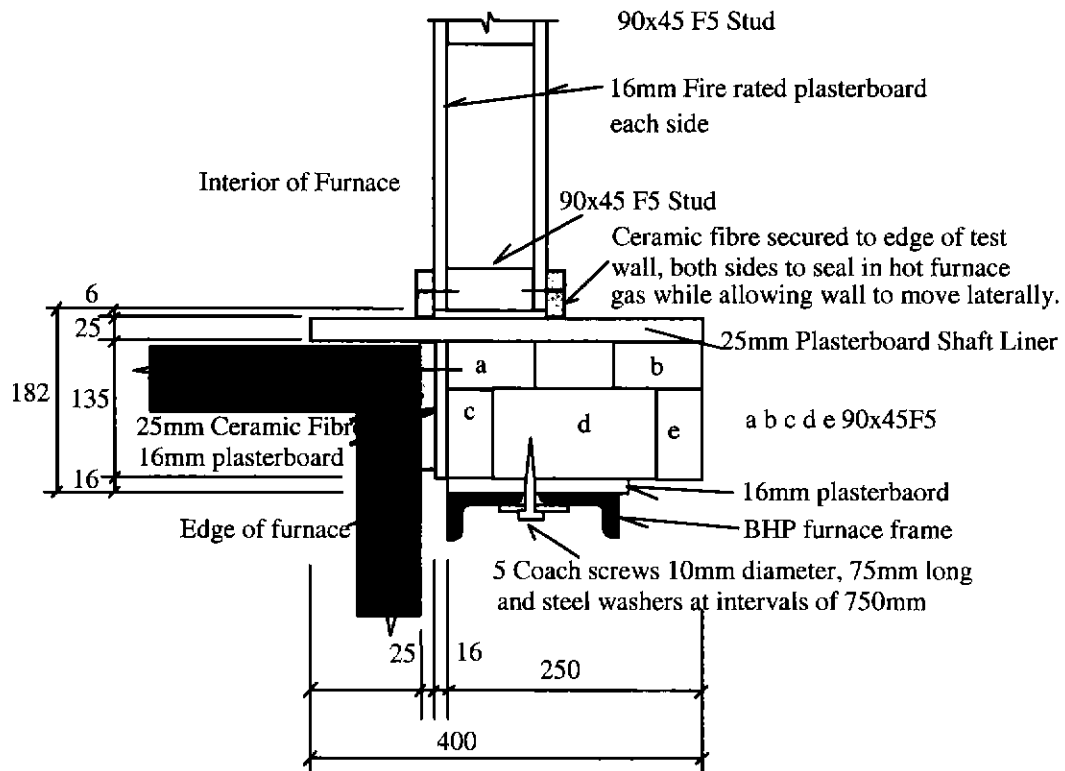
Figure 5.29: Horizontal Section through the Edge of the Wall Section showing the Wiper Seal

Construction Detail

5.3.5.8 Application of Loading

The three 800 kg weights were successively lifted into the loading apparatus (Refer to Figure 5.30) by a small mobile crane just prior to commencement of the experiment. The loading apparatus is shown in Figure 5.31.

Figure 5.30 : *Photograph Showing Steel Weights Being Lifted into Position to Apply Load to Specimen (Note: the smoke is exhaust from the crane, not the furnace)*
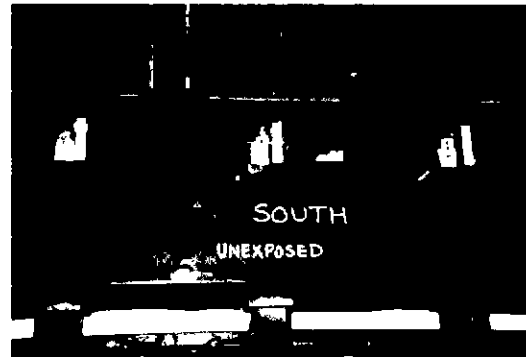
Figure 5.31 : *Loading Apparatus with 800 kg Steel Weights in Position, above each "Plunger" (Note the graduations are used for displacement measurements)*

5.3.5.9 BHP Research, Melbourne Laboratories, Wall Furnace

The wall furnace at BHP Research, Melbourne Laboratories had an opening to heat wall specimens 3 m tall by 1.63 m wide. The furnace was gas powered and was lined with ceramic fibre wool. The wall panel tested that was attached to the furnace was exposed to a heating regime as specified in AS1530.4-1990. The equation describing the heating regime with time was

$$T_f = T_0 + 345\log(8t + 1) \qquad - (5.1)$$

where T_f is the furnace temperature (°C)

T_0 is the ambient temperature (°C)

t is the time after commencement of the test (minutes)

5.3.6 Results

5.3.6.1 Summary of Test Observations

The general test observations on the exposed and unexposed faces of the specimens noted during each test are listed in

Table 5.6 and Table 5.7 respectively.

Table 5.6: General Observations from Full-Scale Fire Resistance Experiments on the Exposed face of the Wall Panels

Time Period After Commencement of Experiment (Minutes)	Observations
0-10	The paper charred to a black colour, then dark grey and gave the appearance of mud-cracking. At the corners of cracks the charred paper curled.
10-20	The stopping material cracked. 5-10% of stopping material cracked and lifted leaving nail heads visible. Where nails were still covered by stopping material, the nail heads showed through as black spots and stopping had sloughed off. No cracks in the plasterboard were apparent. Sheathing around furnace thermocouples was dark red. Plasterboard was dull red. 20-30% of paper had turned to ash. The paper appeared as medium grey and fluffy in appearance indicating the formation of ash.
20-30	The furnace was bright orange. Most of the stopping material over nails fell off during this period. Exposed nail heads were black. The plasterboard sheet was still flat; not warped. The paper was light grey and very fluffy in appearance.
30-40	There was further sloughing of stopping tape and material. Cracking was evident in plasterboard either side of lower joint at end of this time period, varying between hairline to 1mm thick.
40-50	There was further dislodging of stopping tape. Cracking of the exposed face continued.
50-60	Gap in lower joint opened up to 2 mm. More than 80% of all stopping had sloughed off revealing nail heads which had turned black in colour. No warping of the plasterboard was apparent at this stage.
60-70	Several cracks apparent across face, several hundred millimetres long and 1 mm wide. The whole face was crazed. There was intensive crazing about lower joint.
70-80	There was local cracking around nails. The exposed face was intact but field nails had pulled through. Crazing was intense about the lower joint, across full width of wall. The gap in the lower joint opened up to 3mm. Cracks elsewhere in wall had opened up to 3-4mm. The plasterboard was very warped.
80-90	Cracks had opened up to 5mm wide. The amplitude of warping increased and appeared to be as large as 50mm.

Table 5.7: General Observations from Full-Scale Fire Resistance Experiments on the Unexposed

face of the Wall Panels

Time Period After Commencement of Experiment (Minutes)	Observations
0-10	Plasterboard was warmer to touch towards the top of cavities behind the unexposed plasterboard sheet.
10-20	Moisture condensed on cool glass surface when placed within 10 mm of the unexposed face. The unexposed face was warm and easy to touch, the temperature was between 50-60°C.
20-30	Steam emitted from some holes in the unexposed face, where thermocouple wires penetrated. The temperature of the face was 60-70°C. Droplets of water fell from the lower corners of wall onto the floor.
30-40	In pin-ended loaded tests, a horizontal crack formed in the lower joint in the unexposed face. The temperature was 70-75°C. Moisture droplets continued to drip from the lower corners of the wall.
40-50	The face was 75-80°C. Dripping water continued but became a black sooty colour.
50-60	In the fixed-ended test, horizontal hairline cracks were observed about the mid-width of the unexposed face about lower horizontal joint.
60-70	Random cracking sounds came from inside the walls. There was a slight darkening of the face. The odour of burning timber was apparent.
70-80	The cracking sounds coming from inside the wall were loud and audible at 6 metres away from it. The surface temperature was 95-110°C.
80-90	Water continued to pool below the corners of wall. The unexposed face surface temperature was 110-120°C.

5.3.6.2 Failure Mode Description and Post Test Observations

5.3.6.2.1 Experiment BFT 683 lasting approximately 30 minutes

The specimen failed through excessive deformation. The timber studs had a large bowing induced, which was permanent. The surface of the studs and noggings were black but the char was very superficial, being less than one millimetre deep.

5.3.6.2.2   *Experiments BFT 679, BFT 680 lasting approximately 35 minutes*

The specimens failed through excessive deformation, with a split being induced in the joint

between the plasterboard sheets on the unexposed face (refer to Figure 5.32). The timber studs had

a large permanent bow (refer to Figure 5.33). No significant charring of the timber studs was

noted, but only shallow charring on surface which was approximately 1mm deep (refer to Figure

5.34).

Figure 5.32: Photograph Indicating the Failure Mode through Excessive Deformation of the

Pin-Pin Ended Restrained Wall. Note the split in the Plasterboard Joint

Figure 5.33 : Photograph Indicating the Permanent Bowing Induced in the Load-bearing Timber Studs After Failure
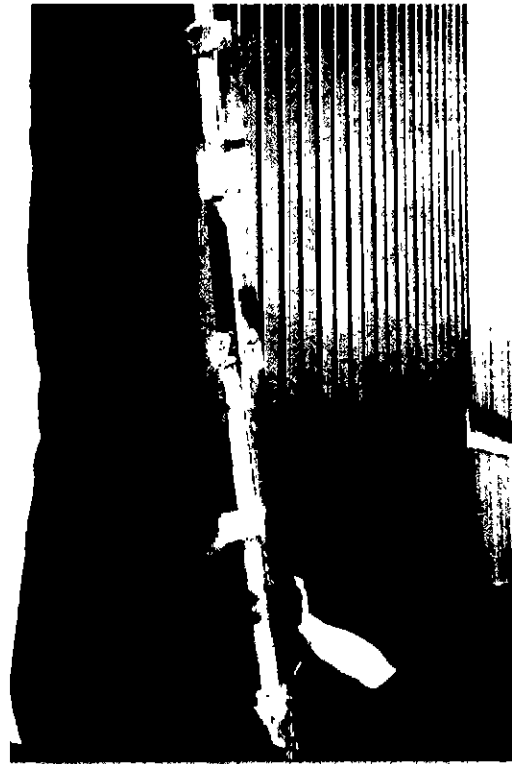
Figure 5.34 : Photograph Indicating the Limited Degradation Induced in the Load-bearing Timber Studs After Failure

5.3.6.2.3   Experiment BFT 682 lasting approximately 40 minutes

Difficulties were encountered with the operation of the furnace for this experiment. At approximately 3 minutes after the experiment commenced, the furnace went out. The furnace was re-started approximately 1 minute later.

The noggings showed no signs of thermal degradation. Very little charring of the timber studs was observed, with no apparent signs of degradation in the top and bottom plates.

5.3.6.2.4   After Experiment BFT 681 lasting approximately 60 minutes

The wall had a rapid failure mode, which occurred through the failure of the timber stud members. The plasterboard on the unexposed face did not fail through a joint, but was ruptured by the failed timber studs (refer to Figure 5.35). The plasterboard seemed to craze much more quickly

immediately after the wall was moved away from the furnace and the exposed face came into

contact with ambient air. A significant proportion (40%) of the cross-section area of the timber

studs had been charred, although the charring process continued for several minutes after the

furnace was shut down and the panel was moved away from the furnace. (Refer to Figure 5.36

which shows the degradation of the load bearing elements).

Figure 5.35: *Failure of the Wall with Rotation*   **Figure 5.36** : *Timber Stud (Viewed from the*

Prevented at the Ends   *Unexposed Side with the Plasterboard*

Sheeting Removed) Remaining after Failure

and Removal of the Wall from the Furnace

(note : degradation continued after failure

whilst the wall panel was safely removed from

the furnace)

5.3.6.2.5   Experiments BFT 668, BFT 669 and BFT 676 lasting approximately 90 minutes

Photographs showing the failure mechanism of a non-load-bearing partition are shown in Figure

5.37 and Figure 5.38. The failure mechanism was through the plasterboard sheeting collapsing on

the unexposed face due to sustaining the self-weight of what remained of the panel and the end plate. The plasterboard seemed to craze much more, immediately after the wall was moved away from the furnace and the sheet on the unexposed face on the furnace side came into contact with ambient air. No uncharred wood was remaining in the wall. The plasterboard on the unexposed face was intact, but warped. Crazing on the plasterboard sheet was intense and extensive.

Figure 5.37: *Photograph Depicting the Edge View of a Non-Load-bearing Panel after Failure at Approximately 90 Minutes Duration*

Figure 5.38: *Photograph Depicting the Unexposed Face of the Non-Load-bearing Panel after Failure at Approximately 90 Minutes Duration*

5.3.6.3 Times-to-Failure

The times-to-failure for each wall panel are summarised in Figure 5.39. Note the time-to-failure for BFT 682 was not reported because of difficulties with the operation of the furnace during the initial stages of the experiment - the same heating regime was not applied and thus a direct comparison could not be made. The time-to-failure reported is one the of collapse of the panel

(integrity) in the case of the non-load-bearing panels and of a structural failure through excessive deflection in the case of the load-bearing panels.
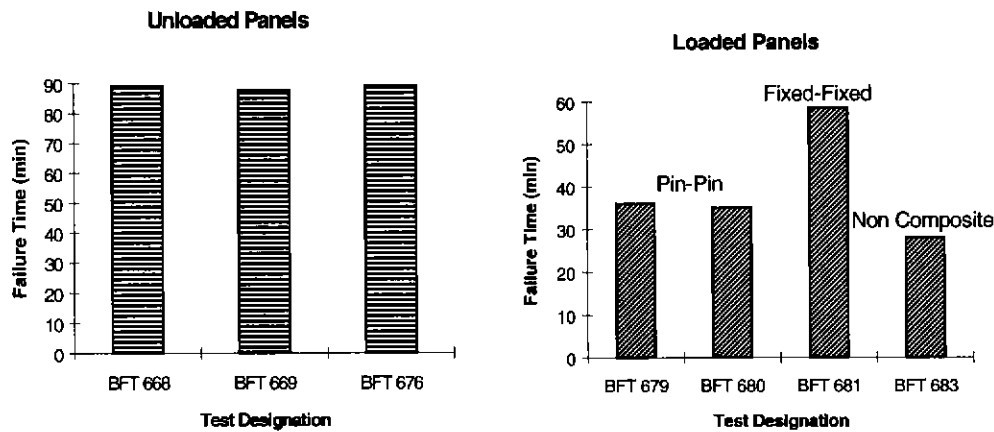
Figure 5.39: *Time-to-Failure for Elevated Temperature Experiments*

Failure through the criterion of insulation as defined in AS1530.4 as an average temperature rise of 140K or maximum temperature rise of 180K on the unexposed face was not observed during the period of temperature measurement (approximately 85 minutes). The surface temperatures on the unexposed face after 85 minutes experiment duration were typically 100°C to 120°C.

5.3.6.4   Temperature Measurements

Extensive details of the temperatures measured during the full-scale wall experiment series are reported elsewhere (Clancy and Young, 1996). The following temperature measurement that are presented are considered directly applicable to the structural response of the wall, and have subsequently been used as input data in runs of the structural model. The average temperatures through the cross-section of the studs/noggings determined at five minute intervals are presented in Figure 5.40 (A) and (B). The isotherms have been determined by using the temperatures recorded during the tests and through interpolation achieved by a Kriging technique by the Surfer V5.00 for Windows software package published by Golden Software Incorporated. The isotherms produced by the software from the experimental data contain some inconsistencies compared with what would be expected in a qualitative sense including for example; the non-linkage of the contours for the cooler regions in the 60 minute and 65 minute profiles. This is related to the interpolation routine selected and is exaggerated by the temperatures specified for the isotherm increments.

Surface temperatures have been determined through extrapolation by the software in addition to estimation of temperatures on surfaces based on adjacent temperatures, with limited data from the experiments being employed to define the temperatures of the surface of the studs/noggings. The primary use of the data presented in these figures was for input into the structural model to define the temperature profile of the cross-section of the timber elements. Some inaccuracy in the surface temperatures from interpolation errors in not considered to significantly affect the determination of the mechanical properties or hence the structural response. This is because the temperature of the materials near the surfaces was generally approaching the char temperature and the thickness of the region was very small, hence the contribution to the overall mechanical performance of the stud would be expected to be small. It should also be noted that for temperatures recorded which were greater than 350°C it is to be expected that some uncertainty would exist with regard to the position of the thermocouples, since significant charring is likely to have occurred at this temperature. This is most evident in the isotherms generated for the 80 minute and 85 minute times.

The comparison between average isotherms determined in the timber studs in non-load bearing tests and in the noggings, and in the noggings in the load-bearing tests, and the variability in the temperatures measured within the timber elements is demonstrated at selected locations within the noggings are presented in Appendix 3.2. of Young (2000)

5.3.6.5 Verification of the Validity in Using Thermocouples located in Noggings to Determine Timber Stud Temperatures in Load Bearing Tests

To demonstrate the suitability of the method of using the noggings for correlation to temperatures within the studs for the load bearing tests, two comparative steps were performed. The first involved a comparison between the nogging and stud temperatures for the non-load bearing tests, the second was a comparison of the temperature distribution between noggings in the non-load bearing and load bearing tests. By referring to the comparative isotherms, the following results can be deduced.

The isotherms for the non-load-bearing stud and noggings were similar. The only times when there were significant differences was during the early stages of the tests (approximately 5-15 minutes after commencement) when it was apparent that convection within the cavity was providing a substantial component of the heat transfer. At times beyond this, when radiation became the more dominant mode in the cavity, the discrepancy between the two profiles up to 85 minutes was very small.

The comparison between non-load-bearing and load-bearing nogging isotherms was quite close, especially up to the failure time of the bulk of the load-bearing tests (<35 minutes). It was apparent that the temperatures measured on one corner of the nogging in test BFT 681 were substantially higher than in other tests, and this has tended to skew the results for times greater than 35 minutes, as this was the only load bearing test to last beyond this time. The result of this single reading gives a slightly hotter profile on one side for the noggings for the load-bearing experiments than the average for those that were non-load bearing, but elsewhere the isotherms matched closely.

The conclusion that can be drawn from the technique of using a thermocoupled nogging for load-bearing experiments was that it gave a close representation of the temperature profile within the stud. The temperature profiles between the noggings and stud compared closely for the non-load-

5 Minutes

10 Minutes

15 Minutes

20 Minutes

25 Minutes

30 Minutes

35 Minutes

40 Minutes
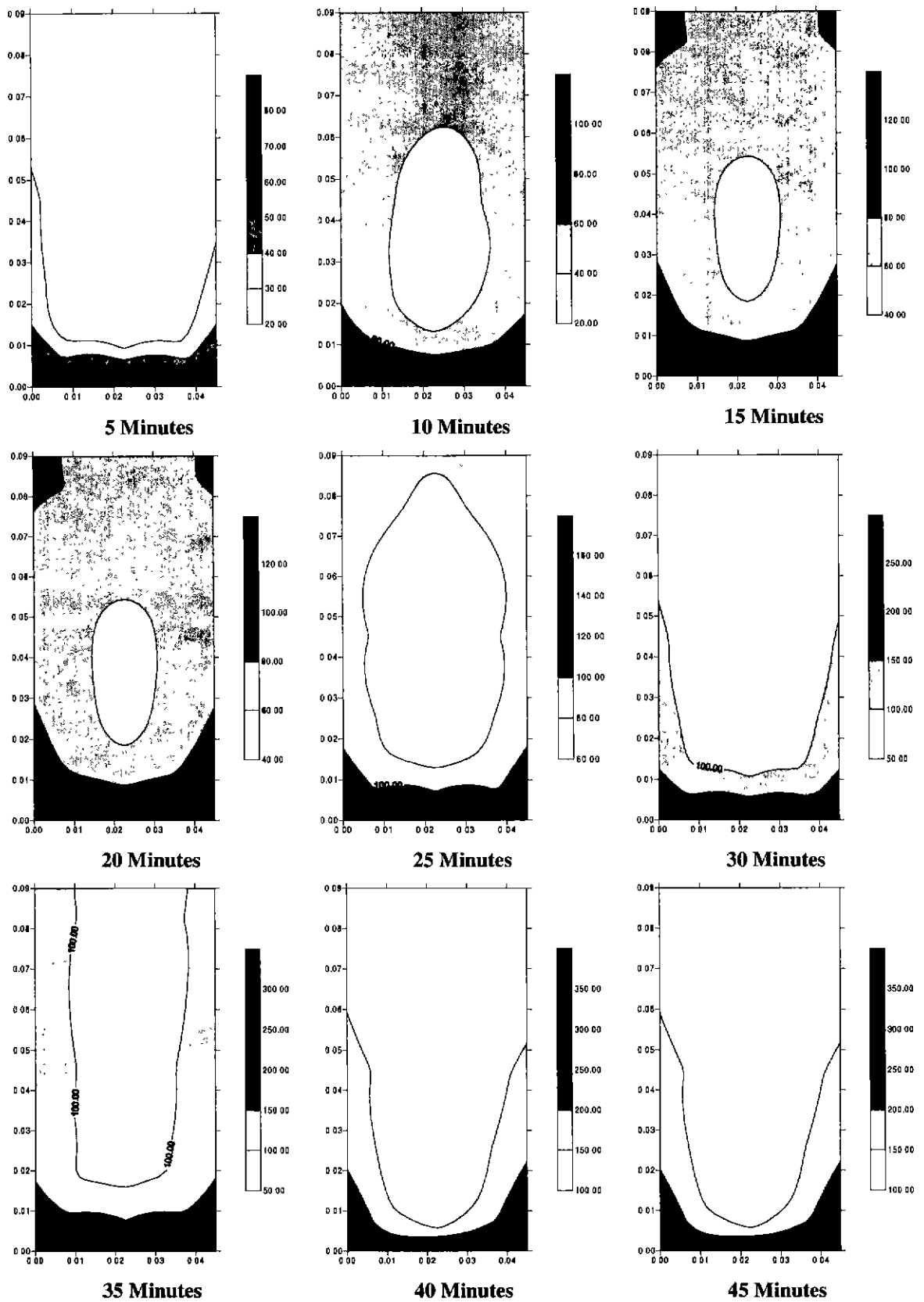
45 Minutes

Figure 5.40(A): *Average Isotherms for the Timber Cross Section (5 - 45 minutes)*

50 Minutes

55 Minutes

60 Minutes

65 Minutes

70 Minutes

75 Minutes

80 Minutes
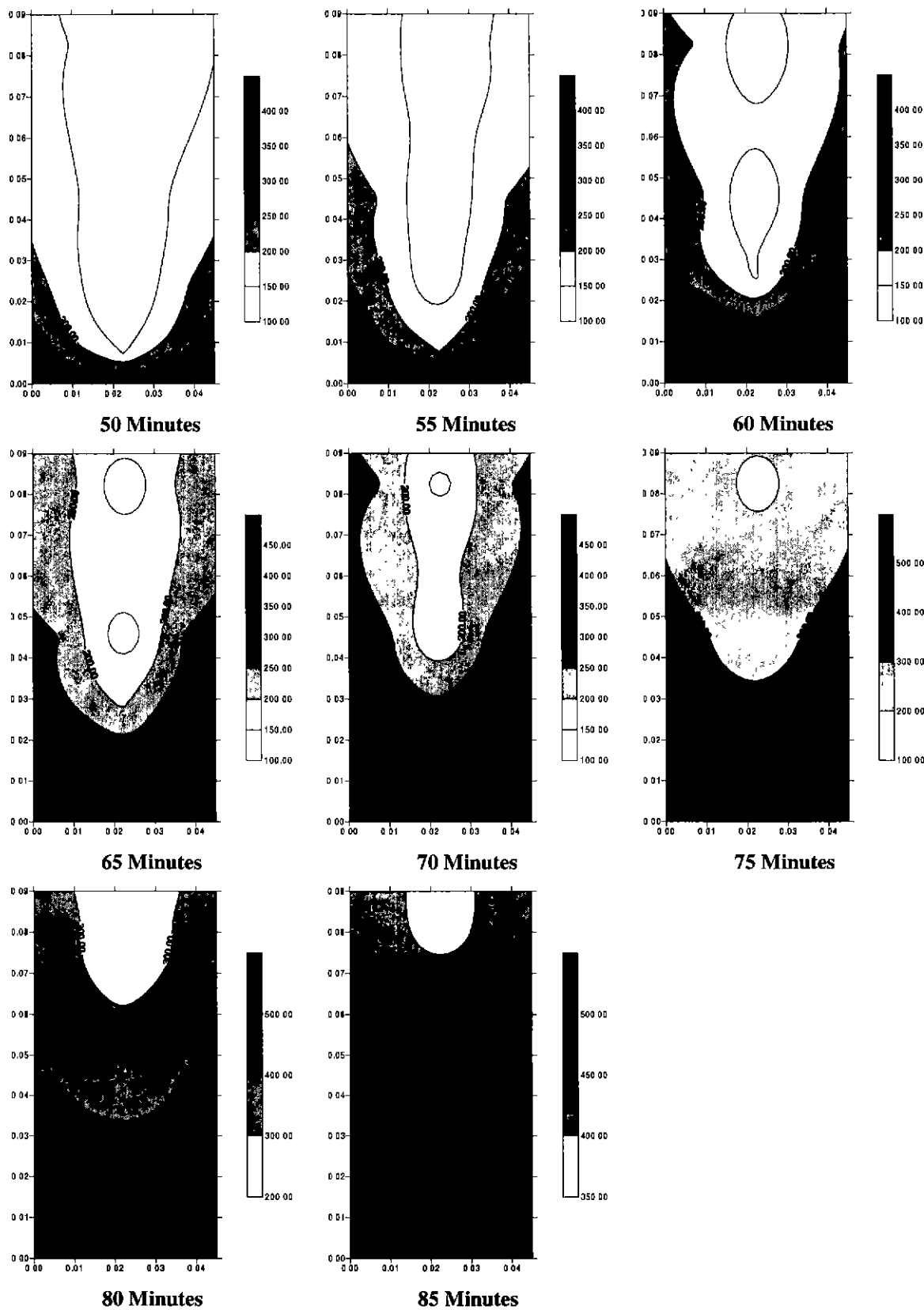
85 Minutes

Figure 5.40(B): Average Isotherms for the Timber Cross Section (50 - 85 minutes)

bearing experiments and further, so did the temperature profiles of the noggings for non-load-bearing and load-bearing experiments. The time period during the test when there was a significant discrepancy in temperature between the two elements was during the initial stages of the experiment when convection was a significant mode of heat transfer. The practice of installing thermocouples within noggings was demonstrated to be a reliable technique of measuring the temperature within timber elements in a load-bearing wall with timber framing and given the cavity temperatures were not affected, was considered to be preferable than using 'dummy' studs.

5.3.6.6 Deflection Measurements

Out-of-plane deflection profiles for the load-bearing experiments are shown in Figure 5.41, Figure 5.42 and Figure 5.43. It must be noted that the deflection profiles have been determined relative to the initial deflection induced by application of the 8 kN per stud loading. In addition the shape of the profile for the column where rotational restrain has been prevented are not accurate at the ends due to the lack of measurements at these locations for all time-steps where measurements were made, evidence of double curvature was apparent in general observations. Wall out-of-plane deflection profiles versus time for each of the experiments are presented in Appendix 3.1 of Young (2000).
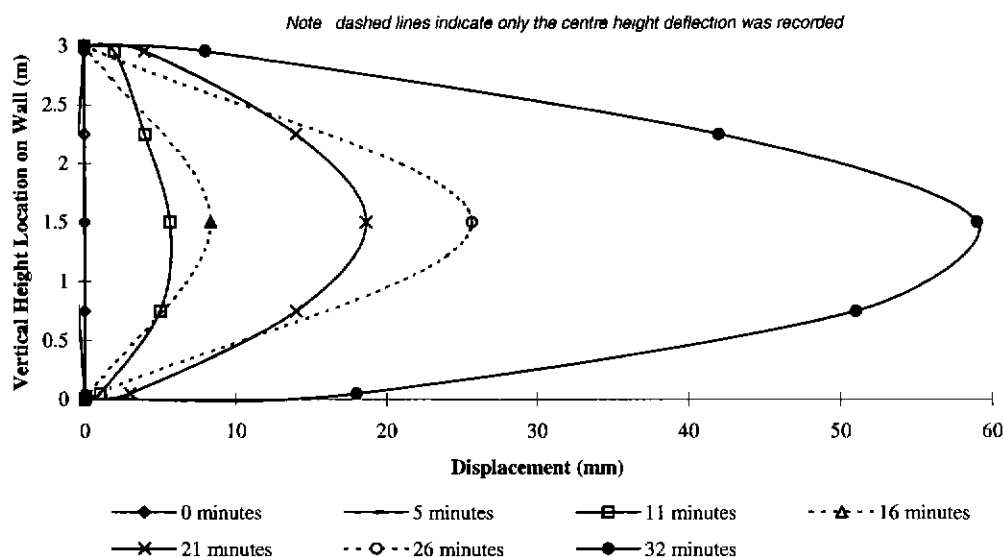
Figure 5.41: Deflected Shape Versus Time for Load Bearing Wall with no Rotational End Restraint (pin-pin) (BFT 680) Note: the lines connecting data points were interpolated by

Microsoft Excel. Due to a single mid-height data point being used for some time intervals (dashed

lines), there is some inaccuracy in the shape prediction near the ends of the walls.
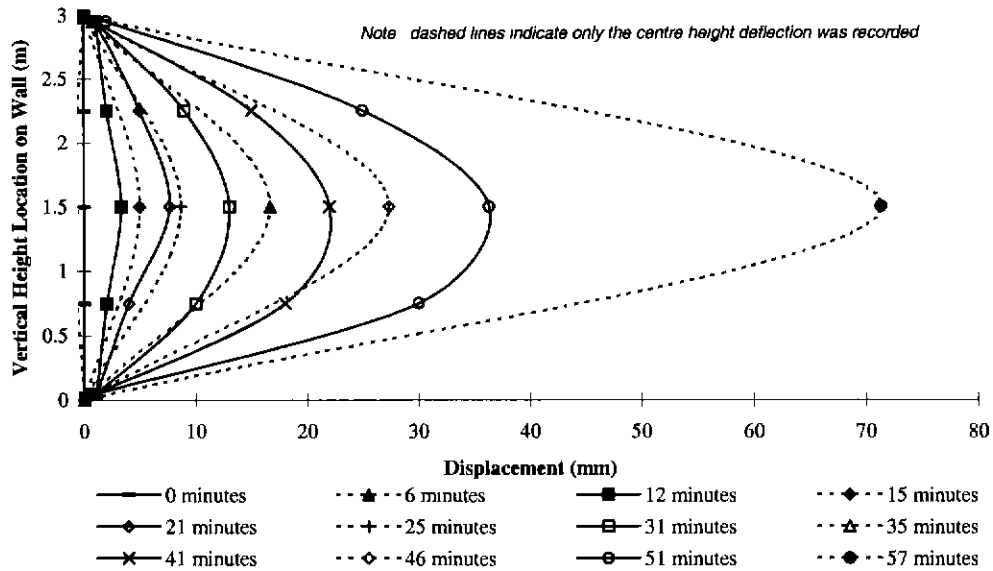
Figure 5.42: *Deflected Shape Versus Time for Load Bearing Wall with Rotational End Restraint*
(BFT 681) Note: the lines connecting data points were interpolated by Microsoft Excel. Due to a
single mid-height data point being used for some time intervals (dashed lines), there is some
inaccuracy in the shape prediction near the ends of the walls.
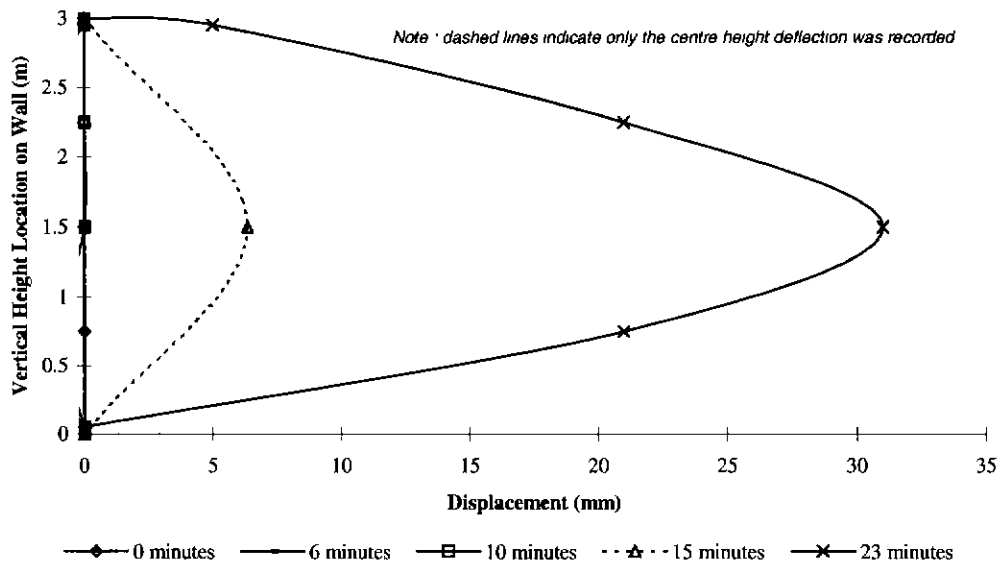
Figure 5.43: *Deflected Shape Versus Time for Load Bearing Wall with no Rotational End*

Restraint (Pin-Pin), No Structural Contribution of Plasterboard Sheeting (BFT 683) Note: the

lines connecting data points were interpolated by Microsoft Excel. Due to a single mid-height data

point being used for some time intervals (dashed lines), there is some inaccuracy in the shape

prediction near the ends of the walls.

5.3.7   Discussion of Results

5.3.7.1   General Discussion : Times-to-Failure

The results obtained for the non-load-bearing and load-bearing full-scale experiments without

rotational restraint showed little variability with regard to the time-to-failure of similar

experiments. The times-to-failure between comparable experimental configurations were within

approximately one minute.

Explanations for the low variability in the times of failure may be related to the selection

procedure employed (§5.2.3.1), which resulted in a low variation in ambient capacity, a low

variation in thermal properties or alternatively a 'heat wave' effect, a discussion of which is

presented overleaf.

The failure mechanism of the wall panels is a buckling phenomenon, that is, the capacity is

proportional to $\dfrac{\pi^2 EI}{L^2}$ where EI is the flexural stiffness of the wall and L is the length of the wall.

Timber framing members were carefully selected such that the mechanical properties relating to

structural response would result in a low variability of the wall capacity. The low variability in the

axial capacity of the timber panels in the ambient tests was demonstrated earlier in this chapter. It

was noted however, in the mechanical property tests in Chapter 6, that there can be considerable

scatter of the modulus of elasticity within groups of specimens, which have been carefully

selected.

The selection of timber studs was based on a density criterion, which may have resulted in a low

variability in the thermal properties. The heat transfer through the panel components is determined

by the thermal diffusivity. The general equation defining heat transfer through diffusion in two

orthogonal directions x, y is $\dfrac{dT}{dt} = \alpha\left(\dfrac{\partial^2 T}{\partial x^2} + \dfrac{\partial^2 T}{\partial y^2}\right)$

where   T is the temperature

          t is the time

          α is the thermal diffusivity $= \dfrac{k}{\rho C_p}$

          where   k is the thermal conductivity

                   ρ is the density

                   C_p is the specific heat

The thermal diffusivity is a function of density, conductivity and specific heat. Examination of the literature for thermal properties of timber as presented in Gammon (1987) indicated that the conductivity was generally defined as related to the density of the timber. The units of specific heat are generally represented as kJ/(kg K) meaning a relationship to the density of the material. Hence it is reasonable to assume fairly similar thermal properties for the specimens in this test series. It is therefore assumed that the chemical changes and associated degradation in mechanical properties would be similar. Thus times and modes of failure would be expected to be similar.

The concept of a 'heat wave' effect is related to the rapid drop in the modulus of elasticity within the timber framing. The drop being rapid and large enough so that the variation between the timber studs mechanical properties is insignificant in comparison. The effect is shown in Figure 5.44. Given that the thermal properties of the timber studs are similar due to the small variation in density, and there is a dwell in the heating of the timber as it approaches 100°C, the time at which a significant proportion of the cross-section timber is approaching 100°C will be similar. Assuming that a rapid drop in the modulus of elasticity occurs as the temperature of the timber approaches 100°C, the timber studs will exhibit a similar rapid drop at a similar time. If the rapid drop is of a large enough magnitude, the initial modulus of elasticity may be irrelevant as the drop could pass through the critical modulus of elasticity at which failure occurs. The likely effect on the variability of the time-to-failure associated with the variability of the mechanical properties is therefore considered to be small.
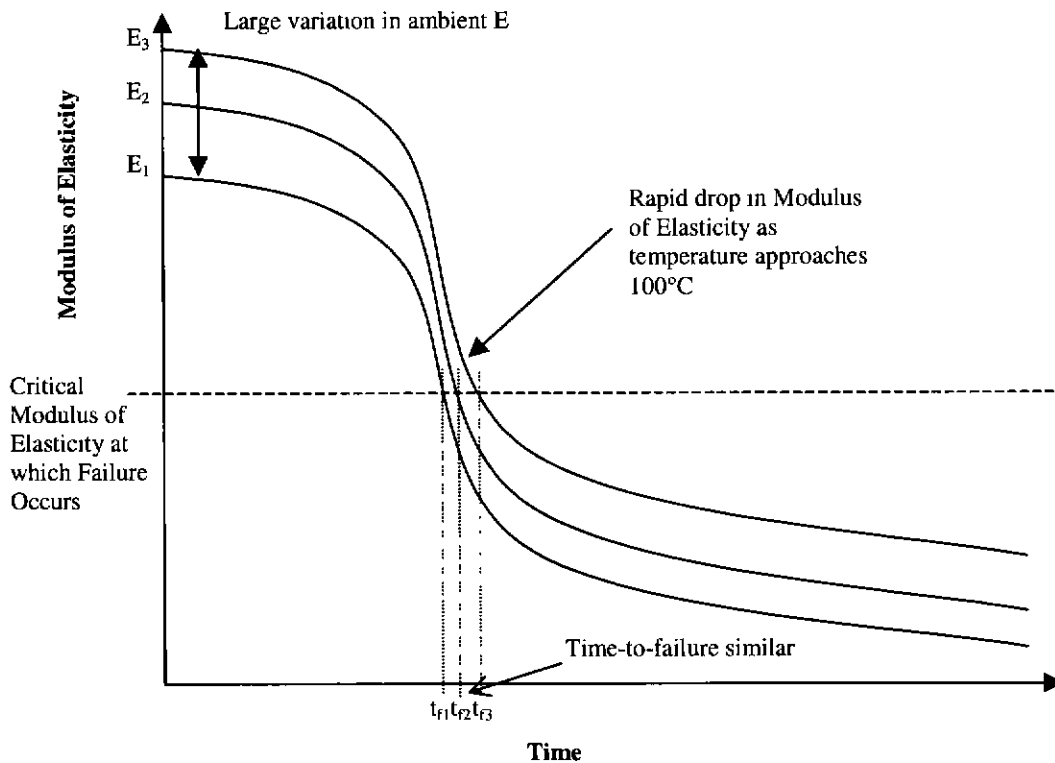
Figure 5.44: *Change in Modulus of Elasticity of Wall Frames versus Time – Diagram Detailing the 'Heat Wave' Effect*

5.3.7.2 Mechanisms of Failure

5.3.7.2.1 Mechanism of the Failure Mode of the Non-load-bearing Walls.

The three non-load-bearing tests gave similar times-to-failure; all being 88.5 ± 1 minutes, most probably associated with the low variability in thermal properties. The failure mechanism was similar for each case. The timber studs were essentially charred completely at failure, with the plasterboard sheeting appearing to be supporting the wall. As the unexposed face of the sheeting reached approximately 120°C, the weight of the plasterboard on the non-fire side face, coupled with the weight of the steel plate providing the end support at the top of the frame, ultimately resulted in the collapse of the panel. An integrity failure occurred immediately at the time of collapse of the panel. It was also noted that the gypsum plasterboard on the fire-side did not slough off during the test.

5.3.7.2.2   *Mechanism of the Failure Mode of the Load-bearing Walls without Rotational*

Restraint at the End Supports.

The time-to-failure of 34 and 35 minutes for the two specimens tested in this configuration

indicated quite low variability. There was little reduction in the dimensions of the timber cross-

section due to charring. The timber had a thin layer of char that was less than 3mm thick, but had

a permanent bow induced in it. The bowing was indicative of irrecoverable deformation, which

had been induced through the heating, moisture and stress conditions that the timber studs had

been subjected to during the test. Examination of the temperature distribution through the cross

section of the nogging (refer to Figure 5.40) indicates that a significant proportion of the cross

section was approximately 100°C at the time of failure. White *et al* (1981) demonstrated the

substantial increase in moisture in a timber slab heated under the ASTM E119 heating regime,

which is similar to that of AS1530.4-1990. They reported the moisture content of the timber

increasing from the initial concentration (generally about 12%) to between 1.26 to 2.0 times this

value as the temperature approached 100°C. The magnitude of the increase was shown to be

related to the permeability of the timber. As the temperature increased above 100°C, the moisture

content of the timber specimens rapidly decreased. White *et al* (1981) concluded that the

movement of moisture within the timber specimen was due to the rapid vaporisation of

hygroscopic water at temperatures approximately equal to 100°C. Thus it is considered likely that

a rapid increase in moisture content will have occurred throughout the majority of the timber

cross-section that was at a temperature of approximately 100°C.

Reference to generalised texts such as the Wood Handbook (1987) indicates that the modulus of

elasticity of clear wood reduces with increased moisture content, which could explain the

increased deformation. However, the deformation induced in the timber studs was permanent.

A possible explanation for the irrecoverable deformation at the increased moisture content was

considered to be the mechano-sorptive creep phenomenon associated with timber under ambient

conditions. This phenomenon is typically associated with the seasonal effects of increasing and

reducing moisture content of load-bearing timber elements and results in a substantial increase in

deflection without a corresponding increase in load. The phenomenon occurring during a fire

resistance test would be equivalent to a single rapid cycle in changing the moisture content of a

load-bearing element. The features associated with the phenomenon for ambient conditions are

summarised in Hoffmeyer *et al* (1989) and Grossman (1976). Pertinent characteristics associated

with the mechano-sorptive phenomenon that relate to observations made during the experiments

are as follows:

- The effects are not directly dependent on time – the increase in deformation occurs rapidly

  with the change moisture content, not the time the moisture content takes to change.

- The deformations increase with both an increase and decrease in the moisture content - it

  may not solely be the process of the rapid localised increase in moisture content within the

  timber as it approaches 100°C, but the rapid drying which follows that contributes to the

  rapid increase in deformation.

- The deformations induced are irrecoverable – this was evident in the tests (refer to Figure

  5.33)

Based on these characteristics, is apparent that a creep/plastification phenomenon that has been

observed in the full-scale fire resistance tests has several similarities with the mechano-sorptive

phenomenon.

5.3.7.2.3   Mechanism of the Failure Mode of the Load-bearing Walls with Full Rotational

Restraint at the End Supports.

Changing the fixity of the ends to prevent rotation at the ends, combined with no initial load

eccentricity resulted in an increased time to failure from approximately 35 minutes for the walls

with ends allowing free rotation at the ends to 58½ minutes, an increase of approximately 66%. It

was observed that the deflections of the wall started to become noticeable at approximately 28

minutes, at which time a substantial proportion of the timber was approaching 100°C, similar to

the wall with no rotational restraint at the supports. The rate of increase of deflection was not as

great as for the walls without rotational restraint at the end supports (refer to Figure 5.41,

compared with Figure 5.42). The deformations continued until failure of the wall, at which time a significant proportion (40%) of the cross-section of the timber elements had been charred. Reference to equations for the buckling capacity of columns (for example, Timoshenko, 1955) demonstrate that a column with rotation at the end supports prevented, has a buckling capacity of four times that of a column with free rotation at the ends. Hence the column with rotation prevented is significantly stiffer and will deflect substantially less, and thus an applied load will induce lower stresses due to P-Δ effects. Given the lower stress conditions, the creep effect was less pronounced, and the timber passed through a critical temperature and associated moisture content changes without sufficient deformations or stresses induced to lead to failure of the panel.

The effect of degradation in the end-plate providing restraint against rotation was examined at the end of each test, in particular the test with rotational restraint substantially prevented. The connection between the top and bottom end plates and the stud was examined after the removal of the specimens from the furnace, substantial degradation was not evident for the load-bearing experiments where no rotational restraint was provided. Given the lack of rotational restraint, it makes sense that there would be no separation within the connection between the top and bottom plates and studs. The comparatively short time of the tests (34,35 and 28 minutes) means the likelihood of substantial deterioration in the end connections is unlikely anyway (refer to Figure 5.40 for temperatures within the timber cross-section at these times).

The load-bearing experiment which had rotation prevented at the end supports exhibited an increased degree of rotational freedom in the top end plate/stud connection, compared with the bottom as the test approached failure. This freedom was apparent from the deflected shape of the wall as the test proceeded. The effect was considered to be a result of thermal degradation in the region of the connection combined with moment induced due to the movement of the neutral axis in the stud. It was most likely that the thermal degradation reduced the effectiveness of the nailed connection and the moment induced due to the movement of the neutral axis of the stud would tend to result in rotation at the connection (Refer to Figure 5.45).
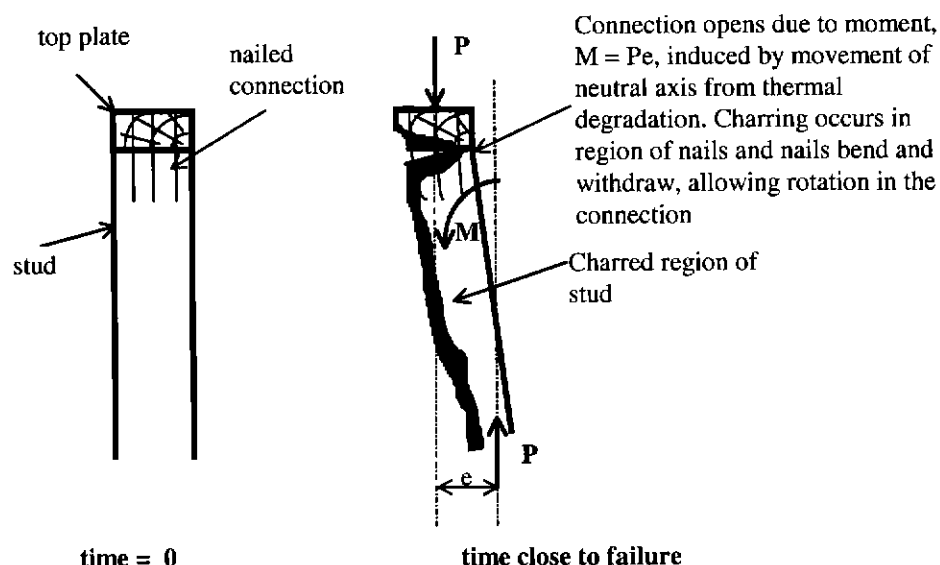
Figure 5.45: *Degradation of the Connection between the Top Plate and Stud during the Fire resistance Test of a Wall with Rotation Prevented at the Supports*

5.3.7.2.4   Determination of the Structural Contribution of the Partial Composite Action provided by the Plasterboard on the Non-fire-side for Walls without Rotational Restraint at the Supports.

The non-composite action test with pin-pin end restraints gave a time of failure 20% earlier than that with full-composite action (Figure 5.39). The mode of failure involved a large bowing in the timber studs. It is assumed that the same phenomenon as occurred with the composite panels with pin supports, was the cause of the excessive deformation. Since the time of fire exposure was only 28 minutes, little degradation in the timber due to charring had occurred (obviously less than the 35 minutes of exposure for the full composite action test). The plasterboard on the non-fire side was thus demonstrated to provide significant tensile resistance as the wall commenced deflecting away from the furnace. The contribution to the ultimate capacity of a wall provided by a sheet fixed on the tensile side had been demonstrated in the ambient test series. The stresses were higher within the timber stud alone, than the test with sheeting providing tensile resistance. It was possible the creep effect may have been induced at a slightly earlier stage, or at a more rapid rate due to the higher levels of stress within the timber stud compared to the stud with plasterboard sheeting attached.

5.3.7.2.5   Examination of the Time-to-failure of the Experimental Series with Documented

Wall Panel Systems Tested in Accordance with AS1530.4

It is noted that the failure time for this specimen which had full restraint against rotation at the

ends (BFT 681) was less (58½ minutes) than the standard system specified for a 60 minute fire

resistance level (Boral Plasterboard, 1994). The difference may appear negligible, but the end

restraint provided in this experiment was considered to be an upper bound with regard to fire

resistance when considering the conditions provided in practice. That is, in practice a conventional

load-bearing timber wall panel would be expected to have end rotational restraint provided which

is somewhere in between the cases of no rotational restraint and full rotational restraint.

The lower performance of the walls constructed for this experimental series compared with

manufacturer's fire resistant systems are considered to be explained with regard to the contribution

of the studs located at the edges of the wall. There is no requirement in AS1530.4 regarding the

position of studs at the edges of the tested panel. It is apparent that timber studs located at the

edges of the wall panel will not be subjected to heating conditions as severe as those in the centre

of the panel, hence additional structural resistance is provided. This effect was demonstrated in the

results from tests performed by Collier (1991). The deflections in this case during a fire resistance

test at 60 minutes duration were half for the two studs near the edges of the panel compared with

the three studs located in the centre, which were subjected to relatively uniform heating conditions.

The procedure employed in the tests series in this chapter removed significantly the contribution of

outer studs in providing resistance. By cutting the member along the length only studs which were

subjected to relatively uniform heating conditions were providing substantial structural resistance.

It was demonstrated in the ambient test series that a single cut may not suffice and the outer studs

should be cut at three locations to reduce the structural contribution of the outer studs, in

combination with the double curvature of the plasterboard.

5.4 Conclusions from Elevated Temperature Experiments

A series of experiments has been conducted for the purposes of examining phenomena and validating models to determine the time-to-failure of timber-framed, plasterboard-clad walls. The experiments have involved the careful selection of specimens to reduce variability, controlled known boundary conditions by using the end supports allowing either free rotation or rotation prevented, and considered the structural contribution of the sheeting to the fire resistance. The following conclusions were gleaned from the series of experiments:

The use of noggings containing thermocouples was demonstrated to be a suitable technique of measuring the temperature within timber elements within a load-bearing wall.

The variability of the time to failure for similar experiments was low. This was assumed to be associated with the selection process employed for the materials, being based on a similar density and similar dynamic modulus of elasticity and a "heat wave effect" related to the rapid decrease in the modulus of elasticity.

The method of failure of the non-load bearing specimens was generally associated with the complete combustion of the studs, complete calcination of the plasterboard on the unexposed side to hemi-hydrate and a subsequent collapse of the wall. The collapse was due to the calcinated plasterboard sheet on the non-fire side being unable to sustain the mass of the end plates at the top of the specimen.

The time-to-failure was substantially greater (approximately 250%) of a specimen without load (0% load ratio) compared with a specimen with a load level of approximately 30% of the short-term ambient capacity with no rotational restraint provided at the end supports. Thus the time-of-failure is sensitive to the load ratio.

The significance on the time-to-failure of the degree of rotational restraint provided at the ends of the wall was demonstrated. This was increased by approximately 70% from a panel free from rotational restraint by preventing rotation at the end supports.

The composite action provided by the plasterboard sheeting on the non-fire side was demonstrated to provide an increase in the time-to-failure of approximately 25% for slender walls.

The mechanism of failure of the load bearing panels, which allowed free rotation at the ends, did not involve a significant reduction in the cross-section through charring. This was considered to be associated with a rapid drop in flexural stiffness when a significant proportion of the cross-section of the timber was approximately 100°C. The cause of the rapid drop in flexural stiffness and permanent bowing induced, referred to hereafter as the creep/plastification phenomenon, may be associated with a mechano-sorptive creep type phenomenon; however, further work is required to investigate this.

Comparison with fire resistance tests performed by other authors indicated the contribution made to the structural response by load bearing elements in the regions of the vertical edges of the panels, which are not subjected to heating conditions as severe. The technique of removing the structural contribution of these elements when validating the results with models is considered essential to have a reliable comparison. Test standards should be reviewed in the light of these findings with more explicitly defined restraint conditions and the spacing of framing members from the edges of the furnace. The outer studs forming the edge of the wall panel should be cut in at least three locations, with the gap being at least 20mm.

6 Mechanical Property Experiments of Radiata Pine in Compression at Elevated Temperatures

6.1 Introduction

6.1.1 General

Timber-framed walls resist loads by the use of slender timber studs subjected to axial compression. The mode of structural failure is therefore most likely to be through buckling, which is dependent on the flexural stiffness and hence the modulus of elasticity in compression. The literature review revealed that there was a lack of knowledge on the degradation of the compression properties with temperature. In particular, no specific experimental data were found that directly calculated the reduction in modulus of elasticity versus temperature for timber in compression parallel to the grain.

In reviewing the results of the full-scale fire resistance experiment series (refer to Chapter 5), it is evident that there was a significant reduction in the modulus of elasticity as the temperature of the wood approached 100°C, which was not highlighted in the literature.

For the structural model developed to give reliable predictions, it was considered essential that the modulus of elasticity (in compression) of the timber was determined for the temperature range of 20°C to 250°C.

6.1.2 Aims

The main objective of the experimental program was to determine the change in the mechanical properties of modulus of elasticity and ultimate strength in compression, due to the effect of elevated temperatures. The methodology employed to determine the reduction in the mechanical properties of timber in compression required careful consideration of the following:

(i)   The variability of compression mechanical properties of timber.

        The testing of specimens to determine the modulus of elasticity (MOE) and ultimate

        strength is destructive. Thus there is some uncertainty in relating the properties of the

        specimen tested at elevated temperature to one tested in ambient conditions. This

        uncertainty must be considered in that ambient timber mechanical properties are highly

        variable (Leicester *et al*, 1988).

        Given mechanical property tests are to be performed in compression, relatively short

        samples will be tested due to propensity of specimens to fail through buckling instead of

        crushing. However, the use of short specimens would tend to result in an increase in the

        variability within a group of samples as the range of defects within a shorter specimen

        will be comparatively lower than in a longer specimen. Madsen (1992) has demonstrated

        this in that longer timber sticks tested in bending had a lower strength than shorter ones.

        To accurately estimate the reduction in ambient mechanical properties of the specimen

        tested subjected to elevated temperatures requires sampling procedures to be developed.

(ii)   Development of a technique of heating the specimens that did not interfere with the

        reliable determination of the mechanical properties.

(iii)   Development of a technique of measuring and recording the compression load-

        deformation behaviour at elevated temperatures to allow for the mechanical properties to

        be deduced.

Thus the following had to be developed to achieve the main aim:

•   An appropriate procedure for selecting timber samples with a small variability of the

        compression properties thereby enabling a small number of samples to be used to determine

        the reduction in mechanical properties with confidence. The technique of specimen

selection for grouping specimens of similar mechanical properties was referred to as a 'batching' procedure.

• A technique of heating each timber specimen such that load and deformation could be accurately measured at elevated temperatures.

• A technique of measuring and recording the compression load-deformation behaviour at elevated temperatures.

6.1.3 Overview of Methodology

Radiata pine (*pinus radiata*) was timber species considered in the experimental series because it was used in the experiments described in Section 5 and it is the most common species in Australia used for timber-framed construction.

To reliably determine the effect of elevated temperatures on the mechanical properties of the timber, two selection techniques were trialed for grouping short specimens to reduce the variability. The first technique (§6.2) was based on grouping specimens on the basis that the specimens were within the low end of the strength distribution of the entire population of a particular stress grade. Initially the aim was to include samples with realistic characteristics, therefore to obtain samples with growth characteristics, it was considered that the selection of low-strength sections of the timber would be more readily performed using visual assessment techniques to achieve this.

The second technique (§6.3) was based on splitting a square cross-section specimen into two separate pieces and being able to relate the mechanical properties of each half. The results obtained from the selection techniques were reviewed, with consideration to the behaviour of the specimen when tested at elevated temperature. The technique found to be most suitable was used in the tests to determine the reduction in mechanical properties in compression of the timber.

A method was developed for heating each timber specimen such that the temperature of the specimen would be known with confidence (§6.4).

The method of heating developed in §6.4 was used in conjunction with the technique developed to measure and record the compression load-deformation behaviour at elevated temperatures. This procedure was used to determine the reduction in mechanical properties of radiata pine in compression (§6.5).

6.2   Grouping on the Basis of Low-End Strengths

6.2.1   Aims

The aims for grouping on the basis of low-end strengths were as follows, to:

(i)   Develop a sampling procedure for timber specimens based upon selection procedures, which grouped specimens on the basis that the specimens were within the lower end of the strength distribution of the population of the stress grade. This was performed by the use of visual grading and Modulus of Elasticity (MOE) testing criteria.

(ii)   Determine statistical parameters for the sampling procedures so that the mechanical properties of specimens chosen through the selection procedures could be predicted.

6.2.2   Procedures

The trial technique for grouping specimens on the basis of low-end strengths involved the following procedure:

As there was no applicable Australian standard, the relevant ASTM standard was used to determine the mechanical properties of short columns of timber in compression. Compression tests were therefore conducted in general accordance with the requirements of ASTM D198 (1994) Sections 12 to 19 for the testing of a short column (L/r<17) parallel to the grain.

All timber sticks from which samples were taken, were 3.0 metres long, of cross section dimensions 90 mm x 35 mm and had been machine stress graded at the sawmill. A 300mm long specimen was cut from the timber sticks that had a reasonable proportion (>50%) of the length

classified with machine stress grading as Grade F5 timberas defined in AS 1720.1-1988 and is the

lowest stress grade for this timber. A secondary criterion for selection of the specimen was that it

have a substantial knot, which would be assumed to initiate failure at a low load. The reason for

choosing a length of 300 mm for specimens was that this length was the maximum length

compliant with the requirements of ASTM D198 for testing specimens in compression parallel to

the grain. The $L/_r = 17.8 \approx 17$ for a 90x35 cross section column, 300 mm long which could not

rotate at the ends. The use of a maximum length would allow a reduced variability between tests

(Madsen, 1992).

Upon identification of an appropriate specimen for tests, the static bending modulus of elasticity

was measured by placing the stick in the machine with the loading point centred about the sample

piece to be removed (refer to Figure 6.1). The stick was orientated to bend about the minor axis.

The machine applied a single concentrated load of 90kg over a span length of 0.9144 metres and

recorded the deflection. This deflection, δ, was inserted into an elementary deflection formula for a

simply supported beam with a single concentrated load, P, at the centre of the span. The average

MOE for the timber over the span was calculated.
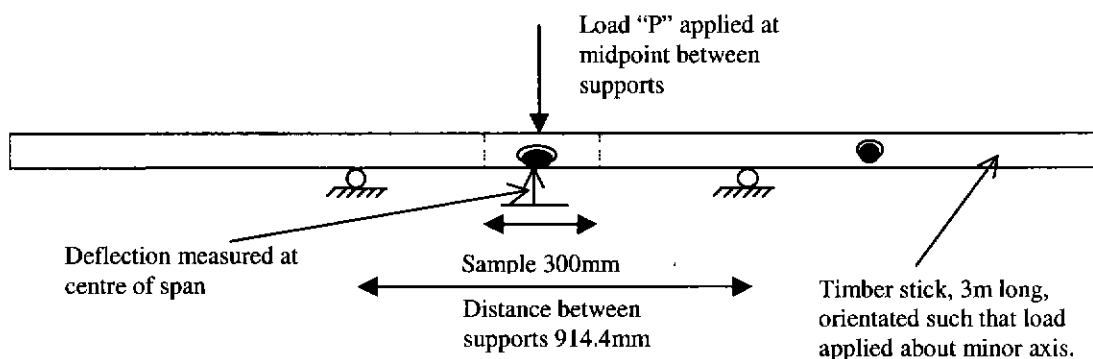
Figure 6.1: Using the Static Bending Modulus Testing Apparatus for Sampling

The specimen was then carefully cut from the stick to ensure that the ends were square to reduce

the likelihood of premature failure due to bearing at the ends and bending cause by eccentricities

in applied loading. Twelve specimens were selected in this manner to comprise a batch.

Before the commencement of each experiment, the specimen was weighed and the moisture content was measured by using a electronic moisture meter. This had been calibrated for the species of timber.

Displacement transducers were attached to the specimen over a gauge length of 55mm about the centre. The specimen was loaded concentrically with respect to the loading platens. Refer to Figure 6.2.
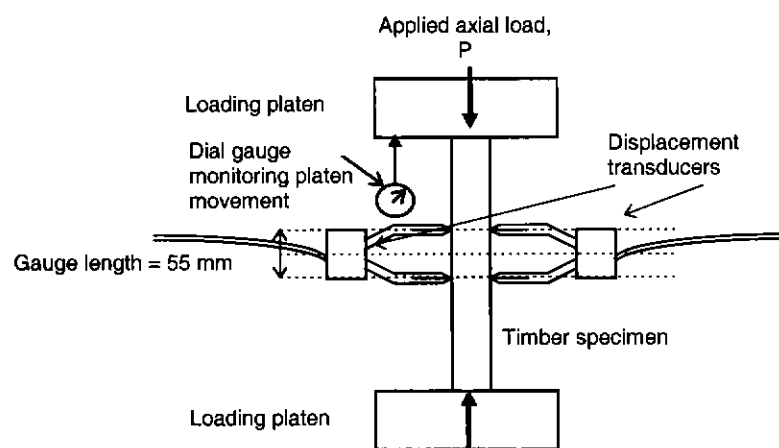
***Figure 6.2**: Schematic of Compression Test Apparatus for both Batching and Split Specimen Procedures*

The compression load and deflection measured over the gauge length were recorded simultaneously on a plotter until the specimen failed. A strain rate of 0.001 $min^{-1} \pm 25\%$ was applied.

The batch selection procedure was repeated for five batches to investigate the suitability of the procedure in being able to relate the mechanical properties calculated between batches.

6.2.3   Results

The relationship between the static modulus of elasticity in bending and the ultimate compressive strength is shown in Figure 6.3.
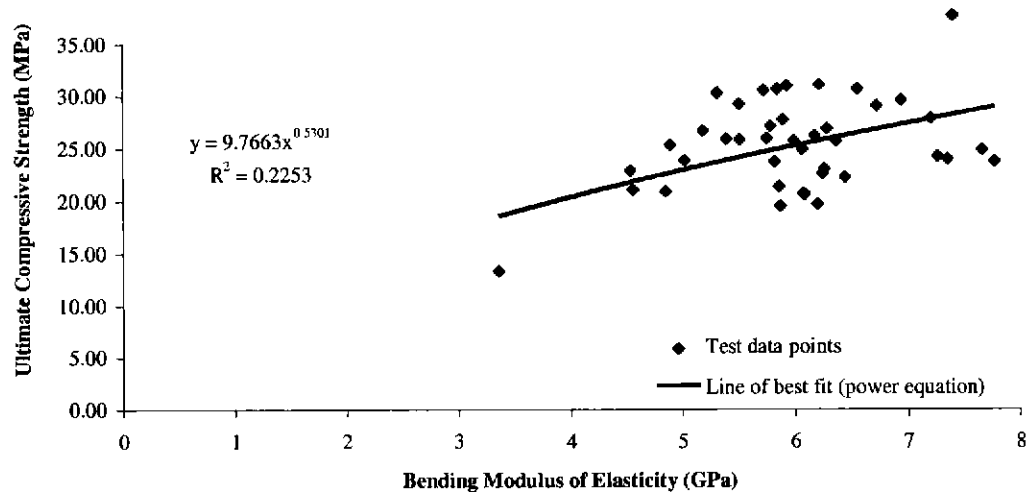
Figure 6.3: Bending Static Modulus of Elasticity Versus Ultimate Compressive Stress: Results of

Batching Procedure

The compressive strength and modulus of elasticity were calculated for each specimen. The

average strength and elastic modulus for each batch were then calculated. The summary of results

obtained for the five batches is shown in Table 6.1. Further details are presented in Young (1996).

Table 6.1: Summary of Results of Low End Specimen Batching Procedures

Batch #	Average σ_{ult} (MPa)	Standard Deviation σ_{ult} (MPa)	Average E_{comp} (GPa)	Standard Deviation E_{comp} (GPa)
1 - (preliminary)	27.38	5.59	5.97	1.88
2	25.54	5.23	5.40	1.83
3	24.22	2.90	5.03	1.75
4	27.02	3.23	5.36	1.44
5	26.13	5.16	5.36	1.44
Average (batches 2-5)	**25.73**	**4.13**	**5.29**	**1.62**

The degree of variability of the average ultimate stresses within each batch remained fairly

consistent, the results for batch #5 were skewed greatly by results from two specimens, when these

results were neglected, the average and standard deviation calculated were similar to those of

batches #2-#4. With the two samples removed from batch #5, the average ultimate compressive

stress was equal to 24.26 MPa, the standard deviation being 2.85 MPa. The average and standard

deviation of the mechanical properties calculated between each batch are shown in Table 6.2.

Table 6.2: Summary of Results of Comparing the Distributions of Low End Specimen Batches

Properties Compared Between Average Results for Each Batch (2-5)	Average σ_{ult} (MPa)	Standard Deviation σ_{ult} (MPa)	Average E_{comp} (GPa)	Standard Deviation E_{comp} (GPa)
Average Value for Batches	25.73	4.13	5.29	1.62
Standard Deviation for Batches	1.18	1.24	0.17	0.20

6.2.4 Discussion

The relationship between the static modulus of elasticity in bending and the ultimate compressive strength demonstrated a very loose trend. By fitting a simple power equation as a line of best fit, it can be seen that the experimental results vary widely about this line. Mathematically this is indicated by the low coefficient of correlation, R^2 value of 0.2253. An R^2 of unity indicates a perfect correlation between the data and the curve of best fit. It must be noted that the static bending modulus of elasticity was calculated over a length (914.4mm) which is more than three times the specimen length (300mm), and the determination of the modulus of elasticity was based on the assumption that the properties along the length were uniform. However, this assumption is not strictly correct as the properties in the region of growth characteristics can change quite markedly from those in the clear wood, which may exist in close proximity. Thus the average MOE over the length could be substantially different to the MOE of a short specimen. The use of the static bending machine gave little improvement in being able to predict the ultimate compressive strength for short specimens, compared with the use of the machine stress grading performed at the sawmill and visual grading techniques.

Based on the sampling procedure employed, it was determined that it would be unlikely for a sample size of 12 specimens that a standard deviation of ultimate compressive strength under 2.5MPa could be obtained, which represents approximately 10% of the mean value.

The modulus of elasticity measured during the compression tests gave similar results for all batches. The mean values were very close, but there was a high degree of variability within each batch. The average standard deviation of the modulus of elasticity was 1.5 GPa, approximately

30% of the mean. It would be difficult to quantify the effect of elevated temperatures on the modulus of elasticity with such a high degree of variability. The short gauge length (55mm) used in this procedure to measure deformations may have also increased the variability of results.

The location of a substantial growth characteristic near the position of the displacement measurement apparatus was observed to result in the disturbance of the correct operation of the apparatus. This was due to localised effects around the growth characteristic such as a knot pushed outward from the specimen, which could subsequently lead to an inaccurate determination of the modulus of elasticity.

The mean and standard deviation of each batch was similar, according to the results presented in Table 6.2, therefore the sampling procedure was considered to be suitable for use in relating the elevated temperature mechanical properties to ambient test results. However, the non-uniformity of knots between specimens within a batch can result in a different distribution of results for elevated temperature response. Furthermore, if correlations are to be made between batches of specimens selected from different packs of timber, either from the same sawmill or more importantly, when comparing batches selected from different sawmills, care must be taken to ensure that any correlations made are reliable.

The procedure was identified as requiring a large number of timber sticks in order to choose appropriate test specimens. The samples obtained for the tests in this section involved approximately 130, 3.0m long sticks being examined, with approximately sixty suitable test specimens being selected.

6.2.5   Conclusions

Use of the static modulus of elasticity as a technique for timber selection proved no more effective when defining the mechanical properties in compression than, machine stress grading which had been performed at the sawmill.

The results using the low end strength batching procedure indicate a high degree of variability of mechanical properties within a batch, the standard deviation being 10% and 30% of the mean for the ultimate strength and modulus of elasticity, respectively.

The modulus of elasticity was identified as a more highly variable parameter between the paired samples than the ultimate strength in compression.

The mechanical properties of the batches obtained by the procedure were statistically similar. Therefore, the sampling procedure was considered suitable in being able to relate the elevated temperature mechanical properties to ambient test results for low-end strength properties. However, problems were identified that were associated with the measurement of deformations to determine the modulus of elasticity. The problems were due to localised effects in the region of growth characteristics. An alternative approach was therefore considered, which involved the splitting of specimens. This is outlined in the next section.

6.3   Grouping on the Basis of Splitting Specimens

Norén (1988) presented the use of split specimens to reduce variability of timber properties in experiments involving timber beams over a furnace in bending. The key difference in this approach from that of Norén (1988) was that the specimens used were comparatively short (300mm compared with 2300mm) and tested in compression instead of bending.

6.3.1   Aims

The aims of the splitting specimen procedure were to:

(i)   Develop and evaluate the efficacy of a procedure for obtaining samples by splitting a 90 mm x 90 mm cross-section specimen into two 90mm x 35mm specimens so to maximise the likelihood of similar mechanical properties in each

(ii)   Determine statistical parameters (mean, standard deviation), which would allow for a given number of split specimens, the mechanical properties in compression to be predicted with a

degree of confidence given that the mechanical properties of one of the samples of the split

pair are known.

6.3.2 Procedure

6.3.2.1 Sample Preparation

The initial specimens to be split were of dimensions 90 mm x 90 mm cross-section, and were cut

along the centre and dressed to give two samples with cross section dimensions of 90 mm x 35

mm. These specimens were visually selected based on the growth rings visible in the ends, which

gave an approximately symmetrical distribution, so the specimen could be split along an axis and

each half would have a similar density (since density is a function of radial position). The density

of timber is proportionally related to the strength. Hence samples with a similar density and

minimal growth characteristics, would be expected to have a similar strength. Refer to Figure 6.4

and Figure 6.5.

Unaccceptable 90x90
- non-symmetrical growth
ring distribution - splitting
gives substantially
different density/strengths

Acceptable 90x90
specimen
- symmetrical growth ring
distribution - can split and
have very similar
densities
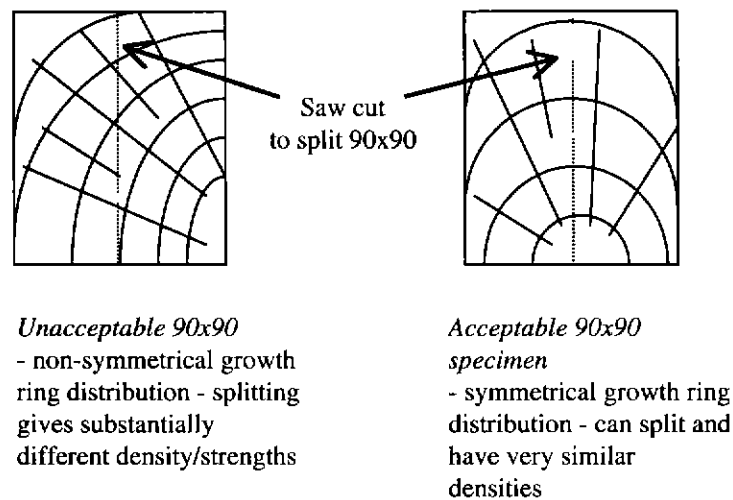
Figure 6.4: *Selection of 90 mm x 90 mm Specimen for Splitting*

To reduce wastage, the 90 mm x 90 mm specimen ideally had minimal growth characteristics such

as knots along the length and the grain was relatively parallel to the length of the specimen.

Grain relatively parallel
to the length of the
specimen

Ideally growth
characteristics along the
length of the specimen
are small.

Direction of sawcut - ideally
perpendicular to growth rings and
symmetrical about the cut.
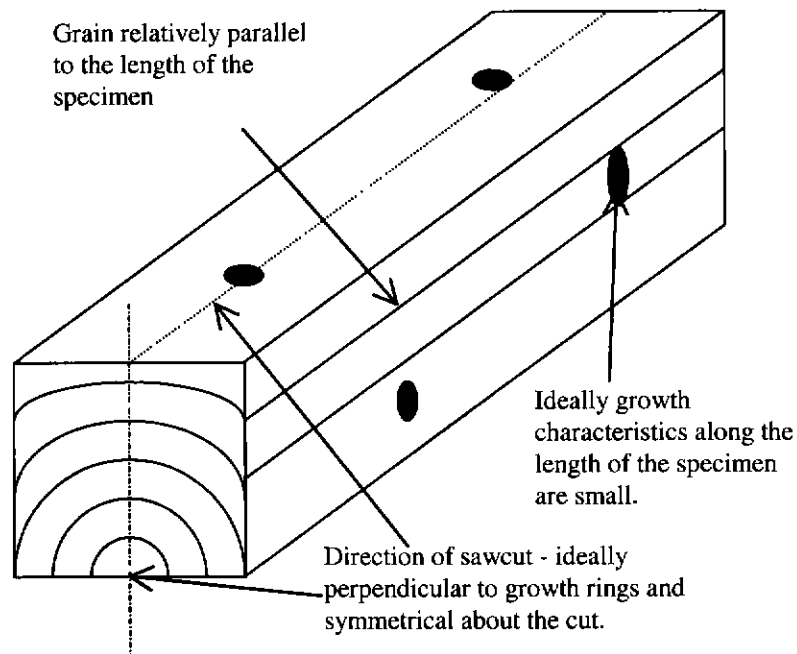
Figure 6.5*: Splitting of 90x90 Specimen into two 90x35 Specimens*

The specimen was marked with identifying letters/numbers along either side of the axis of symmetry so that when the 90mm x 90mm specimen was split, each pair could be identified after the split specimen pairs had been cut into the shorter 300mm length samples. These were cut along the axis of symmetry and dressed to the width of 35 mm. Each half was cut to 300 mm lengths, the maximum length suitable for a compression test to be conducted in accordance with ASTM D198 (1998), Sections 12 - 19. Great care taken to ensure the ends were square so that localised crushing would not be induced in the ends during the compression tests, which could result in premature failure of the sample.

6.3.2.2   Criteria for Acceptance or Rejection for Sample Pairs

Preliminary compression tests were performed to identify some of the key parameters, which defined the variability between each of a pair of split specimens. Samples were visually assessed and the density was measured.

Visual Assessment

A visual assessment of each sample comprising a pair was made. If there were noticeably different growth characteristics in either of the two samples, then the pair was rejected. Ideally each specimen would be clear of growth characteristics such as knots. While this allowed for a significant reduction in variability of the mechanical properties, it resulted in samples that were less representative of in-grade timber.

Density

The density of each sample from a split specimen pair was measured. Sample pairs with a difference in density greater than 10% were rejected. The selection of a figure of 10% was arbitrary. The difference in the mechanical properties of a pair samples was generally found to be most importantly related to the existence of growth characteristics biased to one of the pair of samples.

The difference in density between each of the samples was found to be a secondary factor with regard to the closeness in relating mechanical properties. The density was associated with the relative proportion of growth rings in each half. The relationship between the difference in the modulus of elasticity and difference in density between samples comprising a split pair, which were obtained from the preliminary tests, is shown in Figure 6.6. It was identified that a pair of samples could have a low difference in density, yet have a considerable difference in modulus of elasticity, due to the presence of growth characteristics biased to one of the samples comprising the pair.
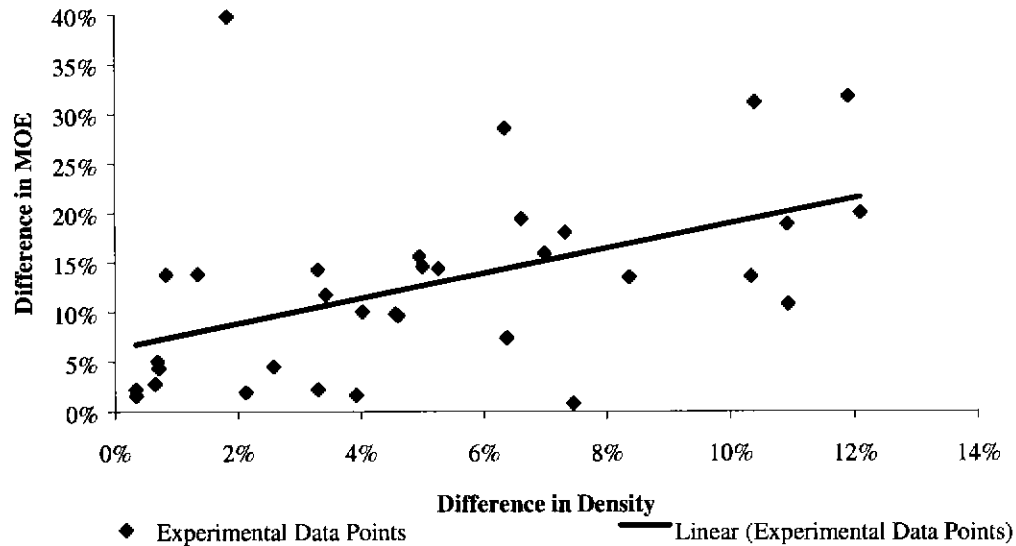
Figure 6.6*: Percentage Difference in Density versus Percentage Difference in MOE for Split*

Sample Pairs from Preliminary Tests

From preliminary experiments, it was clearly identified that if either sample from a split pair contained visible growth characteristics biased more toward one sample than the other, the pair should be rejected as an acceptable pair for which the mechanical properties could reliably be related.

6.3.2.3 Compression Experiments

A similar procedure was used to undertake the compression experiments as detailed in Section 6.2.2, using the same equipment.

A gauge length of 55mm was centred and marked on the specimens to locate the displacement transducers consistently among all samples.

The specimen was placed in the compression testing machine so that the load was applied concentrically and the displacement transducers were attached (refer to Figure 6.2). Compression tests were conducted in general accordance with the requirements of ASTM D198 (1994), Sections

12-19 for the testing of a short column parallel to the grain. A strain rate of 0.001min^{-1} $\pm25\%$ was applied.

The applied load and deflection measured over the gauge length were recorded simultaneously on a plotter until the sample failed.

ASTM D198 (1994) states that the moisture content should be measured before the commencement of the test. However the holes made by inserting the probes of the moisture meter were identified to be the region where failure would be initiated in the samples that were relatively free from growth characteristics. Therefore, an electronic moisture meter measured the moisture content of the sample after it had failed and been removed from the testing apparatus. This was measured away from the region of failure, where the structure of the material was more similar to that before being tested.

6.3.3   Results

6.3.3.1   Absolute Variation in Mechanical Properties between Accepted and Rejected Pairs of Samples

The absolute difference in mechanical properties between accepted and rejected split pairs of samples is shown respectively in Table 6.3 and Table 6.4. A substantial discrepancy between the comparative mechanical properties of those samples accepted as a suitable pair and those rejected is highlighted in these results.

The magnitude of the standard deviation of compressive strength and modulus of elasticity for the accepted pairs (Table 6.3) can be seen to be considerably less than that within the batches selected from the lower end strength batching procedure (Table 6.1).

Table 6.3: Absolute Variation between Mechanical Properties of Accepted Sample Pairs

	Ultimate Compressive Strength	Density	Modulus of Elasticity
Mean	4.06%	2.16%	5.50%
Std Deviation	2.80%	1.23%	5.07%

Table 6.4: Absolute Variation between Mechanical Properties of Rejected Sample Pairs

	Ultimate Compressive Strength	Density	Modulus of Elasticity
Mean	28.35%	4.59%	36.57%
Std Deviation	14.70%	4.26%	25.48%

6.3.3.2 Estimating the Mechanical Properties of an Untested Sample based on the Mechanical Properties of a Tested Sample, for a Split Pair

A statistical study was undertaken to examine the relationship between the mechanical properties of any split pair. The objective was to simulate the situation where the mechanical properties of one sample of a split pair was known (by destructive testing) and the other was estimated based on these properties. The aim was to use the estimated properties at ambient conditions in conjunction with properties measured at elevated temperature conditions to deduce reductions in mechanical properties with temperature. The test results of accepted sample pairs were used and the mean and standard deviation of the mechanical properties between each of the pairs was calculated (refer to Table 6.5).

Table 6.5: Variation between the Mechanical Properties of Accepted Specimen Pairs

	Ultimate Compressive Strength	Density	Modulus of Elasticity
Mean	-0.09%	0.20%	0.20%
Std Deviation	5.23%	2.61%	7.90%

6.3.3.3   Determination of Confidence Limits in Estimating the Mechanical Properties of a Pair of Split Samples, for a Given Number of Samples.

The number of split sample pairs required to be tested at each temperature was determined based on the confidence with which the mechanical properties of one tested sample of a split pair could be related to the other.

Given that there were less than 30 split pairs used in the preliminary tests, use of the normal distribution to apply statistical tests was considered unreliable (Lyman, 1988). As a consequence, the Student's 't' distribution was used because it corrects for the effects of small sample sizes. The confidence limits for Student's 't' distribution, μ_0 are calculated from

$$\mu_0 = \bar{y} \pm t_{\alpha/2} \frac{s}{\sqrt{n}} \qquad \text{- (6.1)}$$

where   s is the standard deviation, $s = \sqrt{\dfrac{n \sum y^2 - \left(\sum y\right)^2}{n(n-1)}}$ - (6.2)

y is the property

n is the number of samples

$\bar{y}$ is the mean

$t_{\alpha/2}$ is the value of the 't' distribution based on the number on the number of degrees of freedom (= n-1) and degree of confidence (1-α).

Curves were constructed (Refer to Figure 6.7 and Figure 6.8) giving the relationship between the number of samples and the confidence limits for specific degrees of confidence using Students 't' distribution. The values were calculated assuming that the mean values for the ultimate compressive strength and modulus of elasticity are centred about zero (the results in Table 6.5 show they are very close to this) and using the values of standard deviation from this Table.
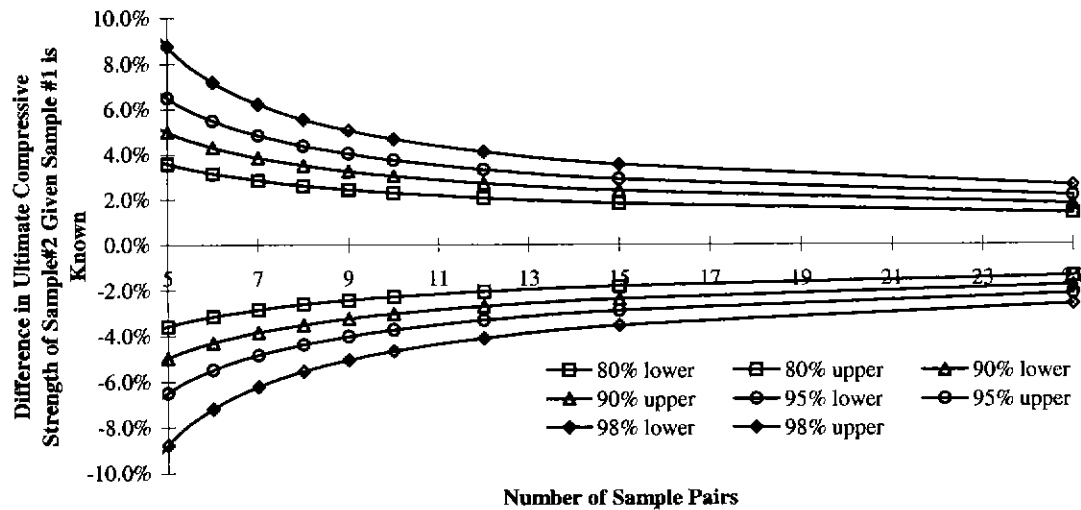
Figure 6.7: *Bounds for the Percentage Difference for Ultimate Strength in Compression of a Pair of Samples versus a Given Number of Samples and Confidence Limit*
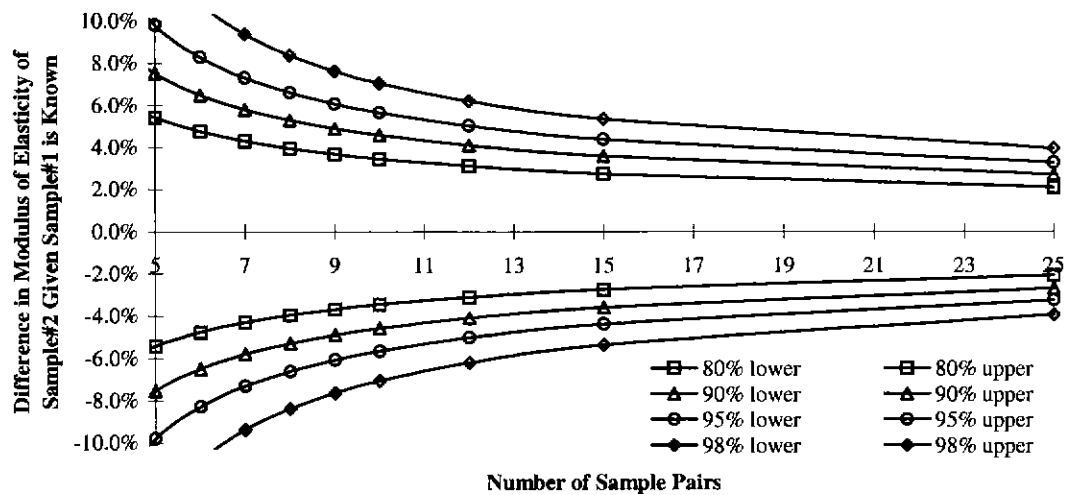
Figure 6.8: *Bounds for the Percentage Difference for the Modulus of Elasticity in Compression for a Pair of Split Samples versus a Given Number of Samples and Confidence Limit*

6.3.4   Discussion of Results

The results obtained demonstrated that in order to relate the mechanical properties of a split pair of samples, there should be no obvious growth characteristics such as knots in either of the pair of samples, and essentially the timber should be clear from visible defects. Observations made of

6-18

split pairs during the procedures indicated that it was highly improbable that perfectly symmetrical growth characteristics would be distributed between paired samples. There would always be a more serious knot in one sample of the pair. The difference in variability within the groups of accepted sample pairs and rejected sample pairs was confirmation of this criterion of no visible defects.

A selection procedure based on split sample pairs with no obvious knots implies that the results obtained from an elevated temperature testing procedure will be for the upper portion of the strength distribution for the grade of timber at the given density. Based on the work of Lau (1996), for tension there was little difference in the specimens that were in the upper and lower bands of the strength distribution. It is therefore considered appropriate to apply results from samples obtained using this procedure to ascertain the reduction in mechanical properties at elevated temperatures and apply them as characteristic of timber of the same species.

The lack of obvious knots within the samples improved the reliability in using the axial deflection measurement apparatus. Several of the experiments conducted for the timber specimens when grouped on a basis of being in the lower portion of the strength distribution (Section 6.2) encountered problems with knots being "pushed" out of samples and interfering with the apparatus. The determination of the modulus of elasticity will therefore be more reliable when the specimens selected based on the splitting technique is employed.

The dominant variable in determining the number of samples required to be tested was the modulus of elasticity. This is because it had a relatively higher variability between samples than the ultimate strength in compression. The gauge length used in this series of experiments was 55mm long, which would most likely increase the variability between samples. The gauge length subsequently used in the elevated temperature experiments, which were performed in a different laboratory, was increased to 135mm, in the expectation that it would reduce the variability.

It was established that a sample size of ten samples should be tested at each temperature because this number gave a prediction of the average variation of the modulus of elasticity of the second

sample being approximately ± 5% of the first, with a 90% degree of confidence. The average variation of the ultimate compression strength of the second specimen being less than ± 3% of the first with a 90% degree of confidence.

6.3.5   Conclusions from Split Specimen Sampling Techniques

If split specimens are to be used to reduce variability for paired sample tests, they should ideally be clear from growth characteristics such as knots to reliably relate the mechanical properties.

Splitting specimens was identified as a successful technique for relating the properties of one sample to another and is ideally suited for application in the elevated temperature mechanical property experiments. This is due to the low number of samples required to give confidence in the results and the time consumed in elevated temperature experiments.

The modulus of elasticity was demonstrated as a more highly variable parameter between the paired samples than the ultimate strength in compression.

Based on the statistical analysis, it was determined that ten pairs of split samples should be tested at each elevated temperature to allow the mean modulus of elasticity to be predicted within an accuracy of ± 5% of the first with a 90% degree of confidence.

6.3.6   Discussion of the Alternative Timber Selection Procedures

The technique of splitting specimens was considered to be a more suitable approach to obtain samples for use in the procedure of determining the compression elevated temperature mechanical properties because:

* The mechanical properties could be more readily related between pairs of samples.

* There was less dependency on ensuring the samples came from the same sawmill or group of timber.

- During the experimental procedure, samples did not cause interference with the deflection measurement apparatus, potentially resulting in an incorrect calculation of the modulus of elasticity.

The use of split samples meant that the change in mechanical properties due to elevated temperature effects of samples with minimal defects would be determined. Application of results determined by use of these properties in structural models involves an implicit assumption that the change in mechanical properties due to elevated temperature effects would be the same reduction factor for samples with substantial growth characteristics. As discussed previously, based on the work of Lau (1996) in performing tensile tests, the reduction in mechanical properties was not significantly different for the upper or lower 20th percentile. However, a further study using the low-end strength batching procedure should be used to validate this assumption. The requirement for further study is mentioned in the Chapter 9, which details recommendations for future research.

6.4 Development of Heating Apparatus and Thermal Calibrations

6.4.1 Introduction

Ideally, thermocouples should be installed within samples to monitor temperatures during the measurement of properties at elevated temperatures. However, it was found during the preliminary experiments that the insertion of thermocouples within heated samples initiated premature failure at half of the expected load, despite the hole in which the wire was inserted being less than 2mm in diameter. It was apparent that the hole drilled in which the thermocouple had been inserted was acting as a stress raiser (refer to Figure 6.9 for a photograph). This concept has been established in conventional plate theory (refer to Timoshenko *et al*, 1970), where a plate subjected to axial stress with a hole drilled in it will have stresses induced in the region of the hole twice those of a plate without a hole.

Figure 6.9: *Preliminary Test Result - Failure Initiated at the Location of a Thermocouple*

Given that split samples were to be used for the elevated temperature experiments and the samples were to be essentially clear of defects, this meant it would be highly probable that premature failure would be induced by insertion of a thermocouple within the specimens.

The use of thermocouples in measuring the temperature of the sample being loaded in compression would require that the thermocouples were inserted in the direction of steepest thermal gradient, that is, through the side of the sample. This direction is perpendicular to the isotherms within the timber when heated, causing heat to flow through the wire and reduce the reliability of the temperature measured. The preferred orientation of a thermocouple wire is one where the isotherms in the timber are followed to reduce the thermal gradient along the wire. Ideally the thermocouples should be placed parallel to the grain, that is, along the length of the sample with holes drilled in the ends. However, in practice this was not feasible to perform whilst loading the sample in an axial compression machine.

Based on the preliminary experiments, in which premature failure was induced in samples, and increased uncertainty in measuring temperature, it was decided that the thermocouples should not be inserted in the samples during the elevated temperature compression tests.

The minimum heating times to achieve a uniform temperature had to be determined before the samples could be tested in the compression-testing machine. Due to a lack of detailed thermal

properties and uncertainty regarding the heat transfer coefficient between the heating apparatus

and the timber samples, it was decided that thermal calibration experiments would be required.

The additional benefit in performing the thermal calibrations was that temperatures measured

would be available for deducing thermal properties for Clancy's (1999) heat transfer model.

6.4.2   Aims

Thus the specific aims of the thermal calibration experiments were to:

(i)   Develop a reliable technique of heating a sample to a required target uniform cross-section

temperature in the minimum time.

(ii)   Develop apparatus and a technique for monitoring the temperature within a timber sample

during heating.

(iii)   Determine the minimum time required heating a sample to achieve a uniform target

temperature through the cross section.

6.4.3   Apparatus and Procedure

6.4.3.1   Techniques to Heat the Timber Sample

The timber samples were 90 mm x 35 mm in cross section and 300 mm in length. The heated

region was 150 mm long, located about the centre of the sample. Two techniques were considered

to heat the timber specimen; namely, gas furnace and electric heating.

The furnaces readily available to perform the test were gas fired and lined with ceramic fibre wool.

Such furnaces are not suited to perform tests at temperatures less than 300°C because there is a

reliance on radiation from the ceramic fibre lining to attain uniform heating throughout. Both

Walker *et al* (1995) and Goncalves *et al* (1996) demonstrated this in a similar type of furnace

when performing elevated temperature tests to determine the mechanical properties of gypsum

plasterboard. Additional concerns regarding the use of a furnace to heat the timber were associated

with the ability to load the samples, make observations, measure deformations and temperatures

through the cross-sections whilst the samples were positioned within the furnace. It was therefore

decided to use an electric heating method, with a device that would allow ready access to the sample so measurements could be taken, load could be applied and a better control of surface temperature would be available.

Two techniques of electrical heating were considered; the first was the use of a heating tape, the second involved the use of steel plates in conjunction with a clamping device.

The heating tape was that conventionally used in industry to maintain the temperature of pipes. While the heating tape has the advantage of flexibility in allowing space to attach measurement probes, there were also several disadvantages:

(i)   The heating capacity of the tape was relatively low. The nature of the material did not produce a high power dissipation (0.5 W/ cm^2). Consequently, it was found that insulation was required to allow heating for temperatures above 125°C.

(ii)   It took a relatively long time to wrap the heating tape around each sample.

(iii)   The heating tape was wrapped tightly around the sample, meaning it provided some resistance to failure, but more importantly, it could be damaged if the sample failed within it.

(iv)   The heating tape was relatively fragile considering the numbers of experiments to be performed.

To overcome the shortcomings of the heating tape, a second technique was adopted which used steel plates within a clamping mechanism to heat the sample. The apparatus consisted of two separate elements attached to an inner steel angle section by means of two clamps at either corner (refer to Figure 6.10). The heating plates had a 6 mm thick piece of steel plate and used conventional heating elements similar to those found in an electric oven or frying pan. The heating potential was much greater than the tape because the materials were less fragile and more substantial in thermal mass and did not allow air to convect heat away. At temperatures approaching 300°C, when heat transfer via radiation becomes more significant, the plates prevented losses though radiation from the surface of the wood.

The time to remove or insert samples in the heating-plate apparatus was considerably less than for the heating tape. It would typically take less than five seconds to release a sample to allow for removal from the apparatus. During testing, the clamping mechanism could be quickly loosened to allow the sample to fail without the apparatus providing resistance. The apparatus was considerably more robust than the heating tape and was more suited to performing many experiments.

The technique of thermal calibration involved drilling longitudinal holes parallel to the grain in the direction where the wire followed the lowest thermal gradient. The samples use for calibration were the same length as the timber samples to be used in the compression experiments. The holes were drilled approximately 100mm deep to ensure that the hot junction forming the thermocouples were positioned just outside the region within of the gauge length (135mm located about the centre) to be used for deflection measurements during the compression experiments. Given timber is a very good insulator, it was assumed that the temperature measured by the thermocouple at this position would be indicative of the temperature of the entire gauge length.

Heating
element

Hinges &
clamping
mechanism

20 mm
diameter

Holes for
displacement
probes to contact
specimen

**Outer - Outside polished
stainless-steel plate / heat
shield**

10 mm

50 mm

15 mm

6 mm
thick

250 mm

40 mm
(outside)

95 mm
(outside)

Inner - Stainless-steel plate
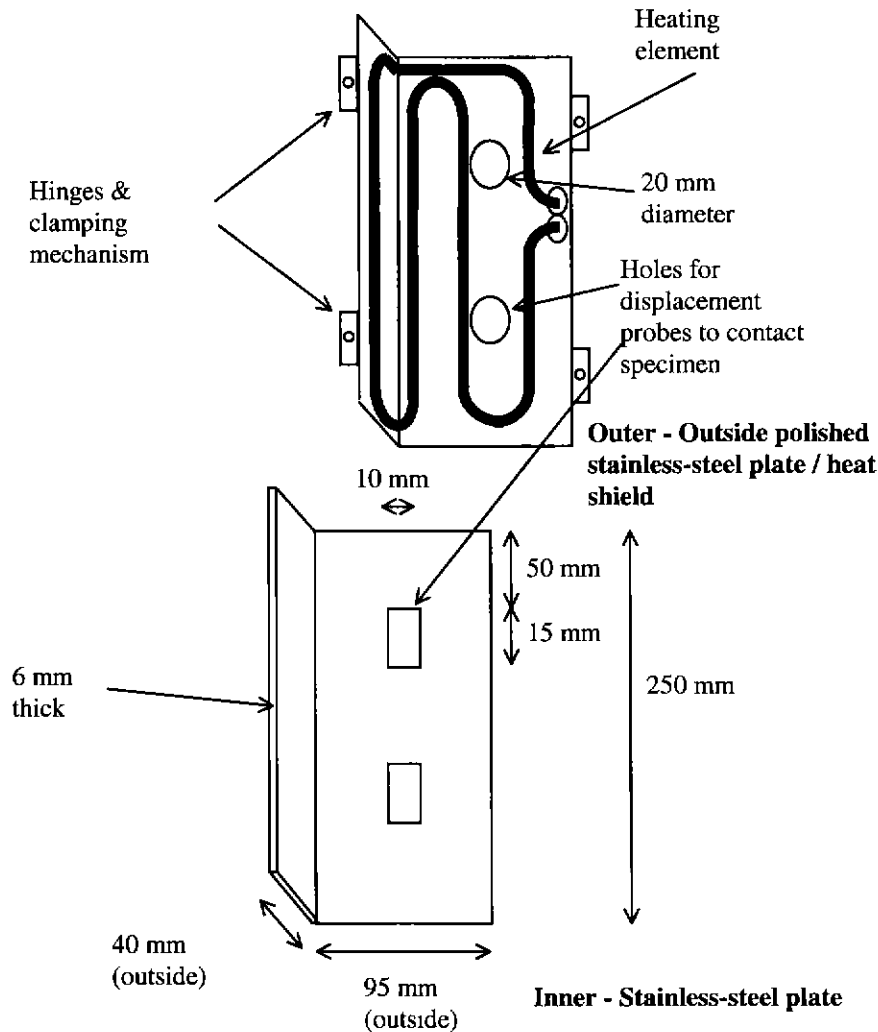
Figure 6.10*: Schematic of Heating Plate Apparatus (Note: plates join together as shown in Plan*

View in Figure 6.11)

The technique of drilling long holes longitudinally in the timber samples required a great deal of

care. Ideally the calibration test samples would have had very straight grain in the longitudinal

direction. Growth rings had to be avoided because they consisted of harder material (late wood)

than the surrounding wood. Hence if the drill bit encountered a growth ring, the drill bit would

tend to drift off into the softer wood, creating a hole which was not parallel to the length of the

sample. Similarly, samples were not used for thermal calibrations that contained growth

characteristics (e.g. knots) of a significant size in the vicinity of the location of the holes. To

maximise the control of drilling the holes a drill press was used to drill the holes. A high drilling

speed was used in conjunction with several short passes to ensure the drill was always clear. The

procedure was checked by cutting open the samples after testing. Hole centres were generally accurate to within 1 mm of the correct position.

6.4.3.2   Measurement of Temperatures

Temperatures were measured using 'K' type thermocouples. The wire was 2.4 mm in diameter and had fibreglass insulation on both the wires and the outer sheath. The thermocouple, created as a hot junction, was constructed in accordance with the requirements of AS 1530.4-1990.

Heating element

90 mm

Outer stainless steel plate heat shield

Thermocouples placed at 15mm centres along depth, in centre of breadth

35 mm

Clamps holding two sections of apparatus together, and allowing firm contact with timber specimen

Stainless steel plate
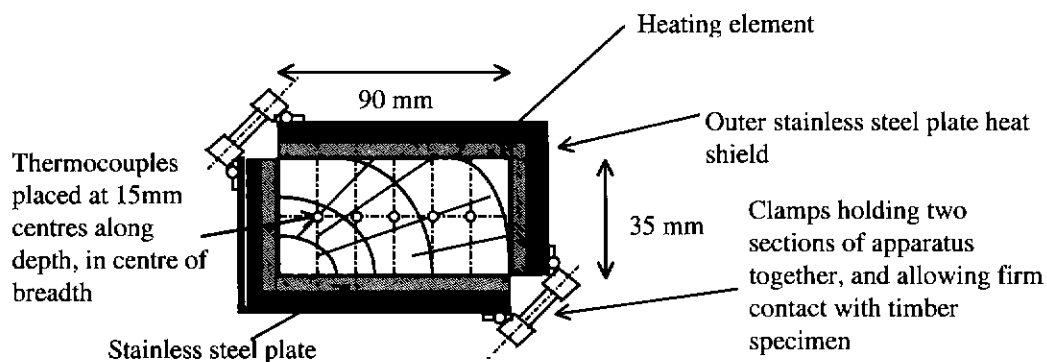
Plan view of heating apparatus

Thermocouple holes drilled 100mm deep, parallel to grain

Test specimen 300mm long

Shaded area covered by heating plates
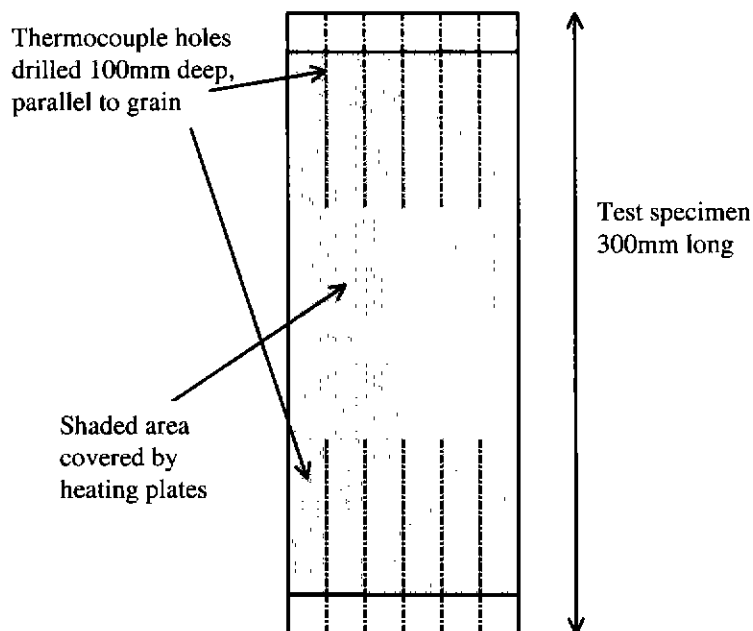
Elevation of Specimen showing Thermocouple Locations for Thermal Calibrations
(details of element/steel plates not shown - refer to Figure 6.10)

Figure 6.11: *Thermal Calibration Apparatus*

The thermocouples were connected to the data acquisition equipment which comprised three

Advantech PCLD-779 integrated signal sampling/amplifier/multiplexer cards connected to an

Advantech PCL-711s analogue to digital conversion card contained within an IBM AT compatible

personal computer (refer to Figure 6.12). The data acquisition cards each had a cold junction

compensation (CJC) circuit that provided a reference temperature. The cards were calibrated to

ensure there was no zero error and that the CJC measured accurate temperatures. Ice and boiling

points were used as further reference checks to monitor the accuracy of the data acquisition

system.

Software was written by the author in Turbo Pascal 7.0 to obtain the temperature data with the

electronic hardware (refer to Young (2000) - Appendix 4.3). The relation between voltage

measured by the data acquisition system and temperature calculated based on the thermocouples

constructed of 'K' type material was obtained from Bentley (1993).
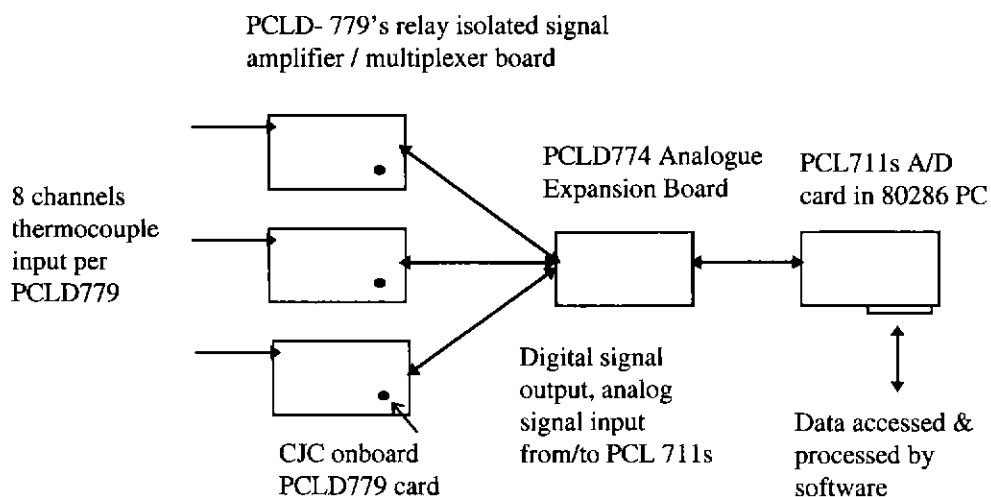
Figure 6.12: Schematic of Data Acquisition Equipment for Thermal Calibration Experiments

6.4.3.3 Experimental Procedure

The following procedure was adopted to heat the samples and also to determine the time of heating

required for the samples to achieve a uniform cross-sectional temperature:

(i)   The samples were prepared by cutting them into 300mm lengths and drilling holes

longitudinally as detailed in Figure 6.11.

(ii)   The samples were weighed and the moisture content was measured using an electronic

moisture meter, which was calibrated through comparisons involving oven drying of the

samples.

(iii)   Each sample was placed in the heating apparatus. Thermocouples were both inserted in the

holes drilled and clamped between the heating plates and the surface of the timber. The

clamps on the heating apparatus were then tightened until the timber was firmly clamped

within. Ceramic fibre wool was then used to insulate the outside of the heating plates to

both improve heating efficiency and protect the surrounding environment from being

damaged by the temperature of the heating plates. Refer to Figure 6.13 for a photograph of

the apparatus.

(iv)   The target surface temperature was set on the temperature-voltage controllers. The

specimen was heated with the surface temperature being controlled by the thermocouple of

the temperature-voltage controller, which was clamped between the surface of the timber

sample and the heating plates.

(v)   Each sample was heated to a specified surface temperature with the plates (Figure 6.13) for

a specific period of time. The internal and surface temperatures of the timber were recorded

with time.

(vi)   Each sample was weighed at the conclusion of the experiment to determine the mass loss

due to heating.
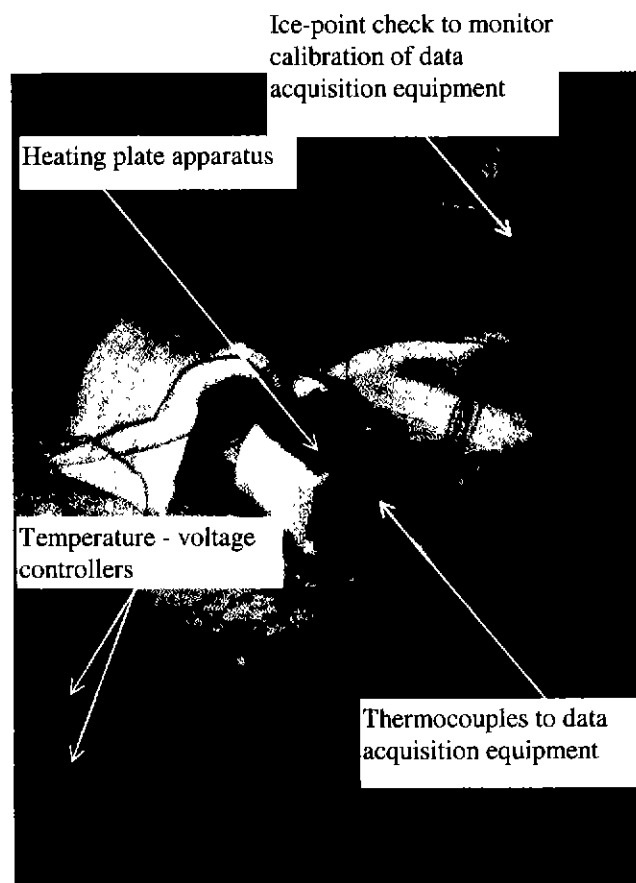
Figure 6.13: Thermal Calibration Apparatus

6.4.4 Results

Temperature versus time results for an experiment with the heating plate surface temperature of

275°C is shown in Figure 6.14. Results for thermal calibrations for several heating plate surface

temperatures are shown in Young (2000) - Appendix 4.1. A noticeable dwell was apparent as the

sample temperatures passed through 100°C. Shrinkage perpendicular to the grain was apparent in

the sample heated to 275°C, which made surface temperatures difficult to sustain because a gap

formed between the clamped heating plates and the surface of the timber. At temperatures of

250°C and less, the shrinkage perpendicular to the grain was not noticeable. The mass loss for

experiments performed at specific temperatures and duration of heating are shown in Table 6.6.
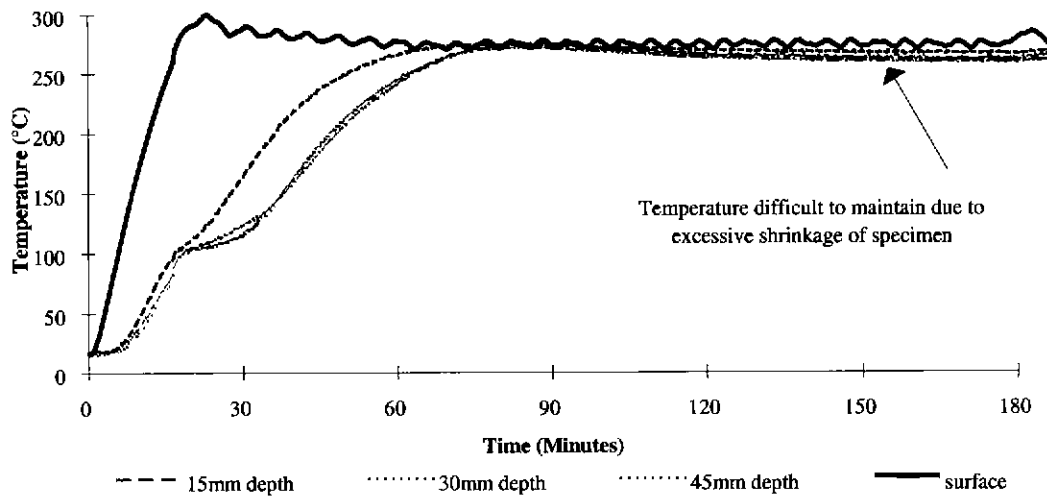
Figure 6.14: *Temperature versus Time for a Sample with the Heating Plate Surface Temperature of 275°C*

Table 6.6: Mass Loss Measured, Moisture Content and Calculated Mass of Moisture for Thermal Calibration Tests

Surface Temperature of Heating Plates	Heating Time (min)	Mass Start (g)	Mass End (g)	Mass Loss (g)	Moisture Content	Mass Moisture (g)
275°C	180	401	297	104	10.3%	37
200°C	120	392	346	46	11.2%	40
200°C	140	404	356	48	11.2%	41
200°C	180	466	416	50	10.5%	44
200°C	150	434	384	50	10.8%	42
200°C	180	392	346	46	11.2%	40
150°C (moist)	180	401	366	35	10.1%	37
150°C (moist)	180	460	415	45	11.4%	47
150°C (dry)	180	403	403	0	0%	0
150°C (dry)	180	398	396	2	0%	0
110°C (moist)	180	409	385	24	10.2%	38
110°C (moist)	180	460	424	36	12.2%	50
110°C (dry)	160	403	403	0	0%	0
110°C (dry)	160	423	423	0	0%	0
70°C (moist)	70	495	492	3	11%	49
70°C (moist)	70	467	463	4	11.1%	47
70°C (dry)	90	413	413	0	0%	0
70°C (dry)	90	365	365	0	0%	0

Note that the heating time listed does not infer the minimum time to achieve a uniform temperature within ±10°C.

6.4.5 Discussion of Results

The results for thermal calibrations demonstrated that the steel heating plate was a reliable technique of heating a timber sample for the compression experiments. The device could be efficiently attached to the sample in a consistent manner each time it was used, giving confidence in the repeatability of the heating procedure. In addition, the device was not damaged during either attachment or removal of the sample nor visibly affected by the heating. The heating tape was found to be unsuitable because it had shortcomings in both of these situations.

As well as developing effective apparatus and procedures for heating samples of wood and determining appropriate periods of time to heat samples, a number of valuable observations of phenomena were observed at various temperatures. These are discussed below.

The thermal calibration tests revealed that it took a long period of time to heat the timber samples containing moisture to a uniform temperature of 110°C and 150°C. The reason for this long period was most likely to be the low temperature gradient driving the moisture from the samples at these temperatures. There were concerns that given the lower input of energy, moisture may condense in the ends of the samples, which were cooler than the heated region in the centre of the sample. This potentially would cause problems with carrying out the tests due to localised moisture induced softening at the supports. It was therefore decided to dry the samples to be tested at 110°C and 150°C.

Heating of the samples to temperatures of 200°C and above showed a dwell in heating (for example refer to Figure 6.14) within the sample within a temperature range between 102°C and 108°C, which was considered to be indicative of the moisture being vaporised from the sample. The temperature was above 100°C due to the confinement of the heated moisture within the structure of the timber, resulting effectively in a superheated vapour.

A heating period of two and a half hours was deemed to be appropriate to ensure the entire cross-section of the timber sample within the gauge length was at uniform temperature for the 200°C and

250°C mechanical property experiments. After this period, the temperature of the sample could be reliably assumed to be at the specified temperature within a range of ± 3°C.

A heating period of seventy minutes was deemed to be appropriate to ensure the entire cross-section of the sample within the gauge length was at uniform temperature for the 70°C, 110°C and 150°C mechanical property experiments.

The time required to achieve uniform temperatures through moist samples was found to be considerably longer than it would take to achieve the temperature within a timber-framing member in a fire resistance test, which had steeper thermal gradients. The comparison between the time required to heat the bulk of the cross-section of the timber framing in the full-scale fire resistance experiments in Chapter 5 and the heating timber for the mechanical property tests are summarised in Table 6.7. It would be difficult to heat the timber at a faster rate than was achieved without overheating the surface layer of the timber, which would result in excessive thermal degradation in this region, and hence a non-uniformity in mechanical properties through the cross-section. The times were however similar for the dried specimens, although the process of oven drying could also affect the mechanical properties of the timber, as indicated in Table 2.2, the natural structure of lignin is altered at 55°C. The lignin does play a significant role in the compression properties of wood (Dinwoodie, 1989).

Table 6.7: Comparison between Heating Time with Metal Plates in Thermal Calibration Experiments and Full-Scale Fire Resistance Experiments Subjected to AS1530.4 Heating Regime

Approximate average cross-section temperature	Time to achieve in Full-Scale Fire Resistance Tests (Refer to Chapter 5)	Time to Achieve Specified Surface Temperature with Thermal Calibrations
110°C	35	160 (wet), 30 (dry)
150°C	50-55	130 (wet), 65 (dry)
200°C	70	150
250°C	80	150

The mass loss measured during the heating procedures indicated that in the case of heating the samples to temperatures of 200°C and above, the mass loss was greater than the mass of moisture within the sample. This indicated that solid wood was being converted to volatiles and hence chemical degradation was occurring. This volatilisation is supported in the literature, which details the degradation of the constituents of timber with temperature e.g. Schaffer (1973). The difference between mass loss and total mass of moisture at 200°C was however not substantial, indicating a small degree of chemical degradation into gaseous compounds.

At 275°C the observed degradation was substantial, further evidenced by the magnitude of shrinkage in the direction perpendicular to the grain observed. A drop in temperature, as shown in Figure 6.14, was recorded as the specimen shrank away from the heating plates for the tests at this temperature. This indicated that the chemical reactions occurring at this temperature were possibly still net endothermic, or heat had escaped via radiation through the gap. A significant drop did not occur due to the influx of cool air into the gap because the samples were well insulated by ceramic fibre wool, which prevented the ready circulation of air in the region of the specimen. Testing the mechanical properties at temperatures at 275°C and above due to the transient degradation appears unfeasible with the heating technique employed. Given the closeness to the documented char temperature of 288°C (Schaffer, 1973), the precise determination of mechanical properties at this temperature or above is not considered significant.

At temperatures of 110°C and 150°C, the moist samples lost less mass than the mass of moisture contained within the sample. This is indicative of moisture migration to the ends of the sample, which were cooler than the heated region in the centre. White *et al* (1981) demonstrated the phenomenon of moisture migration when exposing timber slabs to furnace heating conditions. Dry samples heated to these temperatures exhibited no further mass loss, indicating that chemical reactions involving the conversion of wood to volatiles was not occurring in noticeable amounts at these temperatures.

The moist samples heated to 70°C lost less than 10% of the initial moisture content during the heating procedure. That is, the moisture content decreased from approximately 12% to

approximately 11%. This was deemed an acceptably small change through the heating procedure for which the reduction in mechanical properties could be deduced.

It is possible that the long exposure times needed to heat the timber samples to temperatures from ambient to 200°C and 250°C may have resulted in excessive thermal degradation compared with the full-scale fire resistance tests with timber at the same temperature. It is suggested that further investigation of the effect of heating time on the mechanical properties to validate the results obtained for these two temperatures is required. The literature has established mechanical properties of timber reduce with the time of heating exposure (Schaffer, 1973, Troughton *et al* , 1974), particularly at temperatures of 200°C. Troughton *et al* (1974) showed that at 200°C oxidation reactions were occurring in timber heated in air. Given the heating times are longer than that required for a fire resistance test to achieve the same temperature within a timber specimen, the degradation would be greater than timber in a standard fire resistance test. The results obtained from the mechanical property tests using this heating technique will hence be conservative for design purposes. That is, any calculations using the mechanical properties obtained should underestimate the fire resistance of a timber element and will hence be useful for deterministic design applications. For probabilistic or comparative studies the values may not be reliably applied, particularly if the performance of timber-framing is compared with another framing material as the unknown degree of relative conservatism between materials can skew outcomes towards the material with the less-conservatively derived mechanical properties.

6.4.6   Conclusions from Thermal Calibrations

Apparatus and experimental procedures have been developed to heat timber samples and perform experiments to determine the change in compression mechanical properties due to elevated temperatures.

Substantial chemical degradation of the timber was evident at 275°C indicated by the discolouration, mass loss and shrinkage of the samples.

Evidence in the experiments indicated that the net heat of reaction at 275°C of radiata pine was endothermic, however it is possible that radiant heat losses may be an alternative explanation for this result.

Moisture was removed from timber specimens within a temperature range of 100°C to 108°C.

Specimens to be tested at 110°C and 150°C should be dried due to the long time required to heat the specimens and concern regarding moisture migration to the ends of the specimens and the possibility of degradation of mechanical properties with time.

A heating time of two and a half hours was deemed to be appropriate to ensure the entire cross-section of the specimen within the gauge length was at uniform temperature of 200°C and 250°C.

A heating time of seventy minutes was deemed to be appropriate to ensure the entire cross-section of the specimen within the gauge length was at uniform temperature of 70°C, 110°C and 150°C for all specimens to be tested (moist and dry).

6.5   Elevated Temperature Mechanical Property Experiments

6.5.1   Introduction

The following section documents the experiments conducted to determine the reduction in the mechanical properties in compression of radiata pine. The sampling procedures for splitting specimens (Section 6.3) and the thermal calibration procedures (Section 6.4) previously established were adopted.

6.5.2   Aims

To determine the reduction in the following mechanical properties in of radiata pine when subjected to compression:

(i)   Ultimate strength

(ii)   Modulus of Elasticity

6.5.3   Apparatus

Equipment used in performing the elevated temperature compression experiments on the timber

samples is shown in Figure 6.15. The items of equipment were:

(i)   Heating plates and data acquisition equipment from thermal calibrations.

(ii)   Dial gauge.

(iii)   Linear variable differential transformer (LVDT).

(iv)   Axial compression testing machine.

(v)   Low voltage power supply.

(vi)   Datataker data acquisition equipment for recording LVDT output and power supply

         voltages.

(vii)   Notebook computer.

The particular experiment shown in Figure 6.15 was an ambient experiment to estimate initial

ambient properties of the sample tested at elevated temperature. In elevated temperature

experiments, the heating apparatus was placed around the timber samples.

LVDT electronic
monitoring of platen
movement

Dial gauge to
monitor strain rate
based on platen
movement

Displacement
measurement frame

Notebook
computer for
data storage

Power supplies
for LVDT

Datataker
data acquisition
equipment
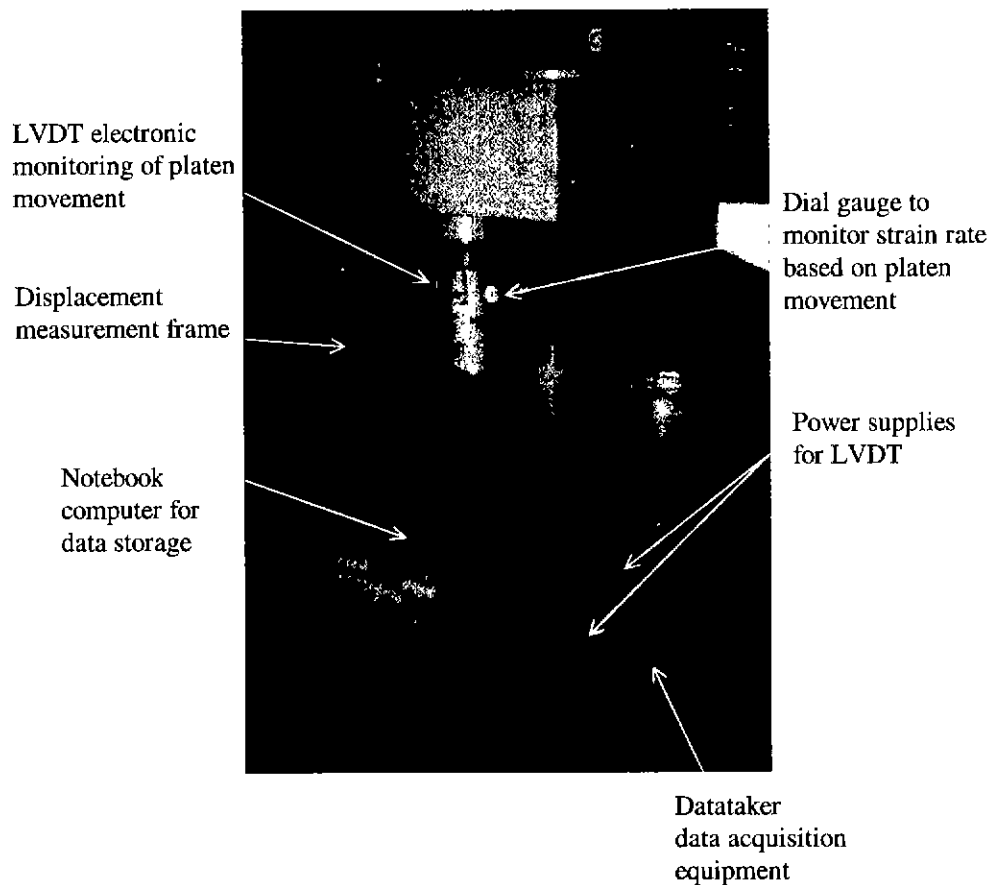
Figure 6.15: Compression Experimental Apparatus (for Mechanical Properties at Ambient

Conditions)

6.5.4   Procedures

6.5.4.1   Calibration of Experimental Apparatus and Preliminary Experiments

The compression-testing machine was calibrated with a proving ring for the range of loading to be

applied.

The LVDT voltage-displacement relationship was determined for several input voltages by

measuring input voltage and output voltage with a Fluke digital multimeter for a given

displacement induced by a micrometer. The input voltage for the LVDT for the experiments

performed was set to almost exactly 10 Volts but some drift in the transformer would cause this to

change by small amounts (±0.01 Volts), although the effect on the displacement-voltage

relationship was minimal. The input voltages for all LVDTs were recorded for all experiments to ensure any drift was monitored and controlled.

Preliminary experiments conducted indicated that it was unsuitable to heat the timber sample whilst it was located within the compression testing machine because of the movement of moisture within the specimen to the cooler ends outside the gauge length. The moisture condensed on the surfaces of the loading platens and subsequently precipitated into the ends of the specimen, resulting in swelling and softening in the ends. As load was applied, considerable deformation occurred in this region (refer to Figure 6.16) which induced bending within the gauge length and could potentially lead to an unreliable determination of the modulus of elasticity. Failure invariably occurred in the ends of the specimen, meaning that the failure load would not be representative as having occurred at the specified temperature as it did not occur within the heated gauge length.

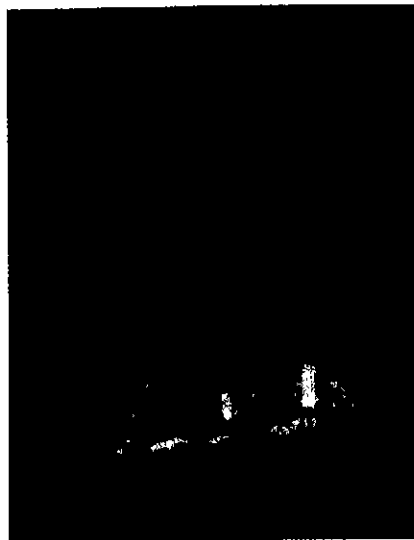*Figure 6.16: Swelling & Softening in the End of a Specimen Heated and Tested in the Compression Testing Machine*

To overcome the problem of moisture migration to the ends of the specimen, it was established that the specimen must be heated outside the testing machine and inserted once the required heating time, determined in the thermal calibrations (§6.4), had transpired.

6.5.4.2   Finalised Procedure for Mechanical Property Compression Experiments

Based on the calibrations and the preliminary experiments, the following procedures were

established and carried out. Split specimens were used and were selected and prepared based on

the procedures outlined in Section 6.3. The samples were heated in accordance with the heating

procedures developed in Section 6.4. Two people were required to conduct the experiment.

Radiata pine specimens of 90 mm x 90 mm cross section were selected, split and sample pairs

were accepted and rejected in accordance with the procedures developed for splitting specimens to

reduce variability (§6.3).

The gauge length of 135 mm was marked about the centre of the samples and the locations for the

displacement probes were lightly marked with a centre punch.

One of the pair of the samples was heated in accordance with the experimental requirements (refer

to Table 6.8), while the other was tested under ambient conditions.

Compression experiments were conducted in general accordance with ASTM D198 (1994)

Sections 12-19 for the testing of a short column parallel to the grain. A strain rate of 0.001 min^{-1} $\pm$

25% was applied. This strain rate corresponded to a shortening of 0.10 mm per 20 seconds over

the length of the sample, which was monitored by means of measuring platen movement with a

dial gauge, in addition to measurements of the change in the gauge length.

At the commencement the heating procedure for each sample, the heating apparatus was checked

to determine if it had been damaged during the previous experiment. The sample was placed

between the heating plates. Eight thermocouples to monitor the surface temperature were placed

on the surface of the timber sample and the plates were clamped. The sample target temperature

was set on the temperature-voltage controllers and the sample was heated for the required

calibrated time as determined in §6.4.

For safety reasons, the heating plate was disconnected from the power source, before the heating plate containing the sample was placed within the compression-testing machine. The power supply was disconnected to reduce the chance of a short, which would result in an unsafe electrical hazard and possible damage to the data acquisition equipment worth several thousand dollars. The sample, together with the heating apparatus, were then inserted into the compression testing machine.

The sample was placed centrally in the compression-testing machine. The heating apparatus was loosened to prevent the sample bearing on it during the test. The heating apparatus was supported externally so it maintained its position of being positioned centrally over the gauge length and it maintained the temperature over the gauge length by virtue of its thermal inertia and a short testing time, typically between 3 to 5 minutes duration. Cooling in the surface regions of the sample during the experimental procedure was a concern. Temperatures in the air cavity between the loosened heating plate apparatus and timber sample were measured during the course of several of the experiments. The temperature of this air cavity was measured to decrease by approximately 20°C over the course of a compression experiment (generally up to five minutes duration) for an initial surface temperature of 200°C. The disconnection of the power supply to the heating plates, in combination with loosening the plates and creating an air gap were demonstrated to have a minimal cooling effect on the timber sample, with a change in surface temperature of less than 20°C. Given the relatively low thermal diffusivity of timber, the effect was likely to be limited to within a few millimetres of the surface.

A 'preload' was applied to hold the sample in the loading machine while the ends of the displacement probes were located on the sample. A check was made that all LVDTs had enough travel for the direction they were to move during the test.

Two persons were required to conduct the compression experiment. A testing machine operator controlled the compression testing machine to ensure the strain rate was maintained in accordance with the requirements of the test specification and an assistant recorded load readings at regular intervals. The assistant for the experiment synchronised a stopwatch with the testing machine

operator at the commencement of the experiment so that the timer would start at the instant the displacement data acquisition equipment commenced logging.

The assistant called for load readings every 20 seconds, which were read by the compression machine operator. The compression machine operator monitored the strain rate applied to the specimen by monitoring the platen movement to ensure a constant strain rate within the prescribed limits of the experimental procedure was maintained. It should be noted that the strain rate applied was based on the entire section compression, not the potentially greater strain rate experienced over the heated gauge length.

Displacements of the LVDTs, which monitored the probe movement in measuring the change in gauge length and the platen movement, were recorded at two-second intervals by the data acquisition equipment. Input voltages to each LVDT were also recorded at each time interval to ensure a reliable determination of the displacement calculation from the LVDT output voltages.

The sample was loaded until failure occurred which was defined as the peak load the sample could sustain at the prescribed strain rate.

The moisture content of each of the ambient samples tested was measured by weighing before and after oven drying.

6.5.4.3   Schedule of Experiments

The schedule of Experiments performed is shown in Table 6.8.

Table 6.8: Schedule of Experiments

Temperature	Number of Sample pairs	Comments
Ambient (approx 15°-20°C)	10	Samples oven dried
70°C	10	Moist (undried) samples used
70°C	10	Samples oven dried
110°C	10	Samples oven dried
150°C	10	Sampled oven dried
200°C	10	Additional 10 preliminary experiments performed to define / clarify procedures employed
250°C	6	Number of experiments reduced due to problems with smoke production

Note: For the sample (of the sample pair) tested at ambient temperature conditions, the moisture content was approximately 12%.

6.5.4.4   Experiments at Ambient Temperature (15°C-20°C, Dried Samples)

The samples were kept in an oven at approximately 102°C to remove all moisture. The time for complete moisture removal was determined by repeated weighing until no significant change in the mass of the sample was observed. The samples were then removed from the oven and placed in airtight bags containing ceramic fibre wool insulation to prevent the heat from the samples removed from the oven damaging the bags. Silica gel sachets were placed in the bags to prevent any moisture absorption by the timber from the air within the sealed bag or any microscopic leakage that the bags may have (Refer to Figure 6.17).
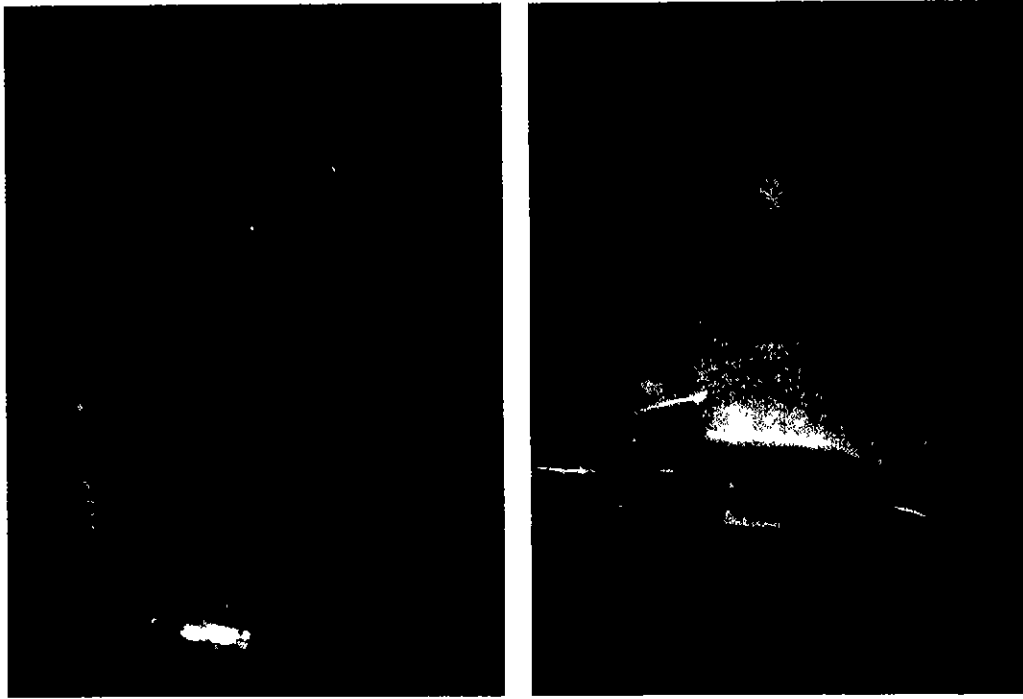
Figure 6.17: Technique of Cooling Samples for Dry Ambient Compression Experiments

The bags were weighed before and after the cooling period of several days to ensure the sample mass

did not increase significantly, giving an indication that a bag had been damaged and moisture had been

allowed to enter and had been reabsorbed by the timber samples.

The samples were weighed before and after completion of the experiments to monitor the

absorption of moisture during the experiment.

6.5.4.5   Experiments at 70°C (Moist)

The samples were weighed before and after completion of the experiment to monitor the loss of

moisture during the heat exposure.

The samples were heated for the duration of seventy minutes with the heating plate set to 70°C.

To allow for the initial overshoot in the surface temperatures at the (relatively) low surface

temperatures, the temperature voltage controller was set to 55°C. The overshoot at this

temperature was generally of magnitude 15-20°C. Thus the duration of exposure of the surface to

temperatures at which moisture would rapidly be removed through overshoot was reduced. After

the initial temperature overshoot, the controller was set to 70°C for the remainder of the duration

of the experiments.

6.5.4.6   Experiments at 110°C, 150°C & 70°C (Dried Samples)

The samples were dried in an oven at 102°C for a period of at least three days. The time for complete moisture removal was determined by repeated weighing until no significant change in the mass of the sample was observed. After drying, the samples were heated for a duration of seventy minutes with the heating plate set to the respective temperature as determined from the thermal calibration experiments (§6.4).

6.5.4.7   Experiments at 200°C & 250°C

The samples were placed in the heating apparatus for a period of two and a half hours (9000 seconds) with the heating plate set to the respective temperature, based on the results from the thermal calibration experiments (§6.4).

6.5.5   Results

6.5.5.1   Introduction

Observations made during the experiments are summarised in §6.5.4.2 - §6.5.4.8. Reference should be made to Young (2000) - Appendix 4.2 for the details of the recorded stress versus strain for each experiment. The calculation of the reduction in mechanical properties is presented in §6.5.4.9.

6.5.5.2   Experiments at Ambient (dried samples)

The failure mode was in some cases explosive (refer to Figure 6.18). The sample would often fail in shear in a direction parallel to the grain direction. If the grain were not straight along the length, the failure would tend to initiate where the grain diverted from the direction parallel to the longitudinal axis of the sample.

Load Applied by Platen

Failure Mechanism - rapid failure - specimen splits
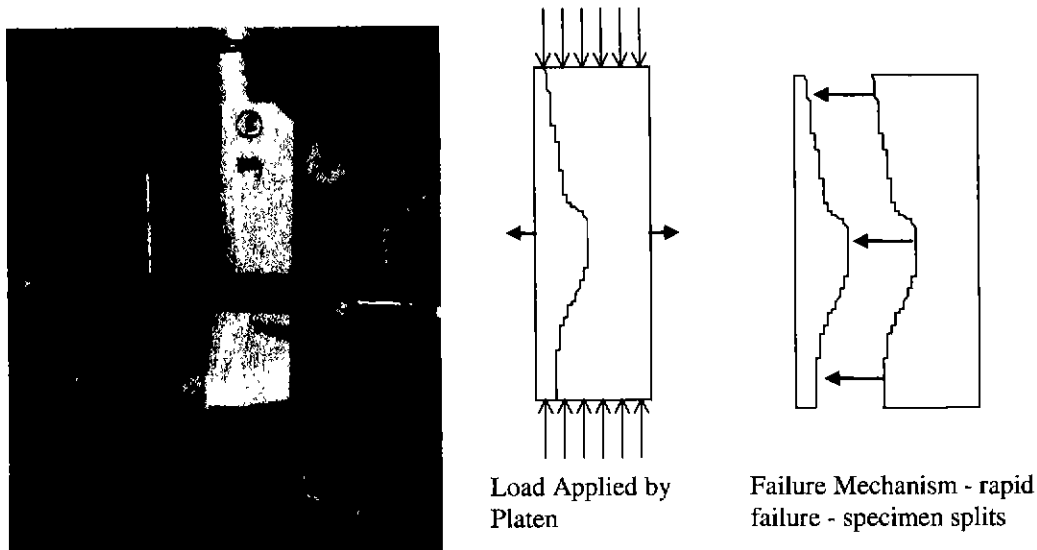
Figure 6.18: Failure of a Dry Timber Sample at Ambient

6.5.5.3 Experiments at 70°C (moist samples)

The timber exhibited a marked increase in ductility and corresponding decrease in ultimate compressive strength. The failure mechanism was that typical of ambient experiments involving clear timber in compression (refer to Figure 6.19). The ductile behaviour was consistent with the assumed stress-strain relationship in compression as shown in Figure 3.7.

6.5.5.4 Experiments at 70°C (dried samples)

No discolouration of the timber was apparent. The dry 70°C timber samples were substantially stronger than the corresponding moist ambient samples. Some samples exhibited shear failure in a direction parallel to the axis. The failure mechanism was similar to that of the experiments involving the dry ambient samples (refer to Figure 6.19).
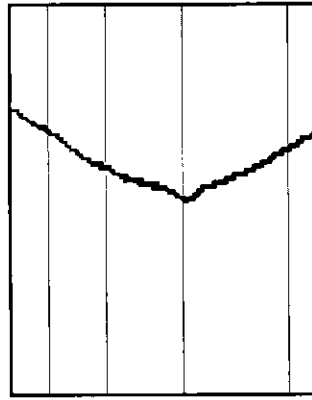
Figure 6.19: *Classical Compression Failure of Timber in Compression*

6.5.5.5   Experiments at 110°C (dried samples)

No discolouration of the timber was apparent. The failure pattern was similar to a classical

compression failure at ambient conditions (refer to Figure 6.19).

6.5.5.6   Experiments at 150°C (dried samples)

No discolouration of the timber was apparent. The failure pattern was similar to a typical

compression failure at ambient conditions (refer to Figure 6.19).

6.5.5.7   Experiments at 200°C

The discolouration of the timber was slight, not to the degree of the specimens tested at 250°C.

The failure mode was quite brittle.

6.5.5.8   Experiments at 250°C

The failure mode was quite brittle. The initial experiment failed at a far lower compressive

strength than predicted. Substantial discolouration was apparent.
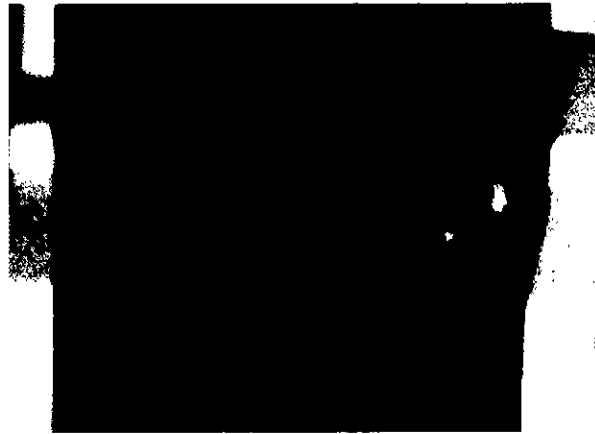
Figure 6.20: *Failure Mode of Timber Sample at 250°. Note the discolouration of the sample.*

The failure mode (refer to Figure 6.20) tended to indicate failure of groups of fibres rather than individual fibres, as would occur for a typical ambient compression failure.

6.5.5.9   Summary of Results

The stress calculated was the force recorded by the testing machine divided by the original cross-section area of the sample. The strain calculated was the change in the gauge length measured by the LVDTs divided by the original gauge length (135mm).

A graph showing the results from the experiments, detailing the reduction from ambient of the ultimate compressive strength versus temperature are presented in Figure 6.21. It was apparent that drying the samples increased the compressive strength considerably, by a factor of 1.65. Heating the samples to 70°C, when moist, showed a sharp drop in compressive strength, a reduction of approximately 35% of the ambient value. A dashed line has been included which extrapolates the results from 70°C to 100°C. Assuming this linear extrapolation, at 100°C, the ultimate strength in compression would be approximately 42% of the ambient value.
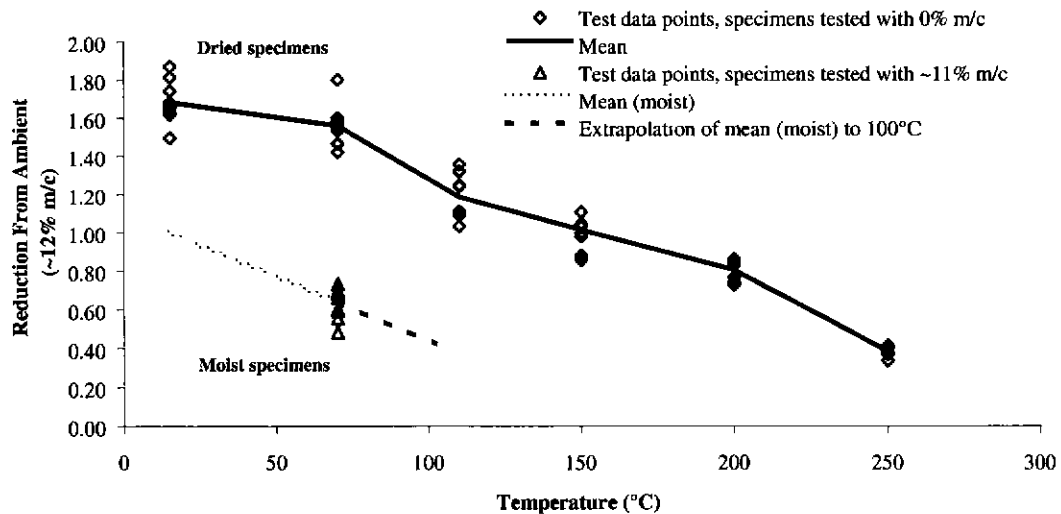
Figure 6.21: Reduction in the Ultimate Compressive Strength versus Temperature

The effect of elevated temperature on the modulus of elasticity is presented in Figure 6.22. There was little change in modulus of elasticity due to the process of oven drying samples. The effect of heating specimens retaining moisture at 70°C showed a sharp drop in modulus of elasticity, a reduction of 35% over the ambient value a numerical reduction equal to the reduction in ultimate compression strength.
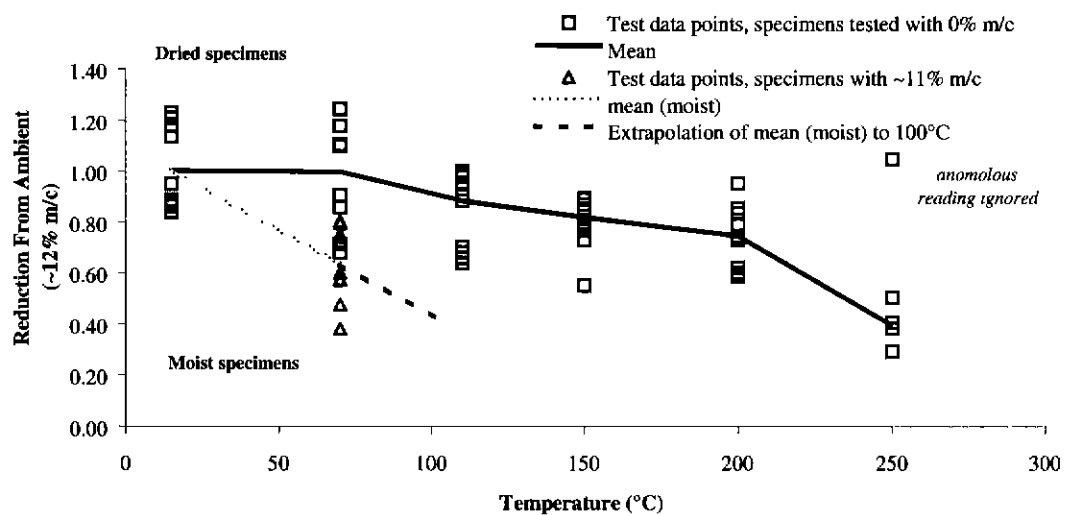
Figure 6.22: Reduction in the Modulus of Elasticity versus Temperature

6.5.6 Discussion of Results

There was a considerable scatter with regard to the results calculated for the reduction in modulus of elasticity at each temperature (Figure 6.22) compared with that of the results obtained for ultimate strength in compression (Figure 6.21). This finding is consistent with the results of the initial study into split samples as detailed in Section 6.3. The variability can be attributed to the length of the samples, and more particularly, the length of the gauge length.

It is interesting to note the variability of the set of the mechanical property experiments shown in Figure 6.22, and the almost identical times of failure for the full scale tests for similar walls. Given three 3.0 metre long studs were used to carry load in each frame in the full-scale tests, it is highly improbable that the mechanical properties could be controlled more effectively than in the small scale mechanical property tests outlined in this chapter. There is some argument that the variability will be less in the mechanical properties of longer specimens (Madsen, 1992), however a better explanation for the lower variability may be due to the 'heat wave' effect discussed in Section 5.3.7.2. The concept of the 'heat wave' effect is that there is a rapid drop in the modulus of elasticity as the timber approaches 100°C due to the combined effects of heat and moisture. As demonstrated in Figure 5.43, due to the magnitude of the reduction in the modulus of elasticity, the variation in the initial value or reduction factor is not important.

The results obtained for dried samples at ambient and 70°C indicated a continual degradation in mechanical properties with increased temperature. It is recommended that in future research, that the technique of oven drying the samples for the experiments should be compared to timber dried with desiccants such as silica gel. This will identify the contribution of oven drying in inducing thermal degradation in samples heated to temperatures less than 100°C. Further repetitions of this procedure are required to determine the relationship between the density of the samples and the reduction in mechanical properties at a given temperature. This will also lead to better defined statistical data for the reduction in the mechanical properties at each temperature, which are essential for probabilistic studies.

Extrapolation of the results beyond 250°C indicates that the compression strength would reduce to zero at approximately 295°C. Extrapolation of the reduction in modulus of elasticity versus temperature results indicates that the value would reduce to zero at approximately 305°C. Both extrapolations give confidence in the results obtained at the higher temperatures, as the char temperature (at which it is assumed there is minimal strength) in the literature is approximately 300°C (Schaffer, 1973). The formation of char is a rate change phenomenon often modelled with an Arrhenius function (Fredlund, 1988). Therefore in furnace tests, the higher thermal gradient would result in a higher temperature at which char is likely to form. Hence the calculated temperature at which zero strength (or char) would occur would be conservative for design purposes.

Extrapolation of the mean reduction in mechanical property of moist samples for temperatures between 70°C to 100°C is difficult. Extension of the line between ambient and 70°C results indicates an intercept at 100°C of approximately 0.42. It is very difficult to heat the specimens in a manner similar to these procedures to determine the reductions close to 100°C. Moisture loss through the surface and internal migration from within the gauge length are difficult to monitor and control beyond 70°C, where the sample moisture content decreased 1%. It is assumed that in the temperature range of 102°C to 108°C, the timber moisture content will reduce (as identified in Section 6.4) and the corresponding strength and modulus of elasticity will increase. It cannot, however, be determined from this type of experiment, the fraction of deformation that is irrecoverable.

6.5.7 Conclusions from Elevated Temperature Mechanical Property Experiments

Procedures have been established and apparatus developed in order to perform compressive experiments on timber samples at elevated temperatures to determine the reduction of the modulus of elasticity and compressive strength from the ambient properties.

A relationship between the reduction of the compression strength and modulus of elasticity versus temperature has been calculated for times of heating of between 1-2½ hours. At temperatures at 200°C and above, when the mechanical properties degrade with time, the relationship obtained was considered to be conservative due to the increased time of heating compared with a standard fire resistance test.

There was considerable scatter with regard to the reduction in modulus of elasticity at each temperature compared with the small scatter in ultimate compression strength. The full-scale experiments did not exhibit such variability, hence the 'heat wave' effect detailed in Section 5 was given further credence.

There was a substantial decrease in strength and modulus of elasticity at temperatures approaching 70°C when moisture is not removed. The decrease for both mechanical properties was 35% from the ambient value.

The strength of radiata pine increases considerably when oven dried at 102°C, by approximately 65% for ambient conditions.

Extrapolation of results above 250°C gave confidence in the reliability of the results at temperatures of 200°C and 250°C. The estimated char temperature was between 295°C and 305°C, which was consistent with published values in the literature.

6.6   Conclusions

Two techniques have been trialed for timber specimen selection in order to control the variability, namely grouping on the basis of low-end strengths and splitting specimens. The split-specimen technique was found to be most suitable in obtaining samples to determine the reduction in mechanical properties at elevated temperatures.

Apparatus and a reliable procedure have been developed to heat timber samples to a uniform temperature and allow deformation to be recorded during a compression test.

A technique for recording deformation of timber samples at elevated temperatures tested in compression has been developed.

The change in mechanical properties of radiata pine in compression due to effect of elevated temperature have been determined for relatively clear samples with cross-sections comparable to structural-grade specimens.

Further testing to determine the relationship for specimens with substantial growth characteristics is required. The sampling procedure employed should be based on the low-end strength batching procedure detailed in Section 6.2.

7. Comparisons of Model Predictions with Experimental Results

7.1 Introduction

The structural model has been developed (§3) and validated with numerical models (§4) to demonstrate the numerical accuracy for the field of application (§1.4). Full-scale ambient wall, frame and wall furnace experiments (§5) have been undertaken to determine the structural response of walls in ambient and elevated temperature conditions, utilising reductions in mechanical properties derived (§6).

This chapter will compare the predictions of the structural model with the results obtained from the ambient and elevated temperature full-scale experiments performed. The basis for comparison involves assumptions made regarding certain mechanical properties, which were not measured during the experimental procedures and will examine the sensitivity of specific parameters on the structural response of the wall panel and wall frame structures. The independently obtained reduction in mechanical properties with temperature (§6) will be used as the basis in comparisons for the full-scale wall furnace experiments. The efficacy of the structural model will be examined with regard to being able to predict:

(i)   Load versus deflection and ultimate load in the case of the ambient experiments.

(ii)   Deformation versus time and time-to-failure in the case of the wall-furnace experiments.

The full-scale experimental series performed enabled the contribution of individual phenomena to be evaluated with regard to the structural response, such as the contribution of the plasterboard sheeting, effect of end restraint and load level.

7.2 Comparisons of Model Predictions with Results from Ambient Full-Scale Experiments

7.2.1 Introduction

Section 5 detailed the full-scale experiments. It was considered essential that the structural model could accurately predict the load-deflection behaviour and ultimate capacity in ambient conditions. The series of experiments performed allowed the efficacy of the structural model to be examined with regard to the ability of being able to predict the behaviour of timber alone, timber with sheeting on one side and with sheeting on both sides.

7.2.2 General Mechanical Properties Used in the Comparisons

The stress-strain characteristics of timber considered in the analysis assumed either a linear-elastic or non-linear relationship. The characteristics in tension in both instances assumed a linear-elastic shape to failure, to represent a brittle type fracture. The non-linear stress-strain profile in compression assumed was that shown in Figure 3.7. The column was subdivided into 10 elements along the height. The framing was divided into ten elements vertically for the purposes of modelling.

The modulus of elasticity used in the structural model was the average of the dynamic value measured for the timber studs from which the respective frames were comprised. The modulus of elasticity was assumed as the same in tension and compression for the ambient conditions. The mechanical properties of the studs used in the frames are listed in Tables 5.1 and 5.2. The failure criterion was based on the ultimate strain, which was calculated on the basis of on an assumed failure stress of 24 MPa for the timber (from Leicester *et al*, 1988) and the modulus of elasticity in Tables 5.1 and 5.2. In the case of assuming a linear stress-strain distribution, the failure mode in compression and tension was assumed as brittle elastic, hence the ultimate strain was calculated by dividing the ultimate stress by the modulus of elasticity.

The mechanical properties of the plasterboard sheeting were assumed to have the modulus of elasticity of 0.48 GPa, based on the experiments of Walker *et al* (1995). The ultimate strength in tension was assumed as 1MPa based on the same experiments.

7.2.3 Comparisons for Timber Framing without the Sheeting

7.2.3.1 Introduction

The experiments were performed as two series, each containing five frames, and are detailed more comprehensively in Section 5.2. The steel bracing, which was used to prevent an in-plane failure, was attached to the tensile face in one series and the compressive side in the other series. The experimental results, with which the analytical model were compared excluded single experiments that gave a markedly different result (refer to Chapter 5 for details of the experimental results). For the timber frames tested, the result for Frame O, which was significantly stiffer than the other frames was excluded, as it contained a single, very stiff stud. Similarly the result for Frame H was excluded, as it was evident that significant deformations were induced in the frame due to the initial imperfections in construction.

7.2.3.2 Results

The comparison between the structural model predictions and experimental results of mid-height deflection versus load (refer to Figure 7.1 and

Figure *7.2*) demonstrates the effect of the steel bracing on the structural response.
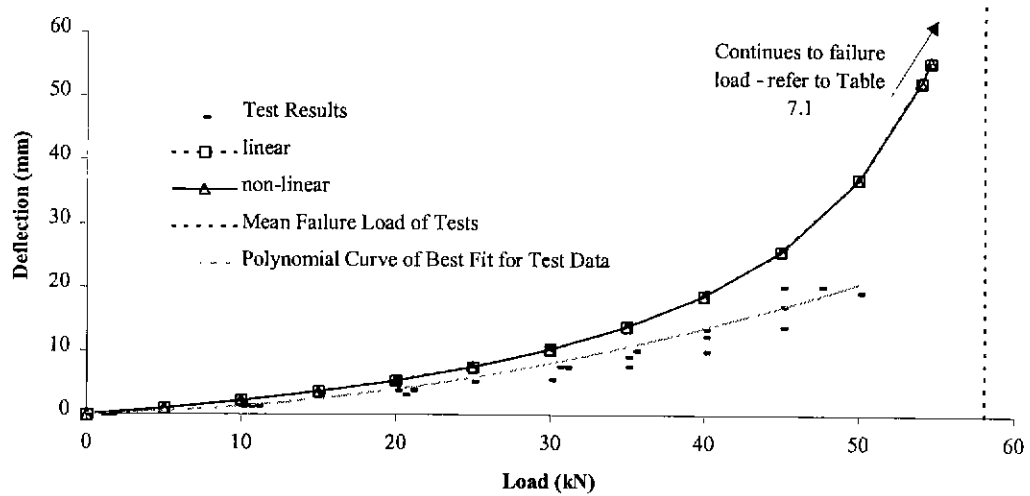
Figure 7.1: *Comparison between the Experimental Results for Frames (F,G,I & J) with Bracing Attached to side of the Studs in Tension and the Structural Model Prediction of Mid-Height Deflection versus Load*
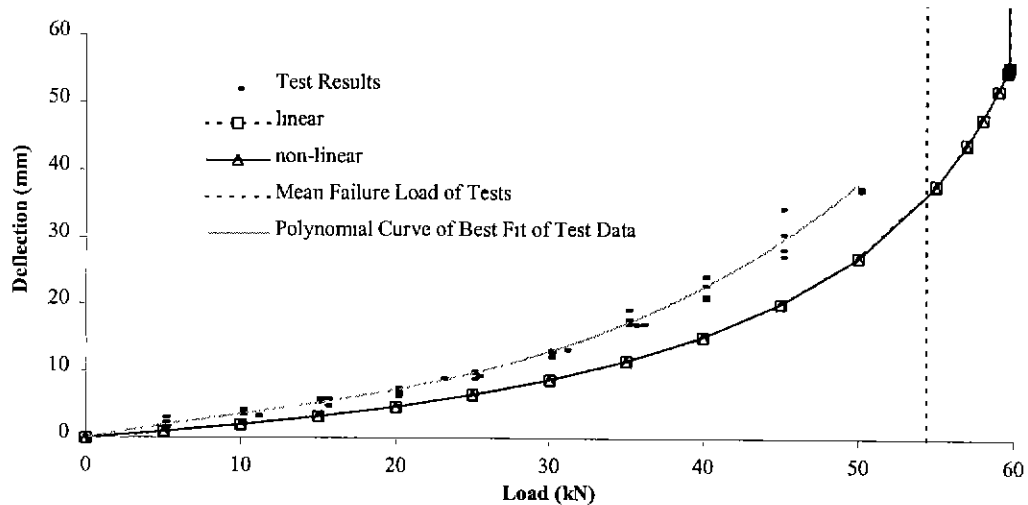
Figure 7.2: *Comparison between the Experimental Results for Frames (K-N) with Bracing Attached to Side of Stud in Compression and the Structural Model Prediction of Mid-Height Deflection versus Load*

The steel bracing attached to the side in tension tended to straighten the wall frame as in-plane effects induced tensile force in the steel. The resultant effect was a reduction in the deflection compared to the walls without the bracing attached. The steel bracing attached to the compression

side of the framing members tended to exacerbate the deformation, as tensile forces induced in the steel bracing induced reactionary compressive force in the timber on the compression side. The substantially lower flexural stiffness in the in-plane direction of the framing resulted in the frame tending to bend in this direction. This resulted in the bracing continuing to be subjected to tension on this face in this direction. Evidence of the bracing being in tension (and performing effectively) was that the wall frame did not have a premature buckling failure in the in-plane direction, and that the bracing cannot transmit substantial compressive forces.

The structural model was therefore considered to give a reasonable prediction of the load versus deflection shape, given it under predicted the deformation on the frames with the steel bracing on the tensile side and over predicted the deflection on the frames with the steel bracing on the compression side.

It was apparent that there was little difference in the deflected shape prediction calculated using an analysis employing either linear elastic or non-linear stress-strain behaviour for the timber for the range of measured deflections in the experiments.

The comparison between the predicted failure load and failure load derived from experiments for the frames is summarised in Table 7.1. The failure loads predicted with the structural model were close to the experimental results. The effect of the steel bracing in increasing or reducing the load at which failure occurred can explain in some part the relatively different error in the prediction between the frames with bracing on the respective sides. However, the errors in failure load prediction are related to the complex failure mechanism of timber associated with local effects in the region of growth characteristics. Invariably during the experiments, the specimens failed locally in tension in the region of a knot, which lead to a sudden failure of the frame. However, given the slenderness of the timber studs, the failure was dominated by the flexural stiffness of the stud and the failure mode was buckling. The localised collapse mechanism was considered a consequence of the buckling failure.

Table 7.1: Comparison between Experimental Results and Model Predictions of Failure Load

	Average Failure Load from Experiments (kN)	Model Predictions of Failure Load (kN)	
		Linear Elastic Mechanical Behaviour	Non-Linear Mechanical Behaviour
Frames with Bracing on Tension Side	58.1	54.4	58.9
Frames with Bracing on Compression Side	54.4	58.6	62.9

The model considered the timber as a homogeneous material for the purposes of computational efficiency and practicality. Further refinement of the stress-strain behaviour to incorporate the failure mechanism via statistical means such as that by Buchanan (1986) was not considered feasible at the current stage of model development due to a lack of available data defining statistically the mechanical properties of timber species at elevated temperatures.

7.2.4   Comparisons for Walls with Plasterboard Attached to One Side – 'T' Panels

The results obtained with the structural model are compared with the experiments involving the timber wall panels with plasterboard sheeting attached to a single side, referred to as a 'T' Panel, to determine the interconnection shear spring stiffness between the stud and sheeting. The relationship between the interconnection shear spring stiffness and flexural stiffness for both 'T' and 'I' panels using the equations (3.9) to (3.13) derived in Chapter 3 is presented in Figure 7.3. It can be seen that the behaviour is essentially represented by the stud alone (i.e. non-composite action) when the shear spring stiffness was less than 10^4 N/m. The behaviour is characterised as essentially fully composite when the shear spring stiffness is 10^8 N/m or greater.
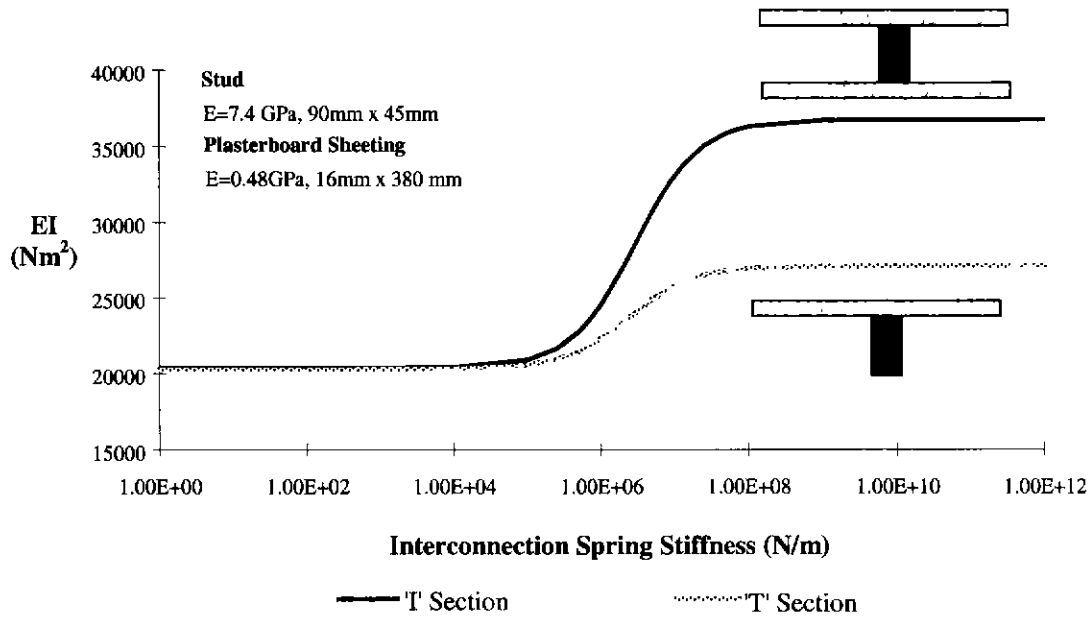
Figure 7.3*: Demonstration of the Flexural Stiffness of the Stud / Plasterboard Assembly versus*

Flexural Stiffness

To ascertain the shear spring stiffness in the experiments, the structural model was used to predict

the load-deformation behaviour for the 'T' panels, employing a variety of values for the

interconnection shear spring stiffness. The values selected represented a range from non-composite

action to full composite action and were based on values from Figure 7.3, varying from 10^4 N/m to

10^8 N/m. The results from this study are presented in Figure 7.4. Note the results from 'T' panel

"P" have not been included, due to the anomaly of the results compared with the other four

experiments. This anomaly in the results from this panel were associated with it having a

substantial increase in deflection in the initial phases of load application, approximately 10mm

deflection at mid height with 6kN applied. This was considered to be most likely due to a

construction defect.

Figure 7.4: *Comparison between the Experimental Results and the Structural Model Predictions for the Load versus Deflection for the 'T' Section for Varying Interconnection Spring Stiffness Values. Note: Structural model predictions using non-linear stress-strain behaviour*

The structural behaviour of the 'T' section obtained during the experiments was indicative (refer to of Figure 7.4) of almost full composite interaction between the sheeting and timber framing for the range of deflection measurements. A general discrepancy of approximately 3mm between the model predictions and experimental results may be due to construction tolerances. That is, the "slack" in the 'T' panels being taken up during the initial phases of the loading. If the initial portion of the load-deformation curve is neglected, the gradient of the curve from the experimental data can be seen to be very similar to that predicted in assuming full composite action.

The relationship between the predicted failure load to the interconnection spring stiffness was compared with the experiments performed, the results are presented in Figure 7.5. This indicates that full composite action was not evident at failure. The calculated interconnection spring stiffness at the mean experiment failure load was $4*10^4$ N/m.
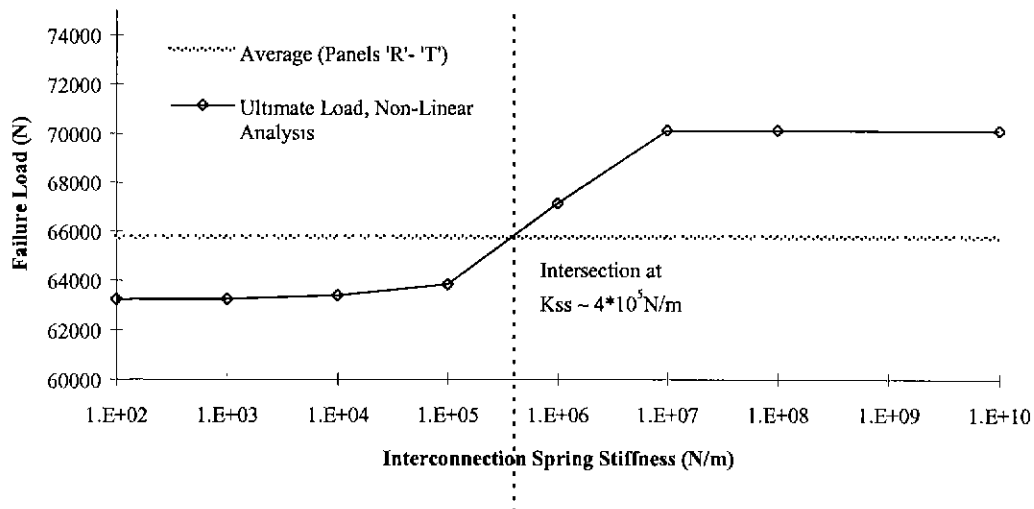
Figure 7.5: Relationship between the Mean Experiment Failure Load and Interconnection Shear

Spring Stiffness for 'T' Panels

7.2.5   Comparisons for Walls with Plasterboard Attached to Both Sides – 'T'

Panels

The comparison between the predicted and experimental load-deflection of the wall panels is

shown in Figure 7.6. From the results of the analysis performed for the 'T' panels, it was assumed

that full composite action between the framing and sheeting would be provided over the range of

deflections measured during the experiments.

The load-deflection behaviour that was predicted by the structural model closely matched that of

the average of the experimental results, although it should be noted that there was some scatter

amongst the experimental results. As with modelling the timber framing, there was little difference

in the predicted load-deflection curves assuming either linear elastic and non-linear elastic stress
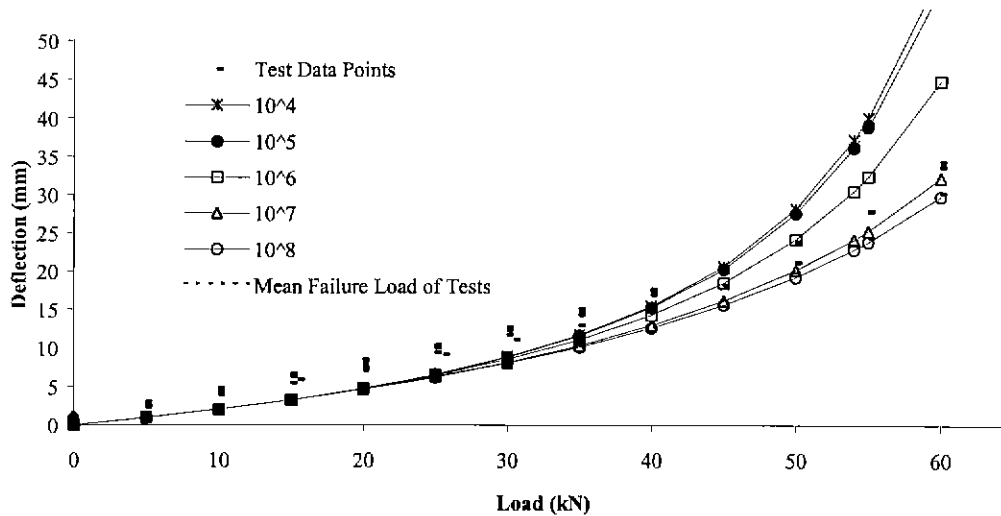
strain behaviour for the timber.
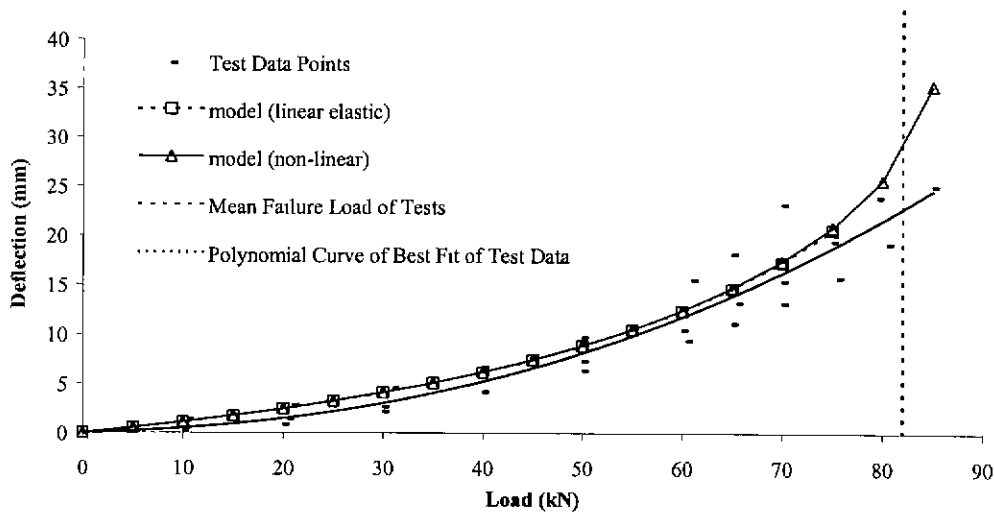
Figure 7.6: Comparison between the Experimental Results and the Structural Model Predictions for Load versus Deflection for the Wall Panels Assuming Full Composite Action

The relationship between the predicted failure load and the interconnection spring stiffness is shown in Figure 7.7. It was demonstrated that full-composite action did not occur at the failure load. However, the degree of composite action was demonstrated to be greater than in the case of the 'T' panel, $k_{ss}=5.75*10^6$ N/m compared with $4*10^5$ N/m for the 'T' panel.
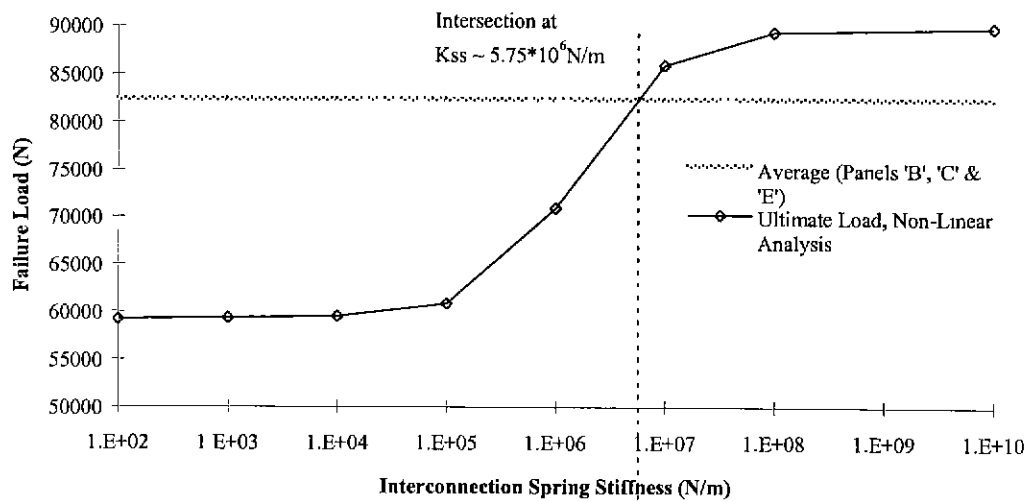
Figure 7.7: Sensitivity of Failure Load to Interconnection Spring Stiffness for Wall Panels

7.2.6   Conclusions

The structural model developed was demonstrated to reliably predict the load-deformation behaviour of timber-framed and clad timber-framed wall panels subjected to an eccentrically applied axial load, based on assuming values of the interconnection shear spring stiffness.

For loads up to approximately 90% of the capacity of the wall panel, full composite interaction between the plasterboard sheeting and timber framing could be assumed. At the time of failure, full-composite action did not occur, the interconnection stiffness was calculated as $4*10^5$ N/m for a 'T' panel and $5.75*10^6$ N/m for an 'I' panel.

Predictions of the failure load of the timber framing were demonstrated to be close to experimental values. However the ability to determine the accuracy of the prediction was limited by the effect of steel bracing attached to prevent in-plane failure. It was considered that the assumption of the timber element to be a homogenous material would result in some inaccuracy in predicting the failure load of the framing.

The analysis demonstrated that for the loaded range (up to approximately 90% capacity) compared with experimental results that there was insignificant difference in the predicted load-deformation behaviour using linear elastic or non-linear elastic stress strain models for timber. The failure mode was considered therefore to be more closely concerned with stability failure. Very close to failure the outer fibres did exceed the ultimate strain, however generally if an iteration of the model occurred where the fibres failed, a stability failure would result. The comparison with the experimental results also indicates within this range that full-composite interaction between the plasterboard sheeting and timber framing can be assumed.

The full-scale furnace experiments had the specimen loaded well below (approximately 30%) the ambient failure load. Thus for the purposes of predicting the time-to-failure for the elevated temperature experiments, it is considered reasonable to assume that stress-strain behaviour of the timber is linear elastic and that full-composite interaction occurs between the timber framing and plasterboard sheeting.

Based on the analysis undertaken within this section it is considered that the structural model has been validated for use in predicting the load-deflection behaviour and failure load of timber-framed, plasterboard-clad walls in ambient conditions.

7.3   Comparisons between Model Predictions and Results from Full-Scale Wall Furnace Experiments

7.3.1   Introduction

Comparisons are made in this section between the results from the full-scale wall furnace experiments presented in Chapter 5 and the structural model predictions.

Given the structural model was demonstrated in §7.2 to give a reliable prediction of the load-deflection behaviour of the wall panels in ambient conditions, the primary consideration in comparing predictions made with the structural model and results from the experiments was the degradation in the mechanical properties with elevated temperature. Since the columns loaded in axial compression were slender in ambient conditions, with the slenderness increasing with thermal degradation, the reduction in the modulus of elasticity in compression was considered the most crucial property to be examined. Predictions based on alternative values given in the literature and Chapter 6 for mechanical properties in compression are compared with the experimental results.

The effects of end-restraint from the experimental results are considered against the idealised assumptions of end-restraint in the structural model.

7.3.2 Consideration of the Mechanical Properties

7.3.2.1 General Mechanical Properties Used in the Comparisons

The initial mechanical properties selected for this analysis were based on the following:

(i)   The ambient modulus of elasticity in tension and compression was equal to the mean values

of the timber studs measured during the procedures of the full-scale experiments detailed in

Section 5.

(ii)   The ultimate strength in tension and compression was assumed as 24 MPa (the same as

used in §7.2), based on Leicester *et al* (1988) conducting extensive tests on radiata pine

studs.

(iii)   The mechanical properties of the plasterboard sheeting were assumed to have a modulus of

elasticity of 0.48 GPa, based on the tests in tension of Walker *et al* (1995). The ultimate

strength in compression and tension was assumed as 1 MPa.

(iv)   Unless otherwise stated, full composite interaction was assumed between the timber studs

and plasterboard sheeting, this assumption was based on the results of the comparisons with

the ambient test series (§7.2.5), which determined that at low load levels, full composite

action could be assumed.

Input data for the temperature distribution through the timber and plasterboard sheeting were

obtained by averaging the measured temperatures from the full-scale experiments (§5).

7.3.2.2 Modulus of Elasticity in Compression – Consideration of Small Scale

Experiments compared with Observed Behaviour for Full-Scale Experiments

As detailed in the literature review, little experimental work had been conducted to determine the

reduction in the modulus of elasticity in compression versus temperature.

The data obtained from the mechanical property experiments (§6) indicate that the reduction in the

modulus of elasticity in compression for a dry sample is significantly less than a moist sample.

Extrapolation of the results presented in Section 6 indicates that the modulus of elasticity in

compression for a moist sample is approximately 42% of the ambient value at 100°C. Samples tested above 100°C were dry and did not demonstrate such a large reduction in the mechanical properties from ambient.

There was evidence that the deformations induced within the timber framing in the full-scale furnace experiments were irrecoverable. There was no obvious increase in the effective modulus of elasticity as the timber framing temperature increased above 100°C-110°C. Otherwise, in maintaining consistency with the results from the mechanical property tests in Section 6, the walls would have straightened as the temperature of the framing passed through this range and the timber dried. Thus the reduction in the modulus of elasticity for temperatures above that in which the timber dries (100°C-110°C) could not be represented by direct application of the reduction in mechanical property results in Section 6, which were given only in terms of temperature.

To implicitly incorporate the phenomenon of irrecoverable deformation, relationships were derived to represent the "effective" reduction in the modulus of elasticity. Two tri-linear reduction relationships, labelled "Case A" and "Case B", were proposed and are shown in Figure 7.8. The initial shapes of the reductions were based on the experimental results obtained in Chapter 6, in they both assumed a constant gradient from ambient (20°C) to the test result at 70°C. Case B was deduced by extrapolating the results linearly at the same gradient from 70°C to a temperature of 110°C, a temperature at which moisture was demonstrated to be removed from heated specimens during the thermal calibrations (§6.3). Case A was also extrapolated linearly from 70°C to 110°C, but at an increased gradient compared with Case B. The reason for the increased gradient was that the tests of White *et al* (1981) had demonstrated a significant increase in the moisture content (approximately 20%) as the temperature approached 100°C. A value of 0.2 at 110°C was chosen, based on comparing model predictions with experimental results.

For both Case A and B, the reduction was assumed constant from 110°C to 200°C. This assumption was based on observations made during the full-scale experiments detailed in Chapter 5, where there was no straightening of the wall with continued exposure to heating by the furnace (for example, Figure 5.41). A linear reduction from the constant value to zero was assumed

between 200°C to the temperature at which the wood would commence charring (288°C, Shaffer,

1973). This assumption was consistent with the findings of the mechanical property tests, where it

was apparent that above 200°C there was a rapid reduction in the mechanical properties of timber

in compression.

Reductions in the modulus of elasticity in compression were included for comparison purposes:

these were selected from specific authors in the literature (Refer to Figure 7.8). The reduction of

the modulus of elasticity in compression of White *et al* (1993) and Gerhards (1982) were

incorporated in Figure 7.8 as these are properties which have been derived from tensile or bending

tests. The use of these property reductions in strength values will be used to examine the suitability

of applying results obtained from tensile or bending tests to members subjected primarily to axial
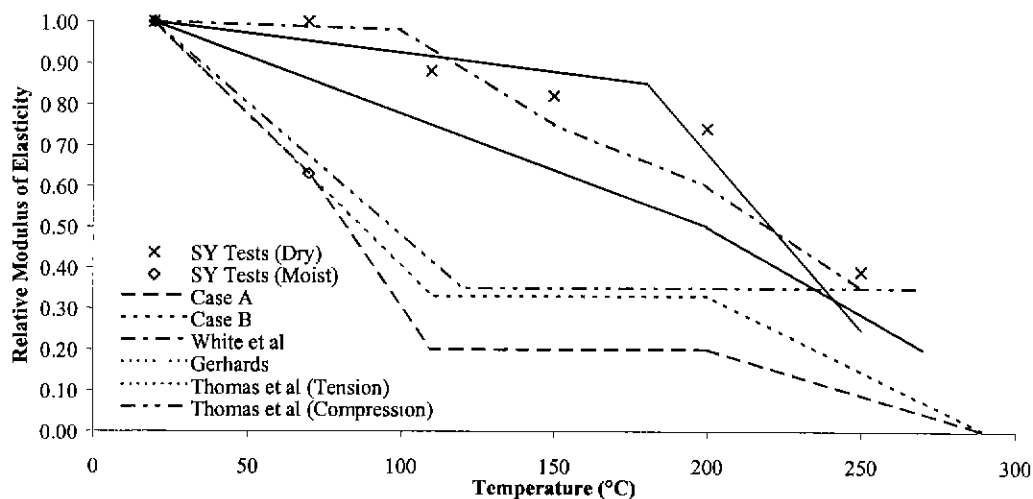
compression.

Figure 7.8: Relative Modulus of Elasticity versus Temperature Relationships of Several Authors

Examined in the Comparisons of Results from the Structural Model with Full-Scale Experiments

Note: SY Tests (Dry) and SY Tests (Moist) Refer to the reductions in mechanical properties

derived in §6

7.3.2.3   Modulus of Elasticity in Tension

The reduction in the modulus of elasticity in tension as used in the Case A and Case B results was that of Thomas *et al* (1996). For the results presented, labeled Gerhards (1982) and White *et al* (1993), the reduction in modulus of elasticity in tension were assumed to be the same as the properties in compression.

Given the failure mechanism of the wall panels is through compressive buckling, the modulus of elasticity in tension is not considered critical in determining the time-to-failure.

7.3.2.4   Ultimate Strength in Compression

The reduction in the ultimate strength in compression for the Cases A and B respectively were obtained directly from the small-scale mechanical property experiments performed in Chapter 6 and are shown inFigure 7.9. The full-scale experiments gave no evidence of a sustained reduction in compression strength after the timber had dried, hence it was assumed that after the specimens are likely to have dried as the temperature reached 110°C, a corresponding increase in strength would result, the continued reduction in the modulus of elasticity at these temperatures (110°C to 288°C) was to account for the irrecoverable deformation induced within the timber. The reductions obtained from Gerhards (1982) and Thomas *et al* (1996) are shown in Figure 7.9. Note for comparisons for White *et al* (1993), the reductions from Gerhards (1982) have been employed.
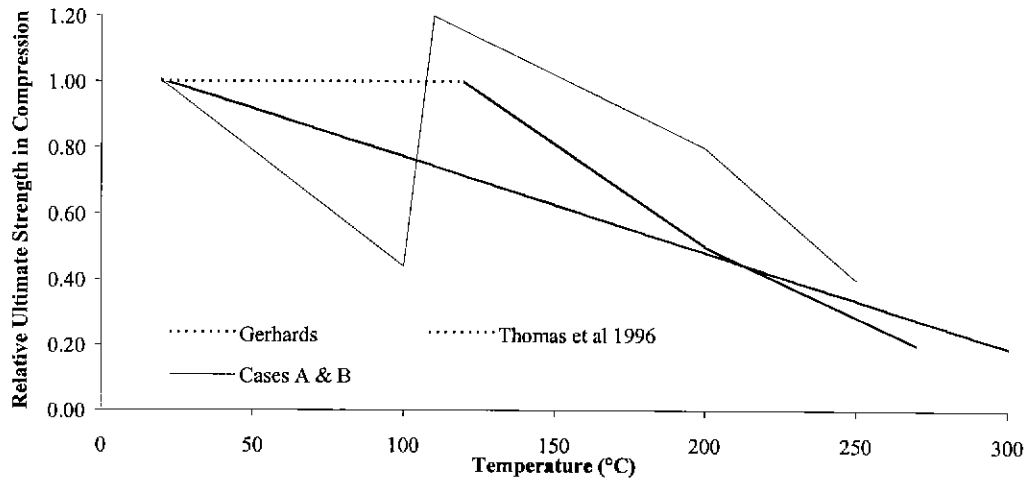
***Figure 7.9**: Relative Ultimate Strength in Compression versus Temperature of Several Authors*

Examined in the Comparisons of Results from the Structural Model with Full-Scale Tests

7.3.2.5 Ultimate Strength in Tension

The ultimate strength in tension was that of the respective authors (Gerhards, 1982, White *et al*,

1993, Thomas *et al*, 1996) as detailed in the literature review in §2.2.3.2. The selected ultimate

strength in tension for Case A and Case B properties was that of Thomas *et al* (1996).

7.3.2.6 Plasterboard Mechanical Properties

The degradation in the mechanical properties of the plasterboard sheeting was based on the data

from tests performed by Walker *et al* (1995) and Goncalves *et al* (1996). However, the lack of data

at temperatures less than 300°C due to heating difficulties required some interpretation beyond the

linear interpolation between 20° and 300°C data points as presented by these authors. Examination

of the mass loss of the gypsum plasterboard versus temperature at a heating regime consistent with

standard fire resistance test as presented by Mehaffey (1991) revealed that the primary temperature

range for mass loss was between these temperatures, which corresponds to the calcination of

Gypsum. The reduction in mechanical properties of the plasterboard was an "Interpreted

Reduction" shown in Figure 7.10. This has been based on an interpretation of the results of

Mehaffey (1991) in that it assumes that the bulk of the plasterboard strength is retained until rapid

calcination of the sheeting commences at approximately 100°C (Mould *et al*, 1974), and has

largely been completed by 150°C. The implication of this is that for temperatures above 150°C

the plasterboard provides a minimal contribution to the structural performance of the wall;

however, it still provides a barrier to reduce the heating of the timber framing members.
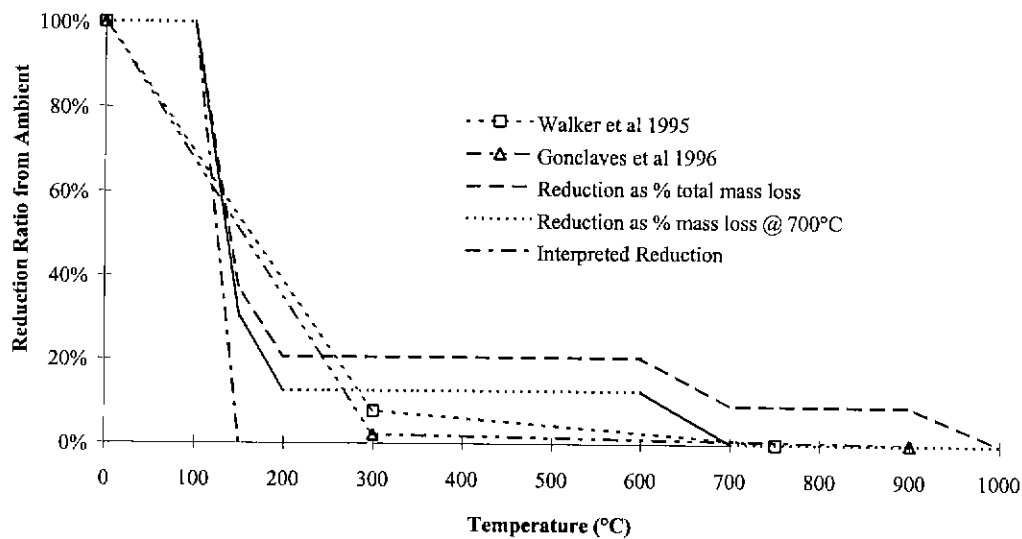
Figure 7.10: Reduction of Plasterboard Modulus of Elasticity versus Temperature

7.3.2.7 Comparisons of Model Predictions with Results from Full-Scale Furnace Experiments

7.3.2.7.1   Walls with End Supports Allowing Free Rotation

Results obtained from the structural model using the reduction in mechanical properties shown in

Figure 7.8 and Figure 7.9 were compared with the results of the full-scale experiments BFT679,

BFT 680 (sheeting conventionally fixed, Figure 5.40) and BFT683 (sheeting on unexposed face

not contributing to composite behaviour, Figure 5.42).

The interconnection stiffness was assumed to provide full composite interaction between the

sheeting and stud for experiments BFT679 and BFT680. It was assumed that there would be a

reduction in interconnection stiffness associated with temperature effects and that this was

considered to be proportional to the reduction in the mechanical properties of the plasterboard. The

temperatures of the plasterboard assigned to the elements, into which the sheeting was discretised, were obtained by linear interpolation between the average temperatures measured on the exposed face and the unexposed face in the full-scale experiments.

The interconnection stiffness was assumed to provide no composite interaction for the comparison with experiment BFT683. This experiment was constructed such that the sheeting on the exposed face provided composite action, and no composite action would be provided on the unexposed face. Although assumed connected in the model, the sheeting on the exposed face would provide little contribution to the structural response of the wall after the average temperature of the sheet exceeded 150°C. This occurred within five minutes of the commencement of the test (refer to Figure 7.11).
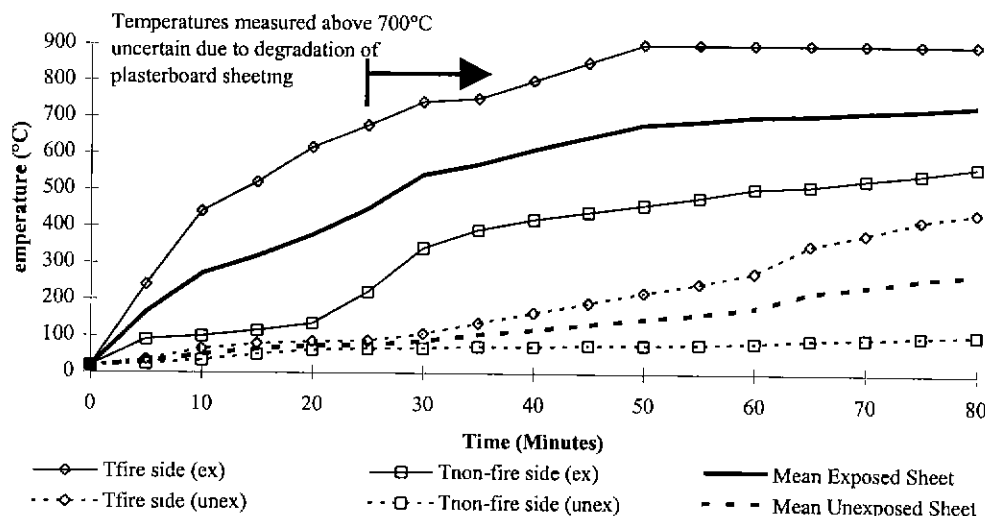
Figure 7.11: Average Surface Temperatures Measured on the Plasterboard Sheeting during the Full-Scale Furnace Experiments

The mid-height deflection versus time were calculated using the structural model, with the timber mechanical properties of Cases A, B and the reductions in mechanical properties (for example Figure 7.7) of the respective authors, Gerhards (1982), White et al (1993) and Thomas (1996). The results obtained from the use of these properties as input data for the structural model and the test results are shown in Figure 7.12 and Figure 7.13. The calculated times-to-failure are listed in Table 7.2.
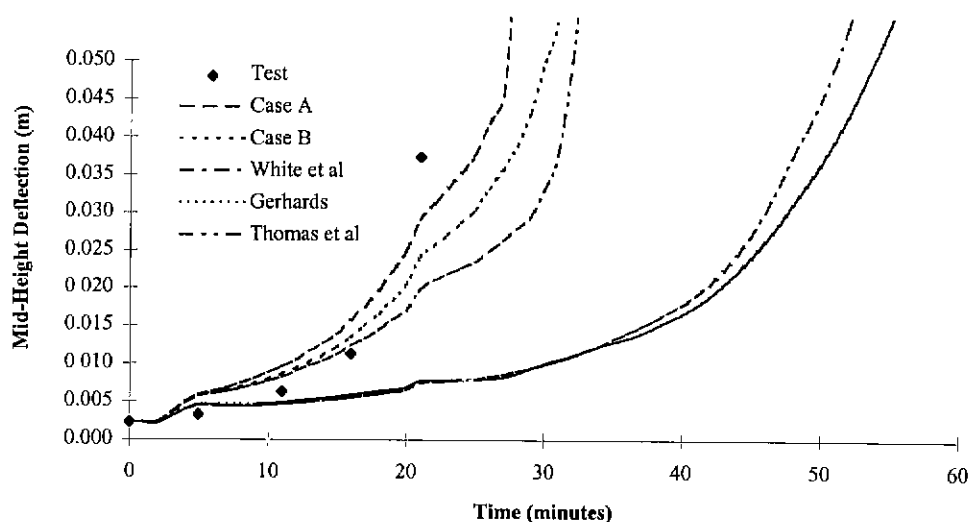
Figure 7.12: *Deflection Versus Time for Wall Panel with No Composite Action between the Plasterboard and Timber Studs on the Unexposed Side: Comparison Between Test (BFT683) and Model Predictions*
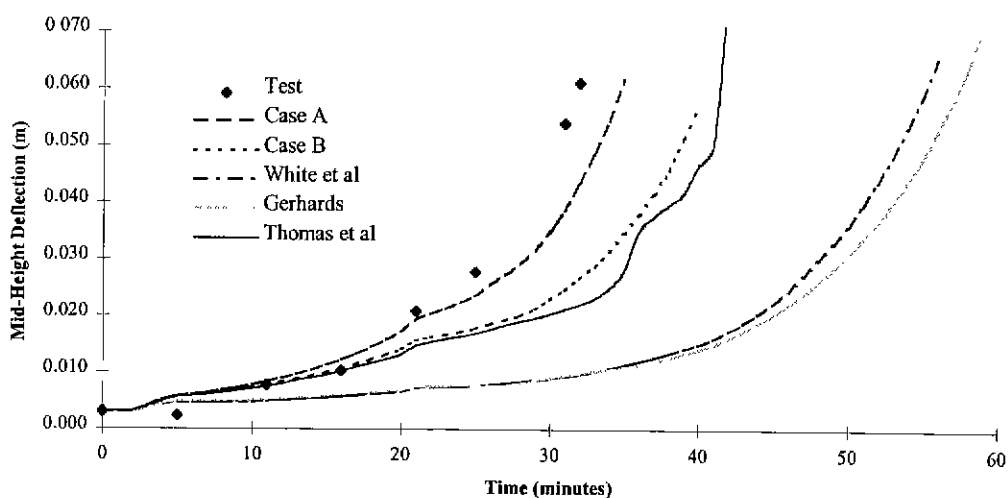
Figure 7.13: *Deflection Versus Time for Wall Panel with Composite Action between the Plasterboard and Timber Studs on the Unexposed Side: Comparison Between Tests (BFT679, BFT680) and Model Predictions*

The results of the analysis indicate that the use of mechanical properties derived from bending or tensile tests such as those by White *et al* (1993) or Gerhards (1982) may not be ideally suited to be applied in structural models to represent members which are primarily subjected to axial compression.

Table 7.2: *Prediction of the Time to Failure (Minutes)*

Source of Compression Mechanical Property Data	No Composite Action between Timber Studs and Plasterboard Sheeting on Unexposed Side	Full Composite Action between Timber Studs and Plasterboard Sheeting on Unexposed Side
Full Scale Test	28.5	35
Case A	26	34
Case B	32	41
White *et al* (1993)	57	57
Gerhards (1982)	60	60
Thomas *et al* (1996)	42	43

It is notable that the reduction in mechanical properties with temperature determined by Thomas *et al* (1996) were derived in using a structural model, which did not incorporate the structural contribution of the plasterboard sheeting on the non-fire side. By ignoring the contribution of the plasterboard sheeting on the unexposed face in providing structural resistance, the mechanical properties of the timber would tend to be overestimated to obtain a reliable comparison with experimental data. Hence the times of 42 and 43 minutes shown in Table 7.2.

The reduction curve defined for Case A gave a more accurate prediction of the time of failure than Case B for wall panels allowed to freely rotate at the ends. The assumption of increased reduction in the "effective" modulus of elasticity in compression as the temperature approaches 100°C appears more valid for this case.

7.3.2.7.2   Sensitivity to Ultimate Strength in Compression

A sensitivity study was undertaken on the change in the ultimate strength in compression by varying it ±25% from the assumed initial ambient value. The time-to-failure using the reduction curve for Case A did not change.

7.3.2.7.3   Wall Prevented from Rotation at the end Supports

The prediction made by the structural model in determining the response of the wall panel with

rotation prevented at the top and bottom end supports was compared with the results from the full-

scale experiment, BFT 681, with these end conditions (Figure 5.41). The same set of mechanical

properties as detailed in Section 7.3.2.7.1 were used in the structural model.

An initial crookedness of 10mm was assumed to initiate the P-Δ analysis. The analysis performed

has examined the applicability of the mechanical properties represented by Case A and Case B,

and the sensitivity of the rotational restraint provided.

It was apparent, based on observations made during the full-scale experiment, that as the

experiment progressed, rotation was not fully prevented where the stud was nailed at the joint

between the top and bottom end supports. At failure, rotation has occurred at the joints. To account

for this, the degree of end restraint was varied, from between being fully prevented to free. The

"degree of rotational restraint", ϕ_{res}, was considered a useful term to define the fraction of full

rotational end restraint. It was defined as:

$$\phi_{res} = \frac{\delta_0 - \delta_{K_\theta}}{\delta_0 - \delta_\infty}$$

- (7.1)

where

δ_0 = mid-height deflection for no rotational restraint

δ_{K_0} = mid-height deflection for rotational restraint of K_θ (kNm/radian)

δ_∞ = mid-height deflection for an infinite rotational spring stiffness at the support ie. fully

restrained against rotation

The relationship between the degree of rotational restraint and the rotational stiffness at the ends of

the wall studs in ambient conditions is shown in Figure 7.14. The mechanical properties used in

generating this relationship were those from the ambient series of experiments (§7.2.1.1).
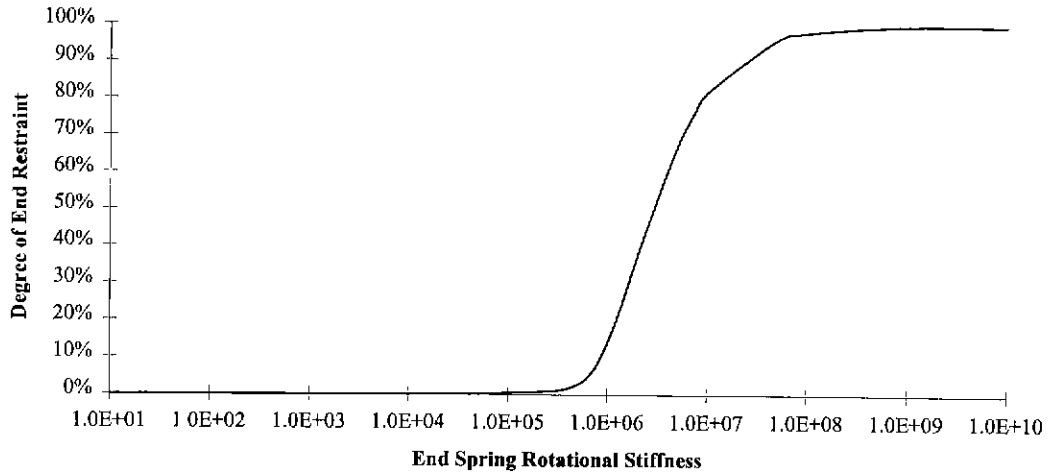
Figure 7.14: *Degree of Rotational Restraint of the Wall Studs versus Rotational Spring Stiffness*

(kNm/radian) at End Supports at Ambient Conditions

The load-deflection plots for the varying end restraint rotational stiffness are compared against the experimental results and are presented in Figure 7.15 and Figure 7.16.
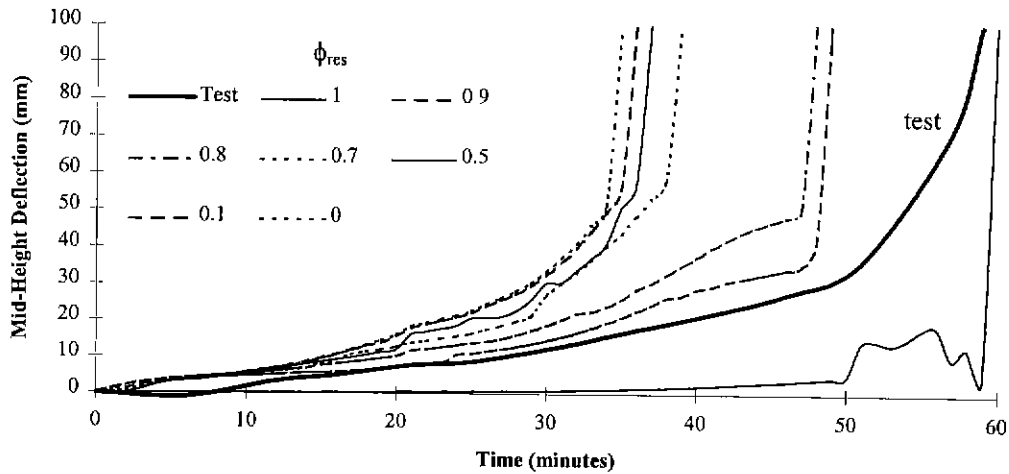
Figure 7.15: *Mid-Height Deflection versus Time for Varying Degrees of Rotational End Restraint,*

ϕ_{res}, utilising mechanical properties from Case A (Note that there is some overlap of the curves

where ϕ_{res} approaches 0)
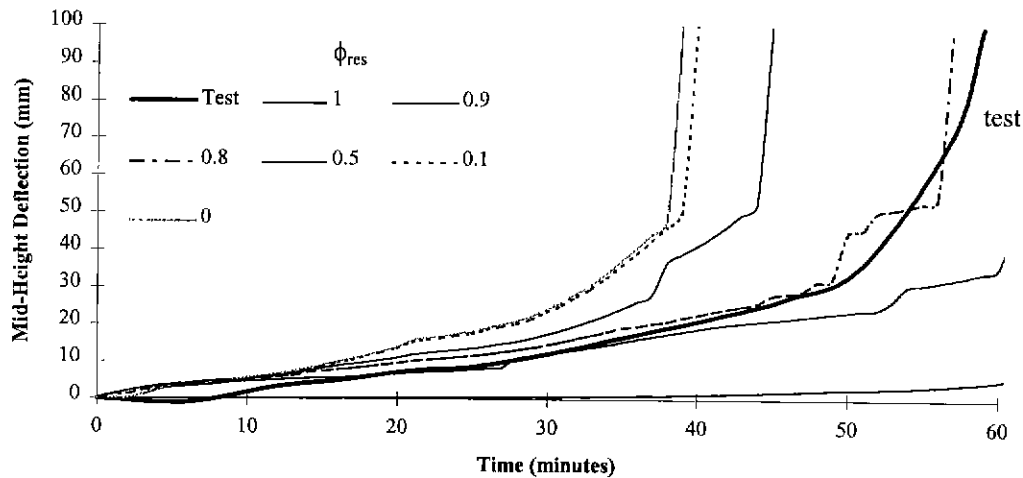
Figure 7.16: *Mid-Height Deflection versus Time for Varying Degrees of Rotational End Restraint,*

ϕ_{res}, utilising mechanical properties from Case B (Note that there is some overlap of the curves

where ϕ_{res} approaches 0)

The predicted time-to-failure by the structural model exactly matches the result obtained from the experiment, 59 minutes, if full rotational restraint is assumed and the mechanical properties from Case A are employed in the model. However, reference to Figure 7.15 indicates that the load-deflection curve was not closely followed, which implies imperfect modelling of the phenomena which occurred during the experiment. The unsteady increase in the load-deflection curve predicted before failure is due to the different values of modulus of elasticity in tension and compression, and the use of an "effective" modulus of elasticity to incorporate the effects of irrecoverable deformation in compression. Reference to the remaining curves (0-0.9) for reduced levels of rotational restraint indicates that the use of mechanical properties from Case A may not be the best to use for this case of rotational restraint.

The time-to-failure derived assuming full rotational restraint with mechanical properties from Case B was 70 minutes. However, given the observation of rotation between the studs and end plates during the experiment, it is expected that the time to failure would be over predicted if full rotational restraint was assumed. The load-deformation curve obtained from the experiments was closely predicted, in assuming the Case B reduction in mechanical properties and with rotational

end restraint factors of 0.9 to 0.8. Whilst the actual rotational restraint provided at the time of failure is uncertain, it is apparent that the reduction in mechanical properties assumed by Case B allows for a better prediction of the load-deformation behaviour than Case A. This can be explained in that the magnitude of creep/plastification induced in the timber as it approached 100°C was less in the case of the wall with rotation prevented at the ends. The deformation was less. There was no fixed eccentricity for load application and the prevention of rotation at the ends resulted in lower stress levels at mid height. Given creep is generally derived for materials as a function of temperature, stress level and moisture content, reducing the stresses on the timber would result in a reduced creep magnitude and hence effectively a higher modulus of elasticity.

Reference to the temperatures of the plasterboard sheets versus time shown in Figure 7.11, demonstrates that the plasterboard sheeting does not play such a significant role in defining the structural response after 60 minutes test duration. However it did play a significant role in the walls without rotational restraint. It would also have reduced the deformation in the wall, prevented from rotating at the ends, and any associated irrecoverable creep-type deformation, and consequently increase the time-to-failure.

7.3.3   Conclusions

The reduction in the modulus of elasticity as a function of temperature was derived for radiata pine for specific rotational end restraint conditions, based on small-scale mechanical property experiments and comparisons with results from full-scale wall furnace experiments. The use of mechanical property data at elevated temperatures derived from tensile and bending tests was demonstrated to not necessarily be applicable to members that are subjected primarily to compression. The applicability of the empirically derived results is dependent on the end restraint conditions prescribed for the wall.

The time-to-failure of a load-bearing timber-framed wall was not sensitive to the ultimate strength in compression of the timber as the failure mode was through buckling.

For the structural model to reliably predict significantly different conditions to those in the experiments performed, it is essential that the creep/plastification phenomenon is studied and a model developed which considers the magnitude of the phenomenon related to the moisture content, stress level, temperature and time.

A wall prevented from rotation at the end plate supports was demonstrated to not be fully restrained from rotation for the duration of the test. The "degree of rotational restraint" calculated for these walls was 0.8, where 1 represents a wall prevented from rotation at the supports and 0 represents a wall which can freely rotate. The assumption of full rotational restraint in models predicting the time-to-failure of timber-framed walls is therefore non-conservative.

The contribution of the plasterboard sheeting to the flexural stiffness of the wall was significantly less after 60 minutes duration for the wall prevented from rotation, than a wall which could freely rotate. However, in incorporating a phenomenon such as creep, which is dependent on the stress and deformation history, the contribution should not be ignored. Similarly, for multiple layered plasterboard sheeting systems, the contribution of the plasterboard sheeting to the flexural stiffness of the wall will be much greater.

7.4   Sensitivity Studies

7.4.1   Introduction

The following sensitivity studies were undertaken using the structural model in conjunction with the temperature data derived from the full-scale wall furnace experiments:

- Time-to-failure as a function of the applied load.

- Time-to-failure as a function of the height of the wall.

Studies of the sensitivity of time-to-failure to other variables such as stud dimensions and thickness of plasterboard sheeting were not possible. Such studies would involve different temperature data, which could only be obtained with further experiments or with a heat transfer model. Obtaining such data through these means is beyond the scope of this research (§1.4). Thus only the sensitivity studies listed above were carried out.

7.4.2   Effect of Load on the Time of Failure

The time of failure for wall panels with free rotation and wall panels with restraint against rotation at the end supports, for varying load levels have been considered (refer to Figure 7.17). The mechanical properties selected were those of Case A for the case of free end restraint and Case B for end restraint prevented, with a rotational restraint factor of 0.8. The results for both cases of restraint indicate that the time of failure is approximately inversely linearly related to the applied load. However, the effect of the creep/plastification phenomenon may cause a distortion of this relationship. As the load level increases, given the rate of creep is generally proportional to the magnitude of applied load, it would be expected that the magnitude of creep would increase. Hence the time-to-failure at higher load levels than those tested would be expected to be less than that predicted in Figure 7.17. Similarly, at lower load levels, the creep deformations would be assumed to be less, hence the time-to-failure would be longer than that predicted in Figure 7.17.
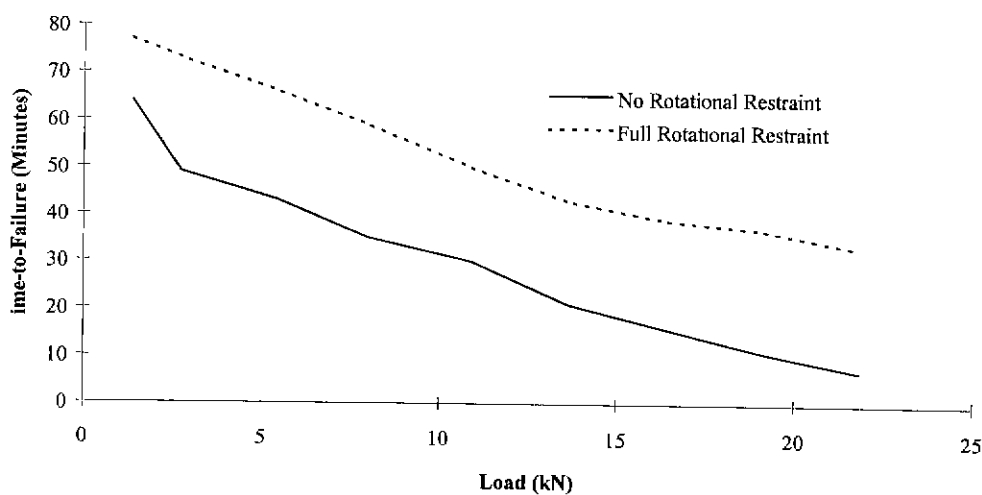
Figure 7.17: Sensitivity Study on the Time of Failure to Load Level

7.4.3   Effect of Wall Panel Height on the Mid-Height Deflection versus Time and on the Time-to-Failure

Results of a study of the sensitivity of the time-to-failure and mid-height deflection versus time to wall panel height are presented in Figure 7.18, Figure 7.19 and Figure 7.20 for both free rotation and full restraint against rotation at the end supports respectively. A load of 8kN was assumed. The results indicated that the time-to-failure was most significantly affected for the wall panel with full restraint against rotation.

The structural model can be used to assess the performance of a timber wall, which is a different height to a tested prototype. However, any results predicted using the derived mechanical properties have implicitly incorporated the creep/plastification phenomenon for the tested systems in Chapter 6. It is feasible for a high wall panel (>3m) that the stress at mid-height would be greater than for a shorter panel and that the creep/plastification phenomenon may be more significant. Thus the "effective" reduction in the modulus of elasticity at a given temperature may be greater. The results predicted by the structural model using this relationship for the reduction in mechanical properties may therefore be non-conservative for walls taller (>3m) than the tested prototypes. The converse would be expected to apply for the shorter wall panels. Due to the non-conservative nature of the prediction, it is necessary that the creep/plastification effect be quantified in future research to reliably use the structural model to extrapolate for wall panels larger than could be tested in a conventional 3 m high furnace.
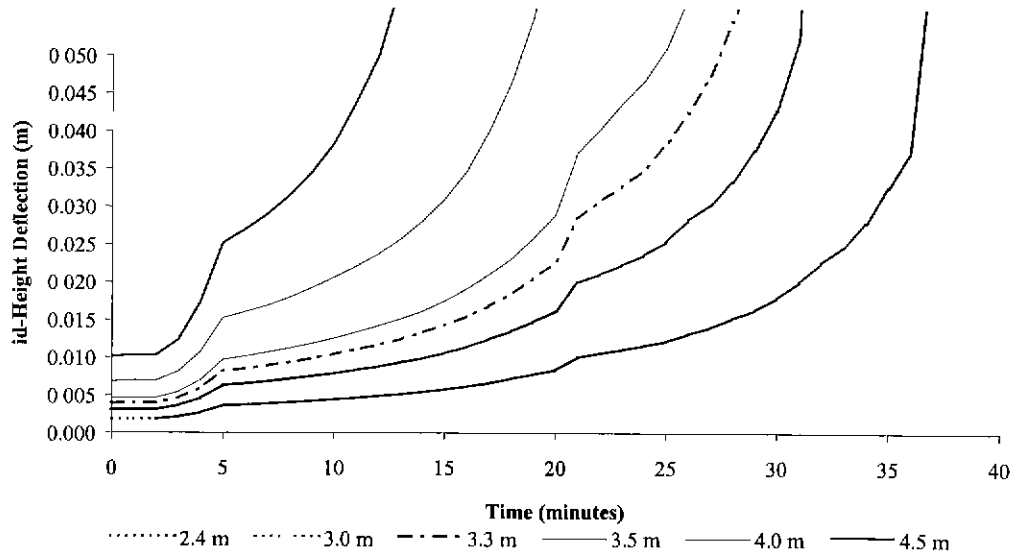
Figure 7.18: *Mid-Height Deflection versus Time for Varying Heights of Wall Panel Utilising*

Mechanical Properties from Case A, No Rotational Restraint at End Supports
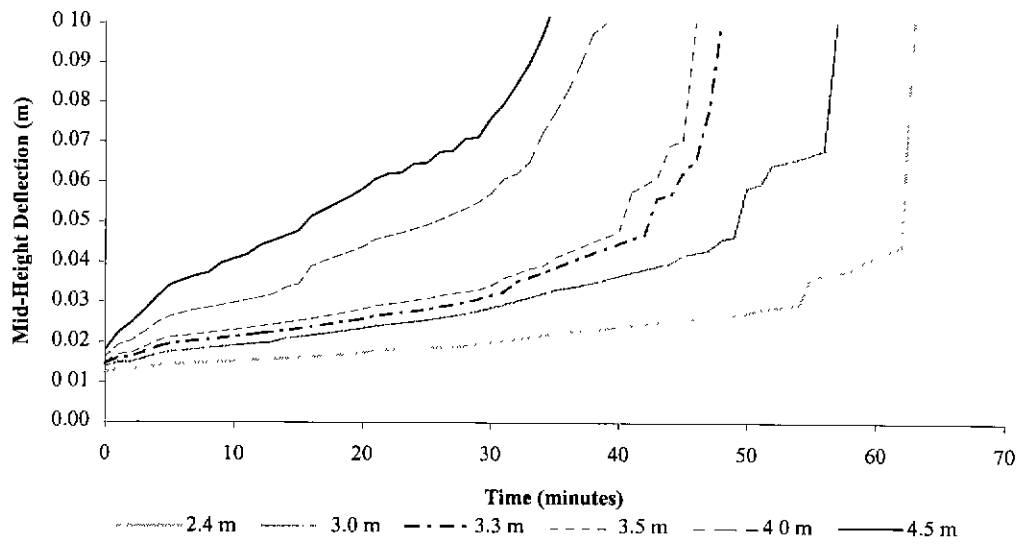
Figure 7.19: *Mid-Height Deflection versus Time for Varying Heights of Wall Panel Utilising*

Mechanical Properties from Case B, Rotational Restraint at End Supports, factor 0.8
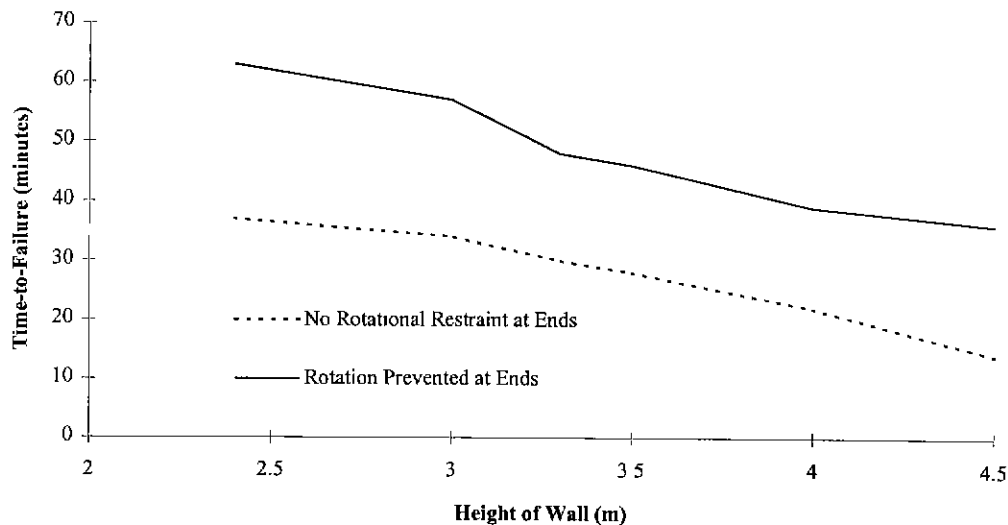
Figure 7.20: Time-to-Failure versus Height of Wall

7.5   Discussion of Results of Comparisons of Model Predictions with Full-Scale Wall Furnace Experiments and Sensitivity Studies

The efficacy of the structural model has been demonstrated for ambient and fire conditions. However, the results demonstrate that the degradation of the mechanical properties of the timber framing must be appropriately selected, especially the modulus of elasticity of timber in compression, for a reliable prediction to be made by the model. Experiments were undertaken to determine the reduction of this modulus with temperature (§6). However, the direct application of some of the results derived could not be performed in the structural model as it does not explicitly account for the creep/plastification deformations induced in timber framing as the temperature of the cross-section approaches approximately 100°C.

Whilst some empirical modification to the test results to account for the irrecoverable deformation was successfully performed, it was shown that a different reduction curve would give a closer representation of the load-deformation behaviour if the end restraint conditions were changed. It is therefore debatable if such properties derived could be applied to timber framing members subjected to different heating conditions or stress levels.

To be confident in the structural model predictions for barriers exposed to real fires, it is essential that the mechanical property reductions used within the model are not only applicable to 'standard' heating regimes such as AS1530.4, ISO834 etc, but must be reliable for different heating regimes, which may alter the significance of the creep/plastification phenomenon.

A more correct approach instead of empirically deriving an "effective" modulus of elasticity, would be to utilise the creep strain term in equation (3.17a). In order to do this, further research needs to be conducted to define a creep sub-model which will allow for the creep/plastification phenomenon. The significance of moisture transfer on this phenomenon in the overall structural response of the wall may necessitate modification of the heat transfer model by Clancy (1999) to incorporate the analysis of moisture transfer.

The lack of sensitivity of the time-to-failure to the ultimate strength in compression is consistent with the timber framing in a wall being effectively slender columns with failure via buckling, which is dependent on the flexural stiffness. As the cross-section of the timber degrades thermally with an increased time of exposure, the slenderness increases and the dependence on the stiffness of the column and the propensity for failure through the mode of buckling increases.

The reduced role of the plasterboard in providing a contribution to the structural performance of the wall decreases with the time of exposure. It is significantly less after 60 minutes test duration compared with 35 minutes test duration for a single layer of 16mm fire rated plasterboard on each side of the stud. However, depending on the load level and height of the wall, the consideration of the plasterboard may provide a significant difference in estimating the time-to-failure. A detailed analysis incorporating the creep/plastification phenomenon, based on the stress level, would also necessitate a correct consideration of the stress history. This would require the contribution of the plasterboard to be incorporated in the analysis, particularly when the apparent modulus of elasticity of the timber rapidly decreases as the temperature approaches 100°C. Consideration of the contribution of the additional stiffness provided through composite action may be more important in predicting the time-to-failure of fire resistant systems constructed of two layers of fire rated plasterboard e.g. standard 90 minute and 120 minute systems.

7.6 Conclusions from Comparisons of Model Predictions with Full-Scale Wall Furnace Experiments and Sensitivity Studies

The structural model was demonstrated to be capable of reliable prediction of the structural response of the full-scale wall panel experimental results, for specific restraint conditions and conditions of composite action. However, the reliability of predictions made by the structural model were demonstrated to be highly dependent on the mechanical properties of the timber, in particular, the reduction in the modulus of elasticity with temperature.

The reduction in the modulus of elasticity as a function of temperature was derived for radiata pine for specific rotational end restraint conditions, based on small-scale mechanical property experiments and comparisons with results from full-scale wall furnace experiments. The use of mechanical property data at elevated temperatures derived from tensile and bending tests was demonstrated to not necessarily be applicable to members that are subjected primarily to compression.

For the structural model to reliably predict significantly different conditions to those in the experiments performed, it is essential that the creep/plastification phenomenon is studied and a model developed which considers the magnitude of the phenomenon related to the moisture content, stress level, temperature and time.

The time-to-failure of a load-bearing timber-framed wall was not sensitive to the ultimate strength in compression of the timber as the failure mode was through buckling.

A wall prevented from rotation at the end plate supports was demonstrated to not be fully restrained from rotation for the duration of the test. The assumption of full rotational restraint in models predicting the time-to-failure of timber-framed walls is therefore non-conservative.

The significance of load level and height of wall panel on time-to-failure has been demonstrated.

The contribution of the plasterboard sheeting to the flexural stiffness of the wall was significantly less after 60 minutes duration for the wall prevented from rotation, than a wall which could freely rotate. However, in incorporating a phenomenon such as creep, which is dependent on the stress and deformation history, the contribution should not be ignored. Similarly, for multiple layered plasterboard sheeting systems, the contribution of the plasterboard sheeting to the flexural stiffness of the wall will be much greater.

8 Summary & Conclusions

8.1 General

A rigorous, phenomenologically based model has been developed to predict the structural response of timber-framed, gypsum plasterboard-clad walls subjected to a wide range of temperature conditions. This model has been successfully integrated into the framework of Clancy (1999). The framework as developed provides a means for predicting the time-to-failure of timber walls when exposed to varied heating conditions and as such provides a substantial advance over empirically derived models in the field of performance-based fire safety engineering design of these passive fire protection systems.

During the research undertaken in developing the model, a number of findings were made. These are outlined in this chapter.

8.2 Conclusions from Model Development

A model was developed to predict the structural response of timber-framed, gypsum plasterboard-clad walls subjected to a wide range of temperature conditions. The model utilises a second-order direct stiffness approach, with a specific element type derived to consider the interaction between the framing and sheeting. The model considered the following phenomena, which have not been all modelled together previously:

- Partial composite interaction between the timber and the plasterboard sheeting.

- Non-linear stress-strain behaviour.

- Non-linear geometric (P - Δ) effects.

- The change in mechanical properties with temperature.

- Thermal expansion.

- Variations in the end restraint conditions including the rotational stiffness provided at the supports.

The results obtained using the model were compared with both numerical solutions and experimental results. The results predicted by the model matched closely with specific closed form and finite element analysis comparisons. The model predictions compare well with full-scale ambient experiments and full-scale furnace experiments.

Clancy (1999) has utilised the structural model in a wide range of studies on the sensitivity of the time-to-failure to parameters including the size of timber framing, spacing between framing, plasterboard thickness and the height of walls. He found that the model met all of the requirements and aims outlined in §1.4.

8.3   Conclusions from Full-Scale Experiments

A series of full-scale experiments was undertaken for both ambient conditions and specimens heated in accordance with a standard fire resistance test regime to provide data to compare with the structural model developed, and further investigate the significance of specific phenomena. The experimental series was carefully controlled, and involved the consideration of the following issues:

- Construction of wall frames and panels of similar capacities through a timber selection process.
- Determination of the ambient capacity in order to determine the load ratio on the elevated temperature specimens.
- End restraint conditions were well controlled so the results of the tests could reliably be used to compare with the models developed.
- Ensuring load-bearing timber framing were subjected to approximately similar heating conditions.
- The structural contribution of the plasterboard sheeting on the tensile side, in ambient and elevated temperature tests.

The findings of the test series were as follows:

- Selection of timber studs with a similar average modulus of elasticity on the basis of machine stress grading in conjunction with a density criterion resulted in little variability in the predicted load-deformation behaviour and ultimate capacity of a wall.

- The variability amongst similar elevated temperature experiments with regard to time-to-failure was low. The concept of a 'heat wave effect' was put forward as an explanation of the very similar times of failure. The 'heat wave effect' concept proposes that as the mean temperature of the timber specimen approaches a specific value, there is a rapid drop in modulus of elasticity. This rapid drop is large enough such that the time-to-failure of different walls may be similar and any minor initial variation in mechanical properties is negated. For the timber walls in this experimental series, the 'heat wave effect' occurred when the bulk of the framing cross-section reached approximately 100°C.

- The results of other authors such as Polensek (1976) were confirmed in that the attachment of plasterboard sheeting to light timber framing results in a significant increase in the flexural stiffness and ultimate capacity of the wall.

- The time-to-failure for walls in a fire resistance test is significantly related to load level. It was demonstrated in the experimental series, that for a wall with no restraint preventing rotation at the ends, a non load-bearing wall may have a time-to-failure through collapse 150% greater than a load-bearing wall sustaining a load ratio of 30%.

- The amount of rotational end restraint provided at the end supports will significantly affect the time-to-failure in a fire resistance test. The time to failure was of the order of 67% greater for wall frames with restraint preventing rotation at the ends compared with a wall with no rotational restraint.

- The level of end restraint provided at the end-supports could determine the mode of failure of a load-bearing wall in a fire resistance test. With no restraint against rotation at the end supports, the failure mode was through large bowing and induced irrecoverable deformation. The temperature of the majority of the cross-section at which this occurred was approximately 100°C. With restraint preventing rotation at the ends, the failure mode was associated with the reduction in timber cross-section through charring.

- The rapid drop in apparent flexural stiffness as the temperature of the majority of the cross-section at which this occurred was approximately 100°C may be associated with a

mechano-sorptive creep type phenomenon, however further work is required to confirm the cause.

- The partial composite action provided by the sheeting on the non-fire side was demonstrated to affect the time-to-failure. This was 25% less for wall frames with no composite action provided by the plasterboard on the non-fire side than for a wall with conventional attachment of the sheets.

8.4   Conclusions from Mechanical Property Tests

The mode of failure of a load-bearing wall was through the mechanism of buckling, which is dependent on the modulus of elasticity in compression. It was demonstrated in the literature review that there was a lack of data in the literature determining the reduction in mechanical properties of timber in compression due to elevated temperatures. It is known that given different constituents provide the tension and compression characteristics for timber, and these constituents degrade at different temperatures. Therefore the use of mechanical property data derived from tension or bending tests would be unsuitable in determining the time-to-failure of a wall. No data were presented in the literature that obtained the reduction in the mechanical property directly from tests in pure compression. An experimental series was therefore conducted to determine the reduction in mechanical properties of radiata pine in compression for the range 20°C to 250°C, with some consideration of the effect of moisture content. The experimental series involved the design, development and conduct of the following:

- A sampling procedure to allow for confidence in relating the mechanical properties of specimens at ambient and elevated temperatures.
- Apparatus and procedures for heating the specimen to a uniform cross-section temperature.
- Apparatus and procedures to undertake the elevated temperature tests in compression.

The outcomes of the experimental series were:

- The use of relatively defect free split samples of a similar density was found to provide the closest comparison between the mechanical properties in ambient and elevated temperature conditions for a small number of samples.

- A series of thermal calibrations was performed in order to determine the time required heating a specimen to a uniform temperature. This data has subsequently been used by Clancy (1999) to validate thermal properties of timber up to 250°C.

- The effect of moisture on the reduction in mechanical properties was demonstrated. Compression test specimens were demonstrated to be unsuitable to heat within the testing machine due to condensation in the ends of the specimens resulting in localised failure at the ends.

- The change in the ultimate strength and modulus of elasticity in compression versus temperature for the radiata pine was determined.

- Comparisons between the full-scale test series and the mechanical property experiments indicate that there was apparently significantly less variability amongst the time-to-failure, than would be expected by the variation in mechanical property test data. Based on these considerations, it is apparent that there is a very rapid drop in the flexural stiffness of the timber-framing members as the temperature approaches 100°C. This possibly could give some credence to the 'heat wave effect' put forward to explain the low variability in the full-scale wall furnace tests.

8.5   Comparisons between Model Predictions and Experimental Results, and Sensitivity Studies

Predictions made by the structural model were compared with the results from full-scale experiments, including some sensitivity studies on the mechanical properties, degree of composite action, end restraint, load ratio and wall height. The outcomes determined from these analyses were as follows:

- The structural model gave a reliable prediction of the load-deformation behaviour of the timber framing and wall panel experiments conducted under ambient conditions. It was determined that essentially full composite interaction was occurring up to 90% of the ultimate capacity of the wall panels. At the time of failure, the effectiveness of the connection reduced and full composite action did not occur.

- The structural model was capable of giving reliable predictions of the deformation versus time behaviour of a wall panel subjected to a standard heating regime. The reliability of the prediction was, however, demonstrated to be highly dependent on the assumed reduction in the modulus of elasticity versus temperature of the timber.

- Modifications to the mechanical properties derived with regard to the degradation of the modulus of elasticity versus temperature were required in order to represent the irrecoverable nature of the deformations induced through the mechano-sorptive creep phenomenon. The phenomenon of the rapid reduction and subsequent irrecoverable loss of stiffness in the timber requires further investigation. This investigation should include a series of additional experiments and modelling development for it to be properly incorporated into the structural model.

- The ultimate strength in compression was not a significant parameter in determining the time-to-failure of a load-bearing timber-framed wall in a fire resistance test.

- The structural response of a timber wall in fire and the subsequent time of failure are highly dependent on the flexural stiffness of the wall. The failure mode of a wall was thus associated with the buckling phenomenon.

- The time to failure of the wall was shown to be sensitive to the load level and the height of the partition.

- The plasterboard sheeting was demonstrated to have a lesser structural effect for a wall prevented from rotation at the ends than for a wall, which could freely rotate at the ends.

9. Recommendations for Further Research

9.1 General

Based on the research undertaken in this thesis and with consideration of the application of the model developed within the framework for building code reform, the following issues were identified as requiring further investigation:

- Further modelling of the creep/plastification phenomenon.

- Increased number of mechanical property tests to better statistically define the reduction in mechanical properties with temperature.

- Consideration of the phenomenon of load sharing.

- Further sensitivity studies.

- Thermal properties for timber can be calibrated against the results from the thermal calibrations performed in the mechanical property experiments.

- Full-scale wall furnace experiments should be conducted for different heating regimes

- Enhancement and verification of the model to consider flooring systems.

- Investigation of the miscellaneous effects due to openings, service penetrations and defects

- Effect of localised charring by nails in determining the time-to-failure.

9.2 Modelling the Creep/Plastification Phenomenon

The work performed within this thesis indicates that some advancement of the structural model is required. In particular, advancement associated with the implementation of a creep submodel to address the rapid reduction in modulus of elasticity of timber exposed to temperatures approaching 100°C, which may be caused by something similar to the mechano-sorptive phenomenon. Although the mechano-sorptive phenomenon has been described in the literature as being almost instantaneous, the expression for the creep strain should be defined in terms of stress level, temperature, moisture content and possibly time. Deriving the expression will require an extensive experimental program, which will hold three of the variables constant and examines the effect of the fourth. The transient nature for fixed conditions of the phenomenon should be investigated. If

the creep/plastification phenomenon is shown through experiment to be effectively instantaneous, then only three variables need to be considered, but the applicability of conventional creep models incorporating visco-elastic phenomena through the use of dashpots and springs in parallel and series will need to be carefully examined. This work is currently being undertaken at Victoria University of Technology.

9.3   Increased Data for Mechanical Property Reductions

The data set for the reduction of the mechanical properties of radiata pine in compression with temperature and moisture contents should be enhanced to increase the confidence in the data obtained from the experimental series performed in this thesis. Studies should examine the wood population as a whole, in particular consider specimens which have significant defects. This is required to investigate the implicit assumption made in this thesis that the reduction of mechanical properties in compression is the same for specimens with minimal defects as specimens with a significant number of defects. The relationship between the density of the specimen and the reduction in the mechanical property at a given temperature and moisture content should be examined.

Experiments should be performed to determine the reduction in the mechanical properties of radiata pine in tension due to the effect of elevated temperatures and moisture content. A large number of experiments should be performed to determine the distribution of the reduction in mechanical properties such as performed by Lau (1996). However, the timber should be heated to a uniform temperature, at least on an initial basis to determine approximate reductions at specific elevated temperatures in order to increase the confidence in applying an assumed interpolation technique. The use of a reasonable sized data set for the tensile tests can lead to the derivation of a statistical distribution for the failure stress, and thus consider size effects, such as presented by Buchanan (1986) for ambient specimens.

After the tension and compression mechanical properties have been determined from experimentation, bending experiments should be taken at elevated temperatures to demonstrate the validity of combining mechanical properties in tension and compression in a model for bending.

Further small-scale experiments should be undertaken to evaluate the effects of different heating rates on the mechanical properties and to validate the use of mechanical properties determined from steady-state heating conditions with transient heating conditions whilst loaded, conditions that are associated with a full-scale wall specimen.

9.4   Consideration of the Phenomenon of Load Sharing

The phenomenon of load sharing can be considered to examine statistically the effect of different mechanical properties of timber framing members within a wall. The model which incorporates a single frame element, can be extended to multiple members by modification of the stiffness matrix to account for the transfer of force through the top plate element and the plasterboard sheeting. Direct stiffness equations for beams can be used to transfer the force between connected nodes of the line members. The methodology to implement this method can be deduced from generalised texts on matrix structural analysis such as Coates *et al* (1988). This approach should be further considered in extending the model to floor-ceiling systems, identified as another area of future work in Section 9.7.

9.5   Further Sensitivity Studies

Further sensitivity studies can be performed to examine the effect on time to failure due to changing the wall height when applying the the design load of the wall, in accordance with relevant timber design codes such as AS1720.1. The design load of a wall would decrease with height, and result accordingly in an increase in the time to failure.

9.6 Thermal Properties Should be Derived from Thermal Calibrations

The thermal properties of timber should be derived based on the thermal calibrations undertaken during the mechanical property tests. The boundary conditions are well defined for a temperature range from 70°C up to 275°C, that is the boundary temperature is almost constant throughout the test period. Hence given the boundary conditions are well defined, the thermal properties can be calibrated for heat transfer modelling up to this temperature.

9.7 Full Scale Experiments at Different Heating Regimes

The models have currently been compared with full-scale experiments conducted for wall panels heated using a standard heating regime (AS1530.4). Given the model is to be applied within a framework that is to determine the response of a wall panel subjected to real fires, it is essential that full-scale experiments with similarly controlled boundary conditions are subjected to a different heating regimes. Reference to real fire tests indicates that fire development can be derived in terms of an incipient phase, rapid development phase (leading to flashover), fully developed phase and a decay phase.

Although the incipient phase may have some localised effects on the plasterboard partition, it is the rapid development and fully developed phases of the fire that are considered to threaten the efficacy of the wall partition system in providing a passive barrier against fire spread.

Examination of the literature involving real fire tests revealed that the hydrocarbon curve as defined in the draft pREN standard (1998) for alternative heating conditions and qualifying procedures to be adopted under special circumstances is more closely representative of the rapid development and fully developed phases of real fires in buildings. The equation presented for the hydrocarbon heating regime, with a peak temperature of 1100°C is

$$T = 1080\left(1 - 0.325 * e^{-0.167t} - 0.675 * e^{-2.5t}\right) + 20 \qquad - (9.1)$$

where T is the temperature of the furnace, t minutes after commencement of the test

9.8 Enhancement of the Structural Model to Reliably Represent Floor - Ceiling Systems.

The structural model at the current state of development can approximately represent the structural behaviour of a flooring system, but it should be slightly modified to more correctly represent the structural behaviour of a floor. The primary modification is to incorporate an additional term into the stiffness matrix to represent the effect of the torsional rigidity of a floor system (Foschi, 1982). In comparing his model for timber flooring in ambient conditions to FEAFLO (refer to Thompson *et al*, 1976) he indicated that the contribution to the structural response is significant. Reference to a text on matrix structural analysis such as Coates *et al* (1988) will provide the terms. The effect of temperature on the mechanical properties for the flooring should be calculated, with consideration of the different types of flooring materials. The sensitivity of the contribution of the torsional rigidity terms should be considered with regard to the time of failure. If the contribution of the torsional terms is found to make a significant difference to the calculated time of failure, experimentation will be required to determine the relationship between the shear modulus versus temperature. Further consideration of the linear reduction in the stress-strain relationship beyond the peak stress in compression should be performed in using the equation from Buchanan (1986). Some calibrations to deduce an appropriate gradient will be required to be performed.

Calibration of the model against a series of experiments that carefully control constituent member properties, uniform heating conditions of load bearing members, edge conditions etc, of a similar breadth as undertaken for the wall panels in this thesis should be an essential component of the extension of the work. In particular, careful consideration should be made in correctly modelling when the plasterboard sheeting fails and falls off, as this will significantly affect the outcome in predicting the heat transfer into the remaining sheets and the incipient spread of flame within the ceiling cavity. The modifications to the models developed by Clancy (1999) incorporating the

structural model detailed in this thesis will require a closer interlinking, where the structural response of the sheeting under self-weight and reduced capacity will directly impact on the configuration of the heat transfer model.

9.9 Investigation of Miscellaneous Effects due to Openings, Service Penetrations and Defects

The effects of incorporated openings, construction defects and cavity insulation materials, while outside the scope of this thesis, could critically affect the performance of timber-framed barriers in fire.

- It is highly probable that a fire resistant barrier system will require openings such as doors and services to pass through. Doors interfere with the continuous composite contribution of the plasterboard sheeting, the door and door frame may generate forces within the wall partition, particularly if a steel frame is present. Similarly, penetrating services may transfer additional energy within the cavity through either conduction or leakage of hot gases and result in localised degradation, whilst the penetrating service may interact structurally with the wall and cause a localised stress concentration. In any probabilistic studies considering the performance of the barrier in a global fire model, the effect of this interaction should be studied.

- Alterations from the prescribed construction systems such as the fixing details, joints, holes etc will impact on the heat transfer and composite action between the timber stud and plasterboard sheeting. The effect of defects in wall construction on the fire resistance of a barrier should be considered in probabilistic studies.

- The effect of cavity insulation on the heating of the wall specimens and the associated structural response should be considered.

9.10   Investigation of the effect of Localised Charring in the Vicinity of Nails on the Time-to-Failure

The nails provide a ready medium for the localised heat transfer into the timber framing. In the vicinity of the nails, there was a noticeable increase in the rate of charring.

The analysis of the localised effect in the vicnity of the connectors can be readily incorporated into the structural model, with very minor alterations. It is more dependent on the heat transfer model of Clancy (1999) being extended to consider the three-dimensional effects. It may be determined that the localised growth characteristics, in conjunction with the increased charring in the vicinity of nails are contained within wood subjected to compression may indicate that the effect of localised charring in the case of light-framed timber walls is not significant.

10. Acknowledgments

The author would like to thank the following persons for contributing to the production of this thesis:

- Paul Clancy for initiating the project, obtaining funds from industry to finance the research and for providing significant time in the supervision of the project and review of the work performed.

- Professor Vaughan Beck for providing generalised supervision of the project and a detailed review of the thesis

- Dr. Ian Bennetts for reviewing the thesis and providing valuable input.

- Judith Young for reviewing the thesis and providing valuable input.

- Paul England for reviewing the thesis and providing valuable input.

- David Baker, for many fruitful technical discussions involving both the theoretical modelling and mechanical property testing.

- Gino Catania for graciously providing assistance in performing the experiments within the thesis.

- Dr. Robert Leicester and Mr. Rob MacNamara and other staff at the CSIRO Division of Building, Construction & Engineering, Highett in providing technical input and extensive support with staff and facilities for experiments involving both ambient full-scale wall frames, panels and small scale specimens.

- Staff at the Department of Civil & Building Engineering, Victoria University of Technology in assisting with the small scale elevated mechanical property experiments.

- Staff at BHP Research, Melbourne Laboratories in providing assistance in performing the full scale elevated temperature experiments.

- The National Association of Forest Industries (NAFI) in providing generous financial support for the project.

11 References

American Society for Testing and Materials, "Standard Methods of Static Tests of Timbers in Structural Sizes: ASTM Designation: D198-84", 1994

American Society for Testing and Materials, "Standard methods of fire tests of building construction and materials", 1992, ASTM E119-88

Anderberg, Y., "Fire -Exposes Hyperstatic Concrete Structures - An Experimental and Theoretical Study", 1976, Lund Institute of Technology, Lund

Armana, E.G., Booth, L.G., "Theoretical and Experimental Studies on Nailed and Glued Plywood Stressed-Skin Components : Part I - Theoretical Study", 1967, *Journal of the Institute of Wood Science*, Vol. 4, No. 1, pp. 43-69

Armana, E.G., Booth, L.G., "Theoretical and Experimental Studies on Nailed and Glued Plywood Stressed-Skin Components : Part II - Experimental Study", 1967, *Journal of the Institute of Wood Science*, Vol. 4, No. 2, pp. 19-34

AS 1530.4, "Methods for Fire Tests on Building Materials, Components and Structures Part 4 - Fire-Resistance Tests of Elements of Building Construction", 1990, Standards Australia, Sydney

AS 1720.1, "SAA Timber Structures Code Part 1 – Design Methods", 1988, Standards Australia, Sydney

AS 1748, "Timber – Stress Graded – Product Requirements for Mechanically Stress Graded Timber", 1978 Standards Australia, Sydney

AS4100, "Steel Structures", 1998, Standards Australia, Sydney

Barnfield, J., Cooke, G., Deakin, G., Hannah, M., Jones, T., Law, M. & Malhotra, B., "Draft British Standard Code of Practice for The Application of Fire Safety Engineering Principles to Fire Safety in Buildings", 1993, Warrington Fire Research Consultants

Bender, D.A., Woeste, F.E., Schaffer, E.L. & Marx, C.M., "Reliability Formulation for the Strength and Fire Endurance of Glued-Laminated Beams", 1985, Research Paper FPL 460, USDA Forest Products Laboratory, Madison, Wi

Bennetts, I.D., Culton, M., Dickerson, M.L., Lewins, R.R., Poh ,K.W., Poon, S.L., Ralph, R., Lee, A.C., Beever, P.F., Cooper, R.J., Haggar, P.I., Moore, I.P., Ramsay & Timms, G.R., "Simulated Shopping Centre Fire Tests", 1997, Fire Code Reform Centre Project 6, BHP Research, Melbourne

Bentley, R., "Theory and Practice of Thermoelectric Thermometry; Temperature Measurement Course: Book 1", CSIRO Division Of Applied Physics

Boral Plasterboard, "FIRESTOP Board Evaluation : R2.00-13", 1977, Boral Australian Gypsum Ltd

Boral Plasterboard, "Construction Selector : Fire Rated and Sound-Rated Systems", 1994, Boral Australian Gypsum Limited.

Buchanan, A.H., "Combined Bending and Axial Loading in Lumber", 1986, *Journal of Structural Engineering*, Vol. 112, No. 12, December, pp. 2592-2609

Buchanan, A.H. & Munukutla, V.R, "Fire Resistance of Load-Bearing Reinforced Concrete Walls", 1991, *Fire Safety Science, Proceedings of the Third International Symposium*, pp. 771-780

"Building Code of Australia (including Amendments 1-5)", 1999, Australian Building Codes Board, Canberra

Chang, F.K., "Stress Analysis of Wooden Structures Exposed to Elevated Temperatures",1986, *Journal of Reinforced Plastics and Composites*, Vol. 5, pp. 218-238

Chang, F.K., "Thermal-Mechanical Loading Interaction Effect on Strength and Failure Time of Wooden Structures Exposed to Elevated Temperature",1986, *Journal of Reinforced Plastics and Composites*, Vol. 5, pp. 253-271

Cheng, W.C., "Theory and Application on the Behaviour of Steel Structures at Elevated Temperatures", 1983, *Computers & Structures*, Vol. 16, No. 1-4, pp.27-35

Chen, W.F. and Lui, E.M., "Structural Stability Theory and Implementation", 1987, Elsevier, New York

Clancy, P., "Time and Risk of Failure of Timber Framed Walls in Real Fires", 1999, PhD Dissertation Submitted, Victoria University of Technology, Melbourne, Australia

Clancy, P. and Young, S.A., "Report on Full-Scale Furnace Tests", 1996, Internal Report, Centre for Environmental Safety and Risk Engineering, Victoria University of Technology, Melbourne, Australia

Coates, R.C., Coutie, M.G. & Kong, F.K., "Structural Analysis Third Edition", 1988, Van Nostrand Reinhold International, Hong Kong

Collier, P.C.R., "Design of Loadbearing Light Timber Frame Walls for Fire Resistance : Part 1", 1991, Building Research Association of New Zealand, Study Report SR 36, Judgeford, New Zealand

Collins, G.E., Collier, P.C.R. & MacKenzie, C.E., "Fire Resistance of Timber-framed Floors and Walls", 1993, CSIRO Technical Report 93/5, CSIRO Division of Building, Construction and Engineering

Criswell, M.E., "New Floor Design Procedures", 1983, *from "Wall & Floor Systems Design and Performance of Light-Frame Structures"*, pp. 63-86

Dinwoodie, J.M., "Wood:Nature's Cellular, Polymetric Fibre-Composite",1989 , The Institue of Metals, London

Do, M.H. & Springer, G.S., "Mass Loss of and Temperature Distribution in Southern Pine and Douglas Fir in the Range 100 to 800°C", 1983a, *Journal of Fire Sciences*, pp. 271-284

Do, M.H. & Springer, G.S., "Model for Predicting Changes in the Strengths and Modulii of Timber Exposed to Elevated Temperatures", 1983b, *Journal of Fire Sciences*, pp. 285-295

Do, M.H. & Springer, G.S., "Failure Time of Loaded Wooden Beams During Fire", 1983c, *Journal of Fire Sciences*, Vol. 1,July/August, pp. 297-303

"Draft National Building Fire Safety Systems Code", 1991, Building Review Task Force

Eurocode 5 Part 1.2, "Structural Fire Design", 1995, Final Draft, prEN 1995-1-2

"Fire Engineering Guidelines 1st Edition", 1996, Fire Code Reform Centre Ltd, Sydney

Forest Products Laboratory, "Wood Handbook : Wood as an Engineering Material", 1987, US Department of Agriculture, Washington

Foschi, R.O., "Load-Slip Characteristics of Nails", 1974, *Wood Science*, Vol. 7, No. 1, pp. 69-76

Foschi, R.O., "Load-Slip Charactersitics for Connections with Common Nails", 1977, *Wood Science*, Vol. 9, No. 3, pp. 118-123

Foschi, R.O., "Structural Analysis of Wood Floor Systems", 1982, *ASCE Journal of the Structural Division*, Vol. 108, No. ST7, July, pp. 1557-1574

Fredlund, B., "A Model for Heat and Mass Transfer in Timber Structures During Fire", 1988, Report LUTVDG/(TVBB-1003), Lund University

Fuller, J.J., Leichti, R.J. & White, R.H., "Temperature Distribution in a Nailed Gypsum-Stud Joint Exposed to Fire", 1992, *Fire & Materials*, Vol. 16, pp. 95-99

Gammon, B.W., "Reliability Analysis of Wood-Frame Walls Exposed to Fire", 1987, PhD Dissertation

Gerhards, C.C., "Effect of Moisture Content and Temperature on the Mechanical Properties of Wood: An Analysis of Immediate Effects', 1982, *Wood & Fibre*, pp. 4-36

Goncalves, T., Jong, F., Clancy, P. & Poynter, W., "Mechanical Properties of Fire Rated Gypsum Board", 1996, Department of Civil & Building Engineering, Victoria University of Technology, Melbourne

Goodman, J.R. & Popov, E.P., "Layered Beams with Interlayer Slip", 1968, *ASCE Journal of the Structural Division*, Vol. 94, No. ST11, November, pp. 2535-2547

Grossman, P.A.U., "Requirements for a Model that Exhibits Mechano-Sorptive Behaviour", 1976, *Wood Science & Technology*, Vol. 10, pp. 163-168

Gypsum Association, "GA-600 – 97 Fire Resistance Design Manual", 1997, Washington

Hadvig, S., "Charring of Wood in Building Fires", 1981, Technical University of Denmark, Copenhagen

Hoffmeyer, P. & Davidson, R.W., "Mechano-sorptive creep mechanism of wood in compression and bending", 1989, *Wood Science & Technology*, Vol. 23, pp. 215-227

Hirschler, M.M., "Analysis of Full-Scale Fire Resistance Tests of Wall Linings in Ranch House", 1998, ASTM STP 1336, American Society of Testing and Materials.

Jonsson, R. & Pettersson, "Timber Structures and Fire – A Review of the Existing State of Knowledge and Research Requirements", 1985, Swedish Council for Building Research, Stockholm, Sweden

Kasal, B. & Leichti, R.J., "Non linear Finite Element Model for Light Frame Stud Walls", 1992, *Journal of Structural Engineering*, Vol. 118, No. 11, November, pp. 3122-3135

Khan, M.A. & Idriss Ali, K.M., "Effect of Moisture and Heat on Mechanical Properties of Wood and Wood-Plastic Composite", 1993, *Journal of Polymer-Plastic Technology Engineering*, Vol. 32, No. 1&2, pp. 5-13

King, E.G. & Glowinski, R.W., "A Rationalized Model for Calculating the Fire Endurance of Wood Beams", 1988, *Forest Products Journal*, Vol. 38, No. 10, pp. 31-36

Knudson, R.M. & Schniewind, A.P., "Performance of Structural Wood Members Exposed to Fire", 1975, *Forest Products Journal*, Vol. 25, No. 2, pp. 23-32

König, J., "The Structural Behaviour of Axially Loaded Wood Studs Exposed to Fire on One Side", 1988, Trätek, Rapport I 8808057, Stockholm

König, J., "Modelling the Effective Cross Section of Timber Frame Members Exposed to Fire", 1991, Trätek, Rapport I 9112080, Stockholm

König, J., "Fire Resistance of Timber Joists and Load Bearing Wall Frames", 1995, Trätek, Rapport I 9412071, Stockholm

Lahey, "Lahey FORTRAN 77 Level 3, Version 5.01", 1992, Lahey Computer Systems Inc, PO Box 6091 Incline Village, Nevada 89450

Latham D.J., Kirby B. R., & Thomas G., "The Temperatures Attained by Unprotected Structural Steelwork in Experimental Natural Fires", 1987, *Fire Safety Journal* Vol. 12, pp 139-152.

Lau, P.W.C., "Behaviour and Reliability of Wood Tension Members Exposed to Elevated Temperatures", 1996, PhD Dissertation, Faculty of Graduate Studies, Department of Wood Science, University of British Columbia, Vancouver

Leicester, R.H., Grant, D.J., Rumball, B.L. & Young, F.G., "Structural Engineering Properties of Machine Stress-Graded, Australian Grown Radiata Pine", 1988, DCE Technical Report TR88/1, CSIRO Division of Building, Construction and Engineering, Melbourne

Lyman,O., "An Introduction to Statistical Methods and Data Analysis", 1988, PWS-Kent Publishing Company, Boston.

McCutcheon, W.J., "Method for Predicting the Stiffness of Wood-Joist Floor Systems with Partial Composite Action", 1977, Research Paper FPL 289, USDA Forest Products Laboratory, Madison, Wi

McCutcheon, W.J., "Deflection of Uniformly Loaded Floors A Beam Spring Analog", 1984, Research Paper FPL 449, USDA Forest Products Laboratory, Madison

McCutcheon, W.J., "Stiffness of Framing Members with Partial Composite Action", 1986, *Journal of Structural Engineering*, Vol. 112, No. ST7, July, pp. 1623-1637

MacLean, J., "Effect of Steaming on the Strength of Wood", 1953, *Proceedings of the American Wood Preservers Association*, Vol. 49, pp. 88-112

MacLean, J., "Effect of Heating in Water on the Strength Properties of Wood", 1954, *Proceedings of the American Wood Preservers Association*, Vol. 50, pp. 253-281

MacLean, J., "Effect of Oven Heating and Hot Pressing on the Strength Properties of Wood", 1955, *Proceedings of the American Wood Preservers Association*, Vol. 51, pp. 227-250

McLain, T.E., "Curvilinear load-slip relations in laterally loaded nailed joints", 1975, PhD Dissertation

Madsen, B., "Structural Behaviour of Timber", 1992, Timber Engineering Ltd., Vancouver

Malhotra, S.K. & Bazan, I.M.M., "Bending Strength Theory for Timber Beams", 1980, *Wood Science*, Vol. 13, No. 1, July, pp. 50-63

Mehaffey, J.R, "Development of Fire Endurance Models for Wood Stud Walls : Progress Report", 1991, Forintek Canada Corp.

Mehaffey, J.R., Cuerrier, P. & Carisse, G., "A Model for Predicting Heat Transfer through Gypsum-Board/Wood Stud Walls Exposed to Fire", 1994, *Fire & Materials*, Vol. 18, pp. 297-305

Mould, A.E. & Williams, D.W., "The Effects of High Ambient Temperatures on Gypsum Plasters", 1974, *Building Science*, Vol. 9, pp. 234-245

Norén, J., "Failure of Structural Timber When Exposed to Fire. Part 2", 1988, Trätek, Rapport I 8810066, Stockholm

O'Meagher, A.J. & Bennetts, I.D., "Modelling of Concrete Walls in Fire", 1991, *Fire Safety Journal*, Vol. 17, pp. 315-335

Östman, B.A.L., "Wood Tensile Strength at Temperatures and Moisture Contents Simulating Fire Conditions", 1985, *Wood Science and Technology*, Vol. 19, pp. 103-116

Peacock, R.D., Jones, W.W. & Bukowski, R.W., "Verification of a Model of Fire and Smoke Transport", 1993, *Fire Safety Journal*, pp. 89-129

Pellicane, P.J., Stone, J.L. & Vanderbilt, M.D., "Generalized Model for Lateral Load Slip of Nailed Joints", 1991, *Journal of Materials in Civil Engineering*, Vol. 3, No. 1, February, pp. 60-77

Poh, K.W & Bennetts, I.D, "Analysis of the Behaviour of Loadbearing Members under Elevated Temperature Conditions", 1994, *Proceedings of the Australasian Structural Engineering Conference*, IE Aust, 21-23 September, Sydney, pp.401-406

Polensek, A., "Finite Element Analysis of Wood-Stud Walls", *ASCE Journal of the Structural Division*, 1976, Vol. 102, No. ST7, July, pp. 1317-1335

Popov, E.P., 1978, "Mechanics of Materials Second Edition", Prentice-Hall, New Jersey

"prEN 1363-2: Fire Resistance Tests – Part 2: Alternative and Additional Procedures", 1998, European Committee for Standardization

Press, W.H., Teukolsky, S.A., Vetterling, W.T. & Flannery, B.P., "Numerical Recipes in FORTRAN : The Art of Scientific Computing Second Edition",1992, Cambridge University Press, Cambridge

Purkiss, J.A. & Weeks, N.J., "A Computer Study of Reinforced Concrete Columns in a Fire", 1987, *The Structural Engineer*, Vol. 65B, No. 1, March, pp. 22-28

Sa Ribeiro, R.A., Pellicane, P.J., "Modeling Load-Slip Behavior of Nailed Joints",1992, *Journal of Materials in Civil Engineering*, Vol. 4 , No. 4, November, pp 385-398

Sazinski, R.J. & Vanderbilt, M.D., "Behavior and Design of Wood Joist Floors", 1979, *Wood Science*, Vol. 11, No. 4, April, pp.209-220

Schaffer, E.L., "Effect of Pyrolytic Temperatures on the Longitudinal Strength of Douglas Fir", 1973, *Journal of Testing and Evaluation*, Vol. 1, No. 4, pp. 319-329

Schaffer, E.L., "State of Structural Timber Fire Endurance", 1977, *Wood & Fiber*, Vol. 9, No. 2, pp. 145-170

Schaffer, E.L., "Influence of Heat on the Longitudinal Creep of Dry Douglas Fir", 1982, *Structural Use of Wood in Adverse Environments*, Society of Wood Science & Technology, Van Nostrand Reinhold Company, New York, pp. 21-52

Schaffer, E.L., "Structural Fire Design : Wood", 1984, Forest Products Research Paper FPL 450, Forest Products Laboratory

STRAND 6.13, "Strand 6, Finite Element Analysis System", 1993, G+D Computing Pty Ltd, Suite 1, Level 7, 541 Kent Street, Sydney

Suzuki, S., Tamai, A. & Hirai, N., "Effect of Temperature on Orthotropic Properties of Wood III", 1982, *Mokuzai Gakkaishi*, Vol. 28, No. 7, pp. 401-406

Thomas, G.C. & Buchanan, A.H., "Mechanical Properties of Timber at High Temperatures", 1995a, *Fire and Materials 4*[th] *Conference and Exhibition*, November 15-16, Washington, pp.125-134

Thomas, G.C., Buchanan, A.H., Carr, A.J., Fleishmann, C.M. & Moss, P.J., "Light Timber-Framed Walls Exposed to Compartment Fires", 1995b, *Journal of Fire Protection Engineering*, Vol. 7, No. 1, pp. 25-35

Thomas, G.C., Buchanan, A.H., Carr, A.J., Fleischmann, C.M. & Moss, P.J., "Modelling Structural Fire Performance of Wood Frame Construction", 1996, Proceedings of the International Wood Engineering Conference, New Orleans, pp. 241-248

Thomas, G.C., "Fire Resistance of Light Timber Framed Walls and Floors", 1997, Fire Engineering Research Report 97/7, University of Canterbury, Christchurch, New Zealand

Thomas I.R., Bennetts, I.D., Proe, D.J., Lewins, R.R. & Almand, K.H., "Fire in Offices", 1989, BHP Research, Melbourne Laboratories

Thomas, I.R., Bennetts, I.D., Proe, D.J., Lewins, R.R. & Almand, K.H., "Fire in Mixed Occupancy Buildings", 1990, BHP Steel Structural Development Group, Melbourne

Thompson, E.G., Goodman, J.R. & Vanderbilt, M.D., "Finite Element Analysis of Layered Wood Systems", 1975, *ASCE Journal of the Structural Division*, Vol. 101, No. ST12, December, pp. 2659-2672

Thompson, E.G., Vanderbilt, M.D. & Goodman, J.R., "FEAFLO: A Program for the Analysis of Layered Wood Systems", 1976, *Computers & Structures*, Vol. 7, pp. 237-248

Timoshenko S.P., "Strength of Materials Part I", 1955, Van Nostrand, New York

Timoshenko, S.P., "Strength of Materials Part II", 1956, Van Nostrand, New York

Timoshenko, S.P. & Goodier, J.N., "Theory of Elasticity", 1970, McGraw-Hill, Singapore

Troughton, G.E. & Rozon, L.R., "Heat Effects on Tensile Properties of Douglas-Fir and White Spruce Thin Sections, 1974, *Wood Science*, Vol. 7, No. 2, October, pp. 116-122

Vanderbilt, M.D., Goodman, J.R. & Criswell, M.E., "Service and Overload Behaviour of Wood Joist Floor Systems", 1974, *ASCE Journal of the Structural Division*, Vol. 100, No. ST1, January, pp. 11-29

Walker, D. & Lightfoot, M., "Mechanical Properties of Fire Rated Gypsum Board", 1995, Department of Civil & Building Engineering, Victoria University of Technology, Melbourne

Warren Centre, "Fire Safety and Engineering Technical Papers Books 1 & 2, International Symposium Papers", 1989, The University of Sydney

Warrington Fire Research, "R9701 – Comparative Pilot test of Fire Resistant Board Products", 1997, Warrington Fire Research (Aust) Pty Ltd

Wheat, D.L., Vanderbilt, M.D. & Goodman, J.R., "Wood Floors With Non-Linear Nail Stiffness", 1983, *Journal of Structural Engineering*, Vol. 109, No. 5, May, pp. 1290-1302

White, R.H. & Schaffer, E.L., "Transient Moisture Gradient in Fire-Exposed Wood Slab", 1981, *Wood and Fiber*, Vol. 13, No. 1, pp. 17-38

White, R.H., "Analytical Methods for Determining Fire Resistance of Timber Members",1988, *from SFPE Handbook of Fire Protection Engineering*, Chapter 8, National Fire Protection Association, Quincy, Ma.

White, R.H., Cramer, S.M. & Shrestha, D.K., "Fire Endurance Model of a Metal-Plate-Connected Wood Truss", 1993, Research Paper FPL 522, Forest Products Laboratory, Madison

Wickstrom, U., "TASEF–2 – A Computer Program for the Temperature Analysis of Structures Exposed to Fire", 1979, Report No. 79-2, Lund Institute of Technology, Dept of Structural Mechanics, Lund, Sweden

Wilkinson, T.L., "Theoretical Lateral Resistance of Nailed Joints", 1971, *Journal of Structural Engineering*, Vol. 97, No. ST5, May, pp. 1381-1398

Wilkinson, T.L., "Analysis of Nailed Joints with Dissimilar Members", 1972, Journal of Structural Engineering, Vol. 98, No. ST9, September, pp. 2005-2013

Woeste, F.E. & Shaffer, E.L., "Reliability Analysis of Fire-Exposed Light-Frame Wood Floor Assemblies", 1981, Research Paper FPL 386, Forest Products Laboratory, Madison

Woeste, R.W., "Performance of Light-Frame Redundant Assemblies", 1990, *1990 International Timber Conference*, Tokyo, October, pp. 124-131

Young, S.A., "Elevated Temperature Mechanical Properties of Radiata Pine in Compression", 1996, Internal Report, Centre for Environmental Safety and Risk Engineering, Victoria University of Technology, Melbourne, Australia

Young, S.A. & Clancy, P., "Full Scale Tests on Ambient Walls", 1996, Internal Report, Centre for Environmental Safety and Risk Engineering, Victoria University of Technology, Melbourne, Australia

Young, S.A., "Structural Modelling of Plasterboard Clad, Light Timber-Framed Walls in Fire", 2000, Internal Report IR 00-001, Centre for Environmental Safety and Risk Engineering, Victoria University of Technology, Melbourne, Australia

Zakic, B.D., "Inelastic Bending of Wood Beams", 1973, *Journal of the Structural Division*, Vol. 99, No. ST10, October, pp. 2079-2095

Appendix 1: Derivation of Strain Induced through the Composite Elements by Consideration of Partial Composite Action

A1.1 Introduction

The derivation of strains induced in the plasterboard flanges and stud is presented, given a moment and applied axial force to the composite segment. A depiction of an element indicating the strain distribution through such an element is shown in Figure 1.
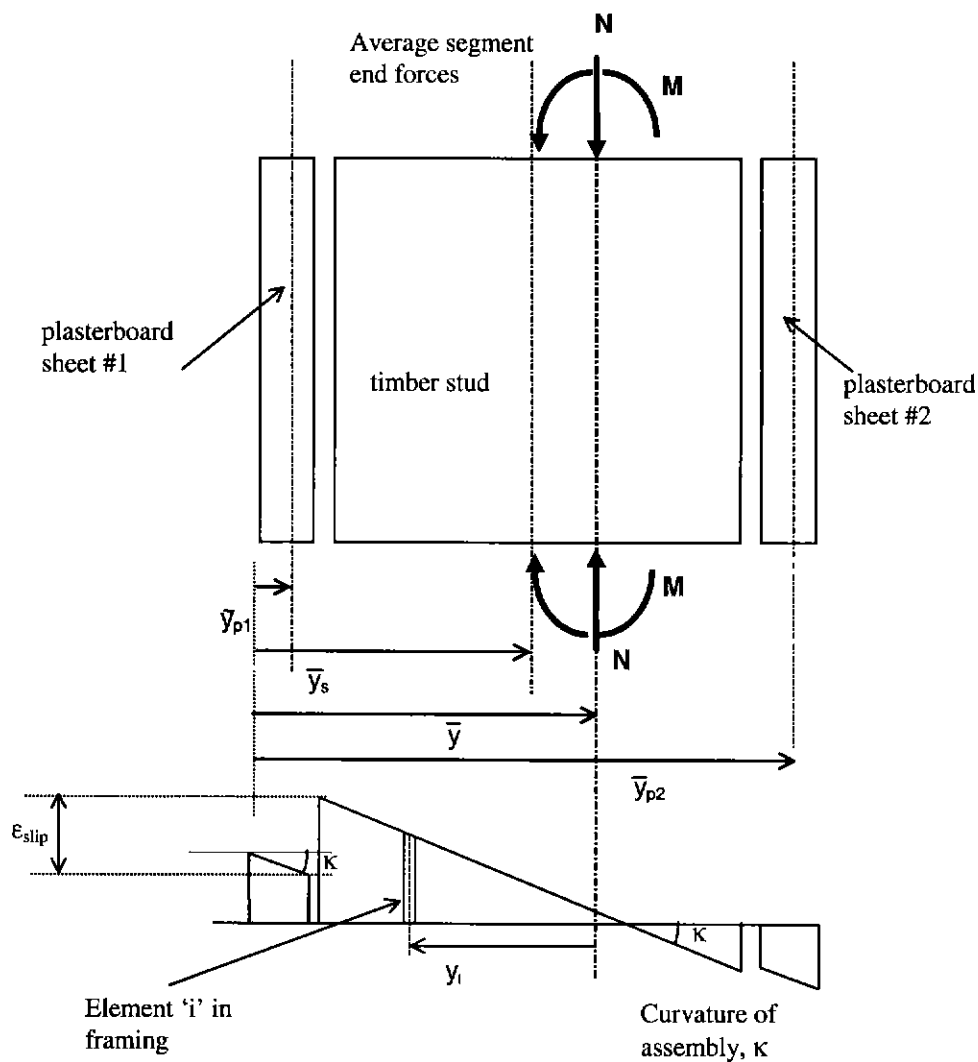

Figure 1 : Details of Strain Distribution Through the Composite Section Cross Section

The total segment axial stiffness, EA, over a segment length L, is determined from the expression

$$EA = L\sum_{i=1}^{3} k_i \qquad \text{- (A1.1)}$$

where k_i represent the contribution to the axial stiffness by each of the components.

$$k_1 = \frac{EA_{p1}k_{ss}}{EA_{p1} + Lk_{ss}}, \quad k_2 = \frac{EA_s}{L} \text{ and } k_3 = \frac{EA_{p2}k_{ss}}{EA_{p2} + Lk_{ss}} \qquad \text{- (A1.2)}$$

where EA_x is the axial stiffness of each of the individual components denoted by the 'x'. The 'p1' subscript refers to the plasterboard sheet #1, 's' refers to the stud and 'p2' refers to the plasterboard sheet #2 as shown in Figure 1.

The centroid of segment, $\bar{y}$, is defined by the expression

$$\bar{y} = \frac{\sum_{i=1}^{3} \bar{y}_i k_i}{\frac{EA}{L}} \qquad \text{- (A1.3)}$$

the segment flexural stiffness, EI, is determined from

$$EI = \sum_{i=1}^{3} \left[k_i L(\bar{y} - y_i)^2 + EI_i \right] \qquad \text{- (A1.4)}$$

A1.2 Determination of the Strain Component Due to Axial Force

Total displacement of the composite segment, Δ, due to axial force, N is

$$\Delta = \frac{NL}{EA} \qquad \text{- (A1.5)}$$

The displacement of the plasterboard sheet, Δ_{p1} is equal to the total displacement less the amount of displacement within the connection ie.

$$\Delta_{p1} = \Delta - \Delta_{ss} \qquad \text{- (A1.6)}$$

where Δ_{ss} = interlayer slip

Given all displacements are assumed to occur over the same length, L, the strain within the plasterboard due to the axial force, ε_{p1n}, may be written as

$$\varepsilon_{pln} = \varepsilon - \varepsilon_{ss1} \qquad\qquad - (A1.7)$$

where ε = strain of segment

The strain in the interlayer connection between the stud and plasterboard sheet #1, ε_{ss1}, is

calculated from

$$\varepsilon_{ss1} = N_{p1} \Big/ Lk_{ss1} \qquad\qquad - (A1.8)$$

where N_{p1} is the force transmitted through the connection into the plasterboard sheet.

hence

$$\varepsilon_{pln} = \frac{N}{EA} - \frac{N_{p1}}{Lk_{ss1}} \qquad\qquad - (A1.9)$$

given

$$N_{p1} = N \frac{\dfrac{k_{ss1}EA_{p1}}{Lk_{ss1} + EA_{p1}}}{\dfrac{EA}{L}} \qquad\qquad - (A1.10)$$

substitution of (A1.9) into (A1.10) yields

$$\varepsilon_{pln} = \frac{N}{EA} - \frac{NL}{EA}\frac{1}{Lk_{ss}}\left(\frac{k_{ss1}EA_{p1}}{Lk_{ss1} + EA_{p1}}\right) \qquad\qquad - (A1.11a)$$

simplification yields

$$\varepsilon_{pln} = \frac{N}{EA}\left(1 - \frac{EA_{p1}}{Lk_{ss1} + EA_{p1}}\right) \qquad\qquad - (A1.11b)$$

A1.3   Determination of the Strain Component Due to Bending

It is assumed that the curvature, κ, between the stud and sheets is constant. Therefore, the

following relationship is applicable.

$$\kappa = \frac{M}{EI} = \frac{M_{p1}}{EI_{p1}} = \frac{M_s}{EI_s} = \frac{M_{p2}}{EI_{p2}} \qquad\qquad - (A1.12)$$

where M represents the bending moment in the respective elements of construction and EI is the flexural stiffness of the respective elements.

The strain in the plasterboard sheet due to bending, ε_{plb}, is calculated with

$$\varepsilon_{plb} = \varepsilon_{section} - \varepsilon_{ss} \qquad\qquad \text{- (A1.13)}$$

where $\varepsilon_{section}$ = strain of the section calculated at a location y from a datum. Therefore

$$\varepsilon_{plb} = \frac{M}{EI}(y - \bar{y}) - \varepsilon_{ss} \qquad\qquad \text{- (A1.14)}$$

The magnitude of slip is proportional to the axial force transferred through the shear spring to the plasterboard sheet, hence equation (A1.8) can be applied.

The magnitude of axial force due to the bending acting through the plasterboard sheet, N_{plb} is calculated from

$$N_{plb} = \frac{M}{EI}(\bar{y} - \bar{y}_{pl})EA_{pl} \qquad\qquad \text{- (A1.15)}$$

direct substitution of (A1.15) into (A1.8) and further substitution into (A1.14) yields

$$\varepsilon_{plb} = \frac{M}{EI}(\bar{y} - y) - \frac{M}{EI}(\bar{y} - \bar{y}_{pl})\frac{EA_{pl}^2}{EA(EA_{pl} + Lk_{ss})} \qquad\qquad \text{- (A1.16a)}$$

simplification gives

$$\varepsilon_{plb} = \frac{M}{EI}\left((\bar{y} - y) - (\bar{y} - \bar{y}_{pl})\frac{EA_{pl}^2}{EA(EA_{pl} + Lk_{ss})} \right) \qquad\qquad \text{- (A1.16b)}$$

A1.4 Calculation of the Total Strain in the Plasterboard Sheeting

The total strain in the plasterboard sheeting is calculated by applying the principle of superposition to combine the bending and compression strain components;

$$\varepsilon_{pltot} = \varepsilon_{pln} + \varepsilon_{plb} \qquad\qquad \text{- (A1.17)}$$

Substitution of (A1.11b) and (A1.16b) gives

$$\varepsilon_{pltot} = \frac{N}{EA}\left(1 - \frac{EA_{pl}}{Lk_{ssl} + EA_{pl}}\right) + \frac{M}{EI}\left((\bar{y} - y) - (\bar{y} - \bar{y}_{pl})\frac{EA_{pl}^2}{EA(EA_{pl} + Lk_{ss})}\right) \text{- (A1.18)}$$